



Titre: Development of a Food-Safe Colorimetric Sensor for Monitoring Fish Spoilage Through Volatile Gases Detection

Auteur: Maryam Ameri

Date: 2025

Type: Mémoire ou thèse / Dissertation or Thesis

Référence: Ameri, M. (2025). Development of a Food-Safe Colorimetric Sensor for Monitoring Fish Spoilage Through Volatile Gases Detection [Thèse de doctorat, Polytechnique Montréal]. PolyPublie. <https://publications.polymtl.ca/65013/>

 **Document en libre accès dans PolyPublie**
Open Access document in PolyPublie

URL de PolyPublie: <https://publications.polymtl.ca/65013/>

Directeurs de recherche: Abdellah Ajji, & Samuel Kessler

Programme: Génie chimique

POLYTECHNIQUE MONTRÉAL

affiliée à l'Université de Montréal

**Development of a food-safe colorimetric sensor for monitoring fish spoilage
through volatile gases detection**

MARYAM AMERI

Département de génie chimique

Thèse présentée en vue de l'obtention du diplôme de *Philosophiæ Doctor*

Génie chimique

Mars 2025

POLYTECHNIQUE MONTRÉAL

affiliée à l'Université de Montréal

Cette thèse intitulée :

Development of a food-safe colorimetric sensor for monitoring fish spoilage through volatile gases detection

présentée par **Maryam AMERI**

en vue de l'obtention du diplôme de *Philosophiæ Doctor*

a été dûment acceptée par le jury d'examen constitué de :

Marie-Claude HEUZEY, présidente

Abdellah AJJI, membre et directeur de recherche

Samuel KESSLER, membre et codirecteur de recherche

Jean-Marie RAQUEZ, membre

Valérie ORSAT, membre externe

DEDICATION

“To my lovely father, Baba Hassan and my dedicated mother”.

ACKNOWLEDGEMENTS

Doing a PhD for me was like living as one of the students in “The Magic School Bus” animated series, with this huge difference that I was alone, without my best friends and maps, heading to unknown destinations with a lot of stop signs in my way. I have tuned myself into different shapes that I never expected. In the journey of my PhD, there are a few people with whom I shared my experiences—in the pain and in the happiness. I could have not been more grateful for their support, kindness, and patience.

I would like to extend my heartfelt gratitude to Professor Abdellah Ajji, my esteemed research supervisor. Your patience, extensive knowledge, thoughtful guidance, and unwavering support have been invaluable throughout my Ph.D. journey.

To my co-supervisor, Samuel, for his constant support, even with thousands of kilometers distance. You always patiently listened to me, educated me, and shaped my mind. None of the words in the world are powerful enough to express how much I appreciate all your support, advice, supervision, and sense of your humanity. Always, I am thankful for creation of such a warm, friendly, and enthusiastic research environment where I overcame my stress and pursue my PhD much easier. Your motivation has profoundly inspired me, and it has truly been a privilege to work under your mentorship.

Besides my supervisors, I would like to thank the rest of my thesis committee, namely Professor. Marie-Claude Heuzey, Professor Jean-Marie Raquez, Professor Orsat for accepting to evaluate my thesis.

I would like to acknowledge Professor Alexandra Furtos, Mass Spectrometry Facility Director at the Université de Montréal, who kindly allowed me to have access to their lab equipment, and Dr. Marc-Antoine Vaudreuil, Research Assistant of the Mass Spectrometry lab, who contributed to accomplishing the objectives of this research project.

I also want to express my sincere appreciation to Dr. Amir Saffar, Dr. Bentolhoda Helli, Dr. Marian Rofeal and Dr. Farid Radmeher for their insightful comments and academic advice, which have greatly enriched my research.

A special thank you goes to our dedicated technical staff in the Chemical Engineering Department, particularly Mr. Matthieu Gauthier and Mrs. Claire Cerclé, whose assistance has been instrumental.

There is a group of people I spent time with more than any others in the past years. My lovely friends, Teodora and Maxime, for giving me whatever you could give as true friends: love, compassion, support, thoughtful advice, and encouragement. Thank you, girls, for making my immigration journey easier and for teaching me anything that I was not familiar enough with, especially culture, language and cuisine. Thanks for always being present in my life.

Finally, I wish to thank my family members for their continuous support and love throughout my education. I am eternally indebted to my parents, Baba Hassan Janam, and my spiritual mother, for their unwavering strength, encouragement, love, and prayers, which have helped me persevere through challenges.

I am thankful to my sister, Marzieh, for all her kindness and taking care of my parents during these 4 years. I owe my deepest appreciation and respect to the almighty God for helping me overcome various obstacles during the research work and giving me the strength to continue despite facing several situations.

RÉSUMÉ

L'objectif principal de ce travail était de développer un capteur colorimétrique de sécurité alimentaire intégré dans les emballages alimentaires comme indicateur de fraîcheur et fournir des informations sur la qualité des aliments en utilisant une technique non destructive, in situ et en temps réel. Une formulation de liant avec un extrait de riz noir enrobé sur des films Polyéthylène téréphtalate (PET) traités par corona a été développée.

Dans le premier objectif, nous avons la formulation d'une encre alimentaire capable de changer de couleur à différents pH. Cette encre devait posséder deux caractéristiques importantes, tout d'abord, une forte adhésion à la couche de revêtement/côté imprimable, et deuxièmement, elle devait rester intacte dans l'espace de tête à haute humidité relative des emballages de fruits de mer. L'étude a impliqué la conception d'une formulation d'encre alimentaire sécuritaire affichant des changements de couleur significatifs sur une plage de pH (du rouge au jaunâtre/marron), démontrant une sensibilité aux gaz Total Volatile Base Nitrogen (TVB-N). Les méthodologies clés comprenaient le traitement corona des films en PET pour améliorer l'adhérence, le traitement thermique pour améliorer le collage de l'encre (adhésion et stabilité), et diverses techniques de caractérisation telles que les mesures de l'angle de contact de l'eau, la spectroscopie FTIR, et la spectrophotométrie UV-Vis pour analyser les propriétés de l'encre. Les résultats ont indiqué que les films développés signalent efficacement la détérioration du poisson grâce à des changements de couleur visibles, fournissant une solution pratique pour surveiller la fraîcheur des aliments tout en respectant les réglementations de sécurité alimentaire.

Dans le deuxième objectif, la recherche a impliqué l'examen de l'efficacité du changement de couleur de l'encre formulée dans différentes solutions de pH. Différentes techniques de caractérisation ont confirmé l'efficacité et la stabilité de l'indicateur, qui a démontré des réponses colorées rapides et sensibles aux gaz liées à la détérioration. Les films ont maintenu une stabilité de couleur acceptable lors du stockage à 4 °C, les changements de couleur corrélant avec les dénombrements microbiens et les analyses chimiques, confirmant leur efficacité en tant qu'indicateurs de fraîcheur. De plus, des modèles mathématiques ont été intégrés pour prédire la détérioration en fonction des données expérimentales, montrant de fortes corrélations entre les réponses colorimétriques et les niveaux de TVB-N, validant ainsi la performance du capteur dans la surveillance en temps réel de la fraîcheur. Les indicateurs de pH développés ont été évalués en

étant exposés à de vrais échantillons de poisson afin d'évaluer la réponse colorimétrique durant le stockage du poisson à 4 °C pendant 9 jours. Un changement de couleur visuellement notable de l'étiquette d'emballage est passé du rouge au violet, puis au bleu, au vert et enfin au jaunâtre/marron avec l'augmentation du dénombrement microbien (de 3.80 ± 0.09 à 7.16 ± 0.04 log CFU/g), de TVB-N (de 5.34 ± 0.02 à 36.25 ± 0.14 mg/100 g) et du pH (de 6.93 ± 0.01 à 7.73 ± 0.01) des échantillons de poisson a été détecté.

Dans le dernier objectif, les résultats démontrent efficacement que la détection colorimétrique constitue une méthode fiable pour suivre la fraîcheur des fruits de mer en détectant les gaz TVB-N. La forte corrélation entre les résultats du capteur et les méthodes traditionnelles de chromatographie-gazeuse-spectrométrie de masse (GC-MS) met en lumière son potentiel pour des applications pratiques en matière de sécurité alimentaire. L'efficacité du capteur a été évaluée à travers une série d'expériences impliquant de véritables échantillons de poisson stockés à 4 °C sur une période de 9 jours. Spécifiquement, la transition de couleur du capteur passant du rouge au jaunâtre/marron a été quantitativement liée à la croissance microbienne et aux niveaux de TVB-N. Cette corrélation souligne la capacité du capteur à fournir une surveillance en temps réel et non destructive de la fraîcheur des fruits de mer, améliorant ainsi la sécurité alimentaire et réduisant le gaspillage. L'intégration de ces conclusions soutient l'application potentielle du capteur colorimétrique dans les systèmes d'emballage intelligent, contribuant à une meilleure traçabilité et efficacité dans l'industrie alimentaire.

En résumé, un capteur colorimétrique sûr pour les aliments a été développé, permettant une détection simple, économique, rapide, facile à préparer et visible à l'œil nu des gaz volatils basiques. Cette approche innovante offre une solution pratique pour améliorer la sécurité alimentaire et réduire le gaspillage en fournissant aux consommateurs des signaux visuels clairs concernant la fraîcheur des produits périssables.

Mots-clés : Emballage intelligent, anthocyanines, sûr pour les aliments, indicateur de pH, fraîcheur du poisson.

ABSTRACT

The main goal of this work was to develop a food-safe colorimetric sensor integrated in food packaging as a freshness indicator to provide information regarding food quality using a non-destructive, in situ, and real-time technique. A binder formulation with black rice extract coated on corona treated PET (Polyethylene terephthalate) films were developed.

In the first objective, our aim was to formulate a food-safe ink with the ability of changing color in different pH states. This ink should have two important characteristics: firstly, high adhesive bonding to the coating layer/printable side, and secondly, it should stay intact in the high relative humidity headspace of seafood packages. The study involved designing a food-safe ink formulation that exhibited significant color changes across a pH range (from red to yellowish/brown), demonstrating sensitivity to Total Volatile Base Nitrogen (TVB-N) gases. Key methodologies included corona treatment of PET films to enhance adhesion, thermal treatment to improve ink bonding (adhesion and stability), and various characterization techniques such as water contact angle measurements, FTIR spectroscopy, and UV-Vis spectrophotometry to analyze the ink's properties. The results indicated that the developed films effectively signal fish spoilage through visible color changes, providing a practical solution for monitoring food freshness while adhering to food safety regulations.

In the second objective, the research involved examining effectiveness of the changing color of the food-safe formulated ink in different pH solutions. Various characterization techniques confirmed the effectiveness and stability of the indicator, which demonstrated rapid and sensitive color responses to spoilage-related gases. The films maintained acceptable color stability during storage at 4 °C, with color changes correlating with microbial counts and chemical analyses, confirming their efficacy as freshness indicators. Additionally, mathematical models were integrated to predict spoilage based on experimental data, showing strong correlations between colorimetric responses and TVB-N levels, thus validating the sensor's performance in real-time freshness monitoring.

The developed pH indicators were evaluated by exposing to the real fish samples to assess color response during fish storage under 4 °C for 9 days. A visual noticeable color change in the color of the packaging label from red to purple and then blue to green and finally to yellowish/brown with the increase in the microbial count (from 3.80 ± 0.09 to 7.16 ± 0.04 log CFU/g), total volatile basic

nitrogen (TVB-N) (from 5.34 ± 0.02 to 36.25 ± 0.14 mg/100 g) and pH (from 6.93 ± 0.01 to 7.73 ± 0.01) of the fish samples was detected.

In the last objective, the result effectively showcases colorimetric sensing as a reliable method for monitoring seafood freshness by detecting TVB-N gases. The strong correlation between the sensor's results and traditional gas chromatography-mass spectrometry (GC-MS) methods highlights its potential for practical applications in food safety. The sensor's effectiveness was assessed through a series of experiments involving real fish samples stored at 4 °C over a 9-day period. Specifically, the color transition of the sensor from red to yellowish/brown was quantitatively linked to microbial growth, and TVB-N levels. This correlation underscores the sensor's capability to provide real-time, non-destructive monitoring of seafood freshness, thereby enhancing food safety and reducing waste. The integration of these findings supports the potential application of the colorimetric sensor in intelligent packaging systems, contributing to improved traceability and efficiency in the food industry.

In summary, a food-safe colorimetric sensor was developed which allows for simple, cheap, rapid, easy to prepare and detectable by naked-eye towards volatile basic gases. This innovative approach offers a practical solution for improving food safety and reducing waste by providing consumers with clear visual cues regarding the freshness of perishable products.

Keywords: Intelligent packaging, anthocyanins, food-safe, pH indicator, fish freshness,

TABLE OF CONTENTS

DEDICATION	iii
ACKNOWLEDGEMENTS	iv
RÉSUMÉ.....	vi
ABSTRACT	viii
TABLE OF CONTENTS.....	x
LIST OF TABLES	xvi
LIST OF FIGURES.....	xviii
LISTE OF SYMBOLS AND ABBREVIATIONS	xxiii
LIST OF APPENDICES	xxv
CHAPTER 1 INTRODUCTION	1
Context	1
Objective	3
Plan of dissertation	3
CHAPTER 2 LITERATURE REVIEW	4
2.1 Intelligent food packaging	4
2.1.2 Colorimetric sensors.....	5
2.1.3 Freshness and/or pH Indicators	6
2.1.4 pH-Sensitive Indicator Films: Mechanisms and Stability.....	7
2.1.5 Integration of sensors and indicators.....	11
2.2 Printable Polymeric Films in Food Packaging	12
2.3 Surface modification	13
2.4 Corona treatment (Increasing the surface energy of the substrate)	13
2.5 Surfactant (Decreasing surface energy of adhesive)	15
2.6 Development of Food-Safe coating ink	16

2.6.1 Crosslinking mechanism for developed pH indicator.....	17
2.7 Regulatory and Safety Considerations	17
2.8 Coating process	20
2.8.1 Doctor blade technique.....	20
2.8.2 Adhesion.....	21
2.8.2.1 Adhesion properties.....	21
2.8.2.2 Measurement of Water Contact Angle (WCA) by sessile drop method	21
2.9 Shelf-life monitoring	22
2.9.1 Microbial Activity in Fish Spoilage	22
2.9.2 TVB-N generation.....	22
2.9.3 Methods for Measuring TVB-N	23
2.9.3.1 GC-MS	24
2.9.3.2 Conway Microdiffusion Method.....	24
2.9.4 Microbial growth and TVB-N analysis for shelf-life determination.....	24
2.10 Summary and problem identification	
CHAPTER 3 OBJECTIVES	28
3.1 Specific objectives	28
3.2 Organization of articles	29
CHAPTER 4 ARTICLE 1: CHARACTERIZATION OF A FOOD-SAFE COLORIMETRIC INDICATOR BASED ON BLACK RICE ANTHOCYANIN/PET FILMS FOR VISUAL ANALYSIS OF FISH SPOILAGE	31
4.1 Abstract	33
4.2 Introduction	33
4.3 Materials and Methods	36
4.3.1 Materials.....	36

4.3.2	Senor ink preparation	37
4.3.3	Sensor preparation.....	38
4.4	Characterization of pH indicator	38
4.4.1	Water Contact Angle Measurements (WCA).....	38
4.4.2	Tape test	39
4.4.3	Abrasion Test	39
4.4.4	Fourier-Transform Infrared Spectroscopy (FTIR-ATR).....	39
4.4.5	The spectral characteristics of the ink formulation	39
4.4.6	Color parameters: RGB	40
4.5	Statical analysis	40
4.6	Results and discussions	41
4.6.1	WCA.....	41
4.6.2	Validation of interaction between functional groups for better adhesion properties via FTIR	42
4.6.3	Validation of adhesion: Tape test and Abrasion test.....	44
4.6.4	UV–vis spectra of the ink solution at different pHs and its stability	45
4.6.5	Color response to volatile amines (Ammonia, dimethylamine, and trimethylamine).....	48
4.7	Conclusions	54
4.8	Reference.....	54
CHAPTER 5 ARTICLE 2: ENHANCING SEAFOOD FRESHNESS MONITORING: INTEGRATION COLOR CHANGE OF A FOOD-SAFE ON-PACKAGE COLORIMETRIC SENSOR WITH MATHEMATICAL MODELS, MICROBIOLOGICAL, AND CHEMICAL ANALYSES		62
5.1	Abstract	64

5.2	Introduction	64
5.3	Materials and methods	67
5.3.1	Materials	67
5.3.2	Sensor preparation	68
5.4	Characterization of pH indicators	68
5.4.1	Fourier-Transform Infrared Spectroscopy (FTIR-ATR)	68
5.4.2	TGA	68
5.4.3	Packaging study using RGB	68
5.4.4	Chemical stability and recovery tests	69
5.5	Fish shelf-life monitoring	69
5.5.1	TVB-N content	70
5.5.2	pH measurement	70
5.5.3	Microbial analysis	70
5.6	Mathematical Modeling of fish spoilage based on TVB-N, TVC and Pseudomonas spp experimental data	
5.6.1	Model Evaluation Metrics	72
5.7	Statistical analysis	73
5.8	Results and discussion	73
5.8.1	TGA	73
5.8.2	Application of developed pH-responsive indicators for fish freshness/spoilage monitoring	76
5.8.5	Validation of the pH indicator's efficacy by linking color changes to chemical analysis and microbial growth	86
5.8.5.1	Chemical analysis (TVB-Ns)	86
5.8.5.2	Microbial analysis	87

5.8.6 Correlation of Δ RGB with chemical and microbial analysis	90
5.9 Conclusion and recommendations	92
5.10 Reference.....	94
CHAPTER 6 ARTICLE 3: INTELLIGENT PACKAGING SOLUTIONS FOR FISH AND MEAT PRODUCTS: VOLATILE GAS DETECTION VIA GC-MS, MICROBIAL ANALYSIS AND COLORIMETRIC MONITORING	105
6.1 Abstract	106
6.2 Introduction	107
6.3 Materials and methods	109
6.3.1 Materials.....	110
6.3.2 Sensor preparation.....	110
6.3.3 Freshness monitoring	111
6.3.4 Packaging study using RGB.....	111
6.3.5 Microbial analysis	112
6.3.6 NH_3 and TEA detection using the gas detection tubes.....	112
6.3.6.2 Freshness control in room temperature with gas tube detector	112
6.3.7 GC-MS analysis	113
6.4 Data analysis	115
6.5 Results and discussion.....	115
6.5.1 pH indicator sensitivity towards different TVB-N gases	115
6.5.2 The effect of sensor ink on different food product: fish, meat and chicken breast	117
6.5.3 Rapid Volatile Gas Detection via gas detector tubes: NH_3 and TEA	119
6.5.4 Microbial analysis	121
6.5.5 Method development and performance Assessment for GC-MS.....	122
6.5.6 Gas analytes quantification essays	123

6.5.7 Method validation and Calibration curve.....	124
6.5.8 Quality Control Measures	126
6.5.9 Trend via GC-MS during shelf-life.....	127
6.6 Conclusion.....	130
Limitations/challenges and future work.....	131
6.7 Reference.....	132
CHAPTER 7 GENERAL DISCUSSION	142
CHAPTER 8 CONCLUSION AND RECOMMENDATIONS.....	147
8.1 Conclusion.....	145
8.2 Recommendations	146
REFERENCES	148
APPENDICES.....	162

LIST OF TABLES

Table 2.1 Natural sources of anthocyanins and their applications in various pH indicators [55]...	9
Table 2.2 Summary of Packaging Technologies and Their Applications for Food Spoilage Detection.	11
Table 2.3 Surface energy profiles of commercial films (mN/m) or (dynes/cm) [94, 95].	14
Table 2.4 Provides a concise overview of the regulatory status, safety assessments, and labeling requirements for each main material used in “formulated ink” for direct contact with food products.	19
Table 2.5 shelf-life monitoring for some food products at 4 °C storage condition.....	25
Table 4.1 the ingredients utilized in the production of the ink formulation in this study, along with their corresponding FDA status.....	62
Table 4.2 Analysis of variance of WCA measurements on films. The droplet volume is 2 µl. ..	66
Table 4.3 The mean value of ΔRGB of NH_3 for three distinct pixels for each pH indicator during the time.....	77
Table 5.1 Empirical models for modeling TVB-N, TVC and pseudomonas spp growth.	71
Table 5.2 Measurements for Chemical analysis (TVB-N and pH), microbiological analysis and color change data during fish storage (day).	89
Table 6.1 Measurement of NH_3 and TEA from vials with valve connected to the gas detector tubes for 9 days storage time at 4 °C	121
Table 6.2 The precisions calculated as relative standard deviation (RSD) of QC injections over 6 different days. Since values are under 10% for the targeted analytes, this means that the method is precise.	125
Table 6.3 Identification of detected species using NIST database comparison for scan mode injections.	129

Table A.1 Summary of the ink components and their corresponding design experiments. The selected range highlights the concentrations that were further investigated throughout this research study.....	164
Table B.1 Displays the parameter values derived from models based on TVB-N data obtained from the present study.....	168
Table B.2 Displays the parameter values derived from models based on TVC data obtained from the present study.....	169
Table B.3 Displays the parameter values derived from models based on pseudomonas spp data obtained from the present study.....	171
Table C.1 Limit of detection with (TVB-N gases) at accelerated storage condition.....	178
Table C.2 The measurement data is derived from the ammonia produced during 8 hours of storage at room temperature for various fish sample weights.....	180

LIST OF FIGURES

Figure 2.1 The scheme for intelligent food packaging systems to detect food spoilage [39].	5
Figure 2.2 Materials used in intelligent packaging, fabrication methods of pH indicator based intelligent films and their scope of applications for detecting food freshness or spoilage [55].	7
Figure 2.3 Color changing mechanism of anthocyanin in response to various pH [55].	8
Figure 2.4 Schematic of an industrial corona treater (Enercon Industries Corporation) [97]. The power supply could be a high-frequency generator and a high-voltage output transformer{Burany, 2008 #577}.....	14
Figure 2.5 Wetting of the surface by the paint is highly essential for the uniform coating of the paint on the surface. For paints that do not adequately wet or spread on the surface, drying results in patches remaining adhered to the surface, which eventually peel off over time, as illustrated in (a) and (b), while (c) and (d) highlight the benefits of effective wetting, resulting in a cohesive and durable film [101].	16
Figure 2.6 The TQC Automatic Film Applicator (right side) and solution is spread across substrate using a blade with a small gap between the two (left side).	21
Figure 2.7 Changes in TVB-N and TVC versus the storage time (a) and changes in TVB-N and pH of fish versus the storage time (b) at 4 °C. Sixth day known as the shelf life of fresh fish; 18.2 (mg N/100 g sample), 4.09 (log CFU/g) and 6.67 are the amount of TVB-N, TVC, and pH, respectively[133].	22
Figure 4.1 FTIR-spectra of each component of formulated ink solution.	42
Figure 4.2 FTIR spectra of dried solution ink (INK I-Dried), fabricated colorimetric films with thermal treatment (INK I-165-60) and without thermal treatment (INK-I-NTT) and sealant layer (PET corona treated).	43
Figure 4.3 The color alternation of black rice anthocyanin at various pH.	45

Figure 4.4 UV-vis spectra of solution ink at different pH.	46
Figure 4.5 Sensitivity test for examining the response of pH indicator towards NH ₃ gases, a = 25 μL, b = 10 μL, c = 5 μL of (30-33%) ammonium hydroxide.	48
Figure 4.6 Sensitivity test for examining the response of pH indicator towards DMA, a = 25 μL, b = 10 μL, c = 5 μL of dimethylamine solution.....	49
Figure 4.7 Sensitivity test for examining the response of pH indicator towards TMA, a = 25 μL, b = 10 μL, c = 5 μL of trimethylamine solution.	75
Figure 4.8 RGB results for fabricated colorimetric films with and without thermal treatment over time by exposure to the (30-33%) ammonium hydroxide.....	50
Figure 5.1 TGA thermogram for each component of formulated ink as an ink sensor.	75
Figure 5.2 TGA thermogram for the dried ink solution (at room temperature) on the Petri dish, developed pH indicators that were thermally treated at 165 °C for 5 min (INK I TT) and those that were not heated (INK I NTT).....	74
Figure 5.3 The color parameters, sensitivity and color change outcomes for NTT pH indicators (package headspace) at different pH level for their coatings, were stored at 4°C over 9 days.....	76
Figure 5.4 Illustrates the color change outcomes for pH indicators (container headspace) were stored at 4 °C over 9 days. NTT; colorimetric films without heat treatment. TT; colorimetric films with exposure to heat (165 °C) for specific time (5 min). Fish condition at day 4: acceptable; day 6: marginal; day 9: spoiled.	78
Figure 5.5 The RGB value of TT pH indicators towards 100 μL of diluted NH ₃ under accelerated storage conditions (T = 60 °C for 30 min).	80
Figure 5.6 The RGB value of TT pH indicators towards 100 μL of diluted TMA under accelerated storage conditions (T = 60 °C for 30 min).	80
Figure 5.7 The RGB value of TT pH indicators towards 100 μL of diluted NH ₃ under accelerated storage conditions (T = 60 °C for 30 min).	81

Figure 5.8 The RGB value of TT pH indicators towards 100 μ L from each standard dilutions (mix of components) under accelerated storage conditions (T = 60 °C for 30 min).	82
Figure 5.9 The RGB value of TT pH indicators at specific storage condition (T:40 °C for 30 min, RH~ 55%).	83
Figure 5.10 TVB-N, TVC and Pseudomonas growth versus the storage time at 4 °C.	86
Figure 5.11 Δ RGB versus TVB-N gases (a), TVC (b), and pH (c) during fish storage at 4 °C. Correlation between the onset of an increase in microbial population and TVB-N gas release and sensor response (d).....	89
Figure 6.1 A container with a 900 ml capacity, along with an integrated colorimeter sensor and a connected valve for monitoring the volatile gasses produced during a duration of 8 hours.	113
Figure 6.2 The color parameters from various TVB-N gas dilutions (a: NH ₃ , b: TMA, c: DMA) and the TVB-N gas detection limit (d) in accelerated mode are presented.....	115
Figure 6.3 Packaging trials for different types of food products during 9 days of storage at 4 °C, their color parameters (a, b, c) and pictures (d).	117
Figure 6.4 The color alteration of vials set up with an attached colorimetric sensor contain a homogeneous amount of fish samples, kept for 9 days at 4 °C.	118
Figure 6.5 The TVC and Pseudomonas spp growth for fish samples during storage at 4 °C for 9 days.....	118
Figure 6.6 Calibration curves of individual targeted analytes when spiking on fish (NH ₃ :a) and (TMA: b).....	123
Figure 6.7 Calibration curves of individual targeted analytes when spiking on solvent (NH ₃ :a) and (TMA: b).	123
Figure 6.8 Calibration curves of individual targeted analytes when spiking on fish (MeOH :a) and (EtOH: b).....	124

Figure 6.9 Calibration curves of individual targeted analytes when spiking on solvent (MeOH :a) and (EtOH: b).	124
Figure 6.10 Trends in the signal intensities of targeted analytes over 9-day storage in the fridge (SIM mode acquisition).....	126
Figure 7.1 Spitless injection of a standard mix at 2.5% (w/w) in pure solvent in SIM acquisition mode.	143
Figure 7.2 Zoomed chromatogram showing overlapping of DMA (green) and TMA (yellow) SIM signals when spiking targeted analytes directly onto the real fish sample.	146
Figure A.1 Final samples with proper thermal treatment (165 °C for 5 min) passed the tape test.....	161
Figure A.2 The left side shows the topographic image and the right side the error-signal image of the same spot. (A) Untreated control; (B) 90 °C for 60 min treatment time; (C) 165 °C for 5 min treatment time.....	162
Figure A.3 The left side root-mean-square (RMS) roughness values and right side DMT modulus. (A) Untreated control; (B) 90 °C for 60 min treatment time; (C) 165 °C for 5 min treatment time.....	163
Figure B.1 Different models curve for TVB-N of Pangasius fillets during 4 ° C storage for 9 days.....	171
Figure B.2 Different models curve for TVC of Pangasius fillets during 4 ° C storage for 9 days.....	172
Figure B.3 Different models curve for Pseudomonas spp of Pangasius fillets during 4 ° C storage for 9 days.....	174
Figure B.4 Sensor Response to Different Fish Weights Over Storage Time.....	175
Figure B.5 Sensitivity trials for NTT pH indicators at T= 60 ° C for 30 minutes.....	175
Figure B.6 Sensitivity trials for NTT pH indicators at T= 40 ° C for 30 minutes.....	176
Figure B.7 Traditional method for lag time assumption: $t_0 \sim 2$ day.....	176

Figure B.8 Colour stability of pH indicators after one month; however, the pH indicator with thermal treatment (165–5) stayed intact and its colour did not wipe out (right side).....	178
Figure C.1 The trend shows an increase in ammonia and then decrease it during 8 hours of fish storage at room temperature.....	182
Figure C.2 Trends in the signal intensities of untargeted analytes over 9-day storage in the fridge (scan mode acquisition).....	183
Figure C.3 Zoomed SIM chromatograms of spoiled fish samples allowing for detection of ammonia and TMA.	185
Figure C.4 Zoomed Scan chromatograms of untargeted species identified using NIST database comparison.	186

LIST OF SYMBOLS AND ABBREVIATIONS

ACN - Anthocyanin

BC - Black rice

CA - Citric acid

CFU - Colony form unit

DMA - Dimethylamine

EFSA - European Food Safety Authority

EtOH - ethanol

FDA - U.S. Food and Drug Administration

FTIR - Fourier-Transform Infrared Spectroscopy

GRAS - Generally recognized as safe

H₂O - Water

H₂SO₄ - sulfuric acid

IP - Intelligent Packaging

LDPE - Low-density polyethylene

LOD - Limit of Detection

M - Molar

MgO - magnesium oxide

mL - milliliter

NH₃ - Ammonia

NIST - The National Institute of Standards and Technology

PCA - plate count agar

PEG - Polyethylene glycol

ppm - parts per million

PVOH - Polyvinyl alcohol

SSO -Specific spoilage organisms

TAC - total anthocyanins content

TGA - Thermal gravimetric analysis

TMA - Trimethylamine

TVB-N - Total volatile bases nitrogen

TVC - Total viable bacterial counts

VOCs - Volatile organic compounds

LIST OF APPENDICES

- APPENDIX A ARTICLE 1: CHARACTERIZATION OF A FOOD-SAFE COLORIMETRIC INDICATOR BASED ON BLACK RICE ANTHOCYANIN/PET FILMS FOR VISUAL ANALYSIS OF FISH SPOILAGE
- APPENDIX B ARTICLE 2: ENHANCING SEAFOOD FRESHNESS MONITORING: INTEGRATION COLOR CHANGE OF A FOOD-SAFE ON-PACKAGE COLORIMETRIC SENSOR WITH MATHEMATICAL MODELS, MICROBIOLOGICAL, AND CHEMICAL ANALYSES
- APPENDIX C ARTICLE 3: INTELLIGENT PACKAGING SOLUTIONS FOR FISH AND MEAT PRODUCTS: VOLATILE GAS DETECTION VIA GC-MS, MICROBIAL ANALYSIS AND COLORIMETRIC MONITORING

CHAPTER 1 INTRODUCTION

Context

In 2020, approximately 5 billion pounds of fish and seafood were produced in the United States, with a market value of around 16 billion \$[1]. Fish and seafood are highly perishable products with an estimated shelf-life of 3-14 days, depending on the type and storage conditions. Current analytical techniques for effective quality control regarding the freshness and spoilage of food products; such as GC/MS, high-performance liquid chromatography (HPLC), UV-Vis spectroscopy, and proton nuclear magnetic resonance (^1H NMR), are often costly, time-consuming, and reliant on laboratory settings [2].

In contrast, colorimetric sensors present a viable alternative, offering advantages such as affordability, user-friendliness, rapid response times, and the ability to provide results that can be interpreted with the naked eye. These sensors can be integrated into packaging materials, allowing for real-time monitoring of food quality throughout the supply chain. However, despite the availability of commercial colorimetric sensors, this technology still faces challenges related to low sensitivity due to indirect contact, which complicates installation and practical use by consumers. To enhance their effectiveness, ongoing research is focused on improving the sensitivity and specificity of these sensors, as well as developing user-friendly designs that facilitate widespread adoption in both retail and home settings.

Fish packaging plays a crucial role in maintaining the freshness and quality of seafood products, as fish are highly perishable and susceptible to spoilage [3]. Intelligent packaging can monitor the condition of packaged food or the environment surrounding the food. Intelligent packaging design for monitoring the quality of fish packages incorporates advanced technologies that enhance food safety and freshness throughout the supply chain [4]. Consumer acceptance of intelligent packaging is influenced by awareness and perceived value [5]. Studies indicate that consumers are more likely to trust products with visible freshness indicators [6], enhancing their confidence in food safety [7]. This innovative approach often includes the integration of sensors, indicators, and smart labels that provide real-time information about the condition of the fish [8].

Intelligent packaging that incorporates anthocyanins and food-safe coating inks as pH indicators offers a promising solution for visually monitoring food quality. Anthocyanins, natural pigments

found in various fruits and vegetables, exhibit color changes in response to pH variations, making them effective indicators of food freshness and spoilage [9]. When integrated into food packaging, these pH-sensitive coatings can provide immediate visual cues about the condition of the food, this color change is in response to specific biochemical changes associated with spoilage, allowing consumers and retailers to assess the quality immediately [10].

The use of food-safe inks ensures that the packaging remains non-toxic and suitable for direct contact with food products, enhancing safety while providing an innovative approach to quality monitoring. This combination of intelligent packaging and natural indicators not only promotes sustainability by using natural components instead of synthetic dyes and reducing the food waste by effective quality monitoring [11]. Anthocyanin-based indicators have demonstrated that they can accurately reflect the freshness of seafood and meat products by correlating color changes with the production of spoilage-related compounds [12, 13]. These indicators provide a practical and visually intuitive method for consumers to assess food quality.

Several design of experiments (DOE) considerations should be implemented to enhance the adhesion bonding of water-based coatings based on anthocyanins to non-polar polymer films [14]. Key factors to investigate include the selection of appropriate printable layer and surface treatments for the non-polar substrates, such as corona treatment as a physical and non-toxic approach, which can increase surface energy and improve adhesion [15-17]. Additionally, varying the concentration of anthocyanins in the coating formulation, along with the incorporation of adhesion promoters such as surfactant or crosslinking agents, can be systematically evaluated to optimize the bonding strength. The experimental design should also include assessments of curing conditions, such as temperature and time, to determine their effects on the final adhesion properties [18].

Accurate shelf-life prediction is essential for minimizing food waste and ensuring product quality. Studies have demonstrated that monitoring volatile amine production can effectively predict the shelf-life of seafood and meat products [15, 19]. The integration of colorimetric indicators into packaging can complement traditional methods, providing a dual-function approach to freshness monitoring [12]. There is a notable absence of literature regarding the use of a food-safe colorimetric sensor that remains intact within seafood packaging and can visually indicate the freshness or spoilage of the product.

Objective

The aim of this research is to develop and characterize sensitive colorimetric sensors utilizing natural dye-based pH indicators for detecting TVB-N gases. Additionally, this study seeks to evaluate the performance of the developed colorimetric sensor during the storage of fish and its potential applications in the food packaging industry.

Plan of dissertation

This dissertation comprises of 8 chapters. The following chapters make up this dissertation:

Chapter 1: Introduction

Chapter 2: Literature review

Chapter 3: Objectives and ordering of the articles

Chapter 4 to 6: Reports of three articles

Chapter 7: General discussion

Chapter 8: Conclusion and recommendations

Appendices

CHAPTER 2 LITERATURE REVIEW

2.1 Intelligent food packaging

Seafood products are highly susceptible to spoilage even during short storage time under freezing conditions [20-23]. Quality control of seafood products by techniques including electrochemical devices or analytical tools are time-consuming, destructive, and requires specific instruments and qualified specialists [24]. The limitation of conventional packaging in showing accurate and real time food expiration dates leads to food waste and foodborne diseases [25], as every year, approximately 600 million people worldwide become ill after eating contaminated food [26]. Food spoilage due to biological, chemical, or physical factors can lead to subtle changes that consumers may not easily notice. Even minor alterations in color, texture, or flavor can result in misjudgments about food quality, contributing to unnecessary food waste [27].

Therefore, addressing the existing challenges of food quality and safety is crucial by 1) detecting changes in food products to prevent consumption by consumers; 2) identifying potential health risks; and 3) implementing strategies to minimize or eliminate these issues [28]. Consumers are increasingly demanding innovative packaging technologies that not only prolong the shelf life of food but also facilitate effective communication regarding the freshness status of food products [8].

Packages generally have four basic functions: protection, communication, convenience and containment. Packages assume a protective role associated to external factors such as light, temperature and contaminants. They are also adjustable to the variable food shape and size and considered easy to use. Packages contribute to an improvement in food commercialization and distribution, ensuring its safe delivery and preservation.

Intelligent packaging (IP) emerged with the aim of detecting and monitoring the interaction between the food, the packaging, and the environment [29, 30], informing the consumer about the quality of food throughout the food chain in a non-destructive way, in situ and in real time [31]. IP systems typically incorporate multiple types of sensors, focusing on various parameters such as gas production, humidity, temperature, and microbial growth [32, 33]. IP innovation can monitor various condition changes in the packaged products, including food quality (freshness, spoilage, or ripeness), microbial activity (generation of organic acids, CO₂, volatile nitrogenous substance, or sulfur derivatives), or other properties (transport and storage history)[34, 35].

While the exact number of sensors can vary depending on the specific application and technology used, these systems generally rely on a combination of indicators, data carriers, and sensors to monitor food quality effectively [32, 36, 37]. For instance, sensors that are a sub-group of intelligent packaging can detect volatile gases produced by spoilage of food products especially seafood and meat products, due to defective transportation or improper storage temperature [38]. **Figure 2.1** shows the framework of IP systems for monitoring food safety and quality [39].

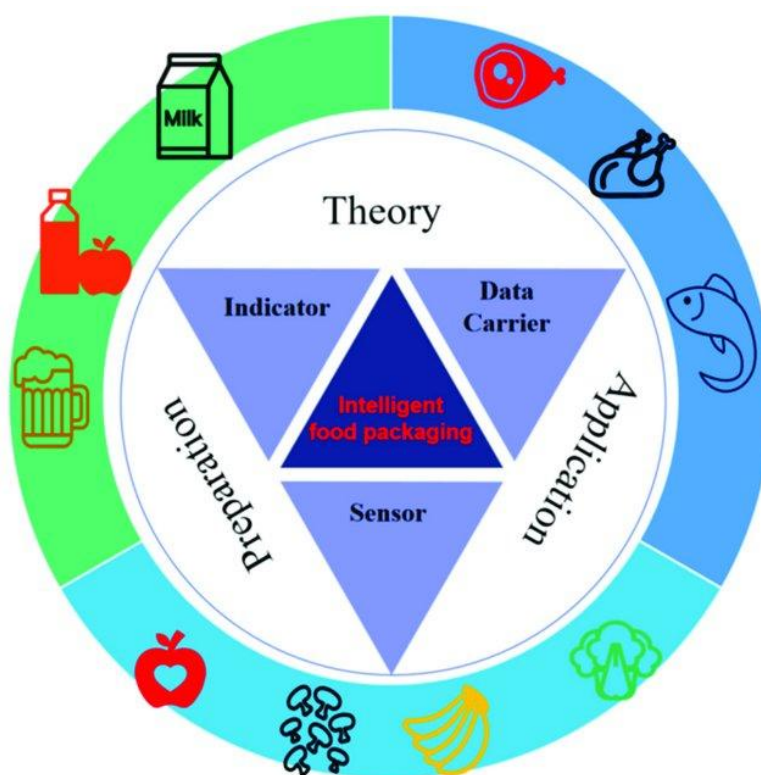


Figure 2.1 The scheme for intelligent food packaging systems to detect food spoilage [39].

2.1.2 Colorimetric sensors

Colorimetric sensors are a subgroup of chemical sensors in intelligent packaging [21, 40]. They are designed to detect specific chemical changes in the environment, often related to the freshness or spoilage of food products [41, 42]. These sensors typically change color in response to certain chemical reactions, providing a visual indication of the quality or safety of the packaged product.

These packaged products are usually containing a detector element that interacts, either with a chemical reaction or physical adsorption, with the preferred analyte, resulting in colorimetric or fluorescent changes on a solid substrate support [41, 43]. Colorimetric sensors are commonly used in applications such as monitoring gas emissions (like TVB-N) or detecting spoilage indicators. These technologies integrate various sensing mechanisms that provide real-time information about the condition of the product.

2.1.3 Freshness and/or pH Indicators

Freshness indicators are a subgroup of direct approaches in intelligent packaging systems [44]. These indicators provide real-time information about the freshness and quality of food products by responding to changes in the environment, such as temperature, humidity, or the presence of specific gases. Recent innovations include the development of pH-sensitive indicators that change color in response to spoilage-related gases, such as TVB-N [15, 45-49]. These indicators can be incorporated into packaging materials, allowing consumers and retailers to visually assess the freshness of seafood products immediately [9, 15, 18, 50, 51]. TVB-N comprises amines trimethylamine (TMA), ammonia (NH_3), and dimethylamine (DMA) [52]. Among TVB-Ns, TMA is produced immediately after the harvest of fish, and the concentration is responsible for the characteristic “fishy” odor [53]. An important index of seafood spoilage is the TVB-N content, which has a direct correlation with the sensory quality of fish, thereby serving as a vital indicator for quality control within the seafood industry [51].

Freshness indicators provide information regarding food quality by assessing microbial activity and/or chemical alterations in food products [54]. Freshness indicators represent a modern approach to food quality assessment that aligns with the demands of today's fast-paced food industry. However, more accurate determination of the shelf life of fish products is essential [53]. Various pH indicators are currently used to detect chemical changes due to microbial growth or food spoilage, applied through techniques such as electrospinning, casting, and immobilization that shown in **Figure 2.2** [55].

A visual pH indicator produced by immobilization technique includes pH-responsive dyes and functional groups which are immobilized on a supporting matrix. The functional quality of a pH indicator primarily depends on the covalently bonded dyes applied to their matrix [23, 56].

For the immobilization of the pH sensing dyes, many solid-based platforms, including glass beads, polymeric materials, hydrogel polymeric membranes, sol–gel matrices are used [30]. Natural and synthetic polymers, including nanocellulose, chitosan, starch, and low-density polyethylene, generally present are applied as structural composites to carry and stabilize the pH indicator dye [57, 58]. PET is an ideal printable layer for food packaging due to its excellent barrier properties, durability, and transparency, which enhance product visibility. Additionally, PET is lightweight, recyclable, and resistant to chemicals, making it a cost-effective and sustainable choice for preserving food quality and safety.

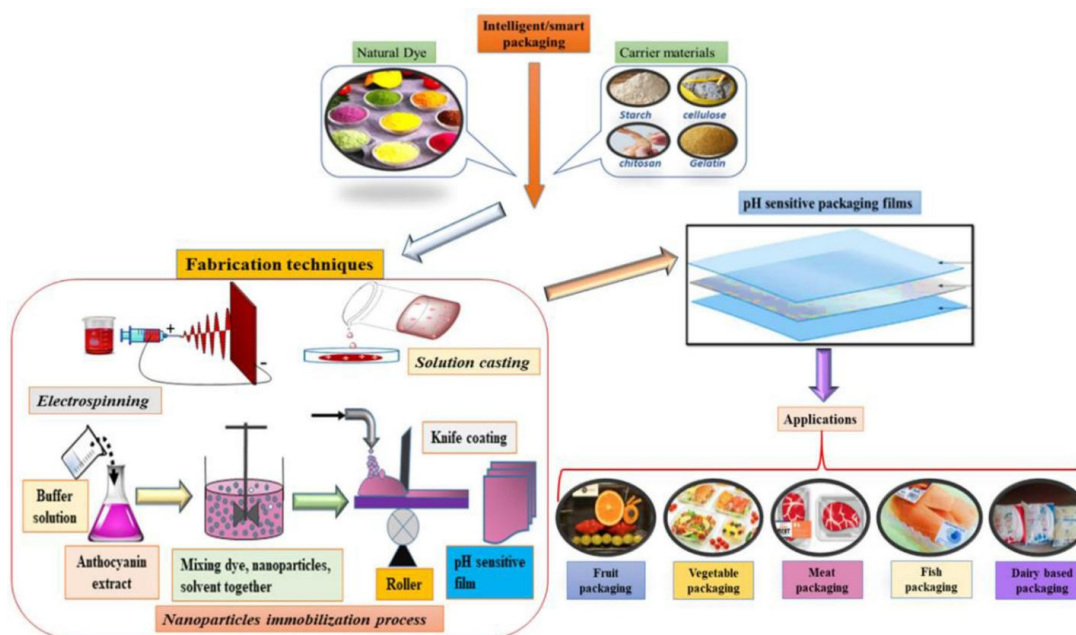


Figure 2.2 Materials used in intelligent packaging, fabrication methods of pH indicator based intelligent films and their scope of applications for detecting food freshness or spoilage [55].

2.1.4 pH-sensitive indicator films: mechanisms and stability

pH-sensitive indicator films change colors in response to variations in the pH of perishable foods, allowing consumers to monitor product quality without opening the package. The pH of food can

change due to microbial decomposition of carbohydrates, fats, and proteins, which is prevalent in fish and meat spoilage, leading to the production of various volatile compounds.

Color changes in anthocyanin-based indicator films are attributed to alterations in the chemical structure of anthocyanins at different pH levels. The color and structure stability of anthocyanins are dependent on a combination of various environmental (including storage conditions) and processing factors including the structure of anthocyanins, oxygen, temperature, light, pH and water activity [69].

Anthocyanins exhibit a reversible color change across different pH levels, ranging from red at pH 2 to bluish-green at pH 9 [70]. The flavylium cation structure of anthocyanins is responsible for this behavior; at low pH, the cyanidin molecule is protonated, forming a positive ion. As pH increases, the molecules become deprotonated, and at high pH, they form a negative ion. Anthocyanins are more stable in acidic environments than in alkaline ones [71].

In mildly acidic (pH 4–5) conditions, the red flavylium cationic state converts to gray carbinol pseudo-bases due to nucleophilic reactions with water. At neutral pH (pH 6–8), these compounds transition to quinoid anhydrous bases, exhibiting a violet color. In highly alkaline environments, the indicator shifts to yellow chalcones, establishing a dynamic equilibrium among these substances (**Figure 2.3**) [55, 72, 73].

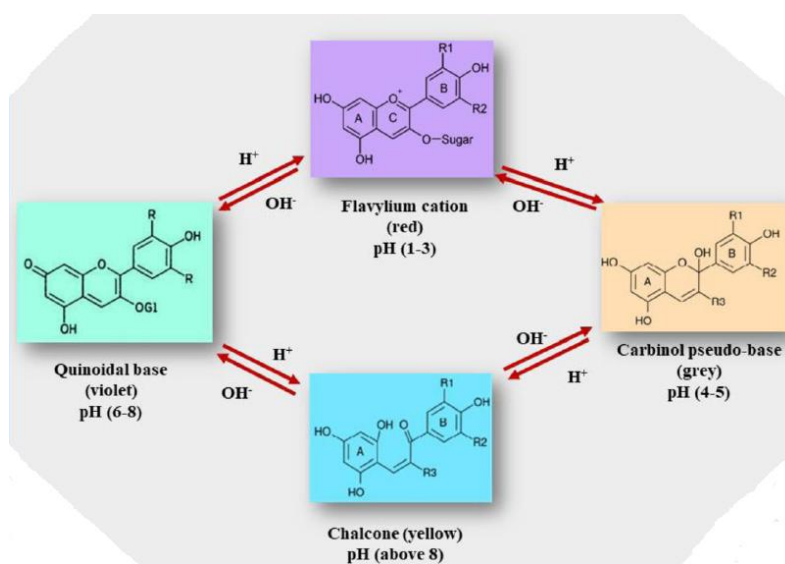


Figure 2.3 Color changing mechanism of anthocyanin in response to various pH [55].

Anthocyanins are water-soluble pigments belonging to the flavonoid class, primarily found in various fruits, vegetables, and flowers, imparting vibrant red, purple, and blue hues [59]. Common types of anthocyanins include cyanidin, delphinidin, malvidin, peonidin, and petunidin, each differing in their chemical structure and color properties [60]. In food packaging, anthocyanins serve as natural colorants and antioxidants, offering a dual function of enhancing visual appeal while providing protection against oxidative degradation [61]. Their ability to change color in response to pH variations makes them valuable as pH indicators in packaging, signaling the freshness and quality of food products. Additionally, anthocyanins offer several advantages, including being natural, non-toxic, biodegradable, and possessing additional health benefits such as antioxidant and antimicrobial properties, making them a promising alternative to synthetic additives in the food industry [62, 63]. **Table 2.1** shows natural sources of anthocyanins and their applications in various pH indicators.

The pH indicator mechanism involves microbial protein spoilage, which generates high levels of TVB-N and biogenic amines. These compounds progressively increase the pH in the packaging headspace, triggering a noticeable color change in the pH-sensitive dye immobilized within the polymer film.

Table 2.1 Natural sources of anthocyanins and their applications in various pH indicators [55].

Type of anthocyanins	Matrix	pH indicator applications	Reference
Red cabbage (Brassica oleraceae)	Bacterial cellulose nanofibers	Applied in cheap and non-destructive smart food packaging to evaluate the quality or spoilage of perishable food products	[64]

Type of anthocyanins	Matrix	pH indicator applications	Reference (Continued)
Black carrot	Bacterial nanocellulose	Used to determine the level of spoilage of rainbow trout and common carp fish fillet at refrigeration storage	[58]
Blueberry/Blackberry pomace extracts	chitosan	Used in antioxidant packaging of fish/meat and evaluated the freshness of food sample based on the color changes of indicator films	[65]
purple tomato	chitosan	Detection of spoilage in milk and fish	[66]
Alizarin (halochromic dye)	Cellulose acetate nanofiber	Used to determine the level and the upper acceptability limit of spoilage	[67]
blueberry powder	corn starch and glycerol	need more research for correlation color changes to the shelf life	[68]

2.1.5 Integration of sensors and indicators

Integrating sensors and indicators into packaging provides critical information about product conditions, enabling timely interventions to prevent spoilage [9, 74, 75]. Colorimetric sensors using anthocyanins effectively detect pH changes in packaging environment related to spoilage through visible color shifts [76]. These sensors can identify specific spoilage-related compounds, such as ammonia and trimethylamine, produced during the microbial degradation of seafood [33, 77]. By monitoring real-time pH variations, these innovative sensors enhance food safety and assist consumers and retailers in making informed decisions about freshness [78]. Utilizing pH-sensitive dyes, the packaging visually signals changes in response to spoilage gases, helping reduce food waste [79, 80] and ensure high-quality products like fish and meat reach consumers [34, 81]. **Table 2.2** shows a summary of packaging technologies and their applications for food spoilage detection.

Table 2.2 Summary of Packaging Technologies and Their Applications for Food Spoilage Detection.

Type of Package	Objective/Purpose	Type of Food	Reference
Metalloporphyrin-based coating	Detection of volatile amines (TMA, TEA, DMA)	Fish	[82]
Colorimetric dye-based indicator	Track increase in volatile amines as an indicator of fish spoilage	Fish	[83, 84]
Polyaniline film	Respond to pH increase due to TVBN accumulation	Fish and poultry meat	[85]

Type of Package	Objective/Purpose	Type of Food	Reference (Continued)
Methyl red/cellulose membrane	Respond to basic volatile amines released during fish spoilage	Fish	[86]
Curcumin/bacterial cellulose membrane	Respond to basic volatile amines released during fish spoilage	Fish	[87]
Chitosan and corn starch film	Colorimetric detection of fish spoilage using red cabbage	Fish	[88]
LDPE film containing the pH sensitive dye bromophenol blue (BPB)	Respond to pH increase due to TVBN accumulation	Fish	[89]
Chitosan matrix with purple tomato	Colorimetric sensor for spoilage detection of fish and milk	Fish and milk	[90]

2.2 Printable Polymeric Films in Food Packaging

In the context of developing colorimetric sensors for food packaging, printable polymeric films, such as PET, offer significant advantages. PET is widely used in food packaging due to its excellent barrier properties [15], mechanical strength [9], and transparency. PET films provide effective protection against oxygen and moisture [91], which are critical factors in preserving the quality of perishable food items, including seafood [8]. PET films coated with anthocyanins, have shown promise as effective freshness indicators [18]. These films not only provide visual cues about

spoilage but also maintain their integrity and functionality over storage periods. The compatibility of PET with various coatings and inks is essential for the development of intelligent packaging solutions. The surface properties of PET can be modified to enhance adhesion and wettability, which are crucial for the effective application of colorimetric indicators and other sensors.

2.3 Surface modification

Polymers are valued for their diverse physical, chemical, and mechanical properties, affordability, and ease of synthesis. However, their surfaces often lack the necessary characteristics for specific applications, limiting their use. Characterizing and modifying polymer surfaces is essential for the effective performance of composite materials, influencing properties such as adhesion, wettability, surface roughness, and chemical stability. These modifications are crucial for applications in decorative coatings, protective films, thin film technologies, and biomaterials. Consequently, surface modification techniques, particularly corona treatment, have become vital in transforming inexpensive polymers into high-value products [92].

Bond strength refers to a permanent chemical attachment formed when the adhesive wets the substrate. Full wetting occurs when the coating surface energy is equal to or lower than the substrate's surface energy. This can be achieved by increasing the substrate's surface energy or using a low surface energy adhesive [93].

2.4 Corona treatment (Increasing the surface energy of the substrate)

PET, being a non-polar polymer, has low surface energy, which can lead to poor adhesion and wettability when applying inks (especially water-based), coatings, or adhesives. Corona treatment involves exposing the PET surface to a high-voltage electrical discharge, which generates a corona discharge that modifies the surface chemistry (schematically shown in **Figure 2.4**). This treatment increases the surface energy of PET by introducing polar functional groups, such as hydroxyl and carboxyl groups, thereby improving its wettability and adhesion characteristics. As a result, corona-treated PET exhibits better ink adhesion, improved print quality, and enhanced bonding with coatings and adhesives. This process is widely utilized in various industries, including packaging, labeling, and textile applications, to ensure optimal performance of PET materials [93]. The surface energy of PET films typically ranges between 42-47 mN/m before corona treatment. After

treatment, it can increase to 50 mN/m or higher [94, 95]. The exact treatment level may vary based on specific applications, the condition of the substrate, and the desired adhesive or coating characteristics [96].

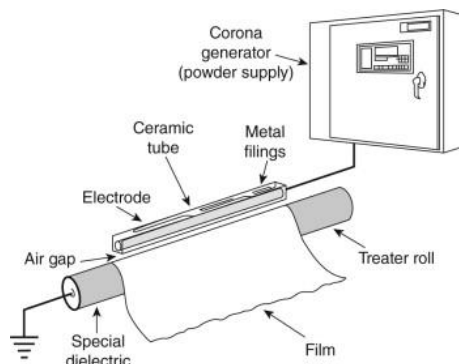


Figure 2.4 Schematic of an industrial corona treater (Enercon Industries Corporation) [97]. The power supply could be a high-frequency generator and a high-voltage output transformer [98].

Table 2.3 Surface energy profiles of commercial films (mN/m) or (dynes/cm) [94, 95].

Polymers	Before surface treatments	After surface treatments
PE (Polyethylene)	27 - 33	NA
PP (Polypropylene)	26 - 30	NA
PS (Polystyrene)	37 - 42	NA
Low Density Polyethylene (LDPE)	32	38-43
High Density Polyethylene (HDPE)	32	38-43
Oriented Polypropylene (OPP)	30	43
Polyethylene terephthalate (PET)	42 - 47	50+

2.5 Surfactant (decreasing surface energy of adhesive)

Surfactants are low molecular weight compounds that lower the surface tension (or interfacial tension) between two liquids, between a gas and a liquid, or between a liquid and a solid. Surfactants are amphiphilic substances, which means that they contain two opposing parts hydrophilic and hydrophobic. Surfactants can be used to enhance print quality, color acceptance, uniformity, and compatibility, especially for water-based inks whose surface tension is high. The value of surface tension for water-based inks is often close to the surface tension of water, which is 72 dynes/cm [99]. An effective ink sensor can be coated if the surface tension of the ink is less than the substrate's surface energy [100]. By doing so, adhesion onto non-porous substrates such as polymers could enhance. The importance of surface wetting in achieving a uniform paint coating is illustrated in **Figure 2.5**.

It is obvious that the choice of surfactants in ink chemistry should take into consideration their negative effects on the ink coating. In this respect, ionic surfactants which normally lead to foam stabilizing conditions are generally avoided in ink formulations. Adding a non-ionic surfactant to water-based ink offers several advantages over ionic surfactants, especially when dealing with substrates that have low surface energy [101]. Non-ionic surfactants improve wetting and spreading on low-energy surfaces without causing charge-related issues. They enhance the ink's adhesion and stability, reducing the risk of flocculation or coagulation that can occur with ionic surfactants [102]. Additionally, non-ionic surfactants are less likely to interact negatively with the ink's components, maintaining the desired properties of the ink while improving its performance on challenging substrates. This results in better print quality, durability, and overall effectiveness of the ink.

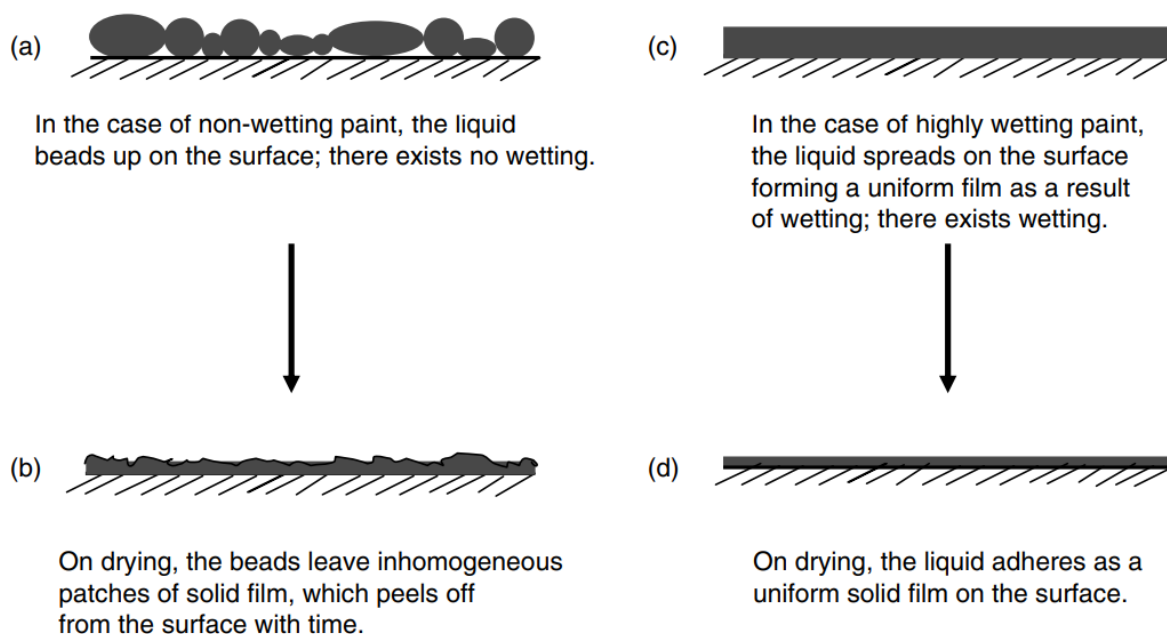


Figure 2.5 Wetting of the surface by the paint is highly essential for the uniform coating of the paint on the surface. For paints that do not adequately wet or spread on the surface, drying results in patches remaining adhered to the surface, which eventually peel off over time, as illustrated in (a) and (b), while (c) and (d) highlight the benefits of effective wetting, resulting in a cohesive and durable film [102].

2.6 Development of food-safe coating ink

Ink formulation could consist of many parts such as colorant (dye), aqueous agents (aqueous vehicle such as water, cosolvents, additives), surfactant (for reducing surface tension), fixing agents for change in the solubility or stability of the colorant and sets the dye in place and strong acid (fully ionized in water) to adjust the pH of fixer fluid composition and used for extraction of anthocyanins as the colorant of ink sensor. Several non-ionic surfactants are considered safe for use in food contact materials, such as Tweens (polysorbates)[103] and Spans (sorbitan esters)[103]. When selecting a non-ionic surfactant, it is crucial to ensure compliance with food safety regulations and suitability for the intended use.

2.6.1 Crosslinking mechanism for developed pH indicator

The reaction between PVOH (polyvinyl alcohol), citric acid, and PEG (polyethylene glycol) involves esterification, a chemical process where hydroxyl groups (-OH) from PVOH and PEG react with carboxylic acid groups (-COOH) from citric acid to form ester bonds (-COO-) and water as a byproduct [104].

To achieve effective crosslinking, it is crucial to remove the water generated during the reaction, as its presence can shift the equilibrium back toward the reactants and hinder the formation of stable crosslinked networks [105]. The removal of water ensures the reaction proceeds efficiently, resulting in a robust, interconnected polymer matrix where PVOH forms ester linkages with citric acid, and PEG may interact with PVOH through hydrogen bonding or additional esterification. Therefore, the process combines chemical crosslinking through esterification of citric acid and PVOH with thermal crosslinking, as heat facilitates the reaction and removes water. This crosslinked structure enhances the material's mechanical and thermal properties [105].

The recommended temperature for removing water during the reaction between citric acid and PVOH typically ranges between 120 °C and 160 °C. This temperature range facilitates efficient water evaporation and promotes crosslinking by driving the esterification reaction forward. The exact temperature may vary depending on the specific setup and materials used [106].

In one study, the effect of crosslinking duration was investigated. It was observed that extending the exposure time of samples to 150 °C enhanced their thermal stability due to improved crosslink density. However, further prolongation of the crosslinking time led to a decline in mechanical properties, likely attributed to thermal degradation of the polymer matrix or excessive crosslinking [107].

On the other hand, extending the duration of crosslinking by exposing samples to elevated temperatures can lead to the degradation of anthocyanins present in the coating [108]. Thermal degradation not only diminishes the visual quality of the coating but also adversely affects the efficiency and functionality of pH indicators, as anthocyanins, essential for accurate colorimetric detection, are highly sensitive to heat-induced structural breakdown [109].

2.7 Regulatory and safety considerations

The implementation of intelligent packaging solutions must comply with food safety regulations, which vary by region. Regulatory bodies require that new packaging technologies demonstrate safety and efficacy before market approval [110].

Various industry standards and guidelines, such as those from the FDA, European Food Safety Authority (EFSA), and other regulatory agencies, provide frameworks for the safe use of ingredients in food packaging. These regulatory bodies require that all ingredients in formulations intended for human consumption or medical use are safe and free from harmful levels of impurities. Each of the components (e.g. PEG) used in this “formulated ink” may contain impurities depending on the manufacturing process, that can have adverse effect. For formulated ink each component should have pharmaceutical grade or food grade. The percentage of contaminants and impurities in each component should be determined and documented. This is essential for ensuring safety and compliance with regulatory standards.

Another aspect is “Biodegradability and Environmental Impact”. For example, PVOH is considered biodegradable under certain conditions, which is an advantage for food packaging applications. However, the environmental impact of its degradation products is also evaluated to ensure safety.

In the European Union, PVOH is regulated under the Framework Regulation (EC) No.1935/2004, which ensures that materials intended to have contact with food do not transfer constituents to food in quantities that could endanger human health.

Regulatory authorities require migration studies to evaluate the possible transmission of substances from the packaging to food. These studies simulate real-life conditions by exposing the food contact material to food simulants under controlled temperature and time, allowing researchers to measure the amount of specific substances that migrate into the simulant. The results are then compared against established migration limits set by regulatory authorities (such as FDA or EFSA) to ensure that any transferred substances do not pose a risk to human health. Such studies are critical for compliance with food safety regulations, ensuring that packaging materials do not contaminate food products [111]. Here in this context, these studies assess the safety of PVOH, PEG, CA, BC, and additives in food applications and assure adherence to prescribed limits. The **Table 2.4** summarizes several crucial regulatory and consideration points for "formulated ink" ingredients. For example, for anthocyanins extracted from edible fruits and vegetables by aqueous processes, changes in composition would not be expected. Anthocyanins are authorised as food additives in

the EU with a total migration limit of 2.5 mg/kg bw/day for anthocyanins from grape skin (as an example). The EU specifications do not indicate which fruits or vegetables can be used to obtain the food additive anthocyanins [112]. However, there is still unanswered questions about possible synergistic interactions of different phenolic compounds (the mix of anthocyanins with each other or with other compounds) [113].

Table 2.4 Provides a concise overview of the regulatory status, safety assessments, and labeling requirements for each main material used in “formulated ink” for direct contact with food products.

Material	Regulatory status	Safety assessments	Labeling requirements
Polyvinyl alcohol (PVOH)	Food-safe by the FDA for food contact applications; regulated under EC No.1935/2004 in the EU[114].	Toxicological evaluations confirm safety; migration studies assess potential transfer to food.	Must comply with specific labeling requirements indicating suitability for food contact.
Citric acid (CA)	Food-safe by the FDA; approved food additive (E330) under EC No.1333/2008 in the EU[114].	Extensive evaluations confirm safety; acceptable daily intake (ADI) of "not specified" by JECFA[115].	Must list as an ingredient in food products.
Anthocyanins	Food-safe by the FDA; approved food additive (E163) under EC No.1333/2008 in the EU[114, 116].	Evaluated for safety with low toxicity; potential health benefits noted; assessed by EFSA.	Must list in ingredient declaration; specific labeling may be required for colorants.

Material	Regulatory status	Safety assessments	Labeling requirements (Continued)
Polyethylene glycol (PEG)	Food-safe for specific uses by the FDA; regulated under EC No.1333/2008 in the EU[114].	Evaluated for safety with low toxicity; acceptable daily intake (ADI) varies by molecular weight and use.	Must comply with labeling regulations indicating presence as an ingredient.

2.8 Coating process

Coating is a process in which one or several layers of material are placed on the substrate's surface. Different coating techniques are now available to address an overall demand for high-quality coating materials on final products while maintaining economically feasible productivity levels. These techniques are Immersion/dip coating, knife or blade coating, transfer coating, roll coating, gravure or engraved roll coating, screen coating, Slot die or extrusion coating, curtain coating, powder coating, spray coating, etc [117].

2.8.1 Doctor blade technique

The doctor blade technique is a lab scale process of flexography printing. Different amount of final solution can be coated on machine direction of corona treated PET. There is a small gap that determines how much solution can get through. Then liquid media is efficiently spread over the substrate. Then, the final thickness is a fraction of the gap between the substrate and the blade as **Figure 2.6** depicts the doctor blade technique. The speed of blade and rod number can be selected by different trials and errors to see, which can load more ink through each passage with homogenous finishing. Viscoelastic properties of the liquid media and the speed of coating could influence the wet film's final thickness [117]. Doctor blading cannot offer the nanoscale uniformity or extremely thin films that spin coating can. However, the scalability, versatility, and simplicity of this technique make it perfect for industrial use [118].

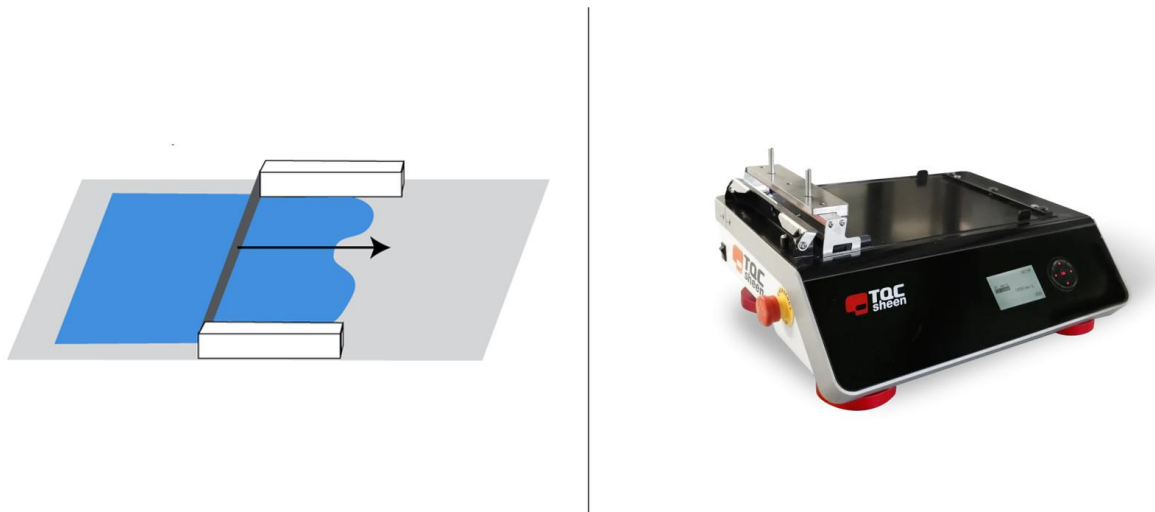


Figure 2.6 The automatic film applicator (right side) and solution is spread across substrate using a blade with a small gap between the two (left side).

2.8.2 Adhesion

2.8.2.1 Adhesion properties

For the initial trials, we selected polymer films as substrates for the colorimetric platform based on their availability, sustainability, and desirable properties such as a high-water barrier, transparency, printability, and mechanical strength. We then evaluated the substrate's ability to adhere to inks.

2.8.2.2 Measurement of Water Contact Angle (WCA) by sessile drop method

Wetting is the ability of liquids to form interfaces with solid surfaces and highly depends on the polymer layer's surface energy. To determine the degree of wetting, the contact angle (θ) formed between the liquid and the solid surface is measured. The sessile drop contact angle measurement is a valuable and reliable method for surface energy determination. The smaller the contact angle and the smaller the surface tension, the greater the degree of wetting. The effect of the corona treatment on surface energy can be evaluated using contact angle measurements conducted by the sessile drop method [119]. The determination of the static contact angle, at the three-phase line of contact relies on the fitting of the drop profile, often using the Young-Laplace equation [120]. Young's equation defines the relationship between a static contact angle and surface energy forces, presented in Equation (2.1), from the interfacial tensions where Y_{sv} = solid-vapor interaction, Y_{sL} = solid-liquid interaction, and Y_{LV} = liquid-vapor interaction [117, 121, 122] .

$$Y_{sv} = Y_{sL} + Y_{Lv} \cos\theta \quad (2.1)$$

After this experiment, we conducted the “Tape test”, which is a simple and accessible method with abrasion tests (dry and sponge tests) to assess the efficiency of the coating's adhesion bonds.

2.9 Shelf-life monitoring

2.9.1 Microbial Activity in Fish Spoilage

Microbial activity plays a crucial role in the spoilage of seafood, with specific bacteria contributing to the production of TVB-N gases. Generally, 7 log₁₀ CFU/g is considered as the higher acceptability limit of fish spoilage. However, standards often use a lower total viable count for safety [123]. However, the level of specific spoilage organisms (SSO) can effectively indicate the remaining shelf life of a product when SSO are significant [124]. *Pseudomonas* spp. is among the most significant spoilage organisms in fish, thriving in refrigerated conditions and producing various spoilage-related compounds, including TMA and ammonia [15, 75, 124]. The colony morphology of this microorganism is “light blue transparent colonies”[125]. The TVC of bacteria is often used as an indicator of microbial load and can correlate with the levels of TVB-N in fish products [46, 126].

2.9.2 TVB-N generation

TVB-N level of 25, 30 and 35 mg N/100 g have been proposed as a rejection limit for fish products and critical TVB-N level of 25 mg/100 g was established for fish spoilage initiation [127]. There was reported that within the first 7 days, the values of TVB-N were lower than 25 mg N/100 g being the implication of the overall acceptability of samples. Describing the exact spoilage threshold could be challenging since it can vary depending on several factors including catch season, catch maturity, geographical origin, species, age and gender of the fish [53, 58, 128].

In one study a halochromic sensor of cellulose acetate nanofibers and alizarin for monitoring real-time fish spoilage was developed [128]. **Figure 2.7** (a) shows that microbial growth and TVB-N rise while fish is stored in the fridge, which is in line with reviews of the literature [56, 129-131]. **Figure 2.7** (b) illustrates the rise in TVB-N and pH during fish storage. The amount of TVB-N reached 22.4 mg N/100 g flesh on the 12th day; at this stage, although it does not exceed from the limit of acceptability, the fish show signs of spoilage and the flesh is soft and watery with an unpleasant smell. The pH of fresh fish was 6.3, and it reached 6.67 after 6 days and 6.94 after 12

days; this correlated with the amount of TVB-N. However, a non-significant decrease in the pH of the fish was observed on the fourth day. The increase in pH value after the sixth day reflected the production of TVB-N from bacterial activity [67].

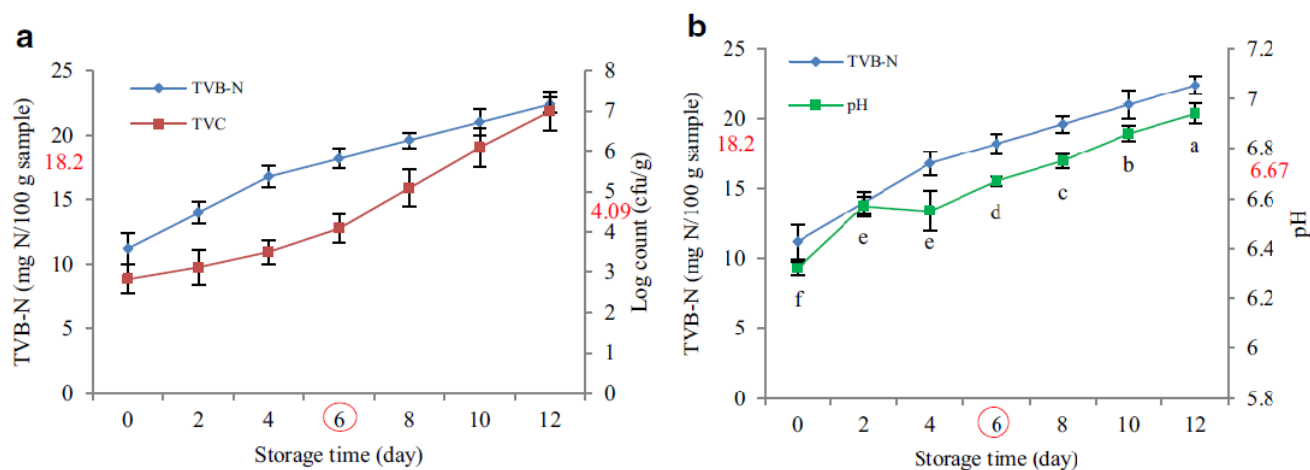


Figure 2.7 Changes in TVB-N and TVC versus the storage time (a) and changes in TVB-N and pH of fish versus the storage time (b) at 4 °C. Sixth day known as the shelf life of fresh fish; 18.2 (mg N/100 g sample), 4.09 (log CFU/g) and 6.67 are the amount of TVB-N, TVC, and pH, respectively [128].

2.9.3 Methods for Measuring TVB-N

Several methods are used for measuring TVB-N. These include the Kjeldahl method [132], the steam distillation method [133], Conway microdiffusion method [134], Ion chromatography method [135], and GC-MS [136].

The Kjeldahl method is a traditional approach that quantifies nitrogen content in a sample, which can be correlated to TVB-N levels. Its advantage lies in its ability to provide a comprehensive nitrogen analysis; however, it is time-consuming and requires hazardous chemicals. The steam distillation method is another widely used technique that involves distilling volatile bases from the sample and measuring the nitrogen content in the distillate. This method is relatively straightforward and provides quick results, but it may not differentiate between various nitrogenous compounds effectively. Ion chromatography, while less common for TVB-N measurement, offers the advantage of high sensitivity and the ability to analyze multiple ions simultaneously. However,

it requires specialized equipment and can be more expensive. Both GC-MS and the Conway microdiffusion method have their advantages and limitations. GC-MS provides high sensitivity and detailed chemical analysis, making it ideal for research applications and in-depth studies of spoilage mechanisms. In contrast, the Conway method offers a more accessible and straightforward approach for routine quality control, although it may not provide the same level of detail. Each method has its own strengths and limitations, making the choice dependent on the specific analytical needs and resources available.

2.9.3.1 GC-MS method

GC-MS is a powerful analytical technique widely used for the quantification of volatile compounds, including TVB-N in seafood. This method offers high sensitivity and specificity, allowing for the accurate detection of low concentrations of spoilage-related gases [137-139]. In GC-MS, the sample is vaporized and separated into its components in the gas chromatography phase, followed by identification and quantification in the mass spectrometry phase. The advantages of GC-MS include its ability to analyze complex mixtures and provide detailed information about the chemical composition of volatile amines. Studies have shown that GC-MS can effectively quantify TMA and other amines in fish samples, providing a reliable assessment of freshness [51].

2.9.3.2 Conway Microdiffusion Method

The Conway microdiffusion method is a titration technique used for quantifying TVB-N in fish and other seafood products [140, 141]. This method involves the diffusion of volatile bases from a sample into a receiving solution, where they can be quantified. The sample is placed in a sealed chamber, and the volatile amines diffuse into a solution containing a known concentration of acid, which reacts with the amines to form a measurable compound [142]. The Conway method is relatively simple and cost-effective, making it suitable for routine analysis in food laboratories. However, it may lack the sensitivity and specificity of more advanced techniques like GC-MS. Nonetheless, it remains a valuable tool for assessing seafood freshness, particularly in settings where access to sophisticated instrumentation is limited [140].

2.9.4 Microbial growth and TVB-N analysis for shelf-life determination

Research has demonstrated a strong correlation between the growth of *Pseudomonas* spp. and the accumulation of TVB-N in fish. As microbial populations increase, the degradation of fish proteins

leads to the production of volatile amines, resulting in higher TVB-N levels [19]. Monitoring TVC can provide valuable insights into the spoilage process, as higher bacterial counts typically indicate a greater likelihood of elevated TVB-N concentrations as some data is available in **Table 2.5**.

Understanding the relationship between microbial activity and TVB-N production is essential for developing effective monitoring strategies in the seafood industry. By tracking both TVC and TVB-N levels, producers can implement timely interventions to maintain product quality and safety. The shelf life of fishery products based on TVB-N at a storage temperature of 4 °C varies among different products.

The threshold for TVB-N indicating spoilage typically occurs when levels reach around 20-30 mg N/100 g, depending on the specific type of fish or seafood. Therefore, the shelf life at 4 °C generally ranges from 6 to 9 days for various fishery products before they reach unacceptable TVB-N levels.

Table 2.5 shelf-life monitoring for some food products at 4 °C storage condition.

Type of product	TVB-N (mg N/100 g)	Microbial analysais log (CFU/g)		shelf life (days)	Reference
		TVC	<i>Pseudomonas spp</i>		
Haddock	NA	5.8	3.5	8	[143]
rainbow trout	25>	NA	NA	7–9	[144]
skinless chicken breast	18	NA	NA	6.12	[145]
Shrimp	27.81	NA	6.53	7	[127]
Minced chicken	<10	NA	9.08	7	[127]
Atlantic Cod	NA	7	NA	2	[146]
Shrimp	26.17	6	NA	8	[147]

Type of product	TVB-N (mg N/100 g)	Microbial analysais log (CFU/g)		shelf life (days)	Reference (Continued)
		TVC	<i>Pseudomonas</i> <i>spp</i>		
Silver carp	20	NA		5.62	[129]
Indonesian Fish (O. gouramy)	39.74>	NA		7	[148]
Tilapia	22	NA		6.80	[125]
NA: not available					

2.10 Summary and problem identification

While the use of synthetic colorants in food monitoring is well-documented, there is a notable lack of extensive studies on natural colorants, particularly those derived from sources such as anthocyanins. The limited studies on anthocyanins, may stem from challenges such as their thermal and pH sensitivity, which complicate their stability and application in food systems. Additionally, synthetic colorants have historically dominated the market due to their cost-effectiveness, ease of production, and consistent performance. This gap highlights the need for further investigation into various natural sources and their efficacy as pH indicators in diverse food products. Additionally, the current literature does not adequately address consumer perception and acceptance of natural colorant-based indicators in food packaging, which is crucial for their market adoption and commercialization.

Another significant challenge arises from the inherent properties of natural dyes. These dyes are predominantly water-based, making them susceptible to being washed away from polymeric substrates when in direct contact with high-humidity food packaging, such as fish. Consequently, they may no longer be functional as colorimetric sensors. Furthermore, natural colorants can degrade during preparation processes, such as creating masterbatches or mixing with other resins for colorimetric film production using techniques like extrusion, where the temperature and the residence time of anthocyanins are prolonged. This degradation not only affects the performance of the indicators but also increases production costs.

To address these challenges, we propose several approaches. Firstly, developing pH indicators using eco-friendly materials derived from food-safe sources can significantly reduce potential health risks associated with synthetic colorants. This shift not only enhances safety and non-toxicity but also aligns with the growing consumer demand for environmentally conscious products, thereby improving overall market appeal. Using pH indicators with natural colorants in direct contact with food products offers additional benefits. These methods enhance the responsiveness and sensitivity of the indicators to pH changes, providing more accurate monitoring of freshness and spoilage in food products. Moreover, these approaches can leverage readily available natural colorants, potentially reducing production costs.

To mitigate the issues related to moisture sensitivity, we recommend employing a coating method combined with channel drying or oven thermal treatment as a post-processing step. This technique will enhance the sensors' resistance to moisture, allowing them to maintain their integrity and sensitivity over time.

The migration of components from a colorimetric sensor to food products is generally a concern in food safety. However, if the components used in the sensor are food-safe and the sensor has undergone post-thermal treatment to ensure its integrity in humid environments, the risk of migration can indeed be minimized. This means that, under these conditions, the migration issue would likely be minor.

While the current literature demonstrates the effectiveness of colorimetric sensors during specific storage periods, further research is necessary to evaluate their long-term stability and performance under varying environmental conditions, such as temperature fluctuations and light exposure. Additionally, there is a need for more studies focusing on the real-time dynamics between colorimetric changes and microbial activity, particularly in conjunction with advanced analytical techniques like GC-MS and mathematical modeling.

In summary, addressing the gaps in literature regarding natural colorants, enhancing the stability and performance of pH indicators, and understanding consumer perceptions are essential steps toward the successful commercialization of these innovative solutions in food packaging.

CHAPTER 3 OBJECTIVES

The main objective of this research is:

To develop a colorimetric sensor for detection of spoilage through a direct approach which is applicable in food packaging film.

To achieve the main objective following specific objectives should be followed.

3.1 Specific objectives

3.1.1 Formulate sensor ink with good adhesion bonding to sealant layer:

1. Formulation sensor ink with black rice as natural pH indicator and evaluating its efficiency.
2. Evaluate the effects of surfactants on contact angle and surface tension
3. Investigate the effect of different polymeric substrates on adhesion (effect of surface treatment)

3.1.2 Sensitivity of the ink in different conditions:

1. Checking thresholds of TVBN (limit of detection) and response time/color to different concentrations of TVBNs at different storage conditions (room/ refrigeration temperature).
2. Study of UV – vis spectra of the natural dyes in solution and in the sensing film (wavelength and intensity) and then quantify the wavelength shifts in response to pH change.
3. Evaluate the color changes of pH indicator films for use in monitoring the quality of fish and meat and then investigate the correlation between the color changes of films and fish and meat spoilage during storage conditions at 25 and 4 °C.
4. Evaluating ink stability

3.1.3 Validation of development sensors:

1. Assess the effect of sensor ink on the different types of food, different types of packaging, different processing parameters (Temperature) and different types of bacteria.
2. Find correlation between bacteria growth with and the amount of produced gases.
3. Investigate of the shelf life of products.

The following three chapters contain the articles representing the results of this study:

3.2 Organization of articles

The first article presented in chapter 4 is entitled “Characterization of a Food-Safe Colorimetric Indicator Based on Black Rice Anthocyanin/PET Films for Visual Analysis of Fish Spoilage.” This chapter introduces a food-safe ink formulation designed for coating on the corona-treated PET films. The developed on-package colorimetric sensor was prepared using the doctor blading technique. Characterization of the sensor was conducted through various methods, including FTIR, TGA, UV-Vis spectroscopy, water contact angle measurements, tape tests, and abrasion tests. Finally, the performance of the colorimetric sensors in detecting TVB-N gases was evaluated through sensitivity tests.

The second article presented in chapter 5 is entitled “Enhancing seafood freshness monitoring: integrating color change of a food-safe on-package colorimetric sensor with mathematical models, microbiological, and chemical analyses”. This study demonstrated that colorimetric films based on eco-friendly materials, that can effectively monitor fish freshness and spoilage at 4 °C, exhibiting acceptable color stability throughout the storage period. The efficacy of the on-package colorimetric sensor was rigorously assessed through simultaneous packaging trials, which included the use of chemical biomarkers and microbial analysis, ensuring a comprehensive evaluation of fish quality. Additionally, the integration of mathematical models allowed for the prediction of seafood spoilage, correlating these predictions with the visual assessments provided by the pH indicators. This innovative approach offers a promising solution for enhancing shelf-life predictions and quality assessments of fish products, contributing to smarter, more efficient, and environmentally friendly food packaging practices.

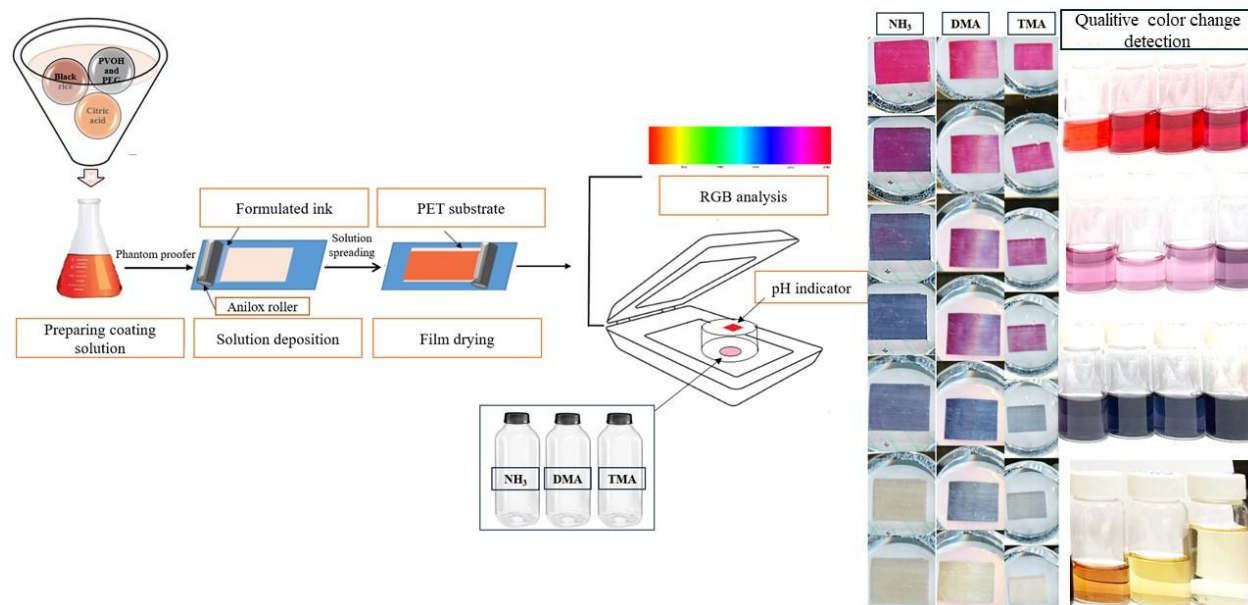
The third article, presented in chapter 6, is entitled “Intelligent packaging solutions for fish and meat products: volatile gas detection via GC-MS, microbial analysis and colorimetric monitoring”. This study employed the colorimetric sensor developed in chapter 4 in various fish shelf-life trials to establish a correlation between fish spoilage and the visual detection of color changes in the sensor. These changes are associated with spoilage due to volatile amine formation and microbial activity in fish products. The colorimetric sensor effectively tracked increases in TMA and NH_3 levels in the packaging headspace, alongside significant growth in TVC, providing a reliable measure of fish freshness. Utilizing GC-MS for headspace analysis, we achieved linear calibration curves and detection limits in the ppm range without the need for laborious pre-treatment or clean-

up. The pH indicator labels exhibited a four-point freshness scale, demonstrating distinct color changes over a 9-day storage period at 4 °C, thus enhancing the practical application of the sensor in monitoring seafood freshness. Furthermore, a strong correlation was observed between the colorimetric results and GC-MS data, reinforcing the sensor's effectiveness as a practical tool for monitoring seafood freshness and suggesting its potential applications in intelligent packaging for food safety and quality assurance.

**CHAPTER 4 ARTICLE 1: CHARACTERIZATION OF A FOOD-SAFE
COLORIMETRIC INDICATOR BASED ON BLACK RICE
ANTHOCYANIN/PET FILMS FOR VISUAL ANALYSIS OF FISH
SPOILAGE**

Credit Author Statement

Maryam Ameri: Conceptualization, Investigation, Experimental work, Data curation, Writing – original draft. Writing – review & editing, bibliographic, Project administration. Abdellah Ajji: Conceptualization, Supervision, Funding acquisition, review & editing. Samuel Kessler: Conceptualization, Supervision, review & editing.



Authors: Maryam Ameri¹, Abdellah Ajji¹, Samuel Kessler², *Corresponding author:
abdellah.ajji@polymtl.ca

1. Chemical Engineering Department, Polytechnique Montréal, Montréal, Québec H3C 3A7, Canada
2. Active/Intelligent Packaging, ProAmpac, Cincinnati, Ohio 45246, United States

Published: Packaging Technology and Science, 17 May 2024

Highlight: This research study displayed an ink formulation design that can be used as a food-safe coating for creating a pH indicator as an on-package sensor. The designed colorimetric sensor demonstrated remarkable color changes at various pH levels and displayed acceptable sensitivities to TVB-N gases. This pH indicator takes benefit of the use of affordable, and eco-friendly dyes, as well as a straightforward printing method, making it suitable for food packaging applications.

4.1 Abstract

The safety of food products is of prime importance for consumers and manufacturers. Many means can be used to validate a food product's safety before it is consumed. This study is about the preparation, characterization, and evaluation of a generally recognized as safe (GRAS) sensitive colorimetric sensor that detects volatile gases (TVB-N) resulting from fish spoilage, thus indicating the pH variation of packaged fish products. This is performed by coating a thin layer of ink sensors on the surface of the supporting matrix (corona-treated PET). Various visual pH indicators were prepared based on black rice anthocyanin as an FDA-approved dye. Black rice contains more than 80% Cyanidin-3-glucoside, which is a prevalent anthocyanin. Because of its low toxicity and high concentration, it can be utilized as a natural food colorant. pH indicators based on black rice can show distinct colors in various pH: From red (low pH) to violet (4-6) and deep purple/blue (6-7), blue (7-9) to yellowish/light brown (9-13) throughout the acid-base reaction by the analyte. The ink formulation was prepared by incorporating a binder system (PVOH-PEG) for higher surface wettability, a crosslinking agent (citric acid) for higher adhesion, an antifoaming agent (natural Vanillin), and acetic acid as a pH fixing agent. Corona treatments affected substrate surface chemistry in this study. The samples with thermal treatment passed the ASTM D3330 tape test, the 8000 passages for dry sponge, and the 25 passages for wet sponge through the abrasion method. The anthocyanin concentration in formulated ink, based on calculation by UV-vis spectra, is 0.240 mg/100 gr. Sensitivity tests towards TVB-N gases were carried out at a temperature of 4°C to evaluate the performance of colorimetric films with formulated ink along with thermal treatment (Temperature: 165 °C, time: 5 min) using the volatile gases emitted by the fish sample inside the package.

Keywords

On-package sensor, pH indicator, anthocyanin, fish spoilage, visual analysis

4.2 Introduction

Fish is one of the most perishable foods on the market, and there are serious health consequences for consuming, once it has spoiled. Evaluation and monitoring of the quality and safety of this high-priced and easily spoiled seafood makes the rapid and non-destructive detection of freshness a crucial need. Currently, food industry utilizes various pH indicators to detect chemical changes

caused by microbial growth or spoilage. By using pH indicators, which can change color, and incorporating this technology into the packaging or even handheld devices, consumers can easily and quickly assess the freshness of the seafood they purchase, ensuring their safety and preventing any potential health hazards. This approach increases food quality and decreases food waste [1-6].

Colorimetric indicators typically exploit pH dependent structural changes of a chemical that shift its characteristic wavelength of absorbance. Specific gases are generated during the microbial spoiling of food products, that can affect the color of pH indicators during the acid-base interaction and can produce rancid aromas. Common markers for gas-targeting food sensors include carbon dioxide, oxygen volatile organic compounds (VOCs), and biogenic amines (BAs). Among these gases the total volatile basic nitrogen (TVB-Ns) is the most present from spoilage of seafood products [7-11]. The presence of volatile amines, including trimethyl amine (TMA), dimethyl amine (DMA), and ammonia (NH₃), contributes to the distinct 'fishy' odor commonly associated with spoiled fish [12]. In accordance with EU regulations, the spoilage threshold for total volatile basic nitrogen (TVB-N) in fish is set at 35 mg per 100 g of flesh. Any concentration exceeding this limit is considered unsuitable for consumption [13]. Changes in concentration of TVB-Ns gases which are produced during spoilage of fish and meat products inside the package can be detected using pH indicator strategy. These indicators are composed of a pH sensor, a natural dye that reacts to pH changes with a noticeable color shift, and a dye carrier. Both components must be non-toxic, fulfill food safety regulations, and be stable at the applied pH [14].

According to the literature, the use of synthetic dyes such as methyl orange, natural red, bromocresol green/purple etc. [15]; as pH indicators is limited due to their high toxicity and genotoxicity [16]. The most common pH indicators are based on natural substances that may be derived from fruits, vegetables, flowers, or even food waste, such as anthocyanins [17].

Anthocyanins are a family of polyphenol-based flavonoids that have sensitive reactions, resulting in color changes, to a broad range of pH (2-9) [18-20]. Also, they meet the safety standards of packaging materials, and can introduce antimicrobial and antioxidant properties, which are relevant for food packaging applications [21]. Moreover, because anthocyanins are ionic, their molecular structure can be altered depending on the pH, resulting in varied colors and hues at different pH levels [14].

Colorimetric indications based on anthocyanins from red cabbage [22], purple sweet potato [23], blueberry [24], Roselle (*Hibiscus sabdariffa* L.)/ curcumin [25], curcumin [26, 27], black carrot [28], shikonin [29, 30], purple tomato [31], black rice bran [32] and other dark purple and black vegetables [33] have been mentioned in studies. The findings revealed that the source of anthocyanin has a significant impact on its functional and physical properties [19, 34].

This study employed phantom proofers (doctor blade), a simple lab-scale flexography printing technology for immobilizing ink solutions that improves coating efficiency.

A suitable substrate is also required for the deposition of formulated ink. In this research, polyethylene terephthalate (PET) was used as the selected substrate due to the many benefits associated with this polymer.

PET is a food-contact polymer with two hydroxyl (OH) groups, a dicarboxylic aromatic acid, and two carboxyl (CO₂H) groups [35]. PET is good for flexible packaging due to its strength, barrier protection (resistance oxygen and other gases), flexibility, transparency, and compatibility [36]. However, PET films have low surface tension in the range of 42-47 [dynes/cm] that might affect coating/printing adhesion [37]. Surface chemical, flame, plasma, corona discharge, and laser ablation are popular procedures for substrate surface modification [38-42]. The material and final goal determine the optimum process.

In this study, the surface chemistry of the substrate has been modified with corona treatments. This objective is to improve surface adhesion, wettability, printability, and coating quality. However, if the bonding of polar molecules does not happen properly, it risks adhesion failure [43, 44]. To address this issue, optimizing the power and speed of the test operation could be beneficial in minimizing the risk of adhesion failure. On the other hand, to attain wetting, the surface energy of the formulated ink must be as low or lower than the surface energy of the substrate to be bonded. To achieve a satisfactory coating, it is important to consider that an increased level of hydrolysis and the higher molecular weight of PVOH, the primary binder in this formulation, can result in greater surface tension and reduced surface tension, respectively [45]. Thus, using appropriate binder can also change the adhesion properties. After selecting polymer films, the substrate's adhesion to inks and their interaction are crucial during printing.

PET shows acceptable barrier properties towards oxygen, however, it is vulnerable against water vapor [46]. Crosslinking agents in the coated ink formulation can improve PET films' water vapor properties so they can be utilized directly with high-humidity food such as fish. Citric acid (CA) is FDA-approved poly-carboxylic acid. At low concentrations, CA can provide COOH groups, crosslink polysaccharides, and produce a chemical bridge between the OH groups of PVOH. To put it simply, the carboxylic groups in citric acid and alcoholic groups in PVOH can react to produce ester groups and water (Fischer's esterification) [47], which can be dissipated by thermal treatment or drying channels during the printing process, making coated films less susceptible to humidity. Adding a co-binder like polyethylene glycol (PEG) can help bridge PVOH chains and reduce coated films' water susceptibility [48-51].

The developed pH indicator presents in this research study, is affordable, user-friendly, non-damaging, and widely accessible. Additionally, there is a possibility of chemical migration from the sensor to the food. Therefore, to develop the ink formulation, we followed the guidelines specified in FDA-approved regulations to demonstrate the practicality of applying this pH indicator to packaging for real-world applications. The effect of thermal treatment on the response time of different types of pH indicators with different ink formulations was investigated. Finally, flexible PET films coated with natural dyes, as air-type packaging, serve as a pH-responsive sensor, exhibit precise visual variations at different pH values, and show high sensitivities to TVB-N gases, which can effectively detect fish deterioration and provide valuable information to customers or sellers about the fish quality.

4.3 Materials and methods

4.3.1 Materials

Starch/LLDPE (linear low-density polyethylene), starch/HDPE (high density polyethylene), and PET films were, all received from ProAmpac flexible packaging company, Terrebonne, Quebec, Canada. Black rice extract 80% from Dongguan Xiherbs Phytochem Co., Ltd, China. Polyvinyl alcohol (87~88% hydrolysis, 145,000 MW), Polyethylene glycol (peg 400), Citric acid (ACS reagent, $\geq 99.5\%$), Vanillin (natural, $\geq 97\%$, FCC, FG), Hydrochloric acid (HCL), Acetic acid, Methanol, Sodium acetate ($C_2H_3NaO_2$), Potassium carbonate (K_2CO_3), Ammonium hydroxide solution (30-33% NH_3 in H_2O), Dimethylamine solution (40 wt. % in H_2O), Trimethylamine

solution (43.0-49.0% in H₂O) and Potassium chloride (KCL) from Sigma-Aldrich, Canada. **Table 4.1** displays the components used in formulating the ink for this project.

Table 4.1 The ingredients utilized in the production of the ink formulation in this study, along with their corresponding FDA status.

Material	Function	FDA status
Black rice anthocyanin (BC)	Natural dye	Anthocyanins are approved for use as food and cosmetic colorants in the EU with E number 163.
Polyvinyl alcohol (PVOH)	Binder	GRAS and FDA-approved.
Polyethylene glycol (PEG)	Co-binder	May be safely used in food in accordance with some terms and conditions ¹ .
Citric acid (CA)	Crosslinking agent	GRAS when used in food and skin product.
Vanillin	Antifoaming	In general, three types of vanillin, namely natural, biotechnological, and chemical/synthetic, are available on the market. However, only natural, and nature-identical (biotechnologically produced from ferulic acid only) vanillin is considered as food-grade additives by most food-safety control authorities worldwide.
Citric acid	Fixing agent	GRAS
1. It contains no more than 0.2 % total by weight of ethylene and diethylene glycols.		

4.3.2 Ink preparation

A heterogeneous mixture composed of PVOH (5.08 g) and deionized water (39 mL) was obtained by mixing the substances in a glass beaker. Once covered with aluminum foil to avoid contamination, the beaker was placed on the magnetic stirrer for mixing at 80 °C with high speed (800 rpm) for 2 hours. To overcome the foaming effect, a 10% (wt./v) solution of vanillin in 95%

ethanol was added to the binder solution. After the solution cooled at room temperature while being stirred constantly, a solution mixer made of 8.69% (wt./wt. of PVOH) PEG, 22.7% (wt./wt. of PVOH) citric acid, 0.56 g (80%) black rice, and 20 ml (wt./wt. of PVOH) DI water was added as a solvent. At the last step, between 50-100 μ L of acetic acid was added to the final solution to fix the pH of the formulated ink. The pH of the solution was recorded by a pH meter (Mettler Toledo, Five easy plus TM, Switzerland). To have acceptable coating process, it should consider the higher degree of hydrolysis and higher molecular weight for PVOH, as main binder in this formulation, can cause larger surface tension and smaller surface tension, consecutively.

4.3.3 Sensor preparation

The coating process was performed using a TQC Automatic Film Applicator (lab scale process of flexography printing). Different amounts of final solution were coated on machine direction (MD) of corona treated PET. The speed of blade and the rod number was 75 mm/s and 60 U, respectively, which can load more ink through each passage. The prepared films dried in different temperature/time conditions (ambient temperature, for 30 min, and 165 °C for 5 min). Print quality was analyzed both visually (tape test) and numerically (color system of RGB). The final thickness of the wet films was calculated based on the amount of ink used (4 ml) and PET surface size (21 mm \times 297 mm).

4.4 Characterization of pH indicator

4.4.1 Water Contact Angle Measurements (WCA)

The effect of the corona treatment on surface energy has been evaluated using contact angle measurements conducted by the sessile drop method, employing optical tensiometers, as well as the dyne pen technique. The sessile drop method involves the use of a precision syringe for carefully dropping a small volume (a few μ L) of probe liquid onto a flat substrate positioned on a platform. The droplet is captured in a cross-sectional view by a camera with great resolution. The determination of the static contact angle, denoted as θ , at the three-phase line of contact relies on the fitting of the drop profile, using the Young-Laplace equation [53]. WCA for starch/LLDPE, starch/HDPE, starch/PBAT, and PET films was determined using the contact angle and surface tension analyzer at ambient temperature and relative humidity 30%.

4.4.2 Tape test

Peel testing was conducted to ensure the presence of proper adhesion bonding between the coating and its respective surface. In this test, a sample of the tape (Tartan 369) being tested is applied to a substrate material and allowed to adhere for a specified amount of time. The tape is then peeled back at a specified angle and speed. According to the ASTM D3330, the specified value of 0.619552 lb/in is the minimum average peel adhesion strength required for a tape to pass this test [54]. This means that if a tape's average peel adhesion strength is lower than this quantity, it fails the test. The test method which used were single coated tape-peel adhesion 180 angle. The sample size is 24 mm (width), and the length is 300 mm. The dwell time was 1 min.

4.4.3 Abrasion Test

The Taber Linear Abrader model 5750 was used for the abrasion test. Before the testing for 24hr, the samples we been in the test atmosphere. The effect of drying and type of coating on the PET films investigated. The type of dry and wet sponge was 133447 from Taber Industries (New York, USA). The test performed in the standard laboratory atmosphere of 23 ± 2 °C with $50 \pm 5\%$ relative humidity. The speed is 25 (cycles/minutes) and the stroke length is 2 in.

4.4.4 Fourier-Transform Infrared Spectroscopy (FTIR-ATR)

The FTIR spectra of the samples were recorded at room temperature using a Perkin Elmer FT-IR spectrometer 65 coupled to an ATR accessory, with a diamond crystal. The data was collected using Perkin Elmer spectrum. The dry starches were clamped directly onto the crystal for analysis, and the spectra were acquired in the range $4000\text{--}600\text{ cm}^{-1}$, with 16 accumulations and a resolution of 16 cm^{-1} .

4.4.5 The spectral characteristics of the ink formulation

Using a UV-Vis Spectrophotometer (Device infinite M200, Tecan, Polytechnique Montreal, CA) and the pH differential method, the total anthocyanin content of roasted black rice in the ink was found to be 0.240 mg/g. Briefly, the samples need to be diluted in the 0.025 M KCl solution adjusted to pH 1 until the $\lambda_{\text{vis-max}}$ is within the linear range of the instrument. A separate sample needs to be prepared with the same dilution factor in the 0.4 M $\text{C}_2\text{H}_3\text{NaO}_2$ solution adjusted to pH 4.5. After 15 min, the $A_{\lambda_{\text{vis-max}}}$ and $A_{700\text{ nm}}$ are measured against a water blank [55, 56]. The following formula was used to calculate the anthocyanin pigment concentrations expressed as cyanidin-3-glucoside equivalents [14] (Eq. (4.1)):

$$\text{Monomeric anthocyanin (mg/L)} = A \times \text{MW} \times \text{DF} \times 1000 / e \times l \quad (4.1)$$

Where $A = (l_{vis-max} - A_{700nm})_{pH1} - (l_{vis-max} - A_{700nm})_{pH4.5}$, MW= Molecular weight (449.2 g/mol) for cyanidin-3-glucoside (cyd-3-glu), D_f = dilution factor, and e = molar extinction coefficient (28,000 L/cm.mol) for cyd-3-glu; 1000 is a factor for conversion from g to mg and L = pathlength in cm.

4.4.6 Color parameters: RGB

To evaluate the sensitivity of ammonia gas towards colorimetric platform, 3 cm × 2 cm of the film was cut, and we put it inside the container (600 ml) with one inlet to inject the different volume (1, 5, 10, 25 μ L) of (30-33%) NH_3 in H_2O at ambient temperature. The studied compound automatically volatilized and exposed to the sensor platform which was positioned at the wall of the sealed container. Color responses of the colorimetric film to ammonium hydroxide were captured by the scanner (Epson Canada Ltd, Perfection V550). The pictures and colorimetric information of the films were registered every 2 min (till 1 hr) and after that each one hour till 24 hr as mentioned [23] with modifications. Image analysis was performed, by MATLAB software 2019b, a desired pixel including row, column, and neighborhood window (the window size around the pixel) the from pictures from pH indicator were considered. The test run for 3 different spots (pixels and considering their neighborhood) inside each picture and the mean and standard deviation were calculated. The control sample was choosen as reference image for RGB calculation. The color change of pH indicators during storage period is measured by the total color difference (ΔRGB) according to the following equation [14]:

$$\Delta\text{RGB} = \sqrt{(R - R_0)^2 + (G - G_0)^2 + (B - B_0)^2} \quad (4.2)$$

Where R_0 , B_0 , G_0 are the initial color parameters of indicators and R , G and B were the values at the time of sampling.

4.5 Statical analysis

All measurements were conducted three times. Data were analyzed with Tukey test at a significance level of $p < 0.005$, $p < 0.001$ and $p < 0.001$. The results are reported as the average value \pm standard deviation (SD).

4.6 Results and discussion

4.6.1 WCA

The effect of the corona treatment on surface energy has been evaluated using contact angle measurements conducted by the sessile drop method and dyne pen. As shown in **Table 4.2** among different trial films, PET (film thickness = 12 micron) was the most reliable film packaging material in this context because it showed a lower contact angle result compared to 25% starch/75% HDPE and 40% starch/60% LLDPE and had the lowest sensitivity towards water (compared to the films that have starch). After corona treatment of the PET films, there was a decrease in its contact angle from 104.43 ± 1.45 ($\pm 1.39\%$) to 65.56 ± 6.674 ($\pm 10.18\%$) and surface energy increased from 42 to 50 dynes/cm, respectively.

Surface coatings were applied right away after corona treatment procedure on the surface of PET films. WCA measurements were then taken before and after coating with the designed ink to examine the effect of eliminating water from the samples and the number of passes on adhesion properties. Corona surface treatment and addition of black rice decreased the WCA of the PET film significantly ($p < 0.05$), due to the temporary introduction of hydrophilic functional groups such as $-\text{OH}$, and $-\text{COOH}$ and the hydrophobic nature of black rice. According to the results, thermal treatment decreases sample water sensitivity, which can increase slightly the contact angle. This effect can be enhanced by increasing coating thickness (number of passes). Films are considered hydrophilic when the WCA is less than 65°C [57], according to this criterion, the developed pH indicators films still can be considered hydrophilic films.

Table 4.2 Analysis of variance of WCA measurements on films. The droplet volume is 2 μl .

Type of films	N	Mean	Variance	Standard deviation	Margin of error at confidence level 95%
25% Starch, 75% HDPE	3	113.46	1.10	1.05	113.46 ± 1.19 ($\pm 1.05\%$)

Type of films	N	Mean	Variance	Standard deviation	Margin of error at confidence level 95%
40% Starch,60% LLDPE	3	106.1	3.08	1.75	106.1 ± 1.98 (± 1.87%)
PET	3	104.43	1.64	1.28	104.43 ± 1.45 (± 1.39%)
PET					
PET Corona treated	3	65.56	34.78	5.89	65.56 ± 6.67 (± 10.18%)
After coating ink formulation					
INK I-NTT ² -1st passage	3	51.53	12.86	3.58	51.53 ± 4.059 (± 7.88%)
INK I-NTT 2nd passage	3	56.83	0.37	0.61	56.83 ± 0.69 (± 1.22%)
INK I-165-5 1st passage	3	55.46	0.16	0.41	55.46 ± 0.46 (± 0.84%)
INK I-165-5 2nd passage	3	58.46	3.16	1.77	58.46 ± 2.01 (± 3.44%)

1. NTT is an abbreviation for films without thermal treatment procedures.

4.6.2 Validation of interaction between functional groups for better adhesion properties via FTIR

FTIR tests were applied to confirm the presence of hydroxyl groups, carboxylic groups, and ester groups. As shown in **Figure 4.1**, the Ink components samples (PVOH, black rice, PEG, citric acid) while in **Figure 4.2**, the colorimetric platform samples (Ink I-NTT and Ink I-165-5) all showed similar behavior, with bands in the region of 3400–3200 cm⁻¹, which were assigned to the stretching vibration of the O-H group.

4.6.2.1 Formulated ink

The bands at 1638 (C-O stretching) and 1572/1517 are related to protein content of roasted black rice. The bands at 1441–1323 cm^{-1} were assigned to C-H bending vibrations, while the band at 1242 cm^{-1} was ascribed to the O-H bending vibrations [43]. The bands at 1157 and 1008 cm^{-1} corresponded to the ring vibrations juxtaposed with the stretching vibrations of the lateral groups (C-OH) and to C-O-C glycoside vibrations [58]. By adding black rice in ink formulation, the peak intensity for OH groups increased and shifted to higher wavelength. This shift could indicate a change in the chemical environment of the OH group. This shift can be attributed to alterations in molecular polarity or hydrogen bonding, variations in the system's temperature during analysis, or changes in the solvent composition or pH conditions.

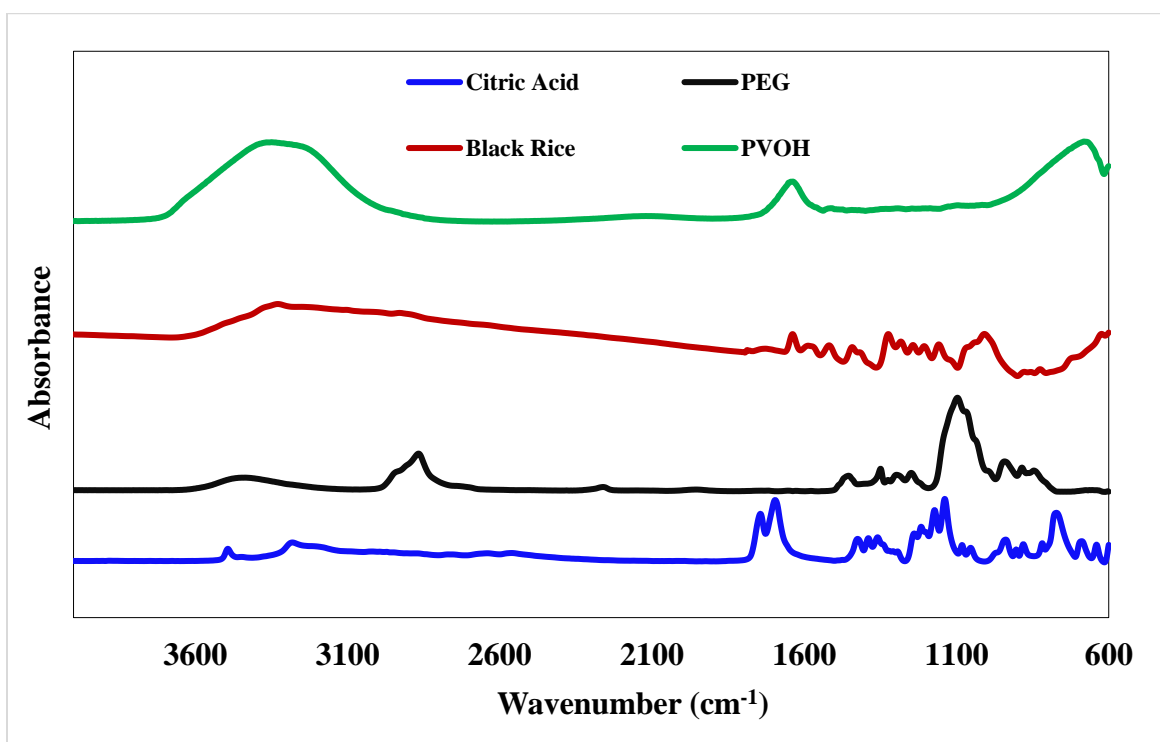


Figure 4.1 FTIR-spectra of each component of formulated ink solution.

4.6.2.2 Colorimetric platform

There is a new peak at 2919 cm^{-1} in coated PET films with INK I formulation, which may be due to the presence of PEG, causing an additional bridge between PVOH groups. The intensity of hydroxyl bands decreases significantly after heat treatment of samples, indicating transitory water loss and a lower number of accessible water molecules from hydrogen bonding because of

dehydration. This suggests that the crosslinking was caused by removal of the solvent and alcohol that leaked from the samples, as well as the presence of citric acid as a crosslinking agent. The absorption of 1713 cm^{-1} was assigned to a C=O stretching vibration and could be attributed to the carbonyl groups in coated film. Also, the $\Delta A = 0.02$ for peak 1713 cm^{-1} (C=O) stretching for the INK I-165-5 intensified. The band at 1230 cm^{-1} , which is connected to the ester C-O stretching (Fisher's esterification), also supports the esterification [59]. This peak can demonstrate that crosslinking between CA and PVOH occurred.

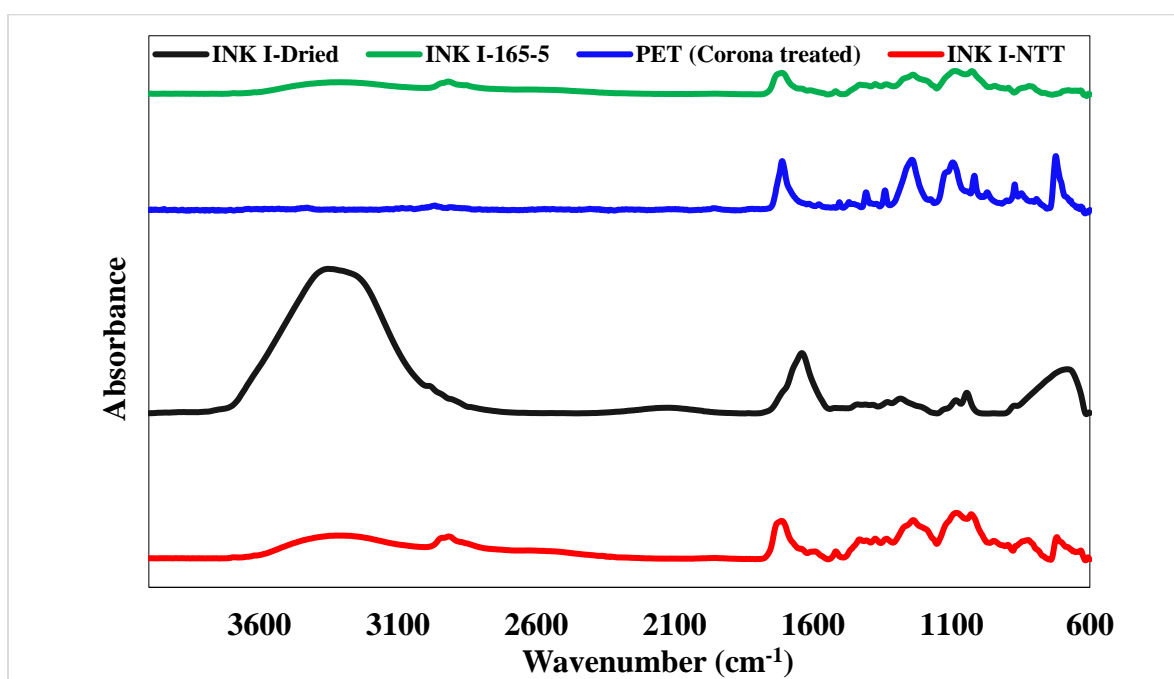


Figure 4.2 FTIR spectra of dried solution ink (INK I-Dried) fabricated colorimetric films with thermal treatment (INK I-165-60) and without thermal treatment (INK-I-NTT) and sealant layer (PET corona treated).

4.6.3 Validation of adhesion: Tape test and Abrasion test

According to the Tape test and abrasion results from several types of PET films coated with these different ink formulations based on black rice and PVOH, films without thermal treatment or with insufficient thermal treatment (90 °C for 60 minutes, 50 °C for 24 hours, 145 °C for 15 minutes) would remove more area, which we did not present results here. The classification of adhesion results was based on the D3359-17 standard [54], in which at least 5-15% of the coating of samples

without thermal treatment was removed when it comes to contact with water (as fish packages have high humidity). Final samples with proper thermal treatment (165 °C for 5 min) passed the tape test. The images displaying the results are not included in this section (**Figure A.1**). Also, these samples passed the abrasion test with 4000 cycles for dry sponge and 25 cycles for wet sponge. Thus, applying the correct thermal treatment to the samples can enhance their adhesion qualities, hence enabling the colorimetric platform to function effectively.

4.6.4 UV–vis spectra of the ink solution at different pHs and its stability

A spectrophotometric titration using a deprotonation–protonation process was performed and monitored at $\lambda = 520$ nm (which sample showed maximum absorbance). The Ink I formulation was diluted using DI water until it reached an absorbance of 1.0271 at 510 nm. This was placed in 20 ml disposable scintillation vials at 23 °C, protected from light, and kept under constant vortex. Aliquots of ammonium hydroxide 0.1 M and HCL 1N were added to the diluted ink for every change of 0.5 in pH, the absorbance was recorded at 520 nm until a pH 10 was reached. (Device infinite M200, Tecan).

The influence of pH to the anthocyanin color stability was investigated by the absorbance of UV light with a wavelength of 400 -700 nm, using UV-VIS spectrophotometer. Roasted black rice exhibited noticeable color changes in different buffers, as reported in a related study under varying pH conditions [58]. Black rice is rich in various anthocyanins, such as Cyanidin-3-glucoside (acidic conditions), delphinidin-3-glucoside (neutral pH), and Petunidin-3-glucoside (alkaline conditions) [60]. The chemical structure of these molecules can change based on the pH levels, influencing the color changes in black rice. Simply explained, the anthocyanin underwent a chemical process that produced a new molecular species (from flavylum cation to hemiketal or quinoidal) with altered absorption characteristics [61-63]. To detect flavonoids in the prepared ink solution, a few droplets of HCl are added to 10 mL of anthocyanin solution, which causes a red solution [61]. In **Figure 4.3**, the color change of black rice anthocyanin at various pH is depicted.

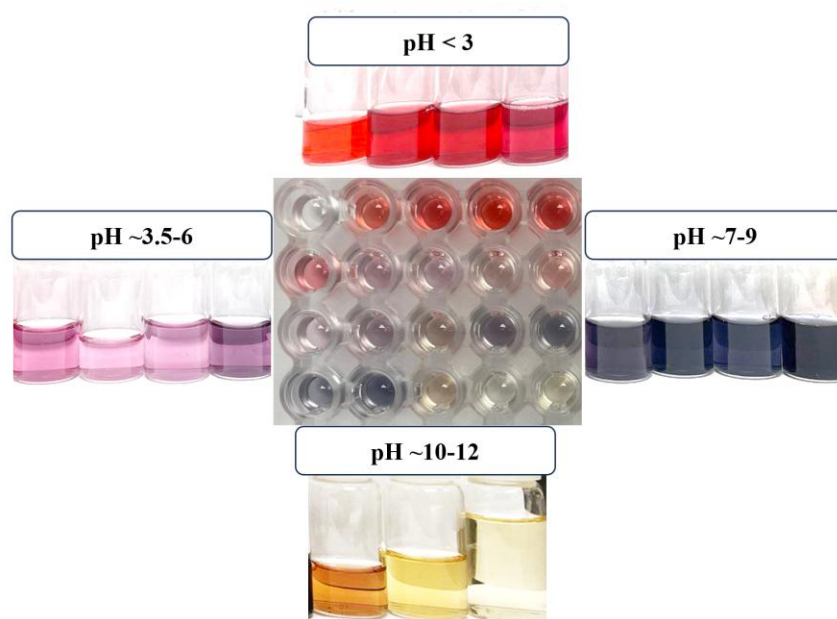


Figure 4.3 The color change of black rice anthocyanin at various pH.

The color change at pH 2-12 was indicated by the change of the distinctive absorbance at a certain maximum wavelength for each sample at each pH condition. The absorption spectrum of the natural pigment anthocyanin covers the entire visible region, and the peak absorbance was observed at 510 nm. The pH for Df = 0.1 is equal to 2.95, and for Df = 0.01 it is equal to 3.35.

In **Figure 4.4**, UV-vis spectra of solution ink at different pHs are presented. The change in pH (from 2-3.5) and molecular structure of anthocyanin inside the ink formulation caused a drop in absorbance peak intensity (at 510 nm) in the UV-visible (UV-vis) spectrum. When the pH increased to 4-6, a bathochromic shift occurred from 510 nm (pH 4) to 560 nm (pH 6). This shifting exhibited a purple color due to the change of anthocyanin structure. At pH 7, the color changed to blue because of the anionic and natural quinoidal bases. At the wavelength of 580, the color intensity increased at sample of pH 7-10 (bluish green), while it decreased from 580 to 520 for the sample with pH 10-11 and finally from pH 11 to 12, the intensity slightly increased with color change from light brown to dark yellow [14].

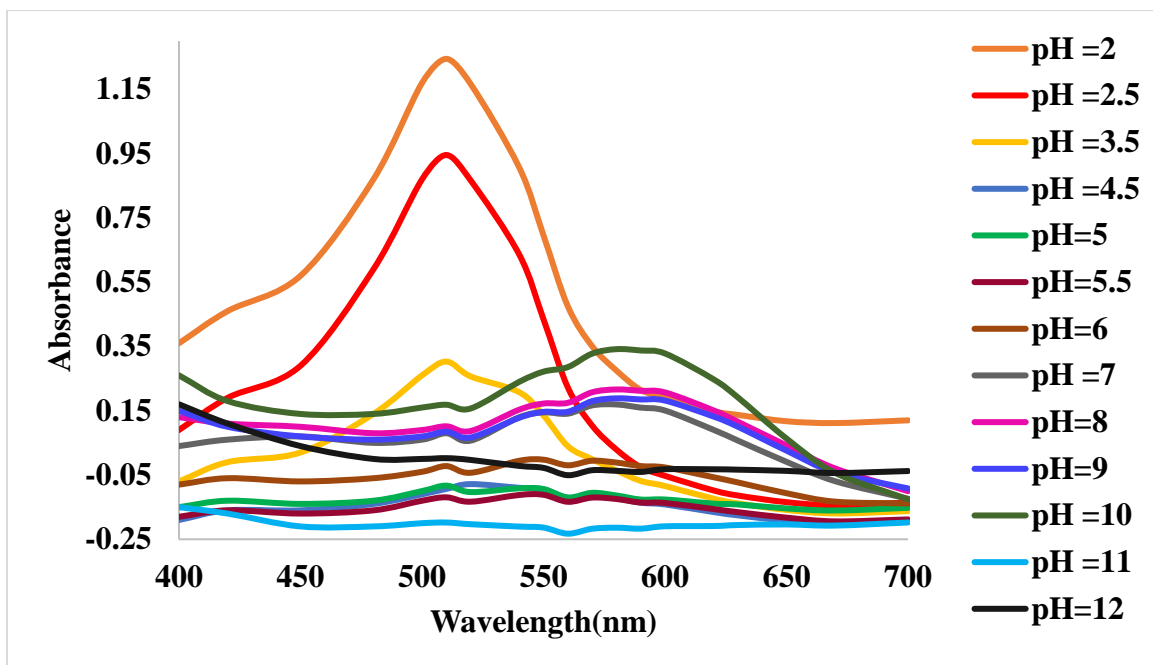


Figure 4.4 UV-vis spectra of solution ink at different pH.

4.6.4.1 Anthocyanin contents

In this study, anthocyanin concentrations were measured using the Giusti and Wrolstad-proposed pH differential method, which is based on the structural transformations of the anthocyanin chromophore as a function of pH. At pH 4.5, the colorless hemiketal form predominates, while at pH=1, the red flavylium form prevails. Instead of quantifying at 520 nm, the approach uses absorbance at the $\lambda_{\text{vis-max}}$ for precision. To avoid haze-induced light scattering, the absorbance at 700 nm was added. The approach also requires the molecular weight (MW) and molar absorption coefficient (ϵ) of malvidin-3-glucoside, the sample's main anthocyanin, to calculate its total amount [56].

Worth to mention that black rice anthocyanin molecular weight varies by component. Cyanidin-3-glucoside, one of black rice's most prevalent anthocyanins. Other black rice anthocyanins have comparable molecular weights. According to the results, the anthocyanin content of Ink I is 0.240 mg/100 g using the above approach. The overall quantity of black rice in this formulation is approximately 0.82 mg/100 g.

4.6.5 Color response to volatile amines (Ammonia, dimethylamine, and trimethylamine)

Colorimetric films react with the production of nitrogen-based compounds (such as NH_3 , DMA and TMA) that can be utilized to check the freshness of high-protein foods like meat and fish. The change in color of the colorimetric platform was recorded by a scanner that is linked to a computer for further analysis. The images were taken before and after exposure of ammonium hydroxide, dimethylamine solution and trimethylamine solution to the colorimetric platform for a duration of 24 hours. The color change exhibited a rapid rate, with most changes occurring within the first 15 minutes. Subsequently, a slower rate of change persisted for an extended duration, as seen in **Figure 4.5**, **Figure 4.6** and **Figure 4.7**. Additionally, it is notable that the quickest color shift was observed in less than one minute. The results indicate that the naked eye is unable to detect the sensitivity to 1 microliter of the stock solution. However, specific details on this observation are not provided in this context. The films undergo a transition in color, progressing from a red hue to a deep purple/blue shade, and to a light brown/dark yellow tone. Dissociation of the H^+ ion from a pH indicator causes its color shift. Note that pH indicators are weak acids and natural colours. The solution changes color when the weak acid indicator dissociates. The observed alterations in color may be attributed to the formation of an alkaline environment around the natural dye, facilitated by the presence of NH_3 gas, which generates OH^- ions upon contact with water [25]. Furthermore, it was noted that there were no discernible changes in color detected in the coated films containing a low concentration of black rice when exposed to various kinds of ammonia gases. This may be attributed to the absence of anthocyanins in the films, as supported by previous research [58].

The assessment of the selectivity of the developed pH indicator is associated with the measurement of the ΔRGB in the presence of several VOCs at a defined concentration. **Figure 4.5**, **Figure 4.6**, **Figure 4.7** illustrate a notable alteration in color upon exposure of the sensor to NH_3 , DMA, and TMA. In contrast, the sensor's color exhibited no alteration upon exposure to various organic substances, including acetone, ethanol, methanol, formaldehyde, and dimethylformamide.

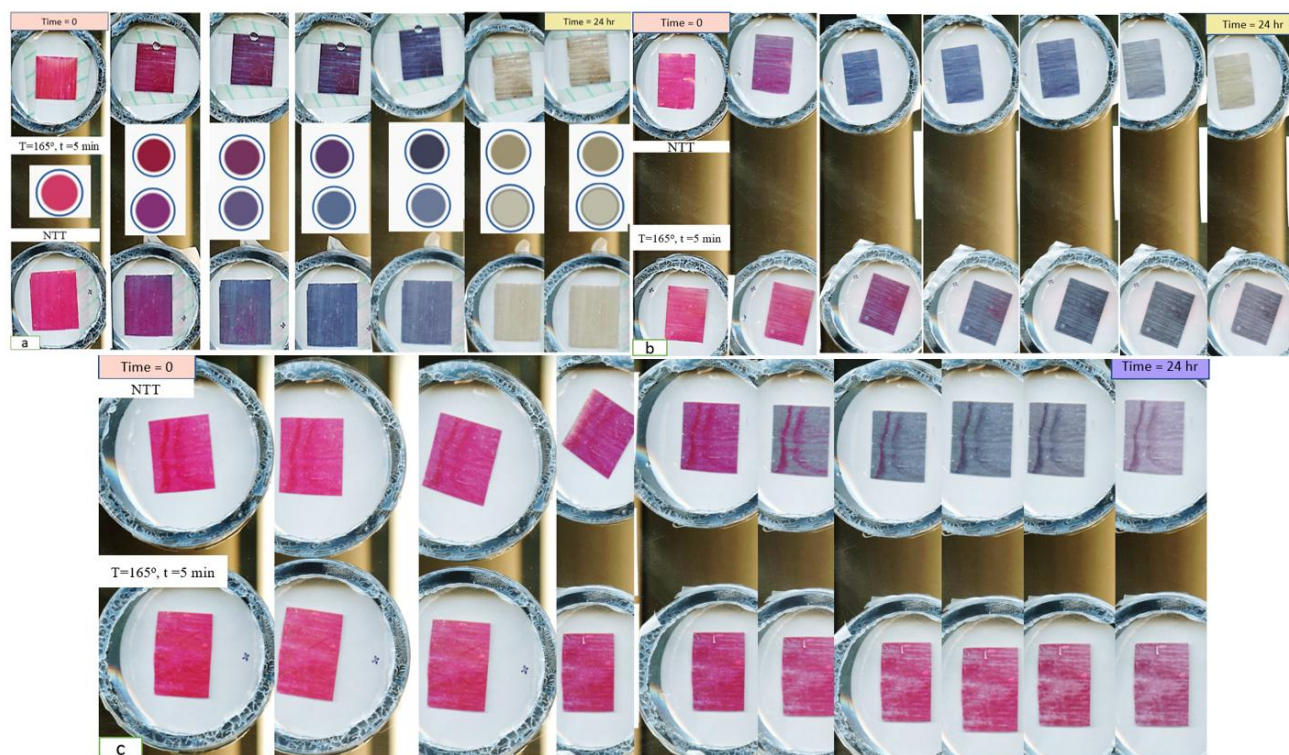


Figure 4.5 Sensitivity test for examining the response of pH indicator towards NH_3 gases, a = 25 μL , b = 10 μL , c = 5 μL of (30-33%) ammonium hydroxide.

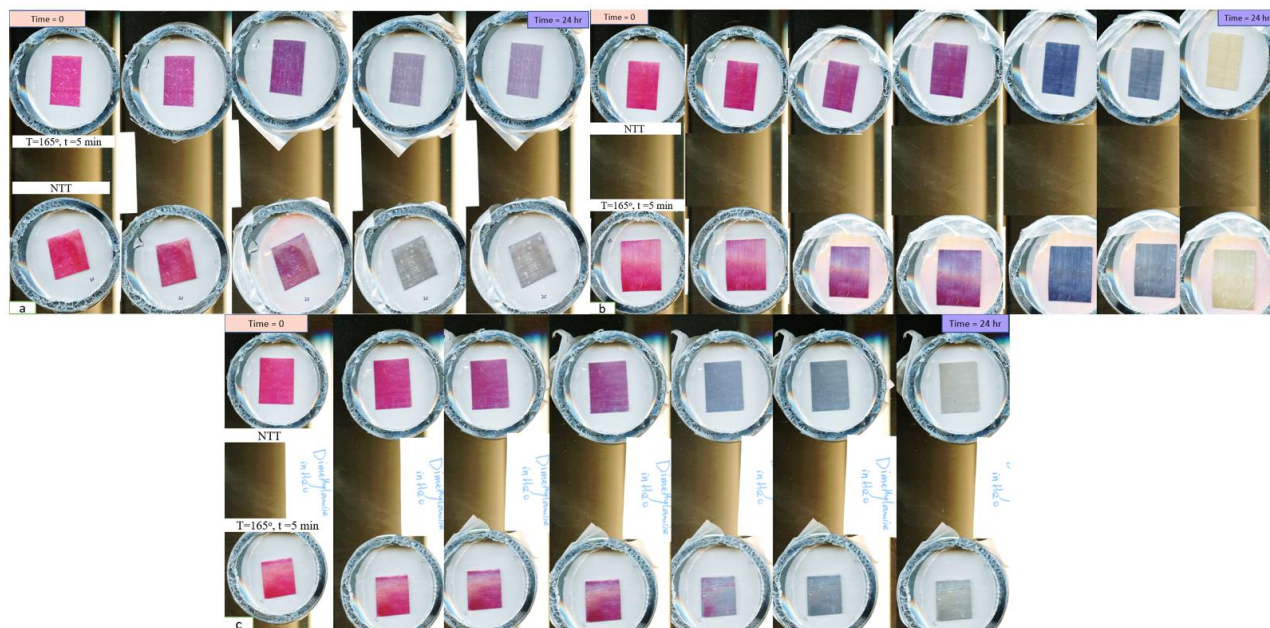


Figure 4.6 Sensitivity test for examining the response of pH indicator towards DMA, a = 25 μ L, b = 10 μ L, c = 5 μ L of dimethylamine solution.



Figure 4.7 Sensitivity test for examining the response of pH indicator towards TMA, a = 25 μ L, b = 10 μ L, c = 5 μ L of trimethylamine solution.

To better understand the color-changing behavior of film indicators, ΔRGB for NH_3 as a function of time is depicted, in **Figure 4.8**. In contrast to dried samples, produced indicators that have not undergone thermal treatment may exhibit a prompt color alteration as time progresses. Compared with the fresh samples, the ΔRGB values of the dried samples were lower. This phenomenon could be attributed to partial destruction of anthocyanins and active components at elevated temperature [64]. **Table 4.3** displays the statistical data, including the mean value of ΔRGB for three distinct pixels for each pH indicator.

In this study, the anthocyanin content in the thermally heated samples at 165 °C was very low, but it did not disappear totally and could alter color change with NH_3 gases. Thus, the pH indicator for fish packing must adjust for lag time correction. This is particularly crucial as the samples come into direct contact with food products, ensuring that the pH sensors will stay intact due to the elevated humidity levels within the packaging.

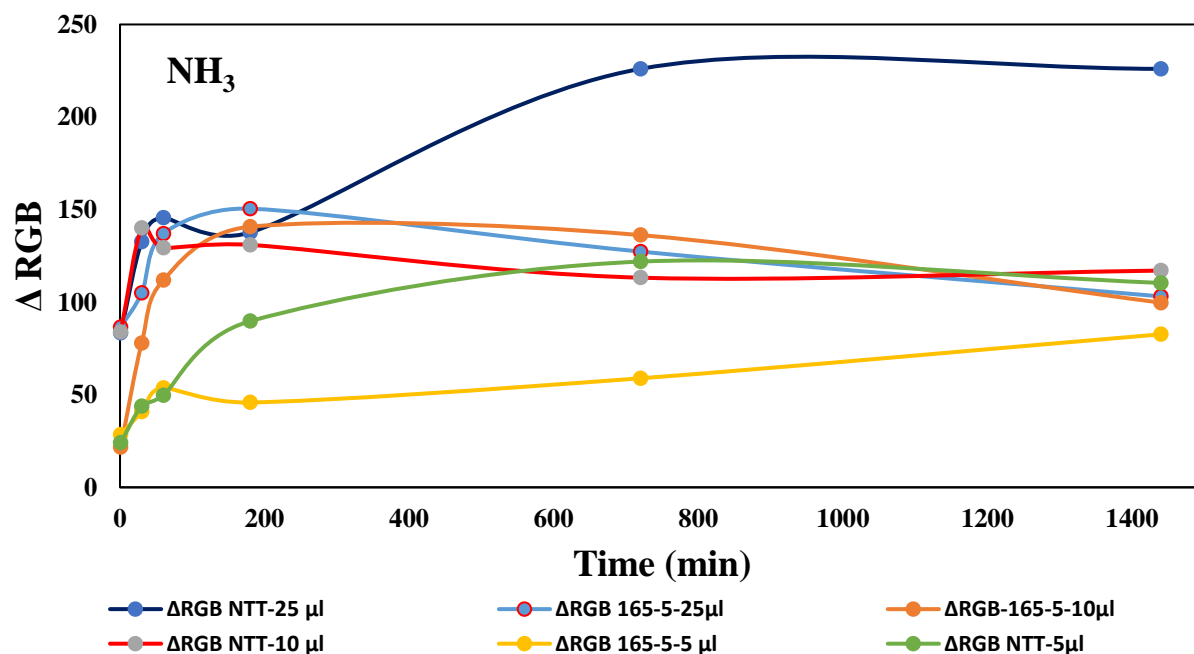


Figure 4.8 RGB results for fabricated colorimetric films with and without thermal treatment over time by exposure to (30-33%) ammonium hydroxide.

Table 4.3 The mean value of ΔRGB of NH_3 for three distinct pixels for each pH indicator during the time.

Type of pH indicator	Time	ΔRGB	SD
Ink I 165-5 25 μL	1	86.51	20.33
	30	104.95	13.98
	60	137.02	9.60
	180	150.48	5.10
	720	127.33	35.71
	1440	103.12	27.80
Ink I NTT 25 μL	1	83.45	8.16
	30	132.60	8.66
	60	145.59	4.78
	180	137.66	6.54
	720	226.02	3.63
	1440	226.02	3.63
Ink I 165-5 10 μL	1	21.722	11.30
	30	77.863	5.13
	60	111.86	4.675
	180	140.73	15.67
	720	136.23	17.07

Type of pH indicator	Time	Δ RGB	SD (Continued)
	1440	99.73	5.41
Ink I NTT 10 μL	1	83.92	16.62
	30	140.04	2.86
	60	129.44	8.40
	180	130.93	1.17
	720	113.23	11.42
	1440	117.07	9.69
Ink I 165-5 5 μL	1	28.50	12.06
	30	40.84	14.74
	60	53.71	15.47
	180	45.82	26.56
	720	58.89	33.93
	1440	82.65	17.05
Ink I NTT 5 μL	1	24.09	11.88
	30	43.89	20.12
	60	49.66	9.01
	180	89.72	33.14
	720	121.92	5.34
	1440	110.39	21.17

4.7 Conclusions

Colorimetric films were successfully developed by coating formulated ink with black rice anthocyanin, on the surface of a corona-treated PET substrate. By using natural dye solutions within the pH range of 2–12, it is possible to visually see a color change when exposed to amine base gases. These gases are generated because of microbial activity during the spoilage of meat and fish products. The FTIR spectra results indicate that the inclusion of PEG as a co-binder can lead to the formation of an additional link between the PVOH groups, validating the interaction between functional groups and enhancing the adhesion properties. The findings from the tape and abrasion tests indicate that the use of thermal treatment for colorimetric films may enhance the adhesive bonding between formulated ink and the substrate by eliminating water. Moreover, heat drying colorimetric indicators at elevated temperatures can cause anthocyanin degradation, which could result in poorer color change. Therefore, optimization of the heating process (time and temperature) and choosing the pH level for ink formulation are two crucial parameters for developing pH indicators. Finally, the developed colorimetric film benefits from using inexpensive, readily available, and environmentally friendly dyes and an easy printing process for food packaging applications. Therefore, this approach will effectively address a significant drawback associated with on-package sensors, namely the potential for chemical migration onto food.

Acknowledgements

The funding for this research project is gratefully acknowledged from the Natural Sciences and Engineering Research Council of Canada (NSERC), 3Spack Industrial Research Chair, Research Center for High Performance Polymer and Composite Systems (CREPEC), Chemical Engineering Department, Polytechnique Montréal, ProAmpac flexible packaging, and Prima. I express my gratitude to Dr. Bentolhoda Heli for her academic and spiritual guidance.

4.8 Reference

[1] W. Huang et al., "Flexible sensing enabled agri-food cold chain quality control: A review of mechanism analysis, emerging applications, and system integration," *Trends in Food Science & Technology*, 2023.

- [2] W. Sun, H. Li, H. Wang, S. Xiao, J. Wang, and L. Feng, "Sensitivity enhancement of pH indicator and its application in the evaluation of fish freshness," *Talanta*, vol. 143, pp. 127-131, 2015
- [3] E. Balbinot-Alfaro, D. V. Craveiro, K. O. Lima, H. L. G. Costa, D. R. Lopes, and C. Prentice, "Intelligent packaging with pH indicator potential," *Food engineering reviews*, vol. 11, pp. 235-244, 2019.
- [4] E. Poyatos-Racionero, J. V. Ros-Lis, J.-L. Vivancos, and R. Martinez-Manez, "Recent advances on intelligent packaging as tools to reduce food waste," *Journal of cleaner production*, vol. 172, pp. 3398-3409, 2018.
- [5] J. K. Heising, G. Claassen, and M. Dekker, "Options for reducing food waste by quality-controlled logistics using intelligent packaging along the supply chain," *Food Additives & Contaminants: Part A*, vol. 34, no. 10, pp. 1672-1680, 2017.
- [6] K. Pounds et al., "Glycerol-based dendrimer nanocomposite film as a tunable pH-Sensor for food packaging," *ACS Applied Materials & Interfaces*, vol. 13, no. 19, pp. 23268-23281, 2021.
- [7] J. Liu et al., "Extract from *Lycium ruthenicum* Murr. Incorporating κ -carrageenan colorimetric film with a wide pH-sensing range for food freshness monitoring," *Food Hydrocolloids*, vol. 94, pp. 1-10, 2019.
- [8] Y. Liu, Y. Qin, R. Bai, X. Zhang, L. Yuan, and J. Liu, "Preparation of pH-sensitive and antioxidant packaging films based on κ -carrageenan and mulberry polyphenolic extract," *International journal of biological macromolecules*, vol. 134, pp. 993-1001, 2019.
- [9] W. Lan, S. Wang, Z. Zhang, X. Liang, X. Liu, and J. Zhang, "Development of red apple pomace extract/chitosan-based films reinforced by TiO₂ nanoparticles as a multifunctional packaging material," *International Journal of Biological Macromolecules*, vol. 168, pp. 105-115, 2021.
- [10] K. Zhang, T.-S. Huang, H. Yan, X. Hu, and T. Ren, "Novel pH-sensitive films based on starch/polyvinyl alcohol and food anthocyanins as a visual indicator of shrimp deterioration," *International Journal of Biological Macromolecules*, vol. 145, pp. 768-776, 2020.

- [11] S. Kang et al., "Colorimetric film based on polyvinyl alcohol/okra mucilage polysaccharide incorporated with rose anthocyanins for shrimp freshness monitoring," *Carbohydrate Polymers*, vol. 229, p. 115402, 2020.
- [12] J. J. Leisner and L. Gram, "FISH | Spoilage of Fish," in *Encyclopedia of Food Microbiology* (Second Edition), A. B. Carl and T. Mary Lou Eds., Second Edition ed. Oxford: Academic Press, 2014, pp. 932-937.
- [13] J. Kerry and P. Butler, *Smart packaging technologies for fast moving consumer goods*. John Wiley & Sons, 2008.
- [14] D. N. Dikmetas, E. Uysal, F. Karbancioglu-Guler, and S. Gurmen, "The production of pH indicator Ca and Cu alginate ((1, 4)- β -d-mannuronic acid and α -l-guluronic acid) cryogels containing anthocyanin obtained via red cabbage extraction for monitoring chicken fillet freshness," *International Journal of Biological Macromolecules*, vol. 231, p. 123304, 2023.
- [15] Y. S. Musso, P. R. Salgado, and A. N. Mauri, "Gelatin based films capable of modifying its color against environmental pH changes," *Food Hydrocolloids*, vol. 61, pp. 523-530, 2016.
- [16] A. Castañeda-Ovando, M. de Lourdes Pacheco-Hernández, M. E. Páez-Hernández, J. A. Rodríguez, and C. A. Galán-Vidal, "Chemical studies of anthocyanins: A review," *Food chemistry*, vol. 113, no. 4, pp. 859-871, 2009.
- [17] P. Shao et al., "An overview of intelligent freshness indicator packaging for food quality and safety monitoring," *Trends in Food Science & Technology*, vol. 118, pp. 285-296, 2021/12/01/2021, doi: <https://doi.org/10.1016/j.tifs.2021.10.012>.
- [18] T. C. Wallace and M. M. Giusti, "Anthocyanins—nature's bold, beautiful, and health-promoting colors," vol. 8, ed: MDPI, 2019, p. 550.
- [19] H. E. Khoo, A. Azlan, S. T. Tang, and S. M. Lim, "Anthocyanidins and anthocyanins: Colored pigments as food, pharmaceutical ingredients, and the potential health benefits," *Food & nutrition research*, vol. 61, no. 1, p. 1361779, 2017.
- [20] G. T. Sigurdson, P. Tang, and M. M. Giusti, "Natural colorants: Food colorants from natural sources," *Annual review of food science and technology*, vol. 8, pp. 261-280, 2017.

- [21] N. Oladzadabbasabadi, A. M. Nafchi, M. Ghasemlou, F. Ariffin, Z. Singh, and A. Al-Hassan, "Natural anthocyanins: Sources, extraction, characterization, and suitability for smart packaging," *Food Packaging and Shelf Life*, vol. 33, p. 100872, 2022.
- [22] T. Liang, G. Sun, L. Cao, J. Li, and L. Wang, "A pH and NH₃ sensing intelligent film based on *Artemisia sphaerocephala* Krasch. gum and red cabbage anthocyanins anchored by carboxymethyl cellulose sodium added as a host complex," *Food hydrocolloids*, vol. 87, pp. 858-868, 2019.
- [23] F. S. Mohseni-Shahri and F. Moeinpour, "Development of a pH-sensing indicator for shrimp freshness monitoring: Curcumin and anthocyanin-loaded gelatin films," (in eng), *Food Sci Nutr*, vol. 11, no. 7, pp. 3898-3910, Jul 2023, doi: 10.1002/fsn3.3375.
- [24] M. Alizadeh-Sani et al., "pH-responsive color indicator films based on methylcellulose/chitosan nanofiber and barberry anthocyanins for real-time monitoring of meat freshness," *International Journal of Biological Macromolecules*, vol. 166, pp. 741-750, 2021. [Online]. Available: <https://www.sciencedirect.com/science/article/pii/S0141813020348716?via%3Dihub>.
- [25] F. S. Mohseni-Shahri and F. Moeinpour, "Development of a pH-sensing indicator for shrimp freshness monitoring: Curcumin and anthocyanin-loaded gelatin films," *Food Science & Nutrition*, 2023.
- [26] S. Roy and J.-W. Rhim, "Preparation of carbohydrate-based functional composite films incorporated with curcumin," *Food Hydrocolloids*, vol. 98, p. 105302, 2020.
- [27] P. Ezati and J.-W. Rhim, "pH-responsive pectin-based multifunctional films incorporated with curcumin and sulfur nanoparticles," *Carbohydrate Polymers*, vol. 230, p. 115638, 2020.
- [28] M. Moradi, H. Tajik, H. Almasi, M. Forough, and P. Ezati, "A novel pH-sensing indicator based on bacterial cellulose nanofibers and black carrot anthocyanins for monitoring fish freshness," *Carbohydrate Polymers*, vol. 222, p. 115030, 2019.
- [29] P. Ezati, Y.-J. Bang, and J.-W. Rhim, "Preparation of a shikonin-based pH-sensitive color indicator for monitoring the freshness of fish and pork," *Food Chemistry*, vol. 337, p. 127995, 2021.

- [30] H. Dong, Z. Ling, X. Zhang, X. Zhang, S. Ramaswamy, and F. Xu, "Smart colorimetric sensing films with high mechanical strength and hydrophobic properties for visual monitoring of shrimp and pork freshness," *Sensors and Actuators B: Chemical*, vol. 309, p. 127752, 2020.
- [31] Y. Li, K. Wu, B. Wang, and X. Li, "Colorimetric indicator based on purple tomato anthocyanins and chitosan for application in intelligent packaging," *International Journal of Biological Macromolecules*, vol. 174, pp. 370-376, 2021.
- [32] C. Wu et al., "Preparation of an intelligent film based on chitosan/oxidized chitin nanocrystals incorporating black rice bran anthocyanins for seafood spoilage monitoring," *Carbohydrate Polymers*, vol. 222, p. 115006, 2019.
- [33] H. Li et al., "Highly pigmented vegetables: Anthocyanin compositions and their role in antioxidant activities," *Food research international*, vol. 46, no. 1, pp. 250-259, 2012.
- [34] J. Shipp and E.-S. M. Abdel-Aal, "Food applications and physiological effects of anthocyanins as functional food ingredients," *The open food science journal*, vol. 4, no. 1, 2010.
- [35] E. Tsochatzis, J. A. Lopes, and M. Corredig, "Chemical testing of mechanically recycled polyethylene terephthalate for food packaging in the European Union," *Resources, Conservation and Recycling*, vol. 179, p. 106096, 2022.
- [36] T. Fernández-Menéndez, D. García-López, A. Argüelles, A. Fernández, and J. Viña, "Industrially produced PET nanocomposites with enhanced properties for food packaging applications," *Polymer Testing*, vol. 90, p. 106729, 2020.
- [37] V. C. Louzi and J. S. de Carvalho Campos, "Corona treatment applied to synthetic polymeric monofilaments (PP, PET, and PA-6)," *Surfaces and Interfaces*, vol. 14, pp. 98-107, 2019.
- [38] M. Lindner, N. Rodler, M. Jesdinszki, M. Schmid, and S. Sänglerlaub, "Surface energy of corona treated PP, PE and PET films, its alteration as function of storage time and the effect of various corona dosages on their bond strength after lamination," *Journal of Applied Polymer Science*, vol. 135, no. 11, p. 45842, 2018.
- [39] L. Penn and H. Wang, "Chemical modification of polymer surfaces: a review," *Polymers for Advanced Technologies*, vol. 5, no. 12, pp. 809-817, 1994.

- [40] S. Siau, A. Vervaet, A. Van Calster, I. Swennen, and E. Schacht, "Influence of wet chemical treatments on the evolution of epoxy polymer layer surface roughness for use as a build-up layer," *Applied surface science*, vol. 237, no. 1-4, pp. 457-462, 2004.
- [41] E. Liston, L. Martinu, and M. Wertheimer, "Plasma surface modification of polymers for improved adhesion: a critical review," *Journal of adhesion science and technology*, vol. 7, no. 10, pp. 1091-1127, 1993.
- [42] C. J. Wohl, M. A. Belcher, S. Ghose, and J. W. Connell, "Modification of the surface properties of polyimide films using polyhedral oligomeric silsesquioxane deposition and oxygen plasma exposure," *Applied Surface Science*, vol. 255, no. 18, pp. 8135-8144, 2009.
- [43] C. Sun, D. Zhang, and L. C. Wadsworth, "Corona treatment of polyolefin films—A review," *Advances in Polymer Technology: Journal of the Polymer Processing Institute*, vol. 18, no. 2, pp. 171-180, 1999.
- [44] P. Fabbri and M. Messori, "Surface modification of polymers: chemical, physical, and biological routes," in *Modification of polymer properties*: Elsevier, 2017, pp. 109-130.
- [45] W.-B. Chu, J.-W. Yang, T.-J. Liu, C. Tiu, and J. Guo, "The effects of pH, molecular weight and degree of hydrolysis of poly (vinyl alcohol) on slot die coating of PVA suspensions of TiO₂ and SiO₂," *Colloids and Surfaces A: Physicochemical and Engineering Aspects*, vol. 302, no. 1-3, pp. 1-10, 2007.
- [46] J. Sarfraz, T. Gulin-Sarfraz, J. Nilsen-Nygaard, and M. K. Pettersen, "Nanocomposites for food packaging applications: An overview," *Nanomaterials*, vol. 11, no. 1, p. 10, 2020.
- [47] E. Y. Malikov et al., "Synthesis and characterization of polyvinyl alcohol based multiwalled carbon nanotube nanocomposites," *Physica E: Low-dimensional Systems and Nanostructures*, vol. 61, pp. 129-134, 2014.
- [48] D. Urban, B. Schuler, and J. Schmidt-Thümmes, "Large volume applications of latex polymers," *Chemistry and Technology of Emulsion Polymerisation*, pp. 253-282, 2013.
- [49] W. J. Auhorn, "Chemical additives," *Handbook of paper and board*, pp. 62-149, 2006.

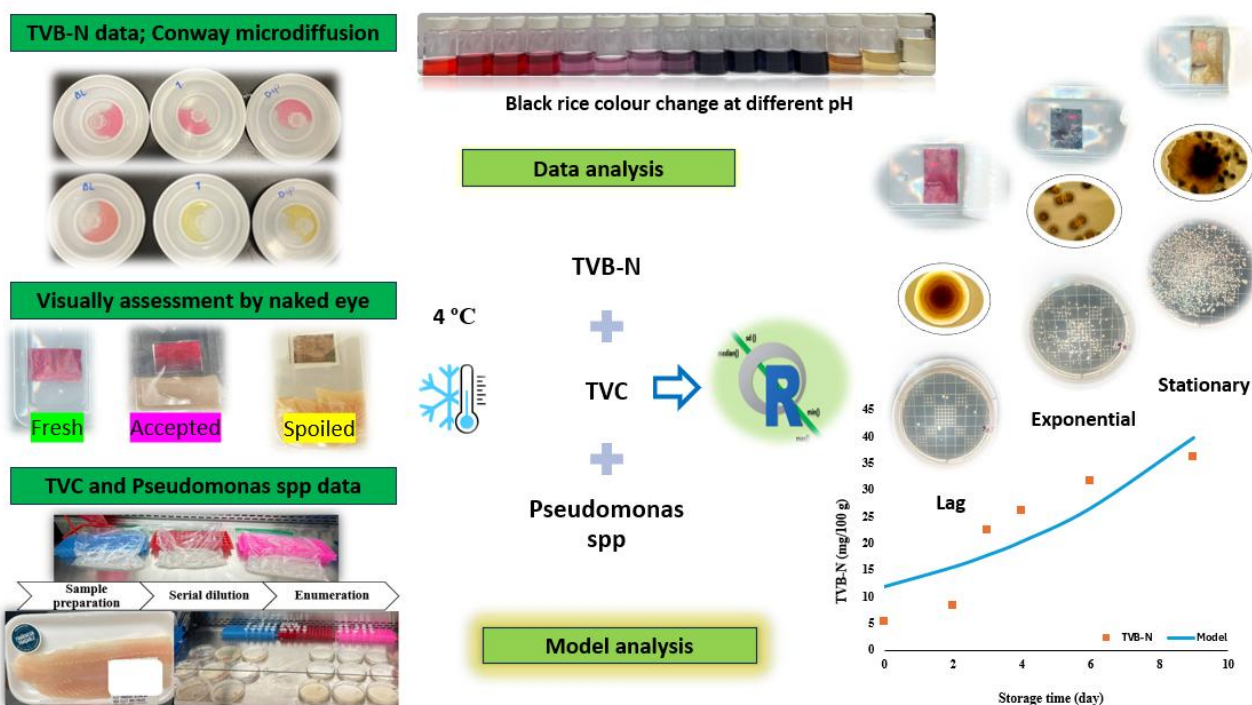
- [50] S. Lorca, F. Santos, and A. J. Fernández Romero, "A review of the use of GPEs in zinc-based batteries. A step closer to wearable electronic gadgets and smart textiles," *Polymers*, vol. 12, no. 12, p. 2812, 2020.
- [51] J. Laine, "Effect of synthetic modifiers on the rheology of coating colours," 2015.
- [52] B. Kuswandi, M. Moradi, and P. Ezati, "Food sensors: Off-package and on-package approaches," *Packaging Technology and Science*, vol. 35, no. 12, pp. 847-862, 2022.
- [53] Y. Yuan and T. R. Lee, "Contact angle and wetting properties," in *Surface science techniques*: Springer, 2013, pp. 3-34.
- [54] S. Tape, "Standard Test Methods for Rating Adhesion by Tape Test1."
- [55] J. Lee, R. W. Durst, R. E. Wrolstad, and Collaborators:, "Determination of Total Monomeric Anthocyanin Pigment Content of Fruit Juices, Beverages, Natural Colorants, and Wines by the pH Differential Method: Collaborative Study," *Journal of AOAC INTERNATIONAL*, vol. 88, no. 5, pp. 1269-1278, 2019, doi: 10.1093/jaoac/88.5.1269.
- [56] R. E. W. M.Mónica Giusti "Acylated anthocyanins from edible sources and their applications in food systems," *Biochemical Engineering Journal*, vol. 14, no. Issue 3, June 2003, pp. 217-225, 2003, doi: [https://doi.org/10.1016/S1369-703X\(02\)00221-8](https://doi.org/10.1016/S1369-703X(02)00221-8).
- [57] E. A. Vogler, "Structure and reactivity of water at biomaterial surfaces," *Advances in Colloid and Interface Science*, vol. 74, no. 1–3, 1 February 1998, pp. 69-117, 1998, doi: [https://doi.org/10.1016/S0001-8686\(97\)00040-7](https://doi.org/10.1016/S0001-8686(97)00040-7).
- [58] H. Yong, J. Liu, Y. Qin, R. Bai, X. Zhang, and J. Liu, "Antioxidant and pH-sensitive films developed by incorporating purple and black rice extracts into chitosan matrix," *International Journal of Biological Macromolecules*, vol. 137, pp. 307-316, 2019.
- [59] A. Musetti, K. Paderni, P. Fabbri, A. Pulvirenti, M. Al-Moghazy, and P. Fava, "Poly (vinyl alcohol)-based film potentially suitable for antimicrobial packaging applications," *Journal of food science*, vol. 79, no. 4, pp. E577-E582, 2014.

- [60] R. Cortez, D. A. Luna-Vital, D. Margulis, and E. Gonzalez de Mejia, "Natural pigments: stabilization methods of anthocyanins for food applications," *Comprehensive Reviews in Food Science and Food Safety*, vol. 16, no. 1, pp. 180-198, 2017.
- [61] M. E. El-Naggar, M. H. El-Newehy, A. Aldalbahi, W. M. Salem, and T. A. Khattab, "Immobilization of anthocyanin extract from red-cabbage into electrospun polyvinyl alcohol nanofibers for colorimetric selective detection of ferric ions," *Journal of Environmental Chemical Engineering*, vol. 9, no. 2, p. 105072, 2021.
- [62] J.-H. B. Hatier and K. S. Gould, "Anthocyanin function in vegetative organs," *Anthocyanins: biosynthesis, functions, and applications*, pp. 1-19, 2009.
- [63] J.-M. Kong, L.-S. Chia, N.-K. Goh, T.-F. Chia, and R. Brouillard, "Analysis and biological activities of anthocyanins," *Phytochemistry*, vol. 64, no. 5, pp. 923-933, 2003.
- [64] J. Wang et al., "The influence of processing conditions on kinetics, anthocyanin profile and antioxidant activity of purple sweet potato subjected to hot air drying," *Journal of Food Process Engineering*, vol. 43, no. 9, p. e13472, 2020.

**CHAPTER 5 ARTICLE 2: ENHANCING SEAFOOD FRESHNESS
MONITORING: INTEGRATION COLOR CHANGE OF A FOOD-SAFE
ON-PACKAGE COLORIMETRIC SENSOR WITH MATHEMATICAL
MODELS, MICROBIOLOGICAL, AND CHEMICAL ANALYSES**

Credit Author Statement

Maryam Ameri: Conceptualization, Investigation, Experimental work, Data curation, Writing – original draft. Writing – review & editing , bibliographic, Project administration. Abdellah Ajji: Conceptualization, Supervision, Funding acquisition, review & editing. Samuel Kessler: Conceptualization, Supervision, review & editing.



Abstract figure:

Highlights

- Food-safe colorimetric films can monitor fish freshness/spoilage at 4 °C during the storage period.
- The efficacy of an on-package colorimetric sensor was assessed in packaging trials with chemical biomarkers and microbial analysis.
- Integrating mathematical models predict seafood spoilage and align these predictions with pH indicators' visual assessments.
- This approach offers a smart, efficient, and eco-friendly solution for improving shelf-life prediction and fish quality assessment.

Authors: Maryam Ameri¹[ID](#), Abdellah Ajji¹[ID](#), Samuel Kessler²

Corresponding authors: Maryam.ameri@polymtl.ca and Abdellah.ajji@polymtl.ca

3. Chemical Engineering Department, Polytechnique Montréal, Montréal, Québec H3T 1J4, Canada.

4. Active/Intelligent Packaging, ProAmpac, Cincinnati, Ohio 45246, United States.

Submitted in Current Research in Food Science journal, 7 October 2024

5.1 Abstract

The study assessed a developed food-safe on-package label as a real-time spoilage indicator for fish fillets. This colorimetric sensor is sensitive to Total Volatile Base Nitrogen (TVB-N) levels, providing an indication of fish freshness and spoilage. This study evaluates and predicts the shelf-life and effectiveness of an on-package colorimetric indicator. The sensor, using black rice (BC) dye with polyvinyl alcohol (PVOH), polyethylene glycol (PEG), and citric acid (CA) as binders and crosslinking agents, is applied to PET films. The food-safe pH indicator, prepared via lab-scale flexography printing, is durable in humid environments, making it suitable for practical packaging scenarios. The sensor visibly monitored fish spoilage at 4 °C for 9 days. Quality assessment included tracking ΔRGB (total color difference), chemical (TVB-N, pH), and microbiological analyses. Results indicate that the fish samples are fresh up to 4 days of storage at 4 °C with the total viable count (TVC), *Pseudomonas* growth, TVB-N contents and pH reaching: 5.2 (log CFU/ml), 4.31(log CFU/ml), 26.22 (mg N/100 gr sample) and 7.48, respectively. Integrating colorimetric sensor data with mathematical modeling can predict spoilage trends over time. An integrated system offers a smart approach to accurately predict shelf-life, aiding in optimizing storage conditions, minimizing food waste, and delivering fresh, high-quality fish products to consumers.

Keywords: On-package sensor, Intelligent packaging, Quality assessment, pH indicator, Anthocyanin, Fish spoilage

5.2 Introduction

Fish is a highly perishable food item, its shelf-life is influenced by various factors, including species, quality, initial microbial load, physical changes, storage temperature, and packaging conditions [1-3]. Spoilage can occur rapidly due to microbial activity, lipid oxidation, and autolysis, rendering the fish inedible [1, 4]. Microbial deterioration is the primary factor affecting the freshness of fish. Under specific storage conditions, specific spoilage organisms (SSOs) decompose various fish tissues, producing off-odors, off-flavors, and volatiles [1, 4-8]. This

microbial spoilage generates volatile bases such as ammonia (NH_3), dimethylamine (DMA), and trimethylamine (TMA), collectively known as total volatile basic nitrogen (TVB-N) [9-11]. These compounds lead to a gradual increase in pH within the packaging headspace, detectable by pH-sensitive indicators to communicate food freshness levels [12].

Intelligent packaging extends traditional packaging functionalities to meet consumer needs and expectations [13]. For example, plant-derived pH-sensitive inks can be used in colorimetric indicators to monitor the freshness/spoilage of fish products, responding to TVB-N concentration increases during spoilage [14-17]. Intelligent packaging use detection means, such as natural dyes, to monitor food freshness, microbiological growth, and chemical changes visually and/or quantitatively in real time [18]. Such strategies can offer a fast, non-invasive and reliable food quality assessment [19]. However, many on-package sensors require direct food contact [20, 21], raising concerns about the migration of substances from the indicator into the food, which poses safety risks [22, 23]. Therefore, the chemical components of the coating must be safe and non-toxic [22, 24].

Recently, researchers have explored anthocyanins—natural dyes recognized as safe—to develop colorimetric pH indicators [25, 26]. These compounds change colors at different pH levels due to molecular structure changes [27]. However, natural pH indicators may degrade over time, especially when exposed to the conditions typically found in food packaging (e.g., high humidity). This degradation can reduce the indicator's effectiveness and accuracy over the product's shelf-life [28]. Producing natural pH indicators with consistent quality and performance can be challenging due to the variability in natural raw materials. This inconsistency can lead to variations in the performance of the indicators [29]. The color changes of natural pH indicators can sometimes be subtle and difficult to perceive accurately with the naked eye. This can lead to misinterpretation of the spoilage status [22].

High humidity in fish packaging poses difficulties for pH-sensitive dyes, as they readily migrate to moisture-laden food [30]. To address this issue, researchers have suggested crosslinking the polymeric matrix to maintain mechanical stability [31, 32]. Citric acid can serve a crosslinking agent to improve anthocyanins' water fastness, as they are prone to dye leaching in humid conditions [33-35], making pH indicator suitable for long-term use [36]. When citric acid reacts with the binder system, consisting of PVOH and PEG, water is produced through Fischer

esterification [37]. The addition of the organic acids without successive thermal treatments has a mere plasticising effect, while their application with thermal treatment has a combined crosslinking and plasticising effect [32]. Therefore, after thermal treatment of film indicators, their vulnerability towards the high humidity area could be decreased, addressing one of the commercialization challenges of pH indicators [33].

Food quality can be monitored through periodic microbiological and chemical analysis (TVB-N and pH) within regular tests [38]. Integrating these analyses with color change analysis, allows for shelf-life estimation [39-44]. The exact spoilage threshold can vary depending on several factors; including catch season, catch maturity, geographical origin, species, age and gender of the fish [14, 22, 45]. Huss [46] and European Commission (EC) [47] reported acceptable limit value for TVB-N as 30–35 mg/100 g and 25–35 mg/100 g, respectively [4]. TVB-N level of 35 mg/100 g fish flesh [48, 49] with a total viable count (TVC) of 7 log CFU/g, is considered the upper limit for fish shelf-life [4, 14, 50]. These metrics guide the pH indicator scaling in this study to reflect the end of the fish samples' shelf-life.

Predictive microbiology anticipates SSO growth to determine the shelf-life of fish products. Specific spoilage bacteria development in fish results from environmental factors and microbial competition. In aerobically packed fish, competition occurs between aerobic gram-negative flora, such as primarily *Pseudomonas* [51]. Empirical models like the Gompertz, logistic, and modified Arrhenius models predict microbial growth kinetics and estimate fish shelf-life based on microbial counts. Kinetic models simulate TVB-N progression and protein degradation during storage at 5° C [52]. However, mathematical models for shelf-life prediction in complex food environments like fish may lack accuracy due to factors affecting microbial development, including food structure and microorganism interaction [53]. This study combined model outcomes with the designed colorimetric sensor's color change response to address this issue. We evaluated the on-package labels for fish freshness monitoring by using microbial counts, chemical analyses [47, 54] and color analysis. This paper builds upon that foundational work and further explores the application and performance of the sensor under varying conditions. In this study, Pangasius (*Pangasius hypothalamus*), a white-fleshed fish with a moderate flavor, was chosen as sample. Fatty fish, such as pangas, have emerged as a highly important aquaculture species economically due to their fast growth, year-round output, and high productivity [55]. The developed pH indicators (flexible PET

films coated with natural dyes) serve as pH-responsive sensor, exhibiting precise visual variations at different pH values. The design minimizes dye leaching and is highly sensitive to TVB-N gases, making it suitable for real-time seafood package monitoring.

5.3 Materials and methods

5.3.1 Materials

We acquired pangasius fillets from a nearby Metro grocery store in Montreal, Quebec, Canada. Initially, the products were sealed in PVC-wrapped packages that displayed a label containing the packaging date and the best before date (which was three days after the packaging date). The samples were placed in an ice container to maintain their temperature and freshness during transportation. Prior to being stored in the laboratory fridge at a temperature of 4°C, they were cleaned using 70% alcohol to eliminate any slime and sanitize the surface [56]. The samples remained in the fridge until they were ready to be use. The Polytechnique Montreal in Montreal, Quebec, Canada, served as the site of all the experiments. Transparent polyethylene terephthalate films (PET, 23 µm) were obtained from ProAmpac Packaging Canada company, Terrebonne, Quebec, Canada. Black rice extract 80% was purchased from Xiherbs Phytochem Co., Ltd (Dongguan, Guangdong, China). Certified amber glass jars with white polypropylene caps and bonded PTFE-faced silicone septa were obtained from Thermo Fisher Scientific, Saint-Laurent, Quebec, to comply with EPA Performance-Based Specifications for volatile organic analysis. Polyvinyl alcohol (87~88% hydrolysis, 145,000 MW), Polyethylene glycol (PEG), Citric acid (ACS reagent, ≥99.5%), Vanillin (natural, ≥97%, FCC, FG), Hydrochloric acid (HCL), Potassium carbonate (K₂CO₃), Trichloroacetic acid (TCA, ACS reagent, ≥99.0%), Boric acid (H₃BO₃, ACS reagent, ≥99.5%), Sodium Chloride (NaCl), Dimethylamine solution (DMA, 2 M in methanol), Trimethylamine solution (TMA, 31-35 wt. % in ethanol, 4.2 M), Ammonium hydroxide solution (NH₄OH, 30-33% NH₃ in H₂O), Conway diffusion cell, Vortex-Genie 2 (120 V) mixer, Agar and Pseudomonas Isolation Agar were purchased from Millipore Sigma Canada Ltd , Oakville, Ontario, Canada.

5.3.2 Sensor preparation

A comprehensive description of the formulated ink and sensor preparation were detailed using a previously reported method with some modification [33]. Specifically, we described the colorimetric sensor's preparation method as follows: PVOH and deionized water were mixed in a glass beaker to create a heterogeneous mixture. A solution mixer made of PEG, C, BC and distilled water was added after the solution cooled at room temperature while being stirred constantly. The coating was carried out with a TQC automatic film applicator (model AB3652). The drying process of the films proceeded at two temperatures: ambient (30 min) and 165 °C (5 min). Samples were labeled NTT (no thermal treatment) and TT (Thermal treated pH indicators, at temperature of 165 °C for 5 min).

5.4 Characterization of pH indicators

5.4.1 Fourier-Transform Infrared Spectroscopy (FTIR-ATR)

The FTIR spectra of the samples were recorded at room temperature using a Perkin Elmer FT-IR spectrometer 65 coupled to an ATR accessory, with a diamond crystal (Waltham, MA, USA). The data was collected using Perkin Elmer spectrum. The spectra were acquired in the range 4000–600 cm^{-1} , with 16 accumulations and a resolution of 16 cm^{-1} . In our previous study, we examined the characterization of the pH indicator including FTIR characterization [18].

5.4.2 Thermogravimetric Analysis (TGA)

A TGA thermal thermogram shows sample mass change vs. temperature. Each compound has a unique thermogram that shows thermal stability, multi-component composition, decomposition kinetics, moisture, and volatile content [57]. Thermogravimetric analysis (TGA) for prepared film indicators and raw material of ink formulation were conducted under a nitrogen atmosphere at a scan rate of 20 °C/min with a Shimadzu DTG-60H thermal analyzer.

5.4.3 Packaging study using RGB

To evaluate the sensitivity of developed pH indicator towards TVB-N gases originated from fish samples, 3 cm × 2 cm films were cut, and put inside the plastic bags and containers with fish samples. Before using these bags and containers, we exposed them to alcohol at 70% purity, and we let them become dry at room temperature for a few hours. Color change of the indicators was measured with an Epson Perfection V550 scanner (Nagano, Japan). The resolution of the pictures

was 800 dpi with reflection mod. The scanning time was approximately 2 minutes, and the type of image was 24-bit color. Blacklight correction was also considered for adjustment. The test run for 3 different spots (pixels and considering their neighborhood) inside each picture and the mean and standard deviation were calculated. Control samples were chosen as reference image for RGB calculation. The color change of pH indicators during storage period is measured by the total color difference (ΔRGB) according to the following equation [27].

$$\Delta RGB = \sqrt{(R - R_0)^2 + (G - G_0)^2 + (B - B_0)^2} \quad (5.1)$$

Where R_0 , B_0 , G_0 are the initial color parameters of indicators and R , G and B were the values at the time of sampling.

5.4.4 Chemical stability and recovery tests

To simulate the long-term storage conditions of pH indicators in a shorter period, we used wide-mouth septa jars with a capacity of 60 ml, which are suitable for analyzing organic volatile compounds. We affixed pH indicator films to the plastic caps of these jars. The indicators were evaluated against external standards at various concentrations: 0.025, 0.125, 0.25, 0.5, 0.75, 1, 1.25, 1.5 (%wt./wt.) by diluting ammonium hydroxide solution, DMA and TMA. We prepared each standard by vigorously mixing them with a vortex for 20 seconds.

As these experiments required us to attach the indicator inside vials for exposure to the TVB-N gases and then removing them to take pictures, some displacement was unavoidable. The images for these experiments were captured using a smartphone (iPhone 12), as scanning was not feasible for certain samples.

5.5 Fish shelf-life monitoring

In a previous study, we developed a colorimetric sensor and evaluated its ability to change color toward TVB-N gases. Also, we tailored the pH sensing properties of the developed pH indicator such as selectivity and sensitivity towards TVB-N gases and response time [33]. It was reported that the microbial population of pangas ranged from 6.213 ± 0.633 to 7.315 ± 0.570 log CFU/g in winter [58]. The Microbiological-and Chemical analysis for shelf-life studies were conducted on Pangasius fish upon storage at around 4°C during the winter of 2024 in Montreal, Quebec, Canada. The day of purchase was taken to be day 0 (the first day the fish was packaged at store for sale).

The results were then compared with the color changing of a pH indicator and chemical analysis, which were conducted simultaneously.

5.5.1 TVB-N content

Conway micro diffusion method was used with some modification in order to quantify the amount of produced TVB-N during fish spoilage [59, 60]. At every sampling point, portions of 5 ± 0.5 g of fish were added to 20 ml of TCA 4% (w/v) and homogenized for 1 min at high speed, then samples filtered with Whatman #1. One side of the exterior of the Conway dish was filled with 1 ml of the prepared sample, and the other side with 1 ml of 50 g K_2CO_3 in 100 ml distilled water. 100 microliters of Conway indicator (methyl red), and 1ml of 2% H_3BO_3 placed inside the inner side of the Conway dish. Some cautions in order to avoid failure to get accurate results were taken into account [61], Eq (5.2):

$$TVB - N \left(\frac{mg}{100g} \right) = (V_S - V_B) \times N_{HCL} \times A_N \times \frac{[(W_S \times \frac{M}{100}) + V_E] \times 100}{W_S} \quad (5.2)$$

Where V_S =Titration volume of HCl for sample (ml), V_B = Titration volume of HCl for blank (ml), N_{HCL} =Normality of HCl, A_N =Atomic weight of nitrogen (14.00), W_S = weight of sample (g), M = Moisture content in sample (%), V_E = Volume of TCA used in extraction (ml).

5.5.2 pH measurement

A 5 g of fish sample were added to 90 ml of distilled water and then homogenized (by the vortex for 2 min). pH of suspension as function of storage time was measured using a pH meter (Mettler Toledo, Mississauga, Ontario, Canada) after 5 minutes incubation at room temperature [62]. The pH meter was calibrated using pH buffer solutions (4.00 ± 0.01 , 7.00 ± 0.01 , 10.00 ± 0.01).

5.5.3 Microbial analysis

During fish storage at 4 °C, the total viable count (TVC) method revealed bacterial growth reaching the spoiling threshold (1×10^7 CFU/ml)[63]. Microbial analysis was performed by weighted fish samples (10 ± 0.5 g) which were placed in sterilized bags. The sterilized NaCl (9 %w/v) saline solution (90 ml) was added to bags and homogenized with vortex for 2 min at room temperature. Serial sample dilutions were made during the fish spoiling tests[64]. For the enumeration of the total microbial population, 100µl of serial dilutions were spread on the surface of dried media Petri dishes and incubated (Economy Incubators IB-11E, 150 L, Biotech Inc, Montréal, Canada) the

plates overnight at 37 °C (ISO,4833:2003) [65]. Also, for the enumeration and *Pseudomonas* spp, 100µl of serial dilutions were spread on the surface of dried *Pseudomonas* Isolation Agar at 25 °C for 44h ± 4h (ISO, 13720:2010).

After the mentioned period for incubation, colonies on the agar plates were counted by a Darkfield Quebec Colony Counter. The results were expressed (according to ISO 7218:2007) as mean log CFU/ml ± standard deviation of 3 replicates.

5.6 Mathematical modeling of fish spoilage based on TVB-N, TVC and *Pseudomonas* spp experimental data

The models were derived from microbiological media observations and chemical experiments in a well-controlled lab. The data points of TVB-N and TVC of the current study were utilized to fit with established empirical models stated in the literature, as presented in **Table 5.1**.

As multiple parameters are necessary to construct a model for the shelf-life prediction [149] we predict different parameters by R software. The models utilized for TVB-N prediction incorporate the following variables: TVB-N content (represented by Y), rate constant (k), and storage time (t in days). Y_0 is the TVB-N content at day 0, i.e., when the fish arrives for storage. The employed microbial growth models for this study were the Modified Arrhenius logistics, logistic, modified logistic and modified Gompertz [67] which are described in **Table 5.1**; where: Y(t) is the TVC at time t, A is the upper asymptote of the curve, representing the maximum TVC, μ_{\max} is maximal growth rate (in day⁻¹), the load capacity of biomass dynamics is stated by B, t_0 is the lag phase or lag time before TVC accumulation begins and t is the storage time.

Table 5.1 Empirical models for modeling TVB-N, TVC and *pseudomonas* spp growth.

Model name	Model equation	Reference
Exponential model	$Y = Y_0 A e^{Kt}$	[150]

Model name	Model equation	Reference (Continued)
Exponential Polynomial	$Y = Ae^{(Kt+Bt^2)}$	Current study
Modified Arrhenius (I)	$Y = Y_0 + K \exp\left(\frac{D}{t+1}\right)$	Current study
Modified Arrhenius (II)	$Y = Y_0 + K \exp(Dt)$	Current study
Howgate	$Y = \frac{Y_{\max} - Y_{\min}}{1 + e^{K(td-t)}}$	[151]
Logistic	$Y = \frac{A}{1 + e^{-K(t-B)}}$	[152]
Modified Logistic	$Y = \frac{A}{1 + Be^{-Kt}}$	[152]
Modified Gompertz	$Y = Y_0 + \frac{A}{e^{e^{\left(\exp(1) \times \mu_{\max} \frac{(t-t_0)}{A} + 1\right)}}}$	[153]

5.6.1 Model Evaluation Metrics

Since the models used for prediction of TVB-N and TVC behaviour are nonlinear; to discriminate the model performance they were discriminated based on the Akaike information criterion (AIC), and root mean square error (RMSE) as follows [71]:

$$RMSE = \sqrt{1/n \sum_{i=1}^n (Y_{i,e} - Y_{i,p})^2} \quad (5.3)$$

$$AIC = n \ln \left(\frac{SS_r}{n} \right) + 2p \quad (5.4)$$

$$AICc = n \ln \left(\frac{SS_r}{n} \right) + 2(p + 1) + 2(p + 1) \left(\frac{p+2}{n-p} \right) \quad (5.5)$$

$$BIC = n \ln \left(\frac{SS_r}{n} \right) + p \ln(p) \quad (5.6)$$

In this context, the experimental value of the i th experiment is denoted as $Y_{i,e}$, whereas the predicted value of the n^{th} experiment determined by the model is represented as $Y_{i,p}$, n indicates the quantity of experimental data points, SS_r represents the residual sum of squares, and p signifies the number of parameters [52]. The selection of the best-fitting model among the models that were tested is based on the criteria of the lowest values of RMSE and AIC.

5.7 Statical analysis

All measurements were conducted three times. Data were analyzed with Tukey test at a significance level of $p < 0.005$, $p < 0.001$ and $p < 0.001$. The results are reported as the average value \pm standard deviation (SD). The fitting parameters were found by using R software version 4.4.3.

5.8 Results and discussion

5.8.1 TGA

TGA was used to evaluate the thermal stability of anthocyanins and polymer components [72]. Understanding thermal stability helps predict polymeric coating durability during processing or application (e.g., curing, printing or coating process) at different temperatures [73]. As anthocyanins are sensitive to heat, TGA measurements can be informative to avoid dye degradation during thermal treatment process [74]. **Figure 5.1** depicts the thermal decomposition results for ink formulation components and **Figure 5.2** depicts thermal decomposition results for colorimetric sensors. For all samples from 40–110 °C, some water desorption and evaporation were observed, consistent with literature [72, 73, 75]. BC anthocyanin decomposed initially at 100 °C and 125–200 °C, respectively, due to the small amount of absorbed and bound water [76]. The initial decomposition of citric acid was observed at 200 °C, and the end of decomposition of citric acid with a weight loss (86%) was above 250–300 °C. This weight loss could be due to the decomposition of citric acid [77, 78].

During the initial region (below 200 °C in this study), a small amount (approximately 1.5 %) of the mass of PVOH is lost as adsorbed water evaporates [79]. The TGA graph demonstrates that the sample of PET coated with INK I, subjected to a thermal treatment at 165 °C for 5 minutes (INK I TT), the PET coated with INK I without thermal treatment (INK I NTT), and the uncoated PET films, all experience weight losses of approximately 94.45%, 98.20%, and 99.62%, respectively, at a temperature of 165 °C.

During the thermal treatment of colorimetric sensors, approximately 3.75% of the degradation can be attributed to this procedure. At this temperature, the weight of BC anthocyanins, PEG, PVOH, CA, and dried ink (with anthocyanins in the coating) decreases by about 95.78%, 96.18%, 97.95%, 99.63%, and 97.30%, respectively. This weight loss may include partial degradation of the dye molecules, loss of functional groups, or minor alterations in the chemical structure. Temperatures higher than 227 °C are the onset temperature of decomposition for formulated ink, as the weight loss reaches approximately 95% and the coating starts to break down chemically. Hence, the thermal decomposition associated with the dried formulated ink, PET films, and thermal treatment procedure is insignificant, resulting in only approximately 5% at a temperature of 165 °C, and the developed pH indicators can be considered thermally stable over the thermal treatment process. Aggressive thermal treatment (temperature and time) can cause the indicator to degrade sooner compared to the sample without thermal treatment [80].

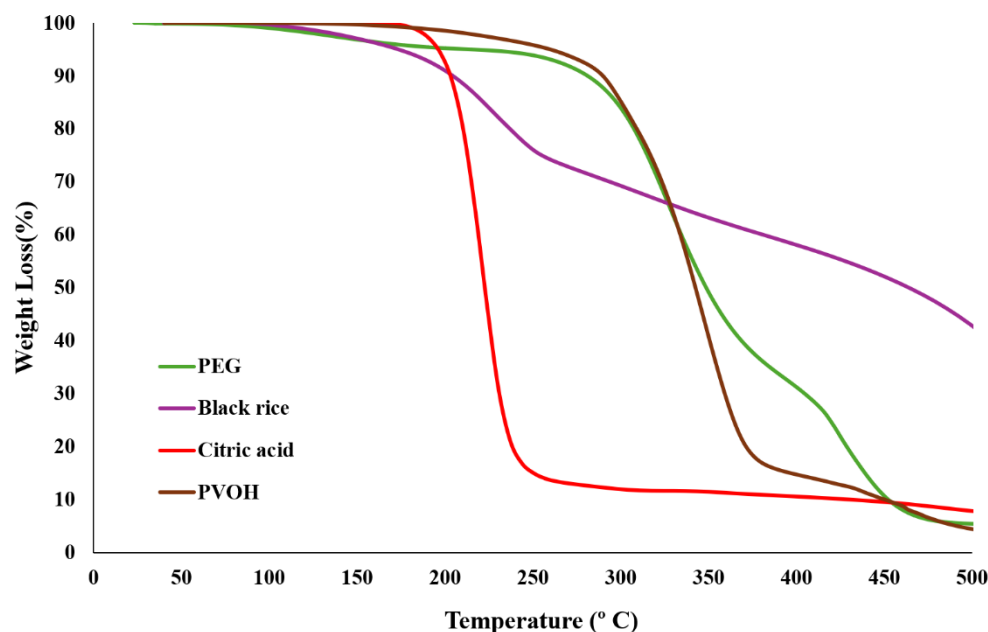


Figure 5.1 TGA thermogram for each component of formulated ink as an ink sensor.

A significant limitation in our method for assessing the process stability of thermally treated pH indicators using TGA analysis was the restricted scope of our sample analysis. Specifically, we analyzed two samples: the INK I TT pH indicator, which had undergone 5 minutes of thermal treatment at 165 °C, and the INK I NTT pH indicator, which had not undergone any thermal treatment. The ideal scenario for evaluating process stability would have involved subjecting the INK I NTT samples to the same thermal treatment protocol—holding them for 5 minutes at 165 °C—rather than using a thermal heating ramp. This approach would have provided a more accurate comparison by ensuring that both sets of samples underwent identical thermal conditions. Consequently, our analysis was limited to speculative comparisons of weight loss between the thermally treated and untreated samples. This limitation restricts our ability to definitively determine the extent of thermal degradation, as the differences in the thermal profiles of the samples could influence the observed weight loss.

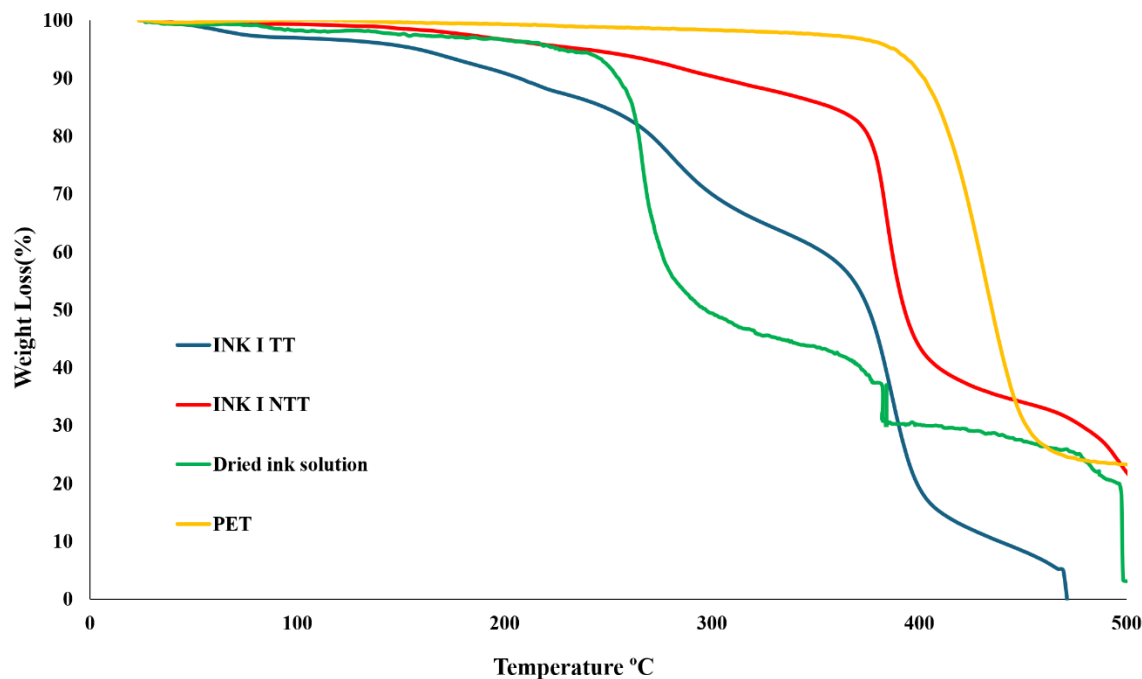


Figure 5.2 TGA thermogram for the dried ink solution (at room temperature) on the Petri dish, developed pH indicators that were thermally treated at 165 °C for 5 min (INK I TT) and those that were not heated (INK I NTT).

5.8.2 Application of developed pH-responsive indicators for fish freshness/spoilage monitoring

To ensure that the dyes in the films exhibit visual reactions to changes in TVB-N, it is necessary for the dyes to retain their pH-responsive properties. It is important that they maintain their protonation and deprotonation states unchanged when they are exposed to varying pH levels.

5.8.2.1 Effects of pH Conditions and Packaging Parameters

Most of current pH indicators for monitoring seafood products depends on the acidic nature of the coatings employed in their production [81]. Selecting an alternative pH for formulated ink was to assess the potential pH adjustment, which can improve the pH indicator's performance, stability, and compatibility and make it more sensitive to the target pH range [23, 24]. This allows for more precise and noticeable color changes at the desired pH levels, which is critical for food packaging spoilage and freshness monitoring [24, 28].

Figure 5.3 shows that three different pH conditions (2, 7.5 and 9) that were examined to determine the impact of the pH level of the formulated ink on the color shift of colorimetric films. The amount of fish and package size were (5 ± 0.5 g) and $19 \text{ cm} \times 17.7 \text{ cm}$, respectively. Fish samples were stored under controlled conditions and monitored using pH indicators with different ink pH coatings. It was observed that pH conditions ranging from 4.5 to 6.5 led to phenomena such as aggregation or precipitation. This can result in a thicker, more gel-like consistency, as seen in this image. This phenomenon can be attributed to the proximity of these pH levels to the isoelectric point of the components in the ink formulation [34, 82] and differences in the solubility of components of the formulated ink at the different pH level. This behavior is significant in various applications, including ink formulation, where achieving the right balance of charge is crucial for stability and performance.

Based on the observation, none of the pH indicators were activated on day 0, showing that the fish samples were fresh. The indicator's color changed over 3 days, when it was exposed to a solution ink (INK I) adjusted to a pH of 2. The pH indicators with a higher pH (pH = 7.5 and 9) were also triggered on the fourth day. This phenomenon may be due to the BC anthocyanin and PVOH, in the ink formulation, which become protonated at lower pH and deprotonated at high pH [83, 84]. As TVB-N gases accumulate in the headspace, the acidic groups in the ink formulation begin to deprotonate, leading to color shifts [85]. Moreover, anthocyanin molecules exist in the flavylum form at low pH values. However, when the pH exceeds 7, the anthocyanins undergo degradation, which is influenced by their substituent groups, and they transform into the carbinol pseudo-base form [86]. Therefore, among the tested indicators, only the one with an acidic coating (pH 2) demonstrated a range of color changes. Also, the sensitivity of this pH indicator can be comparable with a pH indicator at pH level 7.5; however, only for low pH levels, the R parameters decreased, and the G parameters increased, indicating its potential as a reliable tool for monitoring fish spoilage in the early stages. The neutral and alkaline pH indicators did not show significant color changes during initial storage time.

For assessing the fish quality during other parallel trials, different fish sample size and different available headspace, or air volume (zipper seal package: $19 \text{ cm} \times 17.7 \text{ cm}$ and container: 250 ml) were considered. The sensors effectively monitor spoilage over time, with a clear progression in color change corresponding to the spoilage process. The ΔRGB values show a generally linear increase until day 4. Then after its variations in peak and decline suggest, predictable spoilage

progression in the early stages. Variations of color response in later stages, after day 4, indicate the complexity of spoilage dynamics and possible sensor saturation. Samples labeled NTT, consistently show higher ΔRGB values compared to those with thermal treatment. This can suggest how different weight of samples can affect spoilage rates. For example, 100-NTT (Green line) spoils faster and more visibly than 30-TT (Yellow line), as indicated by the higher ΔRGB values. Furthermore, it was reported that a larger sample size (in terms of fish weight) linked with TVB-N emission causes color change to occur sooner, whereas increasing headspace has no significant impact [87] (**Supplementary material**). The color shifting also begins from the side closest to the fish product due to the diffusion of basic gases, whose contact with the indicator's surface occurs sooner.

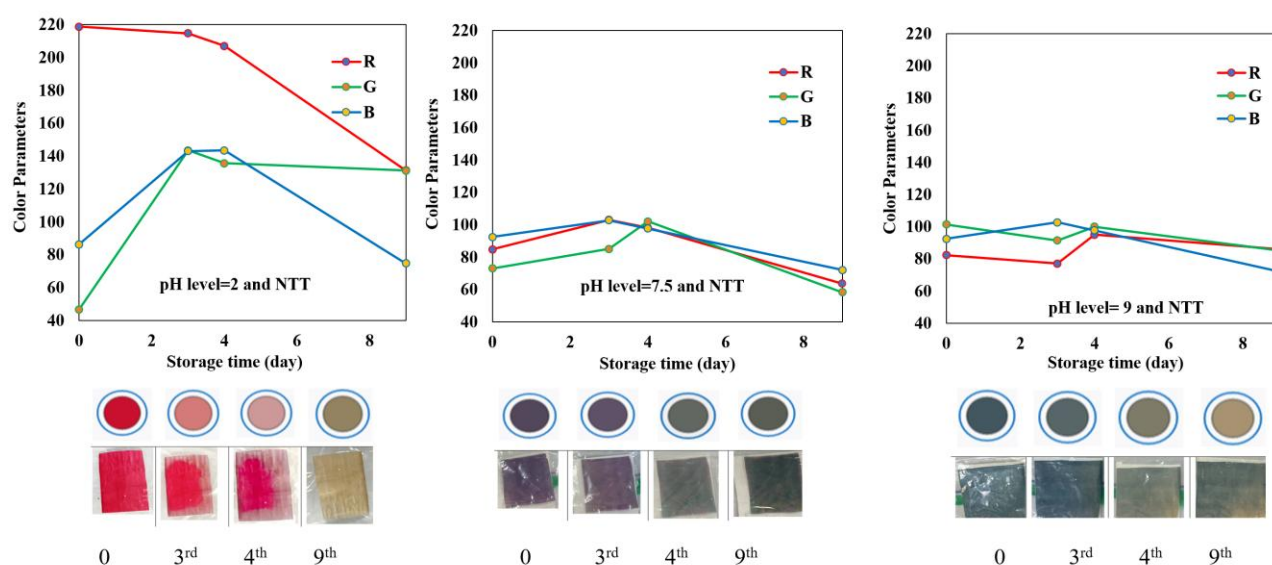


Figure 5.3 The color parameters, sensitivity and color change outcomes for NTT pH indicators (package headspace) at different pH level for their coatings, stored at 4°C over 9 days.

5.8.3 Packaging study and pH Indicator stability in fish packages

The pH indicator was assessed by simultaneous packaging trials including *Pangasius* fish, alongside microbiological and chemical tests. The amount of fish and container size were (50 ± 0.5 g) and 250 ml, respectively. To assess the impact of thermal treatment on packaging application, we used thermally treated fabricated pH indicators with a pH level of 2. These indicators were used

to assess their response time (in terms of color change) and their ability to remain intact upon contact with the headspace of fish packaging.

Figure 5.4 shows, the color changes for pH indicators (container headspace) with pH level of 2, during storage at 4°C over 9 days. The pH indicator exhibited color changes with four-point freshness scale, from red (fresh) to red/purple (acceptable), bluish/green (moderate spoilage/marginal), and yellowish-brown (high spoilage/spoiled). Specifically, color change observations indicated that from days 0-3, the indicator displayed a red color, denoting pristine condition with no spoilage. On days 4-5, the color shifted to red/purple, indicating minimal signs of spoilage while still being safe to eat. By days 6-7, the bluish/green color indicated moderate spoilage, suggesting it may not be safe for consumers, and by day 9, the color intensified to yellowish-brown, clearly indicating spoilage, resulting in the fish being unsafe to eat. The pH indicator effectively differentiated between the freshness levels of fish samples throughout the 9-day storage period, thus serving as a scalar indicator that provides a gradation of color changes corresponding to varying levels of freshness, surpassing a simple binary outcome. This scale offers a clear, reproducible method for categorizing fish freshness, with valuable implications for quality control and consumer safety.

Moreover, the thermal treatment process results in **Figure 5.4** indicate the pH indicators from being dissolved by water, while also causing a minor delay in their response time. This is due to a slight degradation that affects the active sites, which are specific chemical groups that can interact with hydrogen ions or hydroxide ions and are responsible for the acid-base reactions[88]. Consequently, with fewer active sites available, the pH indicator may not respond immediately to changes in pH, leading to a lag time for the active sites to sufficiently interact with ions in the solution to produce a noticeable color change [89].

This may also compromise the sensitivity of the pH indicator, requiring a more substantial change in pH to achieve the same degree of color change as in untreated samples. During fish storage, the R parameter decreased. A match for color changing could be defined for the final application. For this study, the ratio of $\Delta RGB_{NTT}/\Delta RGB_{TT}$ for the sample headspace were 1.07 ± 0.23 . To assess the indicator's stability, all samples were kept under storage conditions for over a month. During this period, there were no signs of dye leaching, color fading, or any alterations in response to the basic environment of the headspace of thermally treated pH indicators. Moreover, removing the

headspace from the container caused the colorimetric sensor to revert to its original color before exposure to an alkaline environment. This is the moment that the sensor will cease functioning.

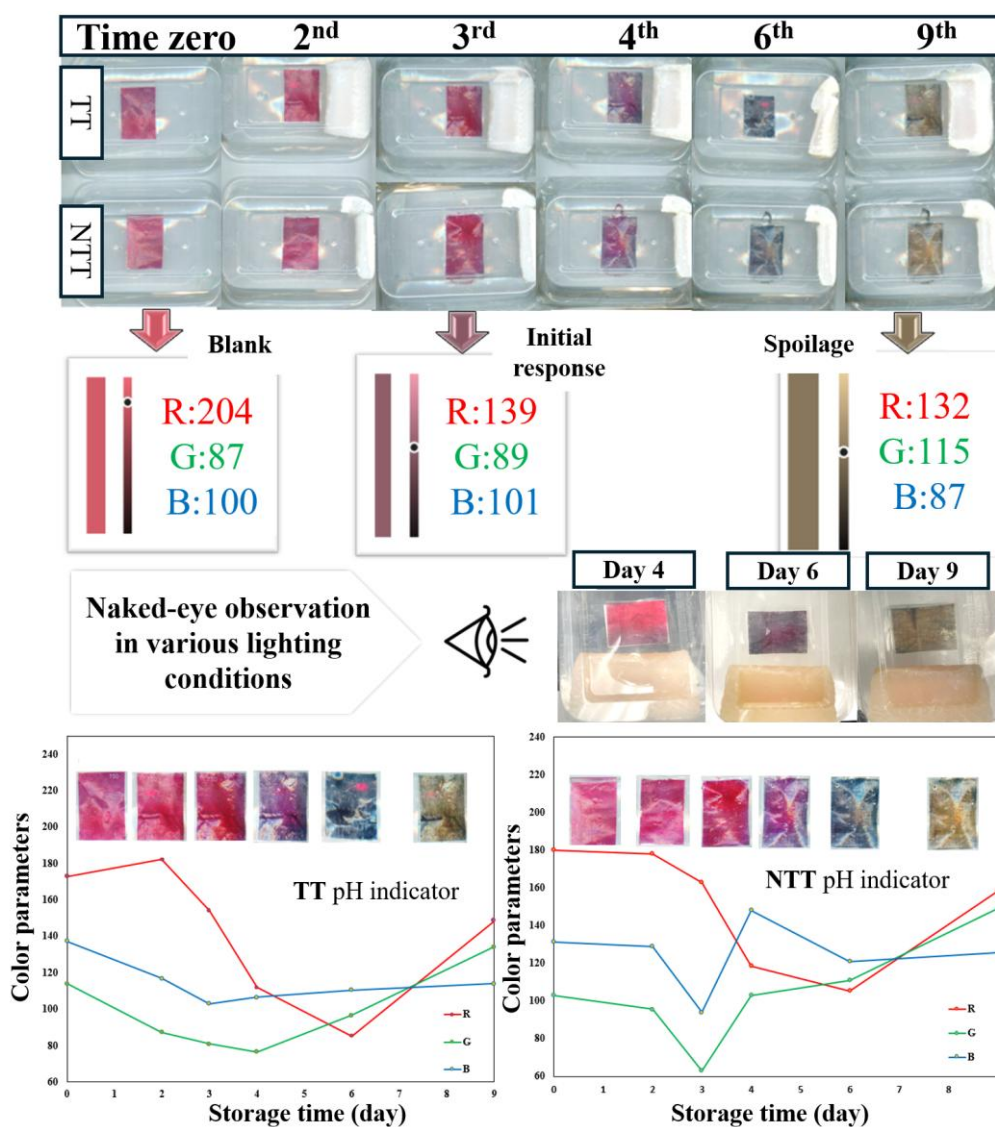


Figure 5.4 Illustrates the color change outcomes for pH indicators (container headspace) stored at 4°C over 9 days. NTT; colorimetric films without heat treatment. TT; colorimetric films with exposure to heat (165°C) for specific time (5 min). Fish condition at day 4: acceptable; day 6: marginal; day 9: spoiled.

5.8.4 Chemical stability and Recovery tests

To ensure the reliable performance of pH indicators, stability tests were performed under varying environmental conditions, specifically temperature and humidity [3]. We decided to stress test the

indicators by exposing to elevated temperatures and humidity which can speedup the reaction kinetics and result in the formation of degradants not typically observed in real-time stability assessments [90]. By analyzing RGB values at varying concentrations and conditions, we could potentially differentiate different stages of spoilage, from initial changes (red to pink/purple) to those indicative of advanced spoilage (pink/purple to blue), emphasizing the importance of both chemical stability and environmental controls.

The indicators underwent testing at two temperatures (40 and 60 °C) across a storage duration of 30 minutes and 1 hour. It was observed that when the samples were soaked at 60 °C for 1 hour, nearly all of them exhibited a complete color change indicating saturation (data not shown). Furthermore, it can generate responses that may not occur naturally in food products, resulting in a false aging mechanism[91]. Consequently, we preserved the samples at the same temperature for a duration of 30 minutes and subsequently observed a gradual alteration in color. We repeated the same procedure for $T = 40\text{ °C}$ as well (supplementary material).

Figure 5.5, Figure 5.6, and Figure 5.7 show the RGB value changes observed across different TVB-N gases, suggesting varying sensitivities among the color channels. Notably, the red channel showed substantial decreases, indicating high sensitivity to color changes. In contrast, the green and blue channels displayed different reaction patterns, with green first increasing and then sharply dropping, while blue consistently decreased as concentration rose. Post-exposure recovery tests investigated the indicators' ability to revert to their initial color following exposure to alkaline environments ($\text{pH} > 10$). Indicators generally reverted to their original color under controlled conditions (lower pH) because of destabilization of the anthocyanin molecule [92, 93]. We observed the variability to return to the original color. The interaction profiles with pH may differ slightly due to the impact of these volatile amines on pH levels. In the current recovery tests, it was observed that exposure to high concentrations of ammonia resulted in irreversible changes due to alterations in the anthocyanin structure.

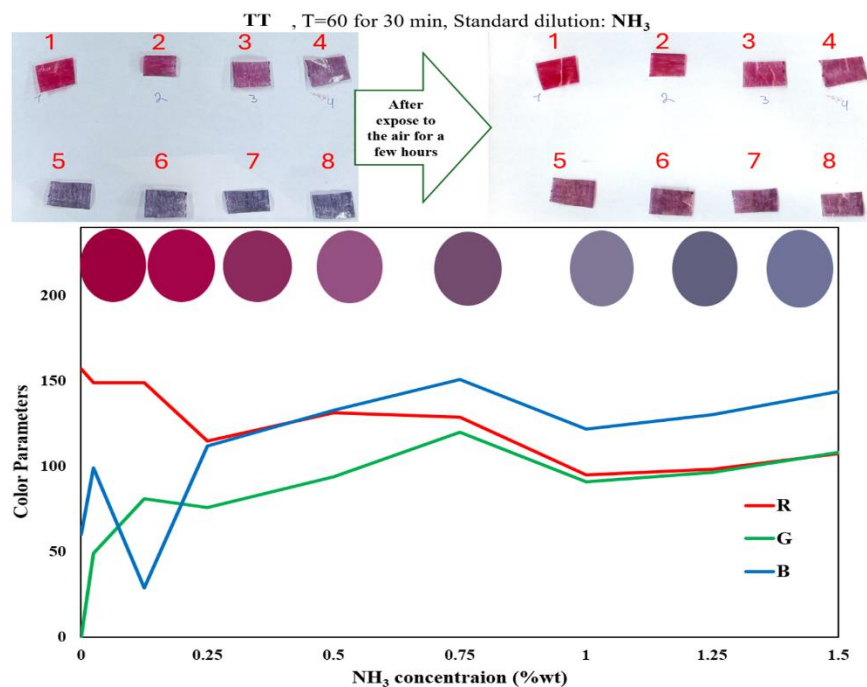


Figure 5.5 The RGB value of TT pH indicators towards 100 μL of diluted NH_3 under accelerated storage conditions ($T = 60$ for 30 min).

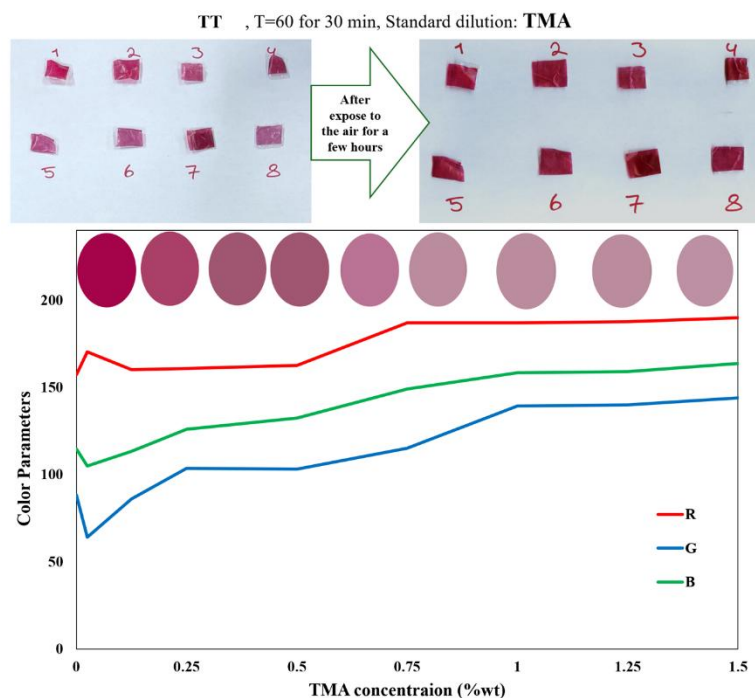


Figure 5.6 The RGB value of TT pH indicators towards 100 μL of diluted TMA under accelerated storage conditions ($T = 60$ for 30 min).

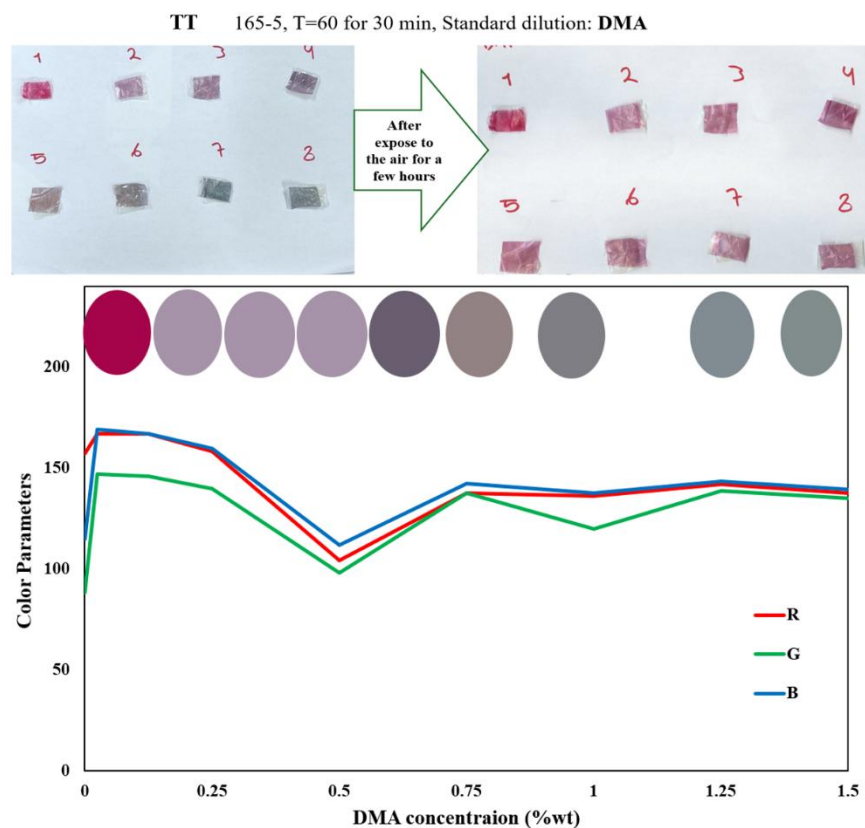


Figure 5.7 The RGB value of TT pH indicators towards 100 μ L of diluted DMA under accelerated storage conditions (T = 60 for 30 min).

In **Figure 5.8**, for samples exposed to the mixture of standards, it seems that the reversibility to the original control sample decreased. In mixed base exposures, NH_3 was identified as the primary contributor to the lack of reversibility. According to literature, anthocyanins can change color from red to orange at temperatures up to 40 $^{\circ}\text{C}$ [94]. As we exposed the pH indicators to each base (NH_3 , DMA, TMA) individually, we observed distinct changes in color behavior, highlighting the individual impact of each base on reversibility.

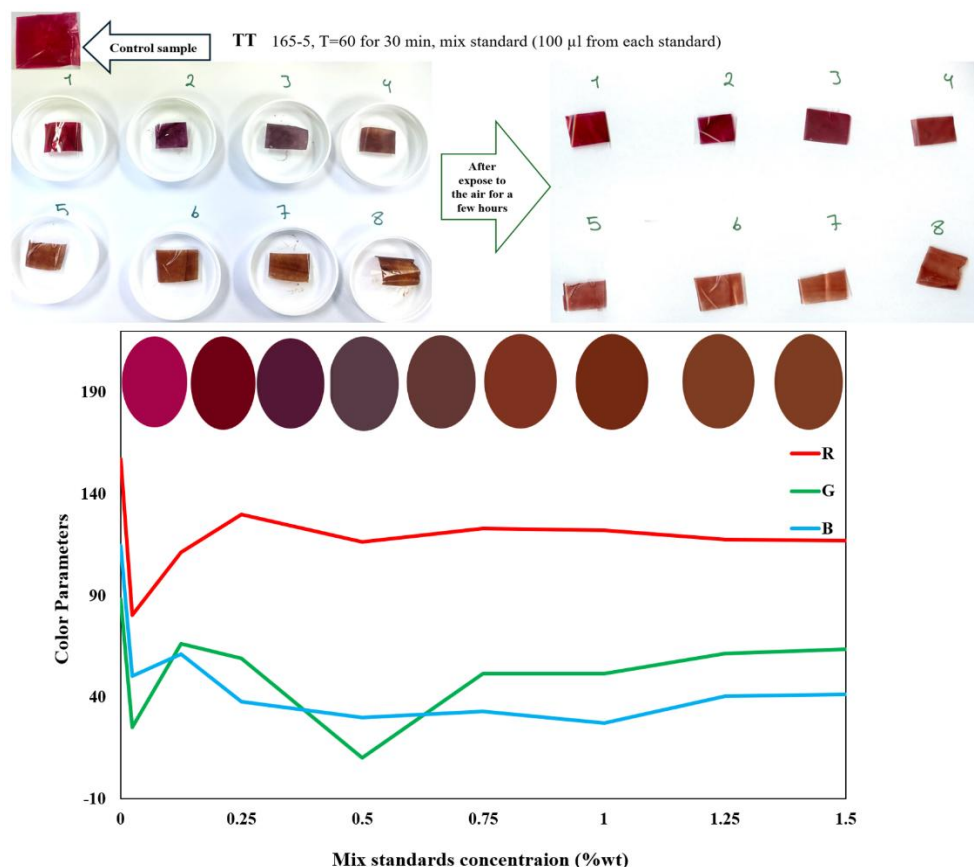


Figure 5.8 The RGB value of TT pH indicators towards 100 µL from each standard dilutions (mix of components) under accelerated storage conditions (T = 60 °C for 30 min).

Figure 5.9 displays the responses of the thermally treated pH indicators to controlled mixtures of NH_3 , DMA, and TMA that were stored in a relative humidity (RH) of 55% for 30 minutes at 40 °C temperature. At 55% RH, the moisture level is sufficient to ensure that the pH indicators remain sensitive to spoilage gases without being overly saturated, which can lead to false readings. Moreover, this RH level helps maintain a balance, making the color change more accurately representative of the spoilage status. According to observations in this storage condition, different color changes can be identified and categorized. Red to pink: may occur at lower pH shifts, indicating initial spoilage stages. Blue typically indicates a highly basic environment, suggesting advanced spoilage. Green represents intermediate stages where mixed gases' effects might overlap, especially in a moist environment. We recorded the RGB values at different concentrations to correlate color changes with gas concentrations. Initially, we tried the same temperature (60 °C);

however, we did not monitor any gradual color change, which could explain why high temperatures and humidity can help us reach the endpoint of color change extensively. The limitation of the climate chamber to provide constant RH in this range caused us to try a lower temperature of 40 °C.

The pH indicators appear to respond differently to TVB-N gas volume. Higher volumes of TVB-N gases can cause stronger color changes, indicating a stronger reaction. By integrating the effects of NH_3 , DMA, and TMA gases on pH indicators under varying relative humidity conditions, it is possible to develop a comprehensive spoilage indicator system.

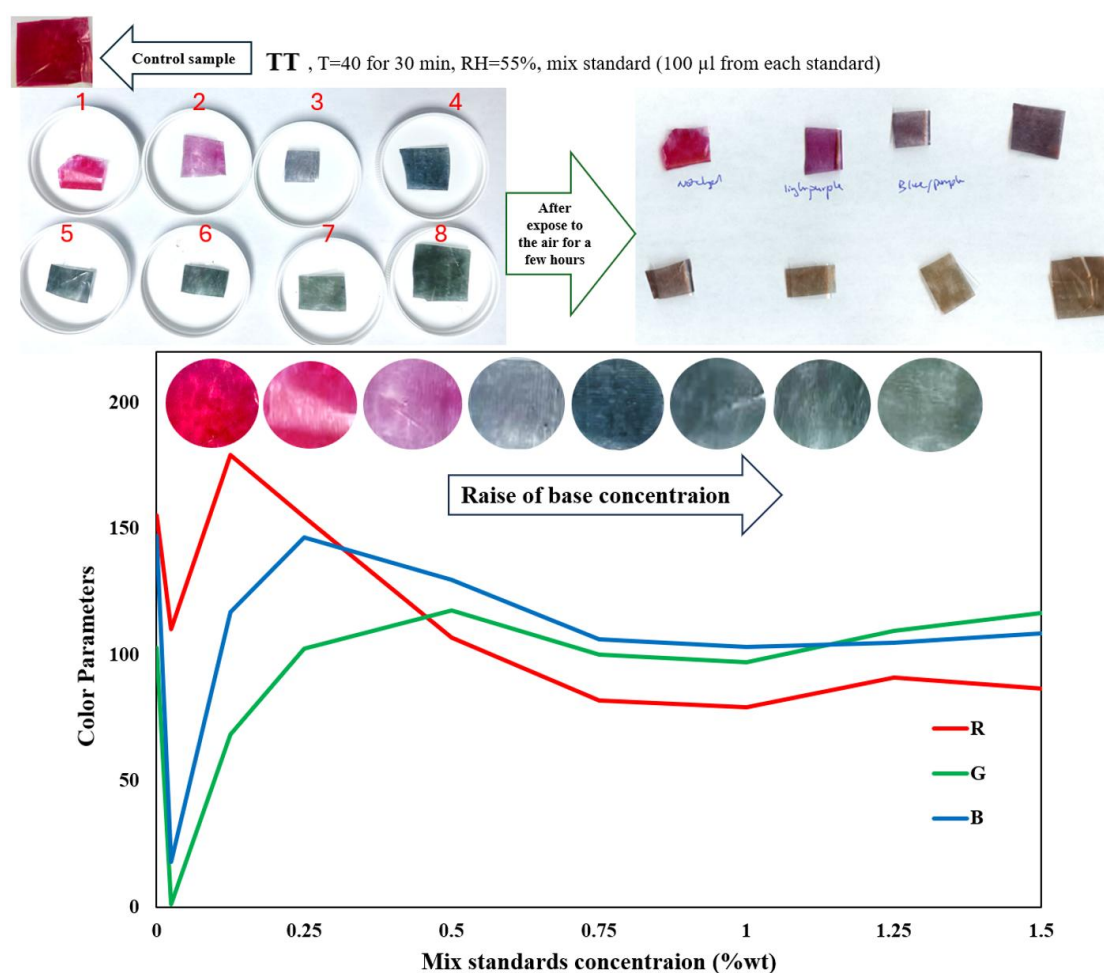


Figure 5.9 The RGB value of TT pH indicators towards 100 μL from each standard dilutions (mix of components) under specific storage condition (T: 40 °C for 30 min, RH~ 55%)

5.8.5 Validation of the pH indicator's efficacy by linking color changes to chemical analysis and microbial growth

Several studies reported the following shelf-life estimates based on the level of TVB-N gases and total microbial population: the TVB-N content was greater than 25 mg/100 g sample, the TVC exceeded 7 log CFU/ml, and the shelf-life was 7 days for rainbow trout fillets stored at 4°C [95]. Another batch of rainbow trout fillets, also stored at 4 °C, had a TVB-N content of 21 mg/100 g, a TVC of 6 log CFU/ml, and a shelf-life of 10 days [96]. Crucian fish fillets were also stored at 4°C, with TVB-N content at 20.7 mg/100 g, and the estimated shelf-life was approximately 6 days [97]. Silver carp fillets, stored under the same conditions, had a TVB-N content of 20 mg /100 g and the shelf-life was reported as 5.62 days [42]. Furthermore, some studies suggest that pH changes in fish can be a good indicator of spoilage [50, 98, 99], while others maintain that the pH test may not always accurately show deterioration in certain foods because of the narrow range that separates acceptable and undesirable quality, making it difficult to definitively determine food freshness [100]. In this study, microbial tests, and chemical analysis along with the color alteration of pH indicator were performed to validate the fish spoilage.

5.8.5.1 Chemical analysis (TVB-Ns)

Immediately after purchasing the fish and transferring it to the laboratory, the TVB-N content was 5.53 ± 0.02 mg /100 g, and the pH of fish was 6.93 ± 0.01 . It indicates that the product was fresh. After 48 hours, the TVB-N content reached to 8.40 ± 0.2 mg/100 g and pH level to 7 ± 0.01 . The colorimetric sensor remained inactive. The TVB-N concentration and pH of the fish reached 22.40 ± 0.2 mg/100 g and 7.34 ± 0.01 , respectively after being stored for 3 days, suggesting a significant drop in its quality. Simultaneously, the pH indicator started to change color, at the edges (depending on the flow direction of produced gases). At the 4th day of storage, the TVB-N content reached to 26.22 ± 0.10 mg/100. Meanwhile, the color of pH indicators was changed to light purple/pink from the edges. At this point, most surface of the indicator, which is located near the fillet, had changed color, signalling the activation of the colorimetric sensor. Indicating that the TVB-N threshold was reached slightly prior to the 4-day storage period. Moreover, the consistency of the fish sample contained inside the packages were watery and squishy. The TVB-N level and the pH of the fish reached 31.65 ± 0.10 mg/100 g and 7.51 ± 0.01 on the 6th day. The TVB-N level at this point is

close to rejection limit which is 35 mg N/100 gr and, the color of indicator almost changed to bluish-purple. At the end of the fish storage period (day 9) the color of indicator reached a dark yellow/light brown. In this point, the TVB-N amount exceeded to 36.25 ± 0.45 mg N/100 gr and pH reached 7.73 ± 0.01 (**supplementary material**).

In current study the pH of the flesh of fish during the storage period increased along with TVB-N content. This is because of the increase of non-protein nitrogen and other volatile amines that were produced because of proteolytic enzyme activities of the microbial flora [96, 101]. However, pH of *Pangasius* fish changed slightly in a narrow range between (6.93-7.73) and cannot be used as the sole indicator of shelf-life [102].

5.8.5.2 Microbial analysis

Microbial activity affects the shelf-life estimation of seafood [103-105]. Small quantities of some spoiling microorganisms are present when storage begins, but they multiply and produce metabolites like TVB-N, which alter texture, color, taste, and smell and lead to sensory rejection [106]. During packaging trials, the TVC counts slowly increased from 3.80 ± 0.09 log CFU/ml during the initial 72 h of storage, which means the *Pangasius* fish fillets used in this study had a relatively good quality up to day 4, with a TVC of 5.21 ± 0.08 log CFU/ml. Initially, the pseudomonas counts were at approximately 63% of the TVC counts rising to approximately 78% at around the end of storage [50]. This suggest that pseudomonas spp could be one of the dominant bacteria involved in fish spoilage at 4°C at both the early and end stages of storage [107]. **Figure 5.10** shows the growth of *Pseudomonas* spp that was isolated from fish samples with TVC and TVB-N. The TVB-N threshold was reached slightly before the fourth day of storage. Both TVC and pseudomonas populations show a gradual increase from the start then rapidly accelerates,

reaching 7.16 CFU/ml and 5.6 log CFU/ml, respectively after 9-day storage. **Table 5.2** presents the measured data points of chemical and microbiological analysis during the packaging study.

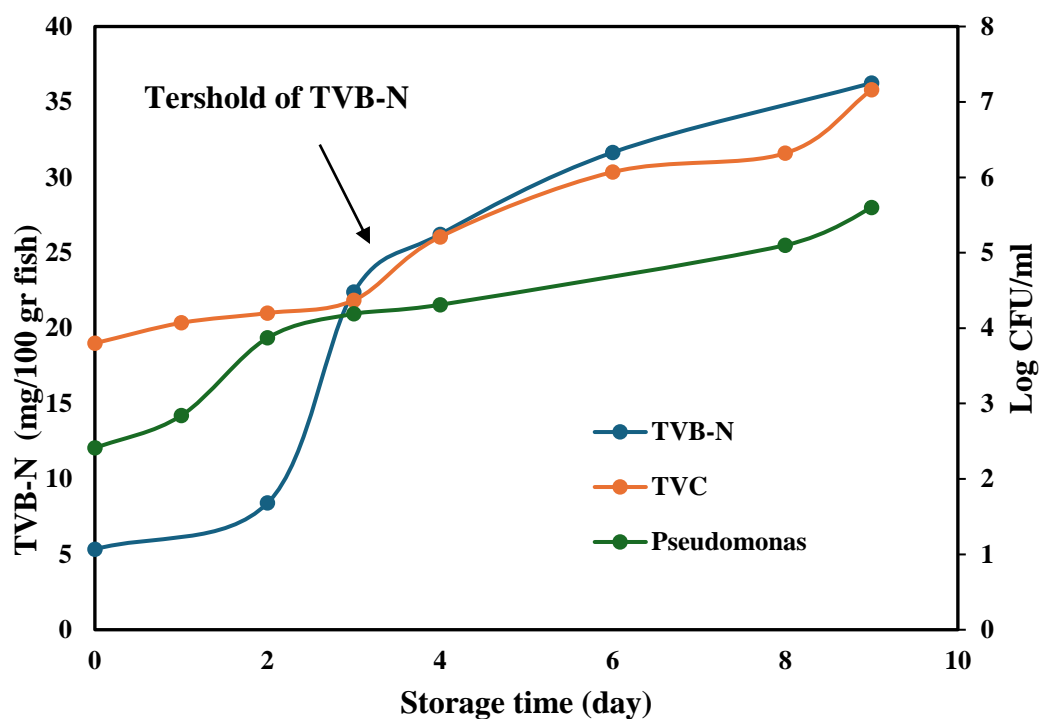


Figure 5.10 TVB-N, TVC and Pseudomonas growth versus the storage time at 4 °C.

The mathematical models fitted to available data from this study and were presented in the appendices (**B.1** till **B.3** sections).

Table 5.2 Measurements for chemical analysis (TVB-N and pH), microbiological analysis and color change data during fish storage (day).

ST	TVB-N	TVC	Pseudomonas	pH	Δ RGB NTT	Δ RGB TT
0	5.34 ± 0.02	3.80 ± 0.09	2.41 ± 0.09	6.93 ± 0.01	0	0
1	NA	4.07 ± 0.09	2.84 ± 0.03	NA	NA	NA
2	8.40 ± 0.2	4.20 ± 0.02	3.87 ± 0.19	7 ± 0.01	16.08 ± 5.68	36.07 ± 7.42
3	22.40 ± 0.20	4.37 ± 0.005	4.19 ± 0.04	7.34 ± 0.01	60.24 ± 4.59	53.34 ± 6.62
4	26.22 ± 0.10	5.21 ± 0.08	4.31 ± 0.03	7.48 ± 0.01	80.03 ± 13.57	78.74 ± 14.87
6	31.65 ± 0.10	6.07 ± 0.02	NA	7.51 ± 0.01	83.04 ± 3.07	93.51 ± 8.78
8	NA	6.32 ± 0.005	5.10 ± 0.10	7.55 ± 0.01	NA	NA
9	36.25 ± 0.14	7.16 ± 0.04	5.60 ± 0.08	7.73 ± 0.01	66.12 ± 5.00	44.42 ± 3.28

NA: not available. All values were expressed as mean \pm standard deviation (n = 3).

NTT; colorimetric films without heat treatment. TT; colorimetric films with exposure to heat (165°C) for specific time (5 min).

ST: storage time

5.8.6 Correlation of Δ RGB with chemical and microbial analysis

Figure 5.11 shows the correlation between Δ RGB and TVB-N gases (a), TVC (b), and pH (c) at 4 °C, showing the high sensitivity of colorimetric sensors to various biomarkers, showcasing their utility in monitoring fish spoilage. The R^2 ratings suggest high sensitivity of colorimetric sensors [108]. **Figure 5.11 (a)** displays a strong correlation ($R^2 = 0.9836$) between Δ RGB and TVB-N concentration. As TVB-N levels increase, the sensor responds significantly by turning deep reddish. This means the sensor reached the initial threshold of TVB-N gas (25 mg/100 g) in the headspace of the fish package [63]. The Δ RGB response showed a linear response to the TVB-N concentration in the range of 5.34 – 26.22 mg/ 100 g at the chilled temperature [109]. **Figure 5.11 (b)** shows the correlation between Δ RGB and TVC with an R^2 of 0.8661, showing the sensor's ability to track microbial growth. The sensor response was captured on day 4, which shows the sensor changed color from the side close to the fish sample to purple. At this time, the microbial activities also increased. **Figure 5.11 (c)** highlights the correlation between Δ RGB and pH ($R^2 = 0.9878$), suggesting that the sensor is highly responsive to pH changes during spoilage. Therefore, these plots show that the sensor response correlates more strongly with chemical analysis than with microbial activities. **Figure 5.11 (d)** shows the different stages of fish condition (fresh, acceptable, moderate spoilage and spoiled) during storage based on the biomarkers. For a food freshness indicator to be effective, it must be able to visually distinguish between fresh, acceptable, and spoiled food [17].

As the alkaline environment increases due to spoilage during fish storage, the color of the sensor changes to green-light brown (a slight reduction in Δ RGB); finally, at the end of storage, the sensor almost reaches the endpoint of its color change and turns to brown yellowish (high reduction in Δ RGB) on day 9. The sensor shows the monitoring of color stability in the basic environment over a period of more than one month. The color did not wipe out or change to its original color before exposure to fish samples for indicators labelled as 165–5 for both container and package storage (**Figure B.8**).

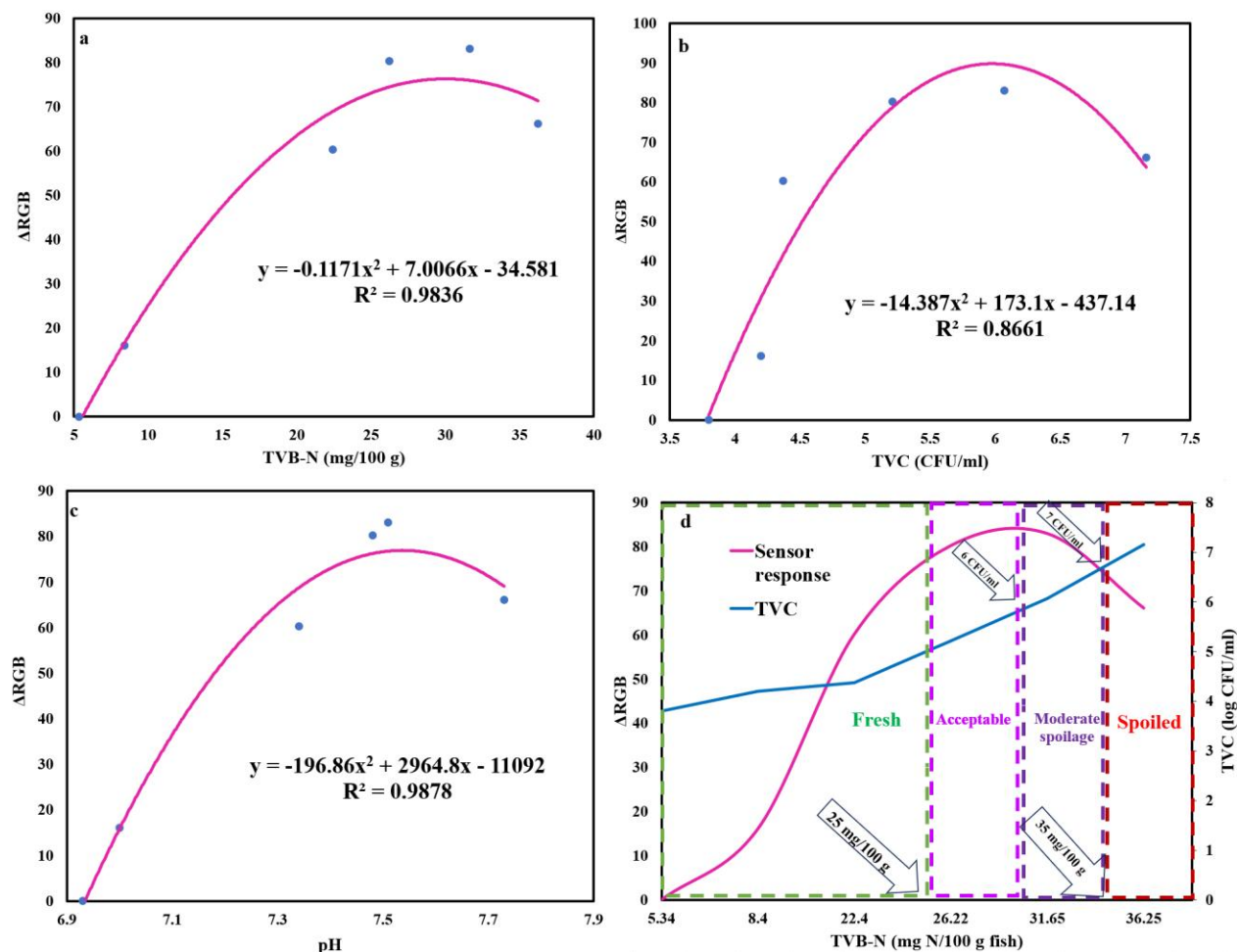


Figure 5.11 ΔRGB versus TVB-N gases (a), TVC (b), and pH (c) during fish storage at 4 °C. Correlation between the onset of an increase in microbial population and TVB-N gas release and sensor response (d).

Numerous limitations exist in these fitting models for predicting fish spoilage using colorimetric sensors. The quadratic nature of the fitted curves indicates non-linear relationships between ΔRGB and the biomarkers (TVB-N, TVC, and pH). This complexity can make the models less intuitive and harder to interpret compared to simpler linear models. The high R^2 values (e.g., 0.9836 for TVB-N and 0.9878 for pH) suggest a strong fit to the experimental data, but they might also show overfitting, where the model captures noise in the data rather than just the underlying trend. There is also a limited number of data points, which might not be sufficient to fully capture the variability and trends in the spoilage process. This can reduce the robustness and generalizability of the model. Moreover, the ΔRGB values eventually plateau at higher biomarker concentrations, indicating that

the sensor response may saturate. This saturation limits the model's ability to differentiate spoilage levels beyond a certain point, potentially reducing its effectiveness in late stages of spoilage.

5.9 Conclusion and recommendations

This study confirmed that an environmentally friendly ink formulation can coat PET films as a scalar pH indicator sensor, and the fabricated films have high potential as an intelligent indicator label for monitoring the freshness of fish products. The novelty of this research project lies in using these pH indicators in direct contact with food products to enhance readability and provide a quicker color change in response to quality changes in seafood. Additionally, it utilizes industrial printing techniques aimed at increasing production rates.

Developed pH indicators can offer a continuum of color variations that correspond to varying degrees of freshness, rather than a simple binary outcome. Hence, color change analysis showed that the developed colorimetric sensor can detect and evaluate gas concentrations through color changes, making it a practical industrial tool for monitoring the food safety and quality of fish packages. The use of crosslinking agents such as citric acid can reduce dye leaching and degradation. Applying controlled thermal treatments can enhance the interaction between anthocyanins and PET films, increasing stability of anthocyanins during fish storage period. The sensitivity of pH indicators at low pH levels is markedly greater compared to those at neutral and alkaline levels, as the latter did not show notable color changes during the initial storage period. Chemical analysis (TVB-N and pH measurement) and microbial analysis (total bacterial population and *Pseudomonas* spp. growth) performed during packaging trials at 4 °C validated the performance of the produced films. After the third day of fish storage during the packaging study, TVB-N gases increased in the headspace, and colorimetric films started to change color. During packaging trials, the TVB-N threshold occurred between the third and fourth days of storage, in transition state from fresh to acceptable state. Additionally, at day 4 of fish storage at 4 °C, we found the pH, TVC, *Pseudomonas* growth, and TVB-N levels to be 7.48, 5.2 (log CFU/ml), 4.31 (log CFU/ml), and 26.22 (mg N/100 gr sample), respectively. At this time, the sensor changed color to reddish-purple. Based on microbial (7 log CFU/ml TVC) and chemical (35 mg/100 g TVB-N) analyses, fish packages stored under atmospheric conditions typically have a shelf-life of less than 9 days. These thresholds are set up to ensure the freshness and safety of both fresh and frozen

fish packages at 4 °C. The sensor response shows a stronger correlation with TVB-N gases than with microbial activities.

The implementation of mathematical models to predict TVB-N content and microbial growth can enhance the utility of this research. These models serve as a robust framework for validating experimental results by correlating initial quality parameters with observed changes in seafood freshness over time. By analyzing historical data and establishing relationships between variables, these models can accurately forecast the shelf-life of seafood products (**appendices**).

Recommendations for future studies

Despite the promising results, this study identified numerous areas for future research to enhance the reliability and applicability of the findings. By addressing these limitations, future research can build on the current study and contribute to more effective monitoring systems for fish freshness and safety.

- The integration of barrier films can extend the shelf life of seafood by minimizing oxygen exposure and inhibiting microbial growth. The coated-PET film can be laminated with various barrier films to create a multilayer intelligent food packaging system. This advanced packaging solution not only protects the seafood product from external contaminants and moisture but also actively contributes to maintaining its freshness. By incorporating pH indicators and other sensory technologies, the packaging can provide real-time information about the product's quality, such as freshness and spoilage levels.
- Complex interactions in biological systems, such as fish microbial spoilage, need a larger dataset for accurate modeling. More experimental data points, cross-validation, error analysis, and studies conducted under varying conditions can significantly improve the predictive model's reliability and robustness. Such enhancements will aid in refining the model's ability to predict TVB-N levels and the corresponding spoilage of fish.
- Another constraint is the reliance on chemical analysis to quantify TVB-N levels in fish samples. Future studies should consider utilizing gas chromatography-mass spectrometry (GC-MS) to collect data from the headspace of the packaging. This approach could prove more effective in quantifying TVB-N gases and establishing correlations between these data, microbiological analyses, and the color response of the developed pH indicator.

Acknowledgements

I express my gratitude to Dr. Marian Rofeal for her proof reading and academic guidance. The funding for this research project is gratefully acknowledged from the Natural Sciences and Engineering Research Council of Canada (NSERC), 3Spack Industrial Research Chair, Research Center for High Performance Polymer and Composite Systems (CREPEC), Chemical Engineering Department, Polytechnique Montréal, ProAmpac flexible packaging, and Prima.

5.10 Reference

1. Banja BA. Shelf-life Trial on Cod (*Gadus morhua* L.) and Haddock (*Melanogrammus aeglefinus* L.) Stored on Ice around 0° C. *Reykjavik, Iceland: UNU-Fisheries Training Programme, Final Project*. 2002;
2. Kuuliala L, Al Hage Y, Ioannidis AG, et al. Microbiological, chemical and sensory spoilage analysis of raw Atlantic cod (*Gadus morhua*) stored under modified atmospheres. *Food Microbiology*. 2018/04/01/ 2018;70:232-244. doi:<https://doi.org/10.1016/j.fm.2017.10.011>
3. Bell LN. Moisture effects on food's chemical stability. *Water activity in foods: fundamentals and applications*. 2020:227-253.
4. Gram L, Huss HH. Microbiological spoilage of fish and fish products. *International journal of food microbiology*. 1996;33(1):121-137.
5. in't Veld JHH. Microbial and biochemical spoilage of foods: an overview. *International journal of Food microbiology*. 1996;33(1):1-18.
6. Valero A, Carrasco E, García-Gimeno RM. Principles and methodologies for the determination of shelf-life in foods. *Trends in vital food and control engineering*. 2012;1:3-42.
7. Nychas G-JE, Skandamis PN, Tassou CC, Koutsoumanis KP. Meat spoilage during distribution. *Meat science*. 2008;78(1-2):77-89.
8. Ghasemi-Varnamkhasti M, Apetrei C, Lozano J, Anyogu A. Potential use of electronic noses, electronic tongues and biosensors as multisensor systems for spoilage examination in foods. *Trends in Food Science & Technology*. 2018;80:71-92.
9. Das J, Mishra HN. A comprehensive review of the spoilage of shrimp and advances in various indicators/sensors for shrimp spoilage monitoring. *Food Research International*. 2023:113270.

10. Rastiani F, Jebali A, Hekmatimoghaddam S, Khalili Sadrabad E, Akrami Mohajeri F, Dehghani-Tafti A. Monitoring the freshness of rainbow trout using intelligent PH-sensitive indicator during storage. *Journal of Nutrition and Food Security*. 2019;4(4):225-235.
11. Miller K, Reichert CL, Schmid M. Biogenic amine detection systems for intelligent packaging concepts: Meat and Meat Products. *Food Reviews International*. 2023;39(5):2543-2567.
12. Kuswandi B, Jayus, Oktaviana R, Abdullah A, Heng LY. A novel on-package sticker sensor based on methyl red for real-time monitoring of broiler chicken cut freshness. *Packaging technology and science*. 2014;27(1):69-81.
13. Kuswandi B, Moradi M, Ezati P. Food sensors: Off-package and on-package approaches. *Packaging Technology and Science*. 2022;35(12):847-862.
14. Pacquit A, Frisby J, Diamond D, et al. Development of a smart packaging for the monitoring of fish spoilage. *Food chemistry*. 2007;102(2):466-470.
15. Luo Q, Hossen A, Sameen DE, et al. Recent advances in the fabrication of pH-sensitive indicators films and their application for food quality evaluation. *Critical Reviews in Food Science and Nutrition*. 2023;63(8):1102-1118.
16. Zhang J, Liu S, Xie C, Wang C, Zhong Y, Fan K. Recent advances in pH-sensitive indicator films based on natural colorants for smart monitoring of food freshness: a review. *Critical Reviews in Food Science and Nutrition*. 2023:1-20.
17. Almasi H, Forghani S, Moradi M. Recent advances on intelligent food freshness indicators; an update on natural colorants and methods of preparation. *Food Packaging and Shelf-life*. 2022/06/01/ 2022;32:100839. doi:<https://doi.org/10.1016/j.fpsl.2022.100839>
18. Mohammadian E, Alizadeh-Sani M, Jafari SM. Smart monitoring of gas/temperature changes within food packaging based on natural colorants. *Comprehensive Reviews in Food Science and Food Safety*. 2020;19(6):2885-2931.
19. Alizadeh-Sani M, Mohammadian E, Rhim J-W, Jafari SM. pH-sensitive (halochromic) smart packaging films based on natural food colorants for the monitoring of food quality and safety. *Trends in Food Science & Technology*. 2020/11/01/ 2020;105:93-144. doi:<https://doi.org/10.1016/j.tifs.2020.08.014>
20. Kuswandi B, Moradi M, Ezati P. Food sensors: Off-package and on-package approaches. *Packaging Technology and Science*. 2022;35(12):847-862. doi:<https://doi.org/10.1002/pts.2683>

21. Mills A. Oxygen indicators and intelligent inks for packaging food. *Chemical Society Reviews*. 2005;34(12):1003-1011.
22. Moradi M, Tajik H, Almasi H, Forough M, Ezati P. A novel pH-sensing indicator based on bacterial cellulose nanofibers and black carrot anthocyanins for monitoring fish freshness. *Carbohydrate Polymers*. 2019;222:115030.
23. Liu D, Cui Z, Shang M, Zhong Y. A colorimetric film based on polyvinyl alcohol/sodium carboxymethyl cellulose incorporated with red cabbage anthocyanin for monitoring pork freshness. *Food Packaging and Shelf-life*. 2021/06/01/ 2021;28:100641.
doi:<https://doi.org/10.1016/j.fpsl.2021.100641>
24. Kaewprachu P, Sai-Ut S, Rawdkuen S. Smart Freshness Indicator for Animal-Based Product Packaging: Current Status. In: Shukla AK, ed. *Food Packaging: The Smarter Way*. Springer Nature Singapore; 2022:107-125.
25. Roy S, Rhim J-W. Anthocyanin food colorant and its application in pH-responsive color change indicator films. *Critical Reviews in Food Science and Nutrition*. 2021;61(14):2297-2325.
26. Singh S, Gaikwad KK, Lee YS. Anthocyanin-A natural dye for smart food packaging systems. *Korean Journal of Packaging Science & Technology*. 2018;24(3):167-180.
27. Dikmetas DN, Uysal E, Karbancioglu-Guler F, Gurmen S. The production of pH indicator Ca and Cu alginate ((1, 4)- β -d-mannuronic acid and α -l-guluronic acid) cryogels containing anthocyanin obtained via red cabbage extraction for monitoring chicken fillet freshness. *International Journal of Biological Macromolecules*. 2023;231:123304.
28. Liu D, Zhang C, Pu Y, et al. Recent advances in pH-responsive freshness indicators using natural food colorants to monitor food freshness. *Foods*. 2022;11(13):1884.
29. Kuswandi B, Nurfawaidi A. On-package dual sensors label based on pH indicators for real-time monitoring of beef freshness. *Food Control*. 2017;82:91-100.
30. Firouz MS, Mohi-Alden K, Omid M. A critical review on intelligent and active packaging in the food industry: Research and development. *Food Research International*. 2021;141:110113.
31. De Dicastillo CL, Rodríguez F, Guarda A, Galotto MJ. Antioxidant films based on cross-linked methyl cellulose and native Chilean berry for food packaging applications. *Carbohydrate Polymers*. 2016;136:1052-1060.

32. Bellelli M, Licciardello F, Pulvirenti A, Fava P. Properties of poly(vinyl alcohol) films as determined by thermal curing and addition of polyfunctional organic acids. *Food Packaging and Shelf-life*. 2018/12/01/ 2018;18:95-100. doi:<https://doi.org/10.1016/j.fpsl.2018.10.004>
33. Ameri M, Ajji A, Kessler S. Characterization of a Food-Safe Colorimetric Indicator Based on Black Rice Anthocyanin/PET Films for Visual Analysis of Fish Spoilage. *Packaging Technology and Science*. 2024;
34. Mulla MA, Yow HN, Zhang H, Cayre OJ, Biggs S. Colloid particles in ink formulations. *Fundamentals of inkjet printing: the science of inkjet and droplets*. 2016:141-168.
35. Ghaani M, Cozzolino CA, Castelli G, Farris S. An overview of the intelligent packaging technologies in the food sector. *Trends in Food Science & Technology*. 2016;51:1-11.
36. Kassal P, Šurina R, Vrsaljko D, Steinberg IM. Hybrid sol–gel thin films doped with a pH indicator: effect of organic modification on optical pH response and film surface hydrophilicity. *Journal of sol-gel science and technology*. 2014;69:586-595.
37. Joseph T, Sahoo S, Halligudi S. Brönsted acidic ionic liquids: A green, efficient and reusable catalyst system and reaction medium for Fischer esterification. *Journal of Molecular Catalysis A: Chemical*. 2005;234(1-2):107-110.
38. Viswanathan S, Radecki J. Nanomaterials in electrochemical biosensors for food analysis-a review. *Polish journal of food and nutrition sciences*. 2008;58(2)
39. Chouhan A, Kaur BP, Rao PS. Effect of high pressure processing and thermal treatment on quality of hilsa (*Tenualosa ilisha*) fillets during refrigerated storage. *Innovative Food Science & Emerging Technologies*. 2015;29:151-160.
40. Fan W, Chi Y, Zhang S. The use of a tea polyphenol dip to extend the shelf-life of silver carp (*Hypophthalmichthys molitrix*) during storage in ice. *Food chemistry*. 2008;108(1):148-153.
41. Prabhakar PK, Vatsa S, Srivastav PP, Pathak SS. A comprehensive review on freshness of fish and assessment: Analytical methods and recent innovations. *Food research international*. 2020;133:109157.
42. Zhai X, Shi J, Zou X, et al. Novel colorimetric films based on starch/polyvinyl alcohol incorporated with roselle anthocyanins for fish freshness monitoring. *Food Hydrocolloids*. 2017;69:308-317.

43. Jia S, Li Y, Zhuang S, et al. Biochemical changes induced by dominant bacteria in chill-stored silver carp (*Hypophthalmichthys molitrix*) and GC-IMS identification of volatile organic compounds. *Food Microbiology*. 2019;84:103248.
44. Khulal U, Zhao J, Hu W, Chen Q. Intelligent evaluation of total volatile basic nitrogen (TVB-N) content in chicken meat by an improved multiple level data fusion model. *Sensors and Actuators B: Chemical*. 2017;238:337-345.
45. Chun H-N, Kim B, Shin H-SJFs, biotechnology. Evaluation of a freshness indicator for quality of fish products during storage. 2014;23(5):1719-1725.
46. Huss HH. *Fresh fish--quality and quality changes: a training manual prepared for the FAO/DANIDA Training Programme on Fish Technology and Quality Control*. Food & Agriculture Org.; 1988.
47. EC.(2005). Regulation No. 2074/2005 of the European Parliament and of the Council. *Official Journal of the European Union*. L338:27-59.
48. Jinadasa B. Determination of quality of marine fishes based on total volatile base nitrogen test (TVB-N). *Nature and Science*. 2014;5(12):106-111.
49. Özoğul F, Özoğul Y. Comparision of methods used for determination of total volatile basic nitrogen (TVB-N) in rainbow trout (*Oncorhynchus mykiss*). *Turkish journal of zoology*. 2000;24(1):113-120.
50. Pacquit A, Lau KT, McLaughlin H, Frisby J, Quilty B, Diamond D. Development of a volatile amine sensor for the monitoring of fish spoilage. *Talanta*. 2006;69(2):515-520.
51. Koutsoumanis KP, Taoukis PS, Drosinos EH, Nychas G-JE. Applicability of an Arrhenius model for the combined effect of temperature and CO₂ packaging on the spoilage microflora of fish. *Applied and Environmental Microbiology*. 2000;66(8):3528-3534.
52. Prabhakar PK, Srivastav PP, Pathak SS, Das K. Mathematical modeling of total volatile basic nitrogen and microbial biomass in stored rohu (*Labeo rohita*) fish. *Frontiers in Sustainable Food Systems*. 2021;5:669473.
53. Koutsoumanis K, Stamatiou A, Skandamis P, Nychas G-J. Development of a microbial model for the combined effect of temperature and pH on spoilage of ground meat, and validation of the model under dynamic temperature conditions. *Applied and Environmental Microbiology*. 2006;72(1):124-134.

54. Crowley K, Pacquit A, Hayes J, Lau KT, Diamond D. A gas-phase colorimetric sensor for the detection of amine spoilage products in packaged fish. *IEEE*; 2005;4 pp.
55. Chowdhury MA, Roy NC. Probiotic supplementation for enhanced growth of striped catfish (*Pangasianodon hypophthalmus*) in cages. *Aquaculture Reports*. 2020;18:100504.
56. Gram L, Melchiorson J. Interaction between fish spoilage bacteria *Pseudomonas* sp. and *Shewanella putrefaciens* in fish extracts and on fish tissue. *Journal of applied bacteriology*. 1996;80(6):589-595.
57. Saadatkhan N, Carillo Garcia A, Ackermann S, et al. Experimental methods in chemical engineering: Thermogravimetric analysis—TGA. *The Canadian Journal of Chemical Engineering*. 2020;98(1):34-43.
58. Hasan MR, Hossain MM, Islam MS, et al. Seasonal variation of quality and the total viable count of lean and fatty fish. *Egyptian Journal of Aquatic Biology & Fisheries*. 2023;27(5)
59. Conway EJ. Microdiffusion analysis and volumetric error. *Microdiffusion analysis and volumetric error*. 1947;
60. Kim D-Y, Park S-W, Shin H-S. Fish Freshness Indicator for Sensing Fish Quality during Storage. *Foods*. 2023;12(9):1801.
61. Conway EJ, Byrne A. An absorption apparatus for the micro-determination of certain volatile substances: The micro-determination of ammonia. *Biochem J*. 1933;27(2):419-29.
62. Lotfi M, Tajik H, Moradi M, Forough M, Divsalar E, Kuswandi B. Nanostructured chitosan/monolaurin film: Preparation, characterization and antimicrobial activity against *Listeria monocytogenes* on ultrafiltered white cheese. *Lwt*. 2018;92:576-583.
63. Karimi Alavijeh D. *Development of Films/Fibrous Nanostructures with Gas and Volatiles Detection Ability*. Master's thesis. Polytechnique Montréal; 2020.
<https://publications.polymtl.ca/4221/>
64. Sobhan A. *"Development of Bio-based Nanocomposites for Biosensor and Indicator Applications in Smart Food Packaging"*. South Dakota State University; 2021.
<https://openprairie.sdstate.edu/etd/5792>
65. <https://www.iso.org/standard/34524.html> IndI.
66. Husain R, Suparmo S, Harmayani E, Hidayat C. Kinetic oxidation of protein and fat in snapper (*Lutjanus* sp) fillet during storage. AIP Publishing; 2016:

67. López S, Prieto M, Dijkstra J, Dhanoa MS, France J. Statistical evaluation of mathematical models for microbial growth. *International journal of food microbiology*. 2004;96(3):289-300.
68. Howgate P. A critical review of total volatile bases and trimethylamine as indices of freshness of fish. Part 2. Formation of the bases, and application in quality assurance. *Electronic Journal of Environmental, Agricultural & Food Chemistry*. 2010;9(1)
69. Peleg M, Corradini MG. Microbial growth curves: what the models tell us and what they cannot. *Critical reviews in food science and nutrition*. 2011;51(10):917-945.
70. Giannuzzi L, Pinotti A, Zaritzky N. Mathematical modelling of microbial growth in packaged refrigerated beef stored at different temperatures. *International Journal of Food Microbiology*. 1998;39(1-2):101-110.
71. Wang L, Heising J, Fogliano V, Dekker M. Fat content and storage conditions are key factors on the partitioning and activity of carvacrol in antimicrobial packaging. *Food Packaging and Shelf-life*. 2020/06/01/ 2020;24:100500. doi:<https://doi.org/10.1016/j.fpsl.2020.100500>
72. Othman N, Azahari NA, Ismail H. Thermal properties of polyvinyl alcohol (PVOH)/corn starch blend film. *Malaysian Polymer Journal*. 2011;6(6):147-154.
73. Kong Y, Wang X, Wu Z, Li Y, Xu F, Xie F. Enzymatic Acylation of Black Rice Anthocyanins and Evaluation of Antioxidant Capacity and Stability of Their Derivatives. *Foods*. 2023;12(24):4505.
74. Prime RB, Bair HE, Vyazovkin S, Gallagher PK, Riga A. Thermogravimetric analysis (TGA). *Thermal analysis of polymers: Fundamentals and applications*. 2009:241-317.
75. Romero C, Bakker J. Effect of storage temperature and pyruvate on kinetics of anthocyanin degradation, vitisin A derivative formation, and color characteristics of model solutions. *Journal of Agricultural and Food Chemistry*. 2000;48(6):2135-2141.
76. Corazzari I, Nisticò R, Turci F, et al. Advanced physico-chemical characterization of chitosan by means of TGA coupled on-line with FTIR and GCMS: Thermal degradation and water adsorption capacity. *Polymer Degradation and Stability*. 2015;112:1-9.
77. Ofori FA, Sheikh FA, Appiah-Ntiamoah R, Yang X, Kim H. A simple method of electrospun tungsten trioxide nanofibers with enhanced visible-light photocatalytic activity. *Nano-micro letters*. 2015;7:291-297.

78. Silva N, Nascimento N, Cividanes L, Bertran C, Thim G. Kinetics of cordierite crystallization from diphasic gels. *Journal of sol-gel science and technology*. 2008;47:140-147.
79. Rowe AA, Tajvidi M, Gardner DJ. Thermal stability of cellulose nanomaterials and their composites with polyvinyl alcohol (PVA). *Journal of Thermal Analysis and Calorimetry*. 2016;126:1371-1386.
80. Ekici L, Simsek Z, Ozturk I, Sagdic O, Yetim H. Effects of temperature, time, and pH on the stability of anthocyanin extracts: Prediction of total anthocyanin content using nonlinear models. *Food Analytical Methods*. 2014;7:1328-1336.
81. Khezerlou A, Alizadeh Sani M, Tavassoli M, Abedi-Firoozjah R, Ehsani A, McClements DJ. Halochromic (pH-Responsive) Indicators Based on Natural Anthocyanins for Monitoring Fish Freshness/Spoilage. *Journal of Composites Science*. 2023;7(4):143.
82. Gratson GM, Lewis JA. Phase behavior and rheological properties of polyelectrolyte inks for direct-write assembly. *Langmuir*. 2005;21(1):457-464.
83. Heredia F, Francia-Aricha E, Rivas-Gonzalo J, Vicario I, Santos-Buelga C. Chromatic characterization of anthocyanins from red grapes—I. pH effect. *Food Chemistry*. 1998;63(4):491-498.
84. Borkowski T, Szymusiak H, Gliszczyńska-Świgło A, Rietjens IM, Tyrakowska B. Radical scavenging capacity of wine anthocyanins is strongly pH-dependent. *Journal of agricultural and food chemistry*. 2005;53(14):5526-5534.
85. Liu Z, Luo F, Chen T. Polymeric pH indicators immobilized PVA membranes for optical sensors of high basicity based on a kinetic process. *Analytica Chimica Acta*. 2004/08/16/2004;519(2):147-153. doi:<https://doi.org/10.1016/j.aca.2004.06.028>
86. Castañeda-Ovando A, Pacheco-Hernández MdL, Páez-Hernández ME, Rodríguez JA, Galán-Vidal CA. Chemical studies of anthocyanins: A review. *Food Chemistry*. 2009/04/15/2009;113(4):859-871. doi:<https://doi.org/10.1016/j.foodchem.2008.09.001>
87. Alamdari NE, Aksoy B, Aksoy M, Beck BH, Jiang Z. A novel paper-based and pH-sensitive intelligent detector in meat and seafood packaging. *Talanta*. 2021;224:121913.
88. Patras A, Brunton NP, O'Donnell C, Tiwari BK. Effect of thermal processing on anthocyanin stability in foods; mechanisms and kinetics of degradation. *Trends in Food Science & Technology*. 2010;21(1):3-11.

89. Loypimai P, Moongngarm A, Chottanom P. Thermal and pH degradation kinetics of anthocyanins in natural food colorant prepared from black rice bran. *Journal of food science and technology*. 2016;53:461-470.
90. Ebrahim A, DeVore K, Fischer T. Limitations of Accelerated Stability Model Based on the Arrhenius Equation for Shelf-life Estimation of In Vitro Diagnostic Products. *Clinical Chemistry*. 2020;67(4):684-688. doi:10.1093/clinchem/hvaa282
91. Muniandy A, Benyathiar P, Ozadali F, Mishra DK. Multi-accelerant approach for rapid shelf-life determination of beverages in polymeric packaging. *Food Research International*. 2023/11/01/ 2023;173:113318. doi:<https://doi.org/10.1016/j.foodres.2023.113318>
92. Etxabide A, Kilmartin PA, Maté JI. Color stability and pH-indicator ability of curcumin, anthocyanin and betanin containing colorants under different storage conditions for intelligent packaging development. *Food Control*. 2021/03/01/ 2021;121:107645. doi:<https://doi.org/10.1016/j.foodcont.2020.107645>
93. Kennedy JA, Waterhouse AL. Analysis of pigmented high-molecular-mass grape phenolics using ion-pair, normal-phase high-performance liquid chromatography. *Journal of Chromatography A*. 2000/01/07/ 2000;866(1):25-34. doi:[https://doi.org/10.1016/S0021-9673\(99\)01038-9](https://doi.org/10.1016/S0021-9673(99)01038-9)
94. Enaru B, Dreţcanu G, Pop TD, Stănilă A, Diaconeasa Z. Anthocyanins: Factors affecting their stability and degradation. *Antioxidants*. 2021;10(12):1967.
95. Jouki M, Yazdi FT, Mortazavi SA, Koochehi A, Khazaei N. Effect of quince seed mucilage edible films incorporated with oregano or thyme essential oil on shelf-life extension of refrigerated rainbow trout fillets. *International journal of food microbiology*. 2014;174:88-97.
96. Aghaei Z, Emadzadeh B, Ghorani B, Kadkhodae R. Cellulose acetate nanofibres containing alizarin as a halochromic sensor for the qualitative assessment of rainbow trout fish spoilage. *Food and bioprocess technology*. 2018;11(5):1087-1095.
97. Yang Z, Zhai X, Zou X, et al. Bilayer pH-sensitive colorimetric films with light-blocking ability and electrochemical writing property: Application in monitoring crucian spoilage in smart packaging. *Food Chemistry*. 2021/01/30/ 2021;336:127634. doi:<https://doi.org/10.1016/j.foodchem.2020.127634>

98. Heising J, Dekker M, Bartels P, Van Boekel M. A non-destructive ammonium detection method as indicator for freshness for packed fish: Application on cod. *Journal of Food Engineering*. 2012;110(2):254-261.
99. Silva-Pereira MC, Teixeira JA, Pereira-Júnior VA, Stefani R. Chitosan/corn starch blend films with extract from *Brassica oleraceae* (red cabbage) as a visual indicator of fish deterioration. *LWT - Food Science and Technology*. 2015/04/01/ 2015;61(1):258-262.
doi:<https://doi.org/10.1016/j.lwt.2014.11.041>
100. Burg SP. *Postharvest physiology and hypobaric storage of fresh produce*. Cabi; 2004.
101. Karaca IM, Haskaraca G, Ayhan Z, Gültekin E. Development of real time-pH sensitive intelligent indicators for monitoring chicken breast freshness/spoilage using real packaging practices. *Food Research International*. 2023/11/01/ 2023;173:113261.
doi:<https://doi.org/10.1016/j.foodres.2023.113261>
102. Zúñiga R, Troncoso E. Shelf-life calculation and temperature-time indicators: importance in food safety. *Chemical Food Safety and Health*. 2013:131-148.
103. Koutsoumanis K, Nychas G-JE. Application of a systematic experimental procedure to develop a microbial model for rapid fish shelf-life predictions. *International Journal of Food Microbiology*. 2000;60(2-3):171-184.
104. Corbo MR, Altieri C, Bevilacqua A, Campaniello D, D'Amato D, Sinigaglia M. Estimating packaging atmosphere-temperature effects on the shelf-life of cod fillets. *European Food Research and Technology*. 2005;220:509-513.
105. Chen L, Wang W, Wang W, Zhang J. Effect of Anthocyanins on Colorimetric Indicator Film Properties. *Coatings*. 2023;13(10):1682.
106. Kim DY, Park SW, Shin HS. Fish Freshness Indicator for Sensing Fish Quality during Storage. *Foods*. Apr 26 2023;12(9)doi:10.3390/foods12091801
107. Tan C, Xiao M, Wu R, Li P, Shang N. Unraveling the Effects of Biochemical Drivers on the Bacterial Communities and Volatile Profiles in Refrigerated Sturgeon Filets at 4°C. Original Research. *Frontiers in Microbiology*. 2022-March-30 2022;13doi:10.3389/fmicb.2022.849236
108. Zhang K, Li Z, Zhao W, et al. Aerogel colorimetric label sensors based on carboxymethyl cellulose/sodium alginate with black goji anthocyanin for monitoring fish freshness. *International Journal of Biological Macromolecules*. 2024:130466.

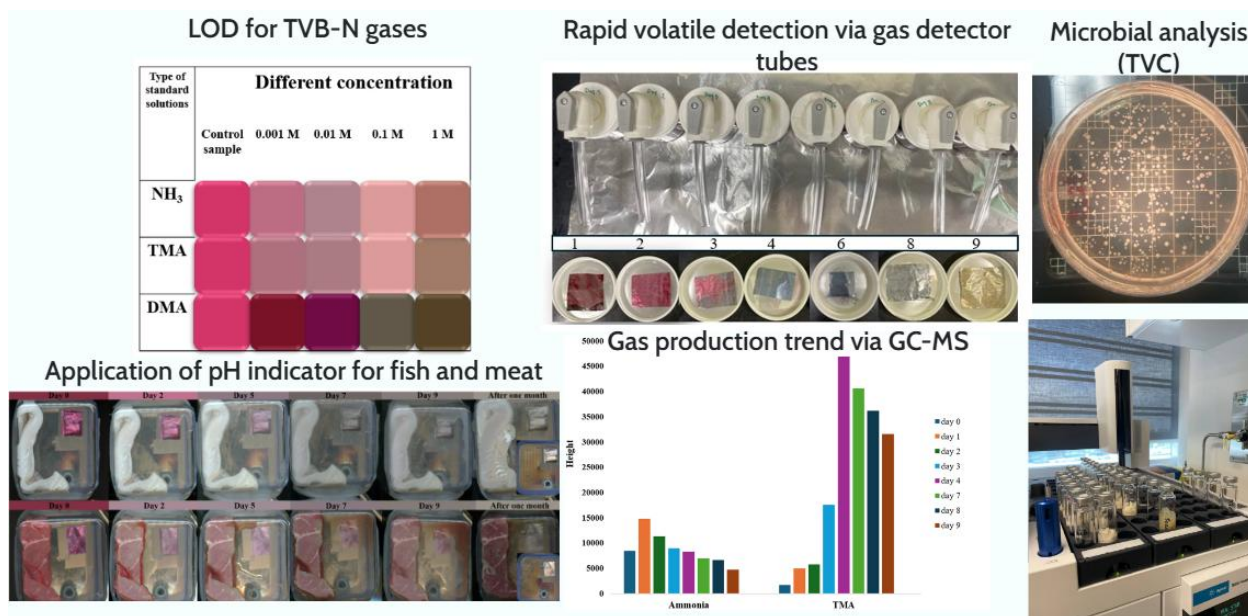
109. Liu X, Chen K, Wang J, et al. An on-package colorimetric sensing label based on a sol-gel matrix for fish freshness monitoring. *Food Chemistry*. 2020/03/01/ 2020;307:125580. doi:<https://doi.org/10.1016/j.foodchem.2019.125580>
110. Hindle F, Kuuliala L, Mouelhi M, et al. Monitoring of food spoilage by high resolution THz analysis. *Analyst*. 2018;143(22):5536-5544.
111. Ogidi OI, Charles EE, Okore CC, Wilfred B, Oguoma LM, Carbom HE. Mathematical modelling of the growth of specific spoilage microorganisms in tilapia (*Oreochromis niloticus*) fish. *ASIO J Microbiol Food Sci Biotechnol Innov*. 2021;6(1):09-15.
112. Yi Z, Xie J. Prediction in the dynamics and spoilage of *Shewanella putrefaciens* in Bigeye Tuna (*Thunnus obesus*) by gas sensors stored at different refrigeration temperatures. *Foods*. 2021;10(9):2132.

CHAPTER 6 ARTICLE 3: INTELLIGENT PACKAGING SOLUTIONS FOR FISH AND MEAT PRODUCTS: VOLATILE GAS DETECTION VIA GC-MS, MICROBIAL ANALYSIS AND COLORIMETRIC MONITORING

Credit Author Statement

Maryam Ameri: Conceptualization, Investigation, Experimental work, Data curation, Writing – original draft. Writing – review & editing , bibliographic, Project administration. Abdellah Ajji: Conceptualization, Supervision, Funding acquisition, review & editing. Samuel Kessler: Conceptualization, Supervision, review & editing. Marc-Antoine Vaudreuil: Experimental work. Writing-review& editing.

Intelligent Packaging Solutions for fish and meat products: Volatile gas detection via GC-MS, Microbial Analysis and Colorimetric Monitoring



Authors: Maryam Ameri¹[ID](#), Abdellah Ajji¹[ID](#), Samuel Kessler², Marc-Antoine Vaudreuil³

Corresponding authors: Maryam.ameri@polymtl.ca and Abdellah.ajji@polymtl.ca

1. Chemical Engineering Department, Polytechnique Montréal, Montréal, Québec, H3T 1J4, Canada.
2. Active/Intelligent Packaging, ProAmpac, Cincinnati, Ohio 45246, United States.
3. Regional Mass Spectrometry Center, University de Montréal, Montréal, Québec, H2V 0B3, Canada.

Submitted in Nature Food, 7 November 2024

6.1 Abstract

A pH-sensitive anthocyanin dye was used as a freshness indicator to detect color changes in fish products due to volatile amine formation and microbial activity during storage at 4 °C. Incremental color changes of the pH indicator response accurately tracked an increase in the total volatile basic nitrogen (TVB-N) content in the packaging headspace of fish products along with increases in total

viable count (TVC). Ammonia (NH_3) and trimethylamine (TMA) production trend were evaluated during the fish storage using headspace analysis with gas chromatography-mass spectroscopy (GC-MS) detection. No laborious pre-treatment, clean-up, or derivatization was required. The GC-MS method optimization yielded linear calibration curves for the targeted analytes, with detection limits in the range of ppm in pure solvent and good method precision, allowing for the analysis of trends in the molecule concentrations formed during real fish sample storage. Scan-mode injections identified methanol (MeOH), ethanol (EtOH), dimethyl sulfide (DMS), butane and pentane (untargeted species) during fish spoilage with high scores ($> 89\%$). In parallel, gas detection tubes were used to quantify NH_3 and Triethylamine (TEA) concentrations in the headspace of homogeneous fish samples across different vial storage conditions and microbial analyses. Correlation analysis between colorimetric results and GC-MS data illustrated a strong relationship in TMA detection, reinforcing the colorimetric sensor's practicality as an efficient monitoring tool for seafood freshness. The experimental outcomes not only highlight the responsiveness of our sensing approach but also suggest potential applications as an intelligent package for ensuring food safety and quality.

Keywords: Intelligent packaging, On-package sensor, Headspace GC-MS, TMA detection, pH indicator, Anthocyanin

6.2 Introduction

The increasing demand for fresh seafood and meat products necessitates effective monitoring systems to ensure food safety and quality [1]. A significant challenge in the storage of fresh fillets is assessing their freshness, as post-mortem microbial activity and endogenous biochemical reactions can rapidly result in quality degradation and a reduced shelf life of the raw fish fillets [2]. Spoilage in perishable food items, such as fish, is predominantly caused by microbial activity, leading to the formation of volatile compounds, including TVB-N, which primarily comprises NH_3 , TMA and dimethylamine (DMA)[3]. Chicken fillets and other types of meat can produce TVB-N as well during their spoilage [4]. However, this indicator is more commonly used as a measure of freshness in seafood products [5]. Moreover, TEA is a volatile organic compound that can be produced during the spoilage of fish and other seafood [5-7]. Traditional methods for assessing spoilage often rely on sensory evaluation or chemical tests that may not provide timely or accurate results [8]. Therefore, there is a pressing need for innovative and reliable indicators that

can monitor spoilage in real-time, ensuring that consumers receive safe and high-quality food products [8-11].

TMA is produced by a small number of specific spoilage organisms (SSO) which is the reason of fishy odour, arising from the bacterial reduction of Trimethylamine N-oxide (TMAO) [12, 13]. Thus the presence of TMA in muscle can give a very good indication of the level of bacterial contamination [14, 15] and often reflects more accurately the degree of spoilage [16, 17]. In a very fresh fish the amount of TMA is low; an average of 2 mg/100g for some fish species from the North-East Atlantic [3]. A TMA content of 5–10 mg/100 g is usually regarded as the sensory rejection limit [18]. However a limit of acceptability of is 8 mg/100g was suggested as well [19]. Studies have indicated that fillet samples can exhibit lower levels of TVB-N and TMA compared to whole fish, likely due to the absence of viscera and head, where microorganisms that convert TMAO to TMA are concentrated [20].

Detecting SSO such as *Pseudomonas* spp. along with TVC for assessing fish product freshness or spoilage [16]. *Pseudomonas* spp. appeared to be responsible for the development of sweet, fruity spoilage odors in haddock fillets. *Pseudomonas* spp. are significantly implicated in the deterioration of haddock fish at refrigeration temperatures, particularly in the initial stages [16]. Studies show that TVC in freshwater fish can attain 6 to 7 log CFU/ml after 3-5 days of storage at 4 °C [21, 22].

In recent years, anthocyanins, natural pigments found in various fruits and vegetables, have gained attention for their potential as pH indicators in food safety applications. These compounds exhibit color changes in response to pH variations, making them suitable for developing indicators that can signal spoilage [10, 23-26]. By integrating anthocyanins into a food-safe pH indicator, we can create a visual tool that not only indicates pH changes but also correlates with the spoilage process in fish and meat products [10, 26-29]. This research aims to evaluate the performance of such an indicator in monitoring spoilage, providing a practical solution for consumers and food industry stakeholders.

Recent studies combining GC-MS with intelligent packaging has shown promising results for monitoring fish spoilage [30]. An electronic nose with metal oxide gas sensors and GC-MS revealed correlations between volatile compounds and fish freshness [31]. Another study demonstrated the use of colorimetric indicators to detect volatile amines and correlated the color

changes with GC-MS measurements [32]. To evaluate the effectiveness of the developed pH indicator, we performed a variety of experiments, including monitoring the color change of pH indicators, microbial analysis to correlate the presence of specific bacteria with the production of spoilage-related compounds, and GC-MS tests to detect NH_3 and TMA levels during fish spoilage. The use of various techniques in GC-MS experiments, such as headspace analysis and direct injection, enabled a thorough understanding of the volatile compounds produced during spoilage.

Scan analysis allowed for detection and identification of non-targeted volatile compounds produced during fish storage. Furthermore, we used gas detection tubes to measure ammonia concentrations in the headspace of fish packages. This multifaceted approach ensures that the developed indicator is not only responsive to pH changes, but also accurately reflects the spoilage process, highlighting the anthocyanin-based pH indicator's potential as a reliable monitoring tool. By combining these methodologies, this study aims to provide an effective structure for evaluating the performance of the developed food-safe pH indicator, resulting in improved food safety and quality control in seafood and meat industries. The main objective of the study was to employ pH indicators based on natural dyes in food packaging that can alter color in reaction to elevated levels of TVB-N gases in the headspace of food containers and the bacterial activity of fish and meat products throughout their shelf life.

The data presented here pertains to method development experiments conducted in January 2024 for the detection and quantification of NH_3 and TMA in three different types of fish: pangas and haddock. Additionally, a storage experiment of haddock fillets was conducted in August 2024 for microbial analysis, TMA trends determination using headspace GC-MS, NH_3 gas detection tubes, and monitoring the color change of these fish fillets simultaneously. The objective was to validate the performance of colorimetric sensor for further application as freshness/spoilage indicator for fishery products. Determination of the end of shelf-life based on microbial analysis and TMA production was compared to the estimation of shelf-life based on the currently developed pH indicator.

6.3 Materials and methods

6.3.1 Materials

We acquired pangasius and haddock fillets from a nearby Metro grocery store in Montreal, Quebec, Canada. Initially, the products were sealed in PVC-wrapped packages that displayed a label containing the packaging date and the best before date (which was three days after the packaging date). The samples were placed in an ice container to maintain their temperature and freshness during transportation. The samples remained in the fridge until they were ready to be use. The Polytechnique Montreal in Montréal, Québec, Canada, served as the site of all experiments except the headspace GC-MS experiments which performed in the Regional Mass Spectrometry Center, Université de Montréal, Montréal, Québec, Canada. Transparent polyethylene terephthalate films (PET, 23 μm) were obtained from ProAmpac Packaging Canada company, Terrebonne, Quebec, Canada. Black rice extract 80% was purchased from Xiherbs Phytochem Co., Ltd (Dongguan, Guangdong, China). Certified amber glass jar with white polypropylene cap with bonded PTFE-faced silicone septa to meet EPA Performance based specifications for volatile organic analysis were from Thermo Fisher Scientific, Saint-Laurent, Quebec. Single-neck round-bottom flask, Polyvinyl alcohol (87~88% hydrolysis, 145,000 MW), Polyethylene glycol (PEG), Citric acid (ACS reagent, $\geq 99.5\%$), Vanillin (natural, $\geq 97\%$, FCC, FG), Hydrochloric acid (HCL), Sodium Chloride (NaCl), Dimethylamine solution (DMA, 2 M in methanol), Trimethylamine solution (TMA, 31-35 wt. % in ethanol, 4.2 M), Ammonium hydroxide solution (NH_4OH , 30-33% NH_3 in H_2O), Diethyl-d10-amine, Vortex-Genie 2 (120 V) mixer, Agar were purchased from Millipore Sigma Canada Ltd , Oakville, Ontario, Canada. Dräger tubes for short term measurement: Ammonia 20/a-D 8101301 (20-1500 ppm), Ammonia 5/a (5-600 ppm), Ammonia 0.25/a (0.25-3 ppm), Triethylamine 5/a (5-60 ppm), and accuro pump Tube-D, were from Dräger Co., Ltd (Mississauga, ON ,Canada).

6.3.2 Sensor preparation

A complete description of sensor preparation was provided with some modifications [9]. Specifically, we described the colorimetric sensor's preparation method as follows: PVOH and deionized water were mixed in a glass beaker to create a heterogeneous mixture. A solution mixer made of PEG, C, BC and distilled water was added after the solution cooled at room temperature while being stirred constantly. The coating was carried out with a TQC automatic film applicator (model AB3652 made in Netherlands). The drying process of the films proceeded at two

temperatures: ambient (30 min) and 165 °C (5 min). Samples were labeled NTT (no thermal treatment) and TT (Thermal treated pH indicators, at temperature of 165 °C for 5 min) [33].

6.3.3 Freshness monitoring

In this study, we conducted a series of simultaneous shelf-life monitoring tests on fish fillets, which included analyses of color change, microbial activity (TVC, *Pseudomonas spp.*), GC-MS for TMA and NH₃ detection, and gas detector tubes for measuring NH₃ and TEA. For monitoring the color change and gas detection, approximately 20 gr of fish samples were prepared in amber vials. For microbial activity assessment, around 5 g of fish were utilized, while 10 gr were allocated for GC-MS analysis. It is important to note that all fish fillets used in these experiments were procured from the same retail outlet, packaged at the same time, and consisted of the same species. Prior to distribution into vials, the fillets were mixed homogenously to ensure uniformity across the samples. The shelf-life was monitored on a haddock fish upon storage at around 4 °C during the summer of 2024 in Montreal, Quebec, Canada. The day of purchase (package date) was considered as day 0 (the day the fish was first packaged at the store for sale), and the 'best before' date on the fish package was set to 3 days from that point.

6.3.4 Packaging study using RGB

We used mentioned procedure from our previous study, with minor modifications, to evaluate the sensitivity of the developed pH indicator towards TVB-N gases originated from fish samples [10]. Color responses of the colorimetric film to produced volatile gases were captured by an Epson perfection V550 scanner (Nagano, Japan). Control samples were chosen as reference image for RGB calculation. The color change of pH indicators during storage period is measured by the total color difference (ΔRGB) according to the following equation [34].

$$\Delta RGB = \sqrt{(R - R_0)^2 + (G - G_0)^2 + (B - B_0)^2} \quad (6.1)$$

Where R_0 , B_0 , G_0 are the initial color parameters of indicators and R , G and B were the values at the time of sampling.

6.3.5 Microbial analysis

During fish storage at 4 °C, the TVC method revealed, the bacterial growth reaching the spoiling threshold (1×10^7 CFU/ml)[35]. Microbial analysis was performed by weighted fish samples (5 ± 0.5 g) which were placed in sterilized 50 ml tubes (Fisher brand). The sterilized NaCl (9 %w/v) saline solution (45 ml) was added to tubes and homogenized with vortex for 2 min at room temperature under biohood. Serial sample dilutions were made during the fish spoiling tests [35]. The rest of experimental part was performed exactly as in our previous work [36]. The results were expressed (according to ISO 7218:2007) as mean log CFU/ml \pm standard deviation of 3 replicates.

6.3.6 NH₃ and TEA detection using the gas detection tubes

The dräger short-term detector tubes along with its pump which can measure toxic gases and vapors in the workplace, were used as fast and cost-effective approach. The measuring range which was used for ammonia gases were 5 to 70 ppm and 0.25 to 3 ppm with 10 times stroke's number and 50 to 600 ppm with once time stroke's number. The approximate measuring time is around 1 minute. For TEA gas detection tubes, the measuring range is 5 to 60 ppm. The number of strokes is 5 and the approximate time for measurement is around 3 minutes, and the standard deviation for all tubes are ± 10 to 15%. The color change principle is based on acid-base reaction which can turn yellow to blue color. Each 1 ppm NH₃ is equal to 0.71 mg NH₃/m³ and 1 ppm triethylamine is equal to 4.2 mg triethylamine/m³. Firstly, we break both tips of the tube and inserted the tube close to the pump. Then inserted the gas sample through the tube and read the entire length of the discolouration.

6.3.6.1 Sample preparation for gas detection tubes

We used amber vials (60 mL) to conduct experiments, filling them with a homogeneous mixture of fish fillets (approximately 20 g). Furthermore, on each sampling day, we used control vials without fish fillets to monitor baseline changes in the headspace gases. On each sampling date, we attempted to measure the gas concentration of each vial as promptly as possible to mitigate variability in gas production that could result from external factors.

6.3.6.2 Freshness control in room temperature with gas tube detector

Ammonia detection tubes with a measurement range of 20–1500 ppm were used to measure the average ammonia concentration over an extended period of up to 8 hours. The ammonia molecules

to be measured independently flow into the tube, which is open at one end, up to reagent layer (bromophenol blue and acid) based on diffusion process in gases. The generated ammonia from fish sample reacts with the chemical on the substrate. A color change for tubes from yellow to blue takes place. The reading is indicated in “ppm × hours”. The length of the color zone and the elapsed sampling time is used to calculate the average ammonia concentration (appendices). For evaluation the ammonia concentration in ppm = tube reading/measurement duration in the hours. The standard deviation for these tubes is ± 15 to 20 % and the accuracy is without calibration. The setup includes a container with an integrated colorimetric sensor, coupled with the connected tube (**Figure 6.1**).

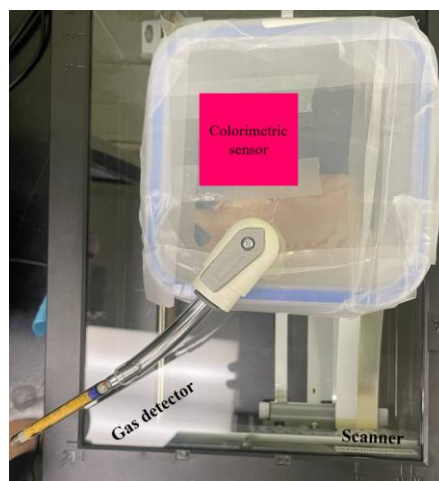


Figure 6.1 A container with a 900 ml capacity, along with an integrated colorimeter sensor and a connected valve for monitoring the volatile gasses produced during a duration of 8 hours.

6.3.7 GC-MS analysis

To achieve the low-level detection of gases generated during the storage of fish samples, specifically DMA, TMA, and NH_3 , a systematic approach was implemented to evaluate different methodologies. Additionally, untargeted (scan mode) analysis was conducted to identify other species present during the storage of fish samples. Various parameters were controlled to ensure consistency across the analytical methodologies employed. The experiments were conducted in two distinct phases. The first phase involved two different fish species, *Pangasius* (commonly known as pangas) and haddock. This phase aimed to develop a standardized laboratory method aligned with the objectives of the project. The second phase focused on performing additional analyses for shelf-life monitoring.

6.3.7.1 Instrumental conditions

The analysis was conducted using a Headspace (model 7697A) coupled with a GC-MS (model 7890A-5975C), all from Agilent Technologies. The gas chromatography utilized a GS-Q column, a narrow bore capillary column, which is appropriate for separation of low molecular weight compounds. The column measures 30 m in length and 320 μ m in diameter. The carrier gas used was helium, with a flow rate of 1.2 mL/min [38]. The headspace temperature was maintained at 80 °C for 30 minutes to achieve optimal vaporization of the analytes.

6.3.7.2 Temperature program for chromatographic column

The temperature program was initiated at 70 °C and held for 2 minutes, followed by a ramp of 10 °C/min until reaching a final temperature of 250 °C, where it was held for an additional 2 minutes. Spitless injection mode was set at an injector temperature of 250 °C to enhance sensitivity for the target analytes.

6.3.7.3 Mass spectrometry conditions

The mass spectrometer was equipped with an electron ionization (EI) source. Acquisition parameters were set to two different approaches: a targeted and an untargeted one. Selected ion monitoring (SIM), focusing on known m/z values 17.0 for NH_3 , 44.1 for DMA, 58.1 for TMA, 32 for methanol, 46 for ethanol and 83.2 for diethyl-d10-amine used as an internal standard was used as targeted method. A scan mode covering m/z 10 to 300 for detection and identification of other volatile species released during fish storage was used as untargeted approach.

6.3.7.4 Calibration curve

A mixture of standards was prepared using stock solutions of individual compounds, with diethyl-d10-amine employed as an internal standard. For the preparation of headspace vials containing standards in pure solvent, 1 mL of water was added to each 20 mL headspace vial, followed by the incorporation of 10 μ L of (25% w/w) diethyl-d10-amine as internal standard. The vials were then spiked with a mixture of standards to achieve final concentrations of analytes ranging from 50 to 38,000 mg/L. Vials sealed with a crimp cap were analyzed on the same day. To verify the retention times of targeted analytes, they were individually injected in pure solvent. The limit of detection (LOD) is defined as the lowest concentration leading to a signal-to noise ratio of 3 [39, 40].

Precision, in terms of relative standard deviation (RSD) was assessed by replicate analyses of spiked samples via studies of inter-day variability. Essays of calibration curves in real matrix were done by adding approximately 10 g of fish to a 20 mL headspace vial and spiking standards directly onto the fish for a final concentration ranging from 700 to 8 000 mg/kg. After sealing the vials with a crimp cap, the content was also analyzed on the same day.

6.3.7.5 Preparation of fish samples for head-space GC-MS

Approximately 10 g of fresh fish was weighed and placed into a 20 mL headspace vial. Following, 10 μ L of diethyl-d10-amine (25% w/w) was added. The vial was sealed with a crimp cap and either analyzed on the same day (day 0) or stored in the refrigerator until analysis on subsequent days (day 1 to day 4 and day 7 to day 9). Alternatively, a manual injection approach was tested by weighing approximately 70 g of fresh fish in 250 mL glass flask. Subsequently, 50 μ L of diethyl-d10-amine (25% w/w) was added, and the flask was spiked with a mixture of analyte standards, with concentrations of 50 to 500 μ g/g for DMA and TMA, and 0.05 to 0.5 μ g/g for ammonia. The flasks were sealed with a silicon septa cap, and headspace samples were extracted using a gas tight syringe and analyzed on the same day.

6.4 Data analysis

Microsoft Excel 365 was used for data processing, to calculate means and standard deviations for all multiple measurements and to generate graphs. Analysis of variance (ANOVA) was applied to the microbial, RGB parameters from colorimetric sensor and TMA quantification. Significant differences were determined by one way ANOVA. An effect was considered significant at the 5% level ($p < 0.05$). Identification of the untargeted compounds made using NIST database comparison (NIST/EPA/NIH Mass Spectral Library with Search Program, data version NIST 05, software version 2.0d).

6.5 Results and discussion

6.5.1 pH indicator sensitivity towards different TVB-N gases

The results from multiple experiments conducted (at room temperature and evaluated temperatures) on the on-package label indicate a clear relationship between the concentration of TVB-N gases (NH_3 , TMA, DMA) and the color parameters measured through ΔRGB . The statistical significance of the 0.01 M concentration ($p < 0.05$) suggests that this level is critical for

detecting changes in color, which can be attributed to the presence of these gases. This concentration level is detectable and has a significant effect on ΔRGB . **Figure 6.2** presents the color parameters associated with the limit of detection measurements based on the pictures captured by the smart phone. The indicators were tested against different standards (TMA, DMA, NH_3) at dilutions (0.001, 0.01, 0.1, and 1 M). The red channel (R) shows a significant decrease for all analytes: NH_3 exhibits the most pronounced decline, followed by TMA, while DMA shows a slightly less dramatic reduction. This trend indicates that NH_3 has noticeable impact on the color change of the pH indicator among the three analytes, as it was observed in our previous research study [37]. DMA's resolution appears better because it maintains a clearer and more stable response across varying concentrations, allowing for more precise differentiation in color intensity, even though its overall effect on color change is less pronounced compared to NH_3 and TMA. This stability can make it easier to detect subtle variations in concentration. For the green channel (G), there is minimal fluctuation across all analytes, with NH_3 and TMA showing slight decreases, while DMA remains relatively stable. In the blue channel (B), a subtle decline is observed for NH_3 and TMA, with DMA exhibiting the least change, indicating that the blue response is less sensitive compared to the red channel.

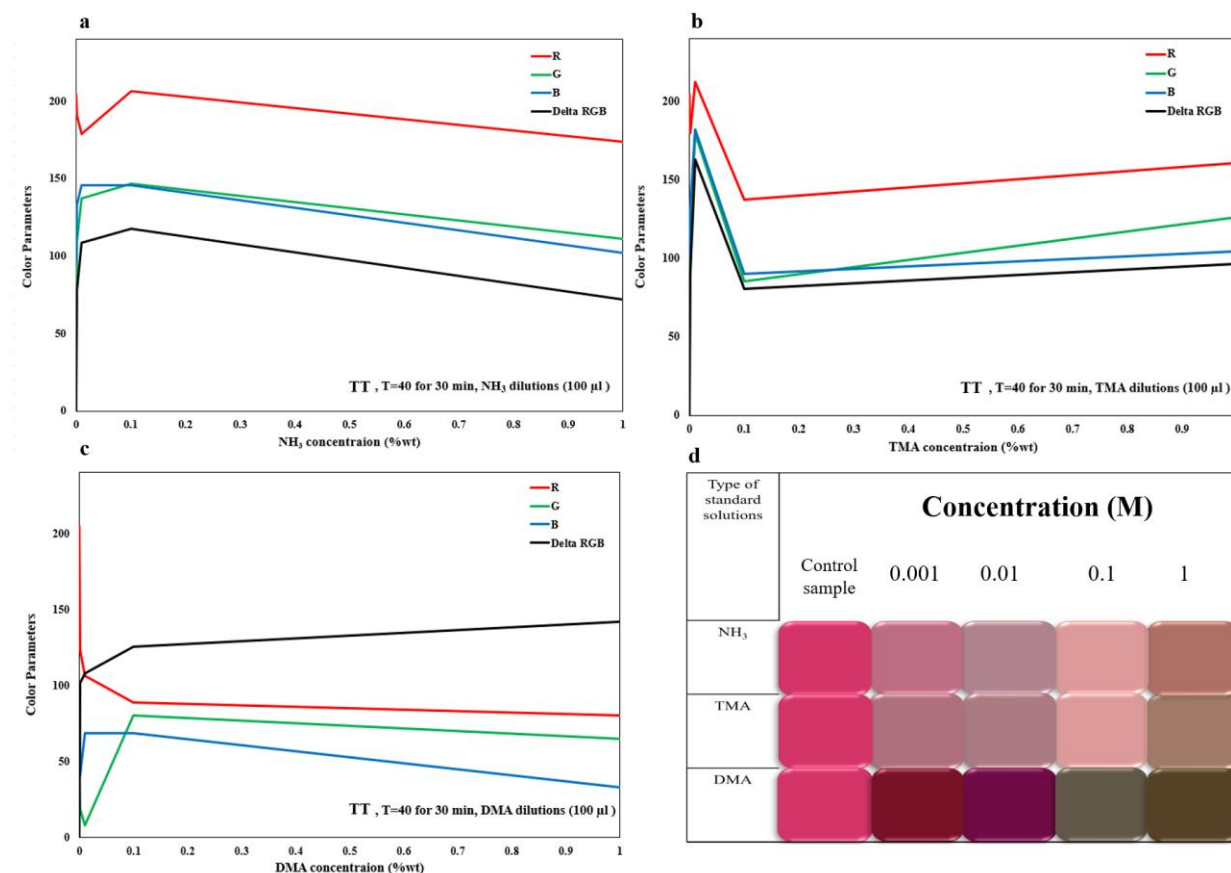


Figure 6.2 The color parameters from various TVB-N gas dilutions (a: NH₃, b: TMA, c: DMA) and the TVB-N gas detection limit (d) in accelerated mode are presented.

6.5.2 The effect of sensor ink on different food product: fish, meat and chicken breast

We assessed the efficacy of pH indicator labels (TT) through packaging trials involving haddock fillets, beef steaks, and chicken breasts, which had best-before dates of 3, 4, and 4 days, respectively. Day 0 marked the packaging date for these products, with trials consisting of samples weighing 100 ± 5 g, contained within 900 ml packages. As shown in **Figure 6.3**, these products were stored at 4°C for a duration of 9 days, during which the pH indicator displayed significant color changes corresponding to the freshness levels of the food items.

The pH indicator was calibrated to exhibit a four-point freshness scale: red for fresh, pink/purple for not fresh/acceptable, light purple for moderate spoilage, and yellowish-brown for high spoilage [37]. Observations indicated that from days 0 to 2, the indicator remained red/pink, signifying pristine conditions with no spoilage. By day 5, it shifted to light purple, reflecting minimal spoilage while still being safe for consumption. On day 7, the haddock sample's indicator changed to

yellowish-brown, indicating spoilage, while the beef and chicken maintained a dark purple hue, suggesting differing spoilage mechanisms between seafood and meat products. By day 9, all meat indicators had also shifted to yellowish-brown, indicating spoilage. Notably, the fish began to exhibit watery conditions by day 2, while the meat products followed by day 3. In order to evaluate the stability of pH indicators, samples were kept for one month after monitoring the shelf life (over 9 days). Despite the high humidity levels in the package, the pH indicators demonstrated excellent color stability, although the product samples appeared visibly watery and squishy.

NH_3 generally increases throughout the storage period for all types of meat, indicating ongoing spoilage. TMA shows a peak around Day 5, followed by a decrease, likely due to its reactivity and potential evaporation. DMA remains relatively stable across the storage period, indicating it may be less affected by spoilage processes compared to NH_3 and TMA. NH_3 , a key volatile compound in TVB-N, significantly contributes to color changes during fish spoilage, as noted in other studies [41, 42]. This observation can be attributed to ammonia is typically more abundant in the early stages of spoilage [43], making it a primary factor in the initial color change of the pH indicator. While TMA becomes more dominant as spoilage progresses [44], accounting for the subsequent changes in the pH indicator's color. Throughout the 9-day storage period, the pH indicator effectively differentiated the freshness levels of food samples, offering a nuanced assessment that surpasses a simple binary outcome.

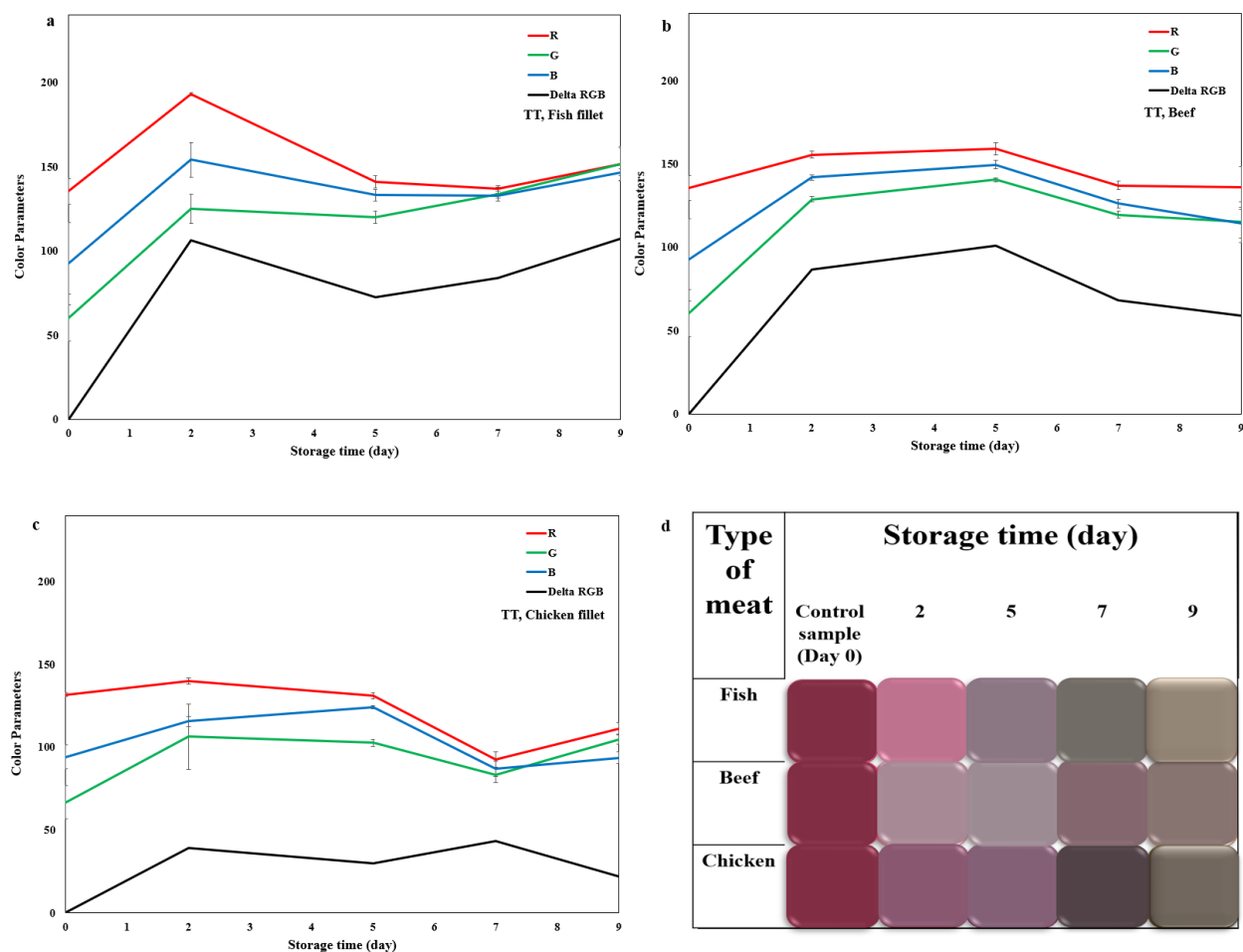


Figure 6.3 Packaging trials for different types of food products during 9 days of storage at 4 °C, their color parameters (a, b, c) and color matching table (d).

6.5.3 Rapid Volatile Gas Detection via gas detector tubes: NH_3 and TEA

The color change parameters and the sensor's color change during these simultaneous experiments, as shown in **Figure 6.4**, were observed by affixing the pH indicator to the upper side of 10 amber vials (60 mL), each containing a homogeneous mixture of fish fillets (approximately 20 g). Over a 9-day period, a gradual but consistent color change in the pH indicator was observed when exposed to fish samples stored at 4 °C temperature. The control sample exhibited no color change, establishing a baseline. By day 2, a noticeable shift occurred, which intensified by day 3. The trend continued, with significant increases noted on days 4–6. Similarly, other research has demonstrated that at 4 °C refrigeration, the chromaticity of the indicator changes gradually [42]. By day 8, the

color change had risen substantially, culminating in the most marked alteration on end of storage period ($\Delta RGB = 113.53$). This progression indicates an increasing reaction correlating with the spoilage and associated chemical changes in the fish samples over time.

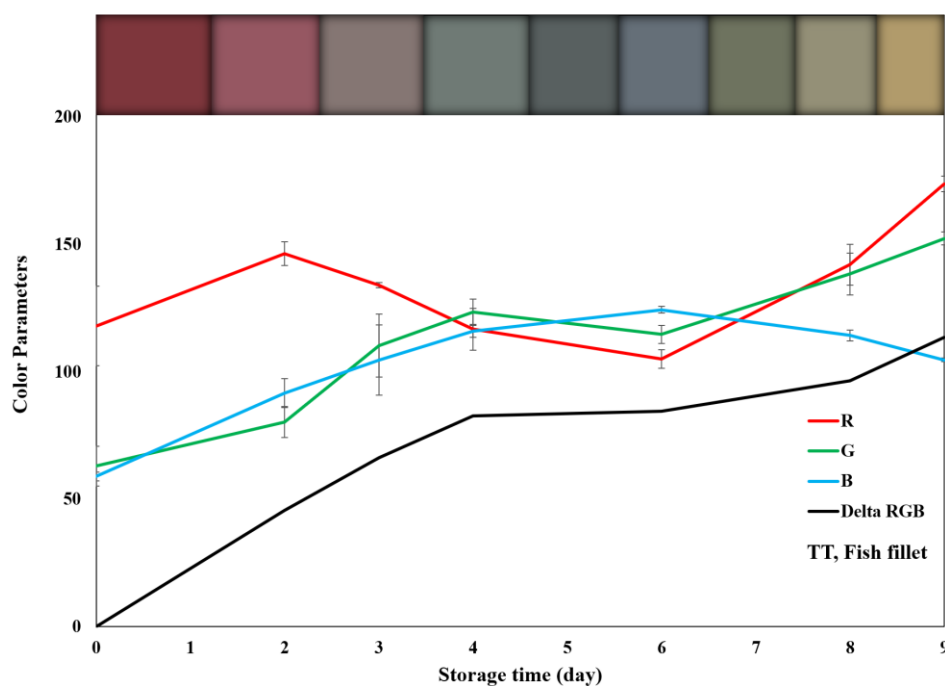


Figure 6.4 The color change of vials set up with an attached colorimetric sensor containing a homogeneous amount of fish samples, kept for 9 days at 4 °C.

Furthermore, we measured the concentrations of NH_3 and TEA generated from fish samples inside vials with securely affixed valves on their caps (with one duplicate), and we prepared the samples uniformly. By using separate vials for each day, we can effectively reduce the risk of gas leakage that can occur when repeatedly sampling from a single vial. This approach helps maintain the integrity of the gas measurements and ensures that we capture the full concentration of NH_3 and TEA gases produced during spoilage.

The concentration of TEA during the initial two days (0–2) was below the detection threshold of this gas detector type. It recommends that the concentration of TEA should be below 10 ppm [45, 46]. The gas detector showed NH_3 and TEA presence but may have biases from co-existing amines and mixed nitrogen components in food matrices which could affect accuracy. The results gathered in **Table 6.1**.

Table 6.1 Measurement of NH_3 and TEA from vials with valve connected to the gas detector tubes for 9 days storage time at 4 °C.

Storage period (days)	0	1	2	3	4	6	7	8	9	10
Concentration (ppm)										
TEA	nd	5<	5<	5	5	5.6 ± 0.1	6	10	15	20
NH_3	nd	0.25	1	1.2 ± 0.1	2.5 ± 0.5	10	20	15	10	10 ± 0.2
ND: Not detect, ppm: parts per million										

6.5.4 Microbial analysis

The microbial analysis was performed on fish fillets during their storage at 4 °C for 9 days, during food packaging trials (**Figure 6.5**). The TVC of the haddock fillets on the day of fillet purchase (day 0; packaging date) were found to be 3.69 ± 0.02 , while *Pseudomonas spp.* was below the detection limit (log 1.3 CFU/mL) on day 0 and first day of storage. After one day of storage, TVC reached 4.03 ± 0.07 , and the initial load of spoilage bacteria, *Pseudomonas spp.*, reached to 3.2 ± 0.05 . Slow increase in bacterial load occurred during the initial storage period (0 to 3) at 4 °C, indicating that fish samples are fresh. From day 4 to day 7, the TVC increases more noticeably from 5.35 to 6.02. This period represents the rapid spoilage phase, where microbial populations grow quickly. Following day 7, the TVC continues to rise but at a slower rate, reaching 7.09 by day 10. This gradual increase suggests the transition toward a stationary phase. In this phase, the growth rate may begin to balance with cell death rates, indicating that the fish is in a declining but measurable state of spoilage. The results were also consistent with the previous study [37].

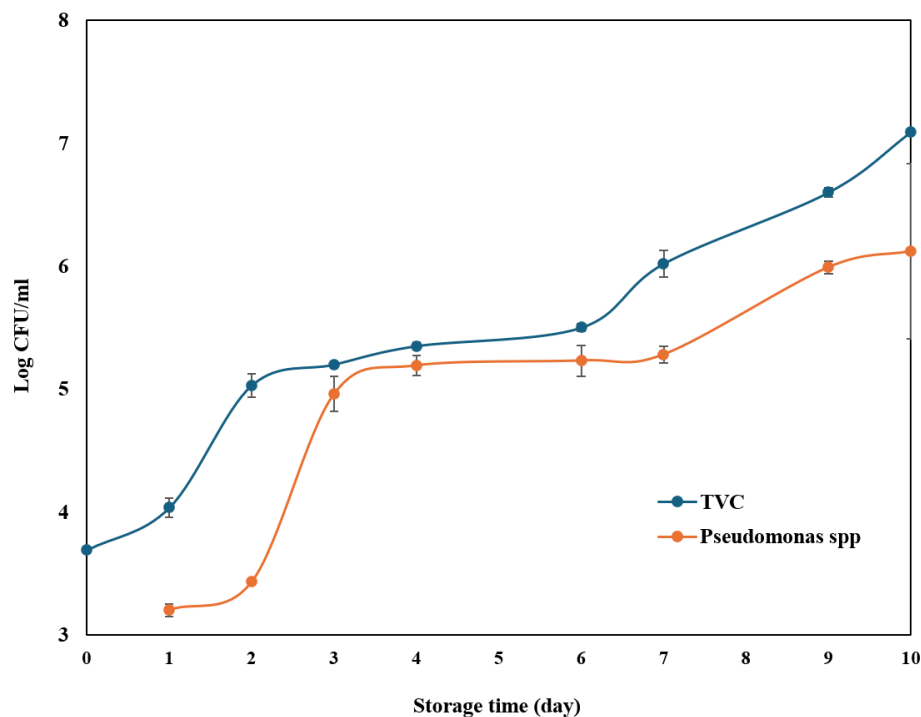


Figure 6.5 The TVC and *Pseudomonas* spp growth for fish samples during storage period at 4 °C for 9 days.

6.5.5 Optimizing GC-MS: method development and performance assessment

Fish samples are inherently complex as a matrix due to their diverse composition [47], variable water contents [48], the presence of interfering substances, and their potential for degradation and transformation to other compounds during their shelf-life [49]. Therefore, it is often challenging to ascertain the exact concentration of specific analytes [50] and to quantify them within fish tissues. This is especially true for small and very volatile molecules such as NH_3 , DMA, and TMA, present in a test portion. This uncertainty complicates the evaluation of the method's success in effectively extracting these compounds from the sample matrix. One effective approach to assess the extraction efficiency involves spiking test portions of fish samples with known concentrations of the analytes (NH_3 , DMA, and TMA). Following the spiking, these portions are extracted, and the concentrations of the analytes are subsequently measured to evaluate the method's extraction performance. Prepared the calibration curve using standard solutions that closely mimic the sample's real conditions by matching the solvent, adding equivalent amounts of sacrificial reagents, or adjusting the pH [51-53]. This helps minimize possible interference from the solution

background [54-56]. Injecting a blank solution, or one taken before the reaction starts, is also highly recommended to correct the sample measurement results [57, 58].

Both scan and SIM acquisition modes were used during this project for characterisation of volatile species and quantification of targeted analytes respectively. The m/z presented in the instrumental conditions were selected by injection of the individual standard of ammonia, DMA, TMA and diethyl-d10-amine as internal standard.

The analytical method was briefly optimized on a GS-Q column; however, the CP-Volamine column can provide better performance due to its specific design for separation of volatile amines [59], even in the presence of water [60-62]. A compromise in the GC gradient was selected to have an appropriate retention for ammonia while allowing to separate closely eluting DMA and TMA with acceptable peak shapes. To analyze multiple compounds by GC-MS, it is necessary to ensure that all target compounds can be adequately separated qualitatively and quantitatively [63, 64].

Different split ratios were tested and spitless injections were selected to achieve as low LODs as possible. The headspace temperature and equilibration times were also optimized to increase the release of ammonia, DMA and TMA to the gas phase of the headspace vial. Headspace vials with a volume of 20 mL were used to maximize the fish sample mass (approximately 10 g) that can be analyzed by the instrument. The trials with larger amounts of fish (approx. 70 g) in 250 mL glass flask did not yield greater signal intensities and this approach was thus discarded due to the use of manual injection which is less precise when compared to the automated headspace extraction.

6.5.6 Gas analytes quantification essays

Matrix-matched calibration trials were performed by spiking the targeted analytes onto fresh fish samples. Only a limited calibration range was obtained: A lower release of targeted analytes to the headspace was observed, impacting the LODs while the signal intensities were rapidly saturated limiting the potential upper limit of quantification. A negative effect on chromatographic performance was caused when injecting a spiked fish sample, resulting in peak broadening and coelution of DMA and TMA. Much lower concentrations of same spiked amounts were observed in real matrix when compared to pure solvent calibration solutions. These results implied a strong interaction between the analytes and the matrix components. This high matrix effect suggested that the quantification of NH_3 and TMA in the fish's headspace might not be directly comparable to

solvent standards. However, the method performance allowed trend analysis of the targeted analytes during fish storage without the success of an accurate quantification.

6.5.7 Method validation and Calibration curve

The method validation was primarily conducted in accordance with the Eurachem Guide [48]. As mentioned in the previous section, linear calibration curves could still be obtained for NH_3 and TMA over a limited range when spiking on to the fish samples (**Figure 6.6**). The linear ranges were first examined to determine how sensitive the instruments are and whether they respond linearly at concentrations expected for real samples [65].

Calibrations curves in solvent (**Figure 6.7**) led to linear curves with correlation coefficient values (R^2) over 0.99. It was observed that TMA signal is rapidly saturated, limiting the calibration range compared to ammonia. On the other hand, TMA is much more sensible than ammonia, allowing for injection of lower calibration points. This is reflected in the instrumental LODs obtained from injection of low spiked concentrations in solvent. Lower spiked concentrations allowed to calculate TMA instrumental LOD that is 30 ppm, while the value for ammonia is 250 ppm. Their linear range are respectively from 250 to 10 000 ppm and from 2 500 to 38 000 ppm. The **Figure 6.8** and **Figure 6.9** present the calibration curve for methanol and ethanol for fish samples and solvent. MeOH and EtOH were not included in the optimization phase, but that first scan tests showed they might be present in the standard mixtures as well, so they were added for the storage/trend's steps. The LOD for MeOH 20 ppm and for EtOH is 10 ppm.

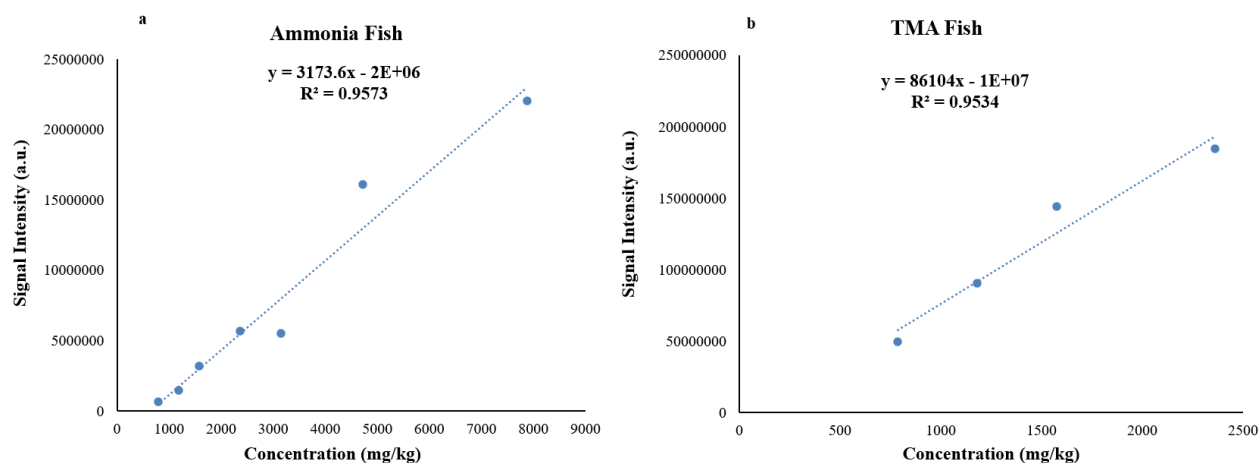


Figure 6.6 Calibration curves of individual targeted analytes when spiking on fish (NH₃ :a) and (TMA: b).

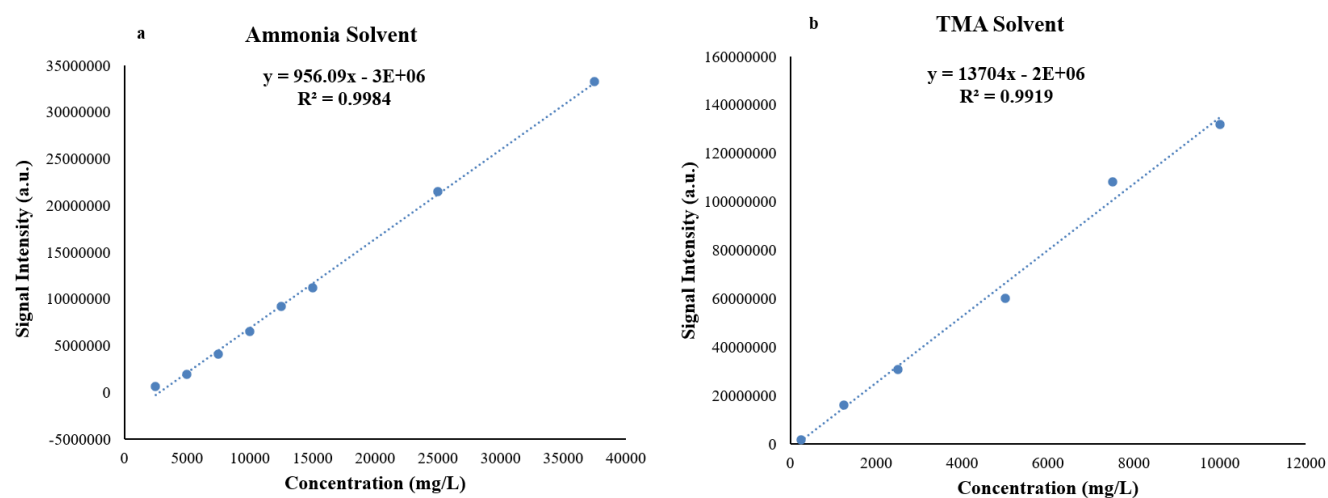


Figure 6.7 Calibration curves of individual targeted analytes when spiking on solvent (NH₃ :a) and (TMA: b).

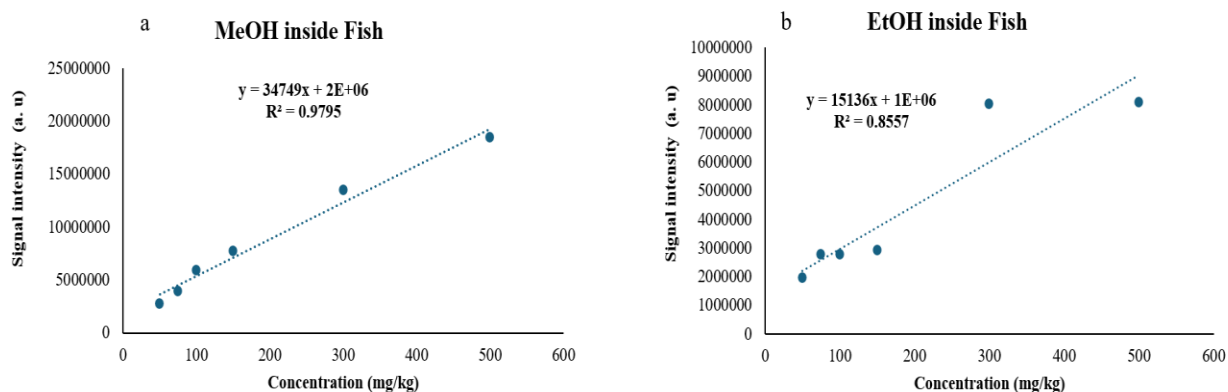


Figure 6.8 Calibration curves of individual targeted analytes when spiking on fish (MeOH :a) and (EtOH: b).

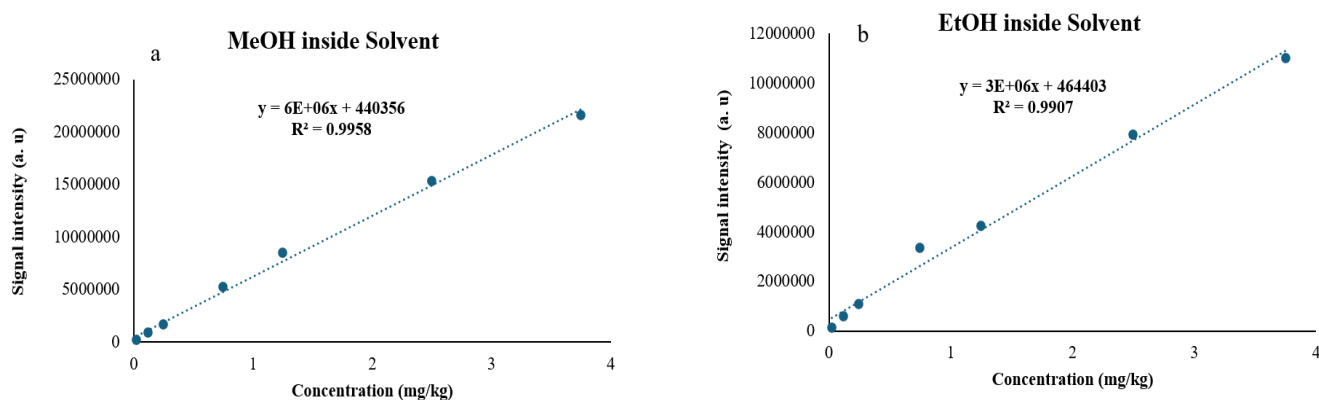


Figure 6.9 Calibration curves of individual targeted analytes when spiking on solvent (MeOH :a) and (EtOH: b).

6.5.8 Quality Control Measures

Quality control (QC) solutions (spiked in solvent) allowed to calculate the system precision for injections on six different days. The RSD values are found to be 4.6 % for ammonia and 8.2 % for TMA. These values are deemed acceptable for this kind of experimental conditions [67]. Even though an accurate quantification could be achieved, the LODs and precision of the method were deemed acceptable to look at the trends in the compounds formed during fish sample storage. Since

the area of the peaks were used for the calibration curves and the trends, area RSD values show in **Table 6.2**.

Table 6.2 The precisions calculated as RSD of QC injections over 6 different days. Since values are under 10% for the targeted analytes, this means that the method is precise.

	NH₃	MeOH	EtOH	TMA
RSD (%)	4.6	4.9	6.9	8.2

6.5.9 Trend via GC-MS during shelf-life

In analyzing the headspace of fish samples stored at 4°C, it is still possible to observe trends in the non-quantifiable signal intensities of the different detected species. One study highlighted the importance of method development for detection and quantification of TMA and DMA during cod fillets shelf-life under melting ice conditions using solid-phase microextraction- gas chromatography-mass spectrometry (SPME-GC-MS). It revealed that TMA and DMA were not effective indicators for detecting the initial decrease in the freshness of the fish samples [68]. Additionally, using more specialized analytical tools such as headspace-SPME-GC-MS has shown that the release of volatile amines is influenced by storage conditions and the fish matrix [39]. These compounds can be correlated with fish freshness [69]. Alternatively, utilizing an ammonia ion-selective electrode (ISE) can measure NH₃ and TMA in fish samples [70]. However, these methods required more specialized equipment, thereby limiting their accessibility for routine analysis.

Figure 6.10 shows the amount of NH₃ seems to be increasing the first day and then is decreasing up to day 9 where the concentration is smaller than initial concentration (at day 0). TMA seems to increase from day 0 to day 3 with a jump in concentration at day 4. The signal is then slowly decreasing for the remaining days of the experiment. The increased moisture content of the fish as it approaches spoilage likely causes volatile amines to remain in the water phase rather than participating in the headspace. Since the vials were heated to 80 °C, the volatile amines might have a greater affinity for water, leading to their probable evaporation during the headspace-GC-MS process [71]. NH₃ and TMA are highly reactive compounds that can change their form during fish

spoilage [72]. This reactivity contributes to their reduced presence in the headspace, which can affect their collection by GC-MS [72]. Despite this decrease in TMA concentration, colorimetric sensors sensitive to TMA continue to show color changes, indicating ongoing chemical reactions or the presence of TMA in the fish samples. The phenomena affecting the concentration of TMA in fish during storage can be attributed to leaching [73] and phase partitioning [71]. As fish spoil, the increased water content leads to volatile amines, like TMA, remaining in the aqueous phase rather than being released into the headspace. This behavior is influenced by the solubility of TMA in water and the physical changes occurring in the fish tissue as it deteriorates. As observed in a recent study, TMA could not be detected using GC/MS without first heating the samples to 200 °C for 10 minutes [74].

To evaluate the difference between the storage headspace content and the total amount of the targeted analytes, a headspace GC-MS method without equilibration at 80 °C could have been used in parallel with the presented method. Although less sensitive, this second method could have provided more information about the partitioning of volatile amines between the fish matrix and the packaging headspace. This approach could also have led to results that better align with the colorimetric sensor data.

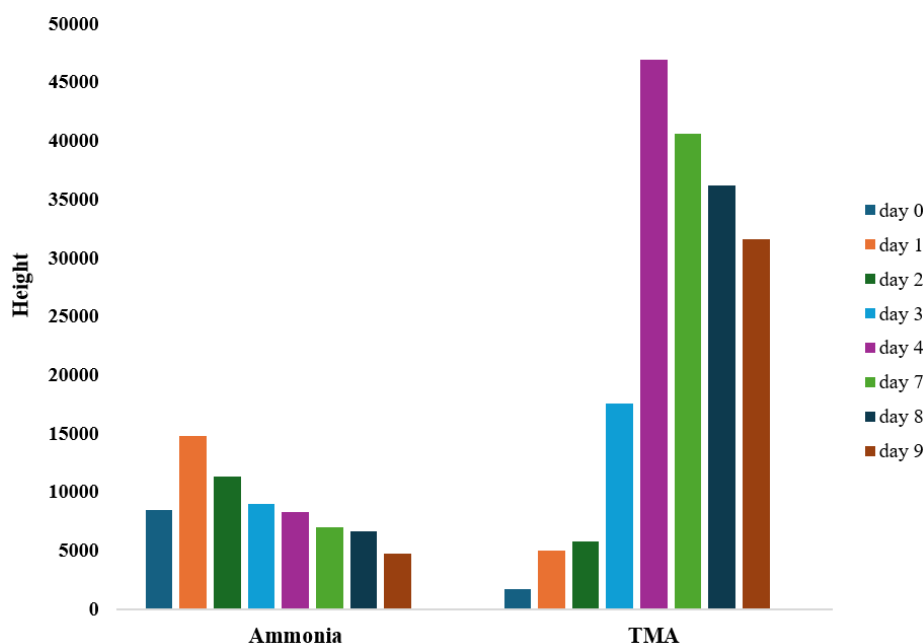


Figure 6.10 Trends in the signal intensities of targeted analytes over 9-day storage in the fridge (SIM mode acquisition).

6.5.10 Scan mode for detection of other analytes

Some untargeted species appear to be released to the headspace after different storage times and could be detected by scan mode injections (**Table 6.3**). Identification of these compounds are made using NIST database comparison of the most intense peak over the 9-day experiment period. High scores (> 89 %) indicate that the mass spectra obtained by scan mode acquisition are matching the theoretical spectra. During the analysis, peaks for methanol and ethanol were observed in the GC-MS spectra. Initially, these compounds were not the primary targets of the study. However, upon their detection, calibration curves were generated, and their LOD were determined to quantify these compounds. This step was taken to provide additional valuable information, given that their presence could offer significant insights into the sample's composition. Consequently, methanol and ethanol were included in the results, despite not being part of the initial target analytes. Injection of an ethanol standard allowed for further confirmation since its retention time match the one in the samples. Although the scan acquisition mode is less sensitive than SIM analysis, some trends could be observed for some of these compounds (**Figure C.2**).

The observed variations in the signals of the compounds in the fish samples stored at 4 °C can be attributed to several biochemical and microbial processes. The increase in ethanol levels during the first eight days, followed by a decrease on the last day, suggests fermentation processes likely facilitated by microbial activity. Various yeasts and bacteria are known to convert sugars into ethanol under anaerobic conditions [75]. The transient elevation of DMS on days 3 and 4 may relate to the breakdown of sulfur-containing amino acids, which is often indicative of microbial spoilage or the degradation of fish tissue [76, 77], and then its amount was stable for the remaining days. The detection of methanethiol starting from day 7, alongside its subsequent increase, points to further microbial activity and the breakdown of organic sulfur compounds, leading to the production of volatile compounds associated with spoilage [78]. Butane does not show a clear pattern while pentane, when discarding day 2, seems to reach its maximum on day 3 and then,

generally, slowly decreases until day 9. These observations underscore the importance of monitoring volatile compounds to assess the freshness and spoilage of seafood products.

Table 6.3 Identification of detected species using NIST database comparison for scan mode injections.

Retention time (min)	Compound name	Score (%)
11.2	Methanethiol	95
12.1	Butane	89
13.8	Ethanol	98
14.7	Dimethyl Sulfide	96
15.4	Pentane	94
15.9	Trimethylamine	99

6.6 Conclusion

This study successfully demonstrates the effectiveness of colorimetric sensing as a practical tool for monitoring seafood freshness through the detection of volatile compounds. The experiment was conducted at $T = 40\text{ }^{\circ}\text{C}$ over 30 minutes, indicating specific storage conditions. ΔRGB shows the sensitivity of the pH indicator to the presence of TVB-N gases. As the concentration of each gas increases, ΔRGB shows a significant decline, particularly at the 0.01 M concentration for each analyte (170.4, 450.9, and 591.1 ppm for NH_3 , DMA, and TMA, respectively), which is statistically significant. The consistent decrease in the red channel across all gases suggests that the pH indicator is effectively responding to the chemical changes induced by the TVB-N gases, leading to a shift in color that can be quantitatively measured through RGB values.

This study aims to evaluate the color response of on-package pH-sensitive anthocyanin dye sensors using headspace GC-MS analysis and microbial analysis to provide a better understanding of the performance of the introduced pH indicator. Additionally, the development of a four-point freshness scale offers a user-friendly method for assessing fish freshness over time, highlighting the potential applications of this intelligent packaging system in ensuring food safety and quality.

Furthermore, the comprehensive analysis of volatile gas concentrations, microbial growth, and colorimetric changes throughout the storage period highlights the multifaceted nature of food spoilage. For GC-MS analysis, amongst the different approaches, the automated headspace injections using 20 mL vials was deemed the more appropriate to analyze volatile species released during fish storage. Linear calibration curves are obtained by spiking standards in pure water, but a significant matrix effect did not allow for an accurate quantification in real fish samples. This effect, along with signal saturation, also led to limited calibration range for the matrix-matched calibration essays on fresh fish. However, the LODs and precisions of pure solvent spiked solutions were deemed acceptable and allowed for trends analysis of compounds produced during storage of fish samples. Such trends were observed for the ammonia and TMA as well as for some untargeted analytes such as ethanol and butane. None of the analyzed headspace of spoiled fish contained detectable amounts of DMA. These results can contribute to future innovations in packaging technologies and freshness indicators, ultimately enhancing food quality and consumer safety.

Limitations/challenges and future work

The complexity of fish samples makes it difficult to determine the exact concentrations of analytes such as ammonia NH_3 , DMA, and TMA. To assess extraction efficiency, test portions can be spiked with known concentrations of these analytes, followed by extraction and measurement. However, a key limitation of this method is that spiked analytes may not bind as strongly as those naturally present, leading to an overestimation of extraction efficiency. This underscores the need for careful interpretation of results from spiked samples in complex matrices. The fact that much lower signals are observed in real fish sample when compared with same amount of spiked standard in pure water indicate an important matrix effect. This and the fact that only a very limited linear range is obtained with a matched-matrix calibration approach, render the quantification of these species very challenging. This matrix effect also had an impact on chromatographic performances, causing the coelution of DMA and TMA. A better retention, sharper peaks and greater signal intensity might be achieved using a more specific column for volatile amines and ammonia such as CP-Volamine but it was not available in laboratory.

Acknowledgements

I would like to express my sincere gratitude to Dr. Alexandra Furtos-Matei, PhD, Mass Spectrometry Facility Manager of the Chemistry Department at the University of Montréal, for her

invaluable collaboration and support throughout the current research project. Her expertise and guidance significantly contributed to the success of this work. The funding for this research project is gratefully acknowledged from the Natural Sciences and Engineering Research Council of Canada (NSERC), 3Spack Industrial Research Chair, Research Center for High Performance Polymer and Composite Systems (CREPEC), Chemical Engineering Department, Polytechnique Montréal, ProAmpac flexible packaging, and Prima.

6.7 Reference

- [1] A. Gordon, "Introduction: effective implementation of food safety and quality systems: prerequisites and other considerations," in *Food Safety and Quality Systems in Developing Countries*: Elsevier, 2017, pp. 1-19.
- [2] J. Li *et al.*, "Spoilage microbes' effect on freshness and IMP degradation in sturgeon fillets during chilled storage," *Food Bioscience*, vol. 41, p. 101008, 2021/06/01/ 2021, doi: <https://doi.org/10.1016/j.fbio.2021.101008>.
- [3] M. Etienne, "Volatile amines as criteria for chemical quality assessment. Seafoodplus traceability," 2005.
- [4] E. Uhlig, M. Bucher, M. Strenger, S. Kloth, and M. Schmid, "Towards Reducing Food Wastage: Analysis of Degradation Products Formed during Meat Spoilage under Different Conditions," *Foods*, vol. 13, no. 17, p. 2751, 2024. [Online]. Available: <https://www.mdpi.com/2304-8158/13/17/2751>.
- [5] C. E. Realini and B. Marcos, "Active and intelligent packaging systems for a modern society," *Meat science*, vol. 98, no. 3, pp. 404-419, 2014.
- [6] B. S. Sá, C. A. Zito, T. M. Perfecto, and D. P. Volanti, "Porous ZnSnO₃ nanocubes as a triethylamine sensor," *Sensors and Actuators B: Chemical*, vol. 338, p. 129869, 2021.
- [7] N. H. Tan *et al.*, "Metal-decorated indium oxide nanofibers used as nanosensor for triethylamine sensing towards seafood quality monitoring," *Colloids and Surfaces A: Physicochemical and Engineering Aspects*, p. 135268, 2024.

- [8] G.-Y. Lee, K.-J. Lim, Y.-H. Lee, and H.-S. Shin, "Development of a Freshness Indicator for Assessing the Quality of Packaged Pork Products during Refrigerated Storage," *Foods*, vol. 13, no. 13, p. 2097, 2024.
- [9] J. Chen *et al.*, "Critical review and recent advances of emerging real-time and non-destructive strategies for meat spoilage monitoring," *Food Chemistry*, p. 138755, 2024.
- [10] M. Ameri, A. Ajji, and S. Kessler, "Characterization of a Food-Safe Colorimetric Indicator Based on Black Rice Anthocyanin/PET Films for Visual Analysis of Fish Spoilage," *Packaging Technology and Science*, 2024.
- [11] I. M. Karaca, G. Haskaraca, Z. Ayhan, and E. Gültekin, "Development of real time-pH sensitive intelligent indicators for monitoring chicken breast freshness/spoilage using real packaging practices," *Food Research International*, vol. 173, p. 113261, 2023.
- [12] Y. Ozogul, "Methods for freshness quality and deterioration," in *Handbook of seafood and seafood products analysis*: CRC Press, 2009, pp. 207-232.
- [13] S. T. Chan, M. W. Y. Yao, Y. C. Wong, T. Wong, C. S. Mok, and D. W. M. Sin, "Evaluation of chemical indicators for monitoring freshness of food and determination of volatile amines in fish by headspace solid-phase microextraction and gas chromatography-mass spectrometry," *European Food Research and Technology*, vol. 224, no. 1, pp. 67-74, 2006/11/01 2006, doi: 10.1007/s00217-006-0290-4.
- [14] P. Malle, P. Eb, and R. Tailliez, "Determination of the quality of fish by measuring trimethylamine oxide reduction," *International Journal of Food Microbiology*, vol. 3, no. 4, pp. 225-235, 1986.
- [15] A. R. Al-Najada, "Quality Assessment of Aquacultured Freshwater Fish Species during Storage in Ice."
- [16] G. Olafsdottir, H. L. Lauzon, E. Martinsdottir, and K. Kristbergsson, "Influence of storage temperature on microbial spoilage characteristics of haddock fillets (*Melanogrammus aeglefinus*) evaluated by multivariate quality prediction," *International Journal of Food Microbiology*, vol. 111, no. 2, pp. 112-125, 2006/09/01/ 2006, doi: <https://doi.org/10.1016/j.ijfoodmicro.2006.04.045>.

- [17] P. Malle and M. Poumeyrol, "A new chemical criterion for the quality control of fish: trimethylamine/total volatile basic nitrogen (%)," *Journal of food protection*, vol. 52, no. 6, pp. 419-423, 1989.
- [18] V. Nikzade, N. Sedaghat, F. T. Yazdi, H. B. Ghoddusi, and M. Saadatmand-Tarzjan, "Development of shelf life kinetic model for fresh rainbow trout (*Oncorhynchus mykiss*) fillets stored under modified atmosphere packaging," *Journal of food science and technology*, vol. 56, pp. 663-673, 2019.
- [19] S. Baixas-Nogueras, S. Bover-Cid, M. Veciana-Nogués, and M. Vidal-Carou, "Suitability of volatile amines as freshness indexes for iced Mediterranean hake," *Journal of Food Science*, vol. 68, no. 5, pp. 1607-1610, 2003.
- [20] S. P. Aubourg, "Damage detection in horse mackerel (*Trachurus trachurus*) during chilled storage," *Journal of the American Oil Chemists' Society*, vol. 78, pp. 857-862, 2001.
- [21] N. Jalali, P. Ariai, and E. Fattahi, "Effect of alginate/carboxyl methyl cellulose composite coating incorporated with clove essential oil on the quality of silver carp fillet and *Escherichia coli* O157: H7 inhibition during refrigerated storage," *Journal of Food Science and Technology*, vol. 53, pp. 757-765, 2016.
- [22] C. Altieri, B. Speranza, M. A. Del Nobile, and M. Sinigaglia, "Suitability of bifidobacteria and thymol as biopreservatives in extending the shelf life of fresh packed plaice fillets," *Journal of applied microbiology*, vol. 99, no. 6, pp. 1294-1302, 2005.
- [23] T. Liang, G. Sun, L. Cao, J. Li, and L. Wang, "A pH and NH₃ sensing intelligent film based on *Artemisia sphaerocephala* Krasch. gum and red cabbage anthocyanins anchored by carboxymethyl cellulose sodium added as a host complex," *Food hydrocolloids*, vol. 87, pp. 858-868, 2019.
- [24] N. Oladzadabbasabadi, A. M. Nafchi, M. Ghasemlou, F. Ariffin, Z. Singh, and A. Al-Hassan, "Natural anthocyanins: Sources, extraction, characterization, and suitability for smart packaging," *Food Packaging and Shelf Life*, vol. 33, p. 100872, 2022.

- [25] L. Chen, W. Wang, W. Wang, and J. Zhang, "Effect of Anthocyanins on Colorimetric Indicator Film Properties," *Coatings*, vol. 13, no. 10, p. 1682, 2023. [Online]. Available: <https://www.mdpi.com/2079-6412/13/10/1682>.
- [26] K. Zhang *et al.*, "Aerogel colorimetric label sensors based on carboxymethyl cellulose/sodium alginate with black goji anthocyanin for monitoring fish freshness," *International Journal of Biological Macromolecules*, p. 130466, 2024.
- [27] A. Khezerlou, M. Alizadeh Sani, M. Tavassoli, R. Abedi-Firoozjah, A. Ehsani, and D. J. McClements, "Halochromic (pH-Responsive) Indicators Based on Natural Anthocyanins for Monitoring Fish Freshness/Spoilage," *Journal of Composites Science*, vol. 7, no. 4, p. 143, 2023. [Online]. Available: <https://www.mdpi.com/2504-477X/7/4/143>.
- [28] X. Zhai *et al.*, "Novel colorimetric films based on starch/polyvinyl alcohol incorporated with roselle anthocyanins for fish freshness monitoring," *Food Hydrocolloids*, vol. 69, pp. 308-317, 2017.
- [29] M. Moradi, H. Tajik, H. Almasi, M. Forough, and P. Ezati, "A novel pH-sensing indicator based on bacterial cellulose nanofibers and black carrot anthocyanins for monitoring fish freshness," *Carbohydrate Polymers*, vol. 222, p. 115030, 2019.
- [30] S. Ibrahim, H. Fahmy, and S. Salah, "Application of interactive and intelligent packaging for fresh fish shelf-life monitoring," *Frontiers in Nutrition*, vol. 8, p. 677884, 2021.
- [31] B. Wang *et al.*, "Intelligent Evaluation and Dynamic Prediction of Oysters Freshness with Electronic Nose Non-Destructive Monitoring and Machine Learning," *Biosensors*, vol. 14, no. 10, p. 502, 2024.
- [32] X. Luo, "Colorimetric Indicator Systems for the Detection of Amines/Terpenes in Intelligent Food Packaging," University of Guelph, 2021.
- [33] A. A. Ameri M, Kessler S, "Enhancing Seafood Freshness Monitoring: Integrating Color Change of a Food-Safe On-Package Colorimetric Sensor with Mathematical Models, Microbiological, and Chemical Analyses," *ChemRxiv*, 2024, doi: 10.26434/chemrxiv-2024-wxznz6.

- [34] D. N. Dikmetas, E. Uysal, F. Karbancioglu-Guler, and S. Gurmen, "The production of pH indicator Ca and Cu alginate ((1, 4)- β -d-mannuronic acid and α -l-guluronic acid) cryogels containing anthocyanin obtained via red cabbage extraction for monitoring chicken fillet freshness," *International Journal of Biological Macromolecules*, vol. 231, p. 123304, 2023.
- [35] D. Karimi Alavijeh, "Development of Films/Fibrous Nanostructures with Gas and Volatiles Detection Ability," Master's thesis, Department of Chemical Engineering, Polytechnique Montréal, 2020. [Online]. Available: <https://publications.polymtl.ca/4221/>
- [36] A. Sobhan, ""Development of Bio-based Nanocomposites for Biosensor and Indicator Applications in Smart Food Packaging," PhD, Agricultural, Biosystems, & Mechanical Engineering South Dakota State University, 2021. [Online]. Available: <https://openprairie.sdstate.edu/etd/5792>
- [37] M. Ameri, A. Ajji, and S. Kessler, "Enhancing Seafood Freshness Monitoring: Integrating Color Change of a Food-Safe On-Package Colorimetric Sensor with Mathematical Models, Microbiological, and Chemical Analyses," *Current Research in Food Science*, p. 100934, 2024/11/23/ 2024, doi: <https://doi.org/10.1016/j.crfs.2024.100934>.
- [38] T. Zhu, Z. Li, X. Liu, C. Chen, and Y. Mu, "Comparative Analysis of Microbial Diversity and Metabolic Profiles during the Spontaneous Fermentation of Jerusalem Artichoke (*Helianthus tuberosus* L.) Juice," *Plants*, vol. 13, no. 19, p. 2782, 2024.
- [39] S. T. Chan, M. W. Yao, Y. Wong, T. Wong, C. Mok, and D. W. Sin, "Evaluation of chemical indicators for monitoring freshness of food and determination of volatile amines in fish by headspace solid-phase microextraction and gas chromatography-mass spectrometry," *European Food Research and Technology*, vol. 224, pp. 67-74, 2006.
- [40] A. Al-Rashdan, M. I. Helaleh, A. Nisar, A. Ibtisam, and Z. Al-Ballam, "Determination of the levels of polycyclic aromatic hydrocarbons in toasted bread using gas chromatography mass spectrometry," *International journal of analytical chemistry*, vol. 2010, no. 1, p. 821216, 2010.
- [41] S. Dodange, H. Shekarchizadeh, and M. Kadivar, "A simple colorimetric volatile nitrogen and hydrogen sulfide indicator based on filter paper and saffron petal anthocyanins to monitor

fish spoilage in intelligent packaging," *Food and Bioprocess Technology*, vol. 17, no. 7, pp. 1785-1796, 2024.

[42] D.-Y. Kim, S.-W. Park, and H.-S. Shin, "Fish freshness indicator for sensing fish quality during storage," *Foods*, vol. 12, no. 9, p. 1801, 2023.

[43] Y. K. Ip and S. F. Chew, "Ammonia production, excretion, toxicity, and defense in fish: a review," *Frontiers in physiology*, vol. 1, p. 134, 2010.

[44] H.-N. Chun, J.-H. Cho, and H.-S. Shin, "Influence of different storage conditions on production of trimethylamine and microbial spoilage characteristics of mackerel products," *Food Science and Biotechnology*, vol. 23, pp. 1411-1416, 2014.

[45] F. Gu, Y. Cui, D. Han, S. Hong, M. Flytzani-Stephanopoulos, and Z. Wang, "Atomically dispersed Pt (II) on WO₃ for highly selective sensing and catalytic oxidation of triethylamine," *Applied Catalysis B: Environmental*, vol. 256, p. 117809, 2019/11/05/ 2019, doi: <https://doi.org/10.1016/j.apcatb.2019.117809>.

[46] Y. H. Cai, S. Y. Ma, and J. S. Wei, "Highly sensitive triethylamine sensor with ppb level detection limit based on SnSe nanofibers," *Ceramics International*, vol. 49, no. 10, pp. 15333-15340, 2023/05/15/ 2023, doi: <https://doi.org/10.1016/j.ceramint.2023.01.117>.

[47] Z. Coppes Petricorena, "Chemical Composition of Fish and Fishery Products," in *Handbook of Food Chemistry*, P. C. K. Cheung and B. M. Mehta Eds. Berlin, Heidelberg: Springer Berlin Heidelberg, 2015, pp. 403-435.

[48] M. a. I. Yeannes and M. a. E. Almandos, "Estimation of fish proximate composition starting from water content," *Journal of Food Composition and Analysis*, vol. 16, no. 1, pp. 81-92, 2003.

[49] D. Martin, C. Joly, C. Dupas-Farrugia, I. Adt, N. Oulahal, and P. Degraeve, "Volatilome Analysis and Evolution in the Headspace of Packed Refrigerated Fish," *Foods*, vol. 12, no. 14, p. 2657, 2023. [Online]. Available: <https://www.mdpi.com/2304-8158/12/14/2657>.

[50] D. Sundaravadivelu *et al.*, "Determination of cyanotoxins and prymnesins in water, fish tissue, and other matrices: A review," *Toxins*, vol. 14, no. 3, p. 213, 2022.

- [51] W. P. Utomo, H. Wu, and Y. H. Ng, "Quantification methodology of ammonia produced from electrocatalytic and photocatalytic nitrogen/nitrate reduction," *Energies*, vol. 16, no. 1, p. 27, 2022.
- [52] K. Johanning *et al.*, "Assessment of metabolic stability using the rainbow trout (*Oncorhynchus mykiss*) liver S9 fraction," *Current Protocols in Toxicology*, vol. 53, no. 1, pp. 14.10. 1-14.10. 28, 2012.
- [53] I. A. Haidar Ahmad, "Necessary analytical skills and knowledge for identifying, understanding, and performing HPLC troubleshooting," *Chromatographia*, vol. 80, no. 5, pp. 705-730, 2017.
- [54] C. Ferrer, A. Lozano, A. Agüera, A. J. Girón, and A. Fernández-Alba, "Overcoming matrix effects using the dilution approach in multiresidue methods for fruits and vegetables," *Journal of Chromatography A*, vol. 1218, no. 42, pp. 7634-7639, 2011.
- [55] K. S. Booksh and B. R. Kowalski, "Theory of analytical chemistry," *Analytical Chemistry*, vol. 66, no. 15, pp. 782A-791A, 1994.
- [56] J. Zhao and M. Riediker, "Detecting the oxidative reactivity of nanoparticles: a new protocol for reducing artifacts," *Journal of nanoparticle research*, vol. 16, pp. 1-13, 2014.
- [57] K. Grob, *Split and splitless injection for quantitative gas chromatography: concepts, processes, practical guidelines, sources of error*. John Wiley & Sons, 2008.
- [58] S. Mitra, *Sample preparation techniques in analytical chemistry*. John Wiley & Sons, 2004.
- [59] A. Technologies. "Optimized Analysis of Ammonia and Volatile Amines Using the Agilent J&W CP-Volamine Column." <https://www.agilent.com/cs/library/applications/an-ammonia-jw-cp-volamine-990-micro-gc-5994-4346en-agilent.pdf> (accessed).
- [60] I. T. Cunha, H. Yang, and P. G. Jessop, "High pressure switchable water: An alternative method for separating organic products from water," *Green Chemistry*, vol. 23, no. 11, pp. 3996-4007, 2021.

- [61] M. Shou and H. Qiu, "Development of a rapid GC-FID method to simultaneously determine triethylamine, diisopropylamine, and 1, 1, 3, 3-tetramethylguanidine residues in an active pharmaceutical ingredient," *Journal of Pharmaceutical Analysis*, vol. 11, no. 2, pp. 251-256, 2021.
- [62] Y. Huang *et al.*, "Highly Efficient Compositional and Compound Specific Isotopic Analysis of Volatile Primary Amines and Ammonia in the Murchison Meteorite Using SPME On-Fiber Derivatization: Optimization for Bennu Sample Analyses," *Rapid Communications in Mass Spectrometry*, vol. 39, no. 7, p. e9979, 2025.
- [63] M.-L. Xu, Y. Gao, X. Wang, X. X. Han, and B. Zhao, "Comprehensive Strategy for Sample Preparation for the Analysis of Food Contaminants and Residues by GC–MS/MS: A Review of Recent Research Trends," *Foods*, vol. 10, no. 10, p. 2473, 2021. [Online]. Available: <https://www.mdpi.com/2304-8158/10/10/2473>.
- [64] M. L. Xu, Y. Gao, X. Wang, X. X. Han, and B. Zhao, "Comprehensive Strategy for Sample Preparation for the Analysis of Food Contaminants and Residues by GC-MS/MS: A Review of Recent Research Trends," (in eng), *Foods*, vol. 10, no. 10, Oct 15 2021, doi: 10.3390/foods10102473.
- [65] B. M. a. U. Ö. (eds.). "Eurachem Guide: The Fitness for Purpose of Analytical Methods – A Laboratory Guide to Method Validation and Related Topics." (accessed.
- [66] N. Lorenzo-Parodi, E. Leitner, and T. C. Schmidt, "Comparison of gas chromatographic techniques for the analysis of iodinated derivatives of aromatic amines," (in eng), *Anal Bioanal Chem*, vol. 415, no. 17, pp. 3313-3325, Jul 2023, doi: 10.1007/s00216-023-04713-8.
- [67] V. T. GL49. "Guidelines for the Validation of Analytical Methods Used in Residue Depletion Studies." International Cooperation on Harmonisation of Technical Requirements for Registration of Veterinary Medicinal Products (VICH). https://www.ema.europa.eu/en/documents/scientific-guideline/vich-topic-gl49-step-4-guidelines-validation-analytical-methods-used-residue-depletion-studies_en.pdf?form=MG0AV3 (accessed.

- [68] A. Dehaut *et al.*, "Development of an SPME-GC-MS method for the specific quantification of dimethylamine and trimethylamine: use of a new ratio for the freshness monitoring of cod fillets," *Journal of the Science of Food and Agriculture*, vol. 96, no. 11, pp. 3787-3794, 2016.
- [69] G. Xuan, M. Guo, H. Lin, J. Sui, and J. Wang, "Study on volatile chemicals as spoilage indexes of salmon by HS-SPME-GC-MS technique during non-frozen storage," *Molecules*, vol. 28, no. 1, p. 13, 2022.
- [70] L. F. Pivarnik, M. Thiam, and P. Christopher Ellis, "Rapid Determination of Volatile Bases in Fish by Using an Ammonia Ion-Selective Electrode," *Journal of AOAC INTERNATIONAL*, vol. 81, no. 5, pp. 1011-1022, 2020, doi: 10.1093/jaoac/81.5.1011.
- [71] C. RUIZ-CAPILLAS, C. M. Gillyon, and W. F. HORNER, "Determination of different volatile base components as quality control indices in fish by official methods and flow injection analysis," *Journal of food biochemistry*, vol. 25, no. 6, pp. 541-553, 2001.
- [72] F. A. Bullard and J. Collins, "An improved method to analyze trimethylamine in fish and the interference of ammonia and dimethylamine," *Fish. Bull.*, vol. 78, no. 2, pp. 465-437, 1980.
- [73] C. Ruiz-Capillas, C. M. Gillyon, and W. F. Horner, "Determination of volatile basic nitrogen and trimethylamine nitrogen in fish sauce by flow injection analysis," *European Food Research and Technology*, vol. 210, pp. 434-436, 2000.
- [74] J. Luo, D. Frank, and J. Arcot, "Forging Prawn and Salmon Flavours with Non-Animal-Based Ingredients," *Foods*, vol. 14, no. 5, p. 820, 2025. [Online]. Available: <https://www.mdpi.com/2304-8158/14/5/820>.
- [75] J. Lee, "Biological conversion of lignocellulosic biomass to ethanol," *Journal of biotechnology*, vol. 56, no. 1, pp. 1-24, 1997.
- [76] V. Lougovois and V. Kyrana, "Freshness quality and spoilage of chill-stored fish," *Food Policy, Control Res*, vol. 1, pp. 35-86, 2005.
- [77] X. Yu *et al.*, "Rapid assessment of meat freshness by the differential sensing of organic sulfides emitted during spoilage," *ACS sensors*, vol. 7, no. 5, pp. 1395-1402, 2022.

- [78] J. Bai, S. M. Baker, R. M. Goodrich-Schneider, N. Montazeri, and P. J. Sarnoski, "Aroma profile characterization of Mahi-Mahi and Tuna for determining spoilage using purge and trap gas chromatography-mass spectrometry," *Journal of Food Science*, vol. 84, no. 3, pp. 481-489, 2019.

CHAPTER 7 GENERAL DISCUSSION

Polymer substrate selection was conducted based on properties such as transparency and moisture resistance. Among the tested films, bio-based and bio-degradable polymeric films were excluded due to their incompatibility with the water-based nature of anthocyanins. Corona treatment was proposed as a non-destructive and physical method to enhance surface properties and improve adhesion bonding between the formulated ink and the polymeric carrier. Alternative methods like chemical modification were considered but deemed potentially toxic, however the selection of corona treatment have been compromised.

Anthocyanins exhibit greater stability at room temperature and in acidic conditions, while they rapidly degrade in alkaline environments. To enhance the stability of anthocyanins, it is advisable to reduce pH and temperature [154]. During this research project, further testing at the other pH levels resulted in agitation and precipitation, leading to the project's continuation with the acidic pH level for developed pH indicators. For instance, Walkowiak-Tomczak and Czapski [155] demonstrated that anthocyanins from red cabbage maintain higher stability at a pH of ≤ 3 . We maintained the main ink's pH below 3 for the final pH indicators. Conversely, increasing the pH diminishes the stability of these compounds. This factor poses a challenge to produce pH indicators using coatings that operate at higher pH levels, as they may increase the risk of coating corrosion. Consequently, there is a need for the development of more specialized coating devices that are less sensitive to acidic conditions, enabling the creation of colorimetric sensors integrated into food packaging.

Altering the synthesis sequence during the preparation of the sensor can significantly impact its performance. When we initially combined all materials and then heated them to increase the solubility of polyvinyl alcohol (PVOH), we observed the creation of heterogeneous mixtures. Specifically, when we formulated the PVOH/PEG masterbatch simultaneously.

We employed the post-treatment technique of heat drying to ensure the integration of pH indicators developed for seafood packaging. The response time of thermally treated samples was evaluated to preserve active sites for color change functionality and enhance stability in humid environments. Results indicated a lag time of approximately one minute for thermally treated samples at specific pH levels, confirming sensor functionality and observable color changes due to the structural transformations of anthocyanins.

Vacuum packaging affects the assessment of fish quality using pH indicators due to the elimination of headspace. To address this, we implemented pH indicators inside atmospheric air packaging (air-type packages) and evaluated their performance. Atmospheric packaging primarily interacts with aerobic bacteria, whereas vacuum packaging involves anaerobic bacteria. As a result, the type of bacteria and the associated grain components vary depending on the packaging method.

In the food trials, we noticed that the color of indicators changed significantly from fresh to spoiled seafood product. However, the color change of indicators in chicken breast was not easily noticeable. Therefore, indicators based on volatile base nitrogen type are considered more appropriate for assessing the freshness of aquatic products [127].

We found that TVBN and shelf-life were strongly correlated with colorimetric sensors as mentioned by other researchers as well [159].

The presence of TMA in real fish samples rendered analysis of DMA, a previously targeted analyte, impossible due to the coelution of the two molecules. Initial analysis of real fish samples did not show presence of DMA and this analyte was ignored for the remaining experiments. However, a more specific column for volatile amine such as CP-Volamine could have better chromatographic results as well as much lower LODs that could be needed for DMA detection in real samples.

Linear calibration curves were obtained for NH_3 and TMA when spiking on fish samples and when spiking in solvent. However, the linear range is very limited due to the signal being observed at much higher concentrations than in solvent and a rapid signal saturation. Once again, this approach is deemed impractical for real samples since the observed signal is much lower than the smallest spiked concentrations. It should be noted that smaller spiked concentrations should be used for future experiments since the type of fish seems to have an important effect on how the analyte can be released to the headspace. Unfortunately, the lower release to the headspace from fish sample and limited calibration range make it impossible to calculate the actual method LODs in real matrix. Calibrations curves in solvent led to comparable results as the initial experiments that we conducted with GC-MS. For both approaches, TMA signal is rapidly saturated, limiting the calibration range compared to ammonia. On the other hand, TMA is much more sensitive than ammonia, allowing for

injection of lower calibration points. This is reflected in the instrumental LODs obtained from injection of low spiked concentrations in solvent (pure water). Lower spiked concentrations allowed to calculate TMA instrumental LOD that is 30 ppm.

In accordance with quality control protocols, we checked the relative abundance of ammonia and trimethylamine in fish samples. Implementing QC points at higher concentrations may assist in assessing the potential for establishing linearity across a broader range. It is essential to ensure these higher concentrations remain within the linear range of the detector, and do not lead to saturation. The precisions calculated as RSD of QC injections over 6 different days. Since values are under 10% (max 8.2 for TMA when using peak areas), this means that the method is precise.

The concentrations of NH_3 and TMA are too low to quantify, making it difficult to generate accurate results. There is a challenge in determining the limit of detection for both ammonia and TMA since the signals are weak and inconsistent. The chromatograms are not showing clear peaks, complicating the analysis. The concentration of TMA and ammonia is lower than the spike in solvent, indicating issues with the sample analysis. To overcome these issues, there is a need to inject significant amounts of each standard into the GC-MS for calibration curves. However, this approach can cause that peaks become saturated. We were not able to calculate a real sample concentration because the signal intensities are much lower, and the peak shapes become even larger. The LODs that were presented are instrumental LODs (the minimum concentration the GC-MS system can detect in pure solvent). **Figure 7.1** presents the injection of a standard mix after the chromatographic optimization. The three targeted compounds as well as the internal standard were detected and identified.

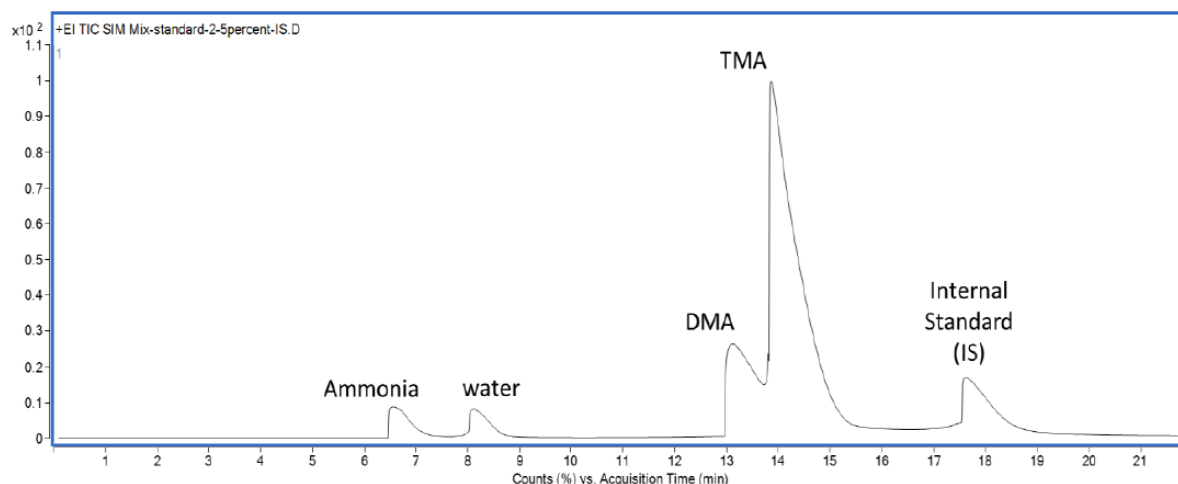


Figure 7.1 Spitless injection of a standard mix at 2.5% (w/w) in pure solvent in SIM acquisition mode.

To better assess the concentrations of detected analytes in un-spiked fish samples, a calibration curve was prepared on same mass of fish as real samples. The spiked concentrations were significantly higher than the ones in pure solvent to increase chances of obtaining linear calibration curves. These higher concentrations with low release from the fish to the headspace during heating cycle caused a broadening of the peaks (see **Figure 7.2**). This drawback and the presence of TMA in real fish samples rendered the analysis of DMA, a previously targeted analyte, impossible due to the coelution of the two molecules. Initial analysis of real fish samples did not show presence of DMA, and this analyte was ignored for the remaining experiments.

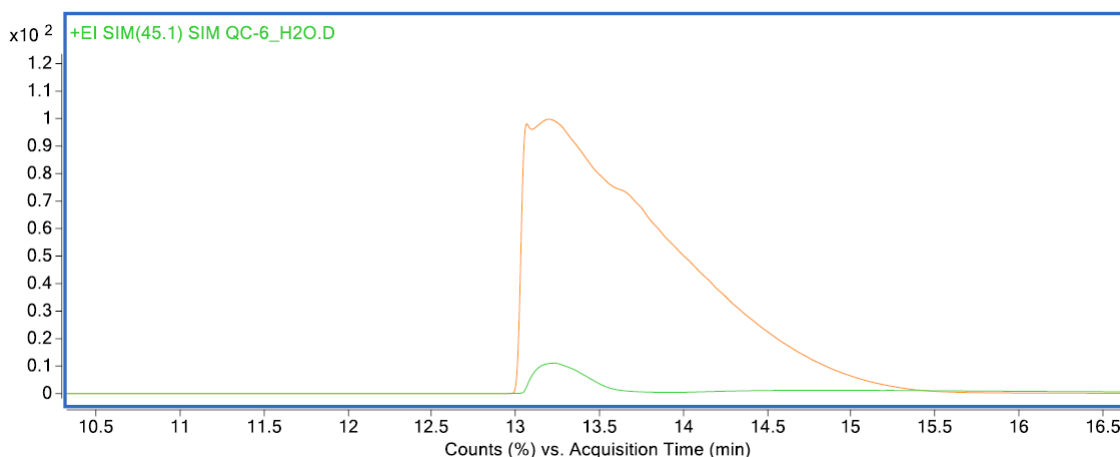


Figure 7.2 Zoomed chromatogram showing overlapping of DMA (green) and TMA (yellow) SIM signals when spiking targeted analytes directly onto the real fish sample.

Some of the images were captured using a smartphone, as scanning was not feasible for certain samples due to their watery consistency at the end of their shelf-life. Despite this limitation, the color changes in the samples were distinctly observable to the naked eye. While we believe this did not affect the color analysis results, we recognize that the clarity was compromised.

We acknowledge minor variations in the size of the indicators and some inconsistencies in their placement across the illustrations. While most indicators adhered to specific dimensions, some discrepancies arose during the shelf-life study. These occurred as the samples were stored in the refrigerator and were not perfectly aligned when placed on the scanner. Greater care should have been taken to ensure neater placement during picture scanning.

CHAPTER 8 CONCLUSION AND RECOMMENDATIONS

8.1 Conclusion

The research demonstrates the successful formulation of colorimetric films using black rice anthocyanin coated onto Corona-treated PET substrates. These films exhibit visible color changes in response to amine base gases produced during the microbial spoilage of meat and fish, providing a practical tool for assessing food safety. The incorporation of polyethylene glycol PEG and CA enhance the adhesion properties of the films, while careful optimization of thermal treatment is necessary to prevent anthocyanin degradation.

The studies validate the effectiveness of environmentally friendly ink formulations as scalar pH indicator sensors, capable of indicating varying degrees of freshness in fish products. The films show a continuum of color changes rather than a binary outcome, allowing for more nuanced monitoring of spoilage. Crosslinking agents, such as citric acid, improve the mechanical stability of the polymer matrix, reducing dye leaching and enhancing the interaction between anthocyanins and the PET substrate.

Chemical and microbial analyses conducted during packaging trials at 4 °C confirm the correlation between colorimetric changes and the levels of TVB-N gases, which indicate spoilage. The studies highlight the importance of further research to enhance the reliability of these indicators, recommending the use of GC-MS for more accurate quantification of volatile compounds in complex seafood matrices and validate the indicators.

Overall, the findings underscore the potential of colorimetric sensing as a reliable, cost-effective method for monitoring seafood freshness, paving the way for innovations in food packaging technologies and improving consumer safety. Future research should focus on refining analytical techniques and expanding the dataset to enhance the predictive capabilities of these freshness indicators.

8.2 Recommendations

To transition from lab-scale development to commercialization of these products, we have the following suggestions.

1. Development of smart packaging systems:

Future studies could focus on developing smart packaging solutions that serve dual functions: informing consumers about shelf life and actively extending the shelf life of food products. Depending on the specific food product, incorporating barrier layers to enhance properties tailored to particular needs could be beneficial. For example, seafood products require robust moisture barrier properties to maintain freshness and prevent spoilage.

2. Optimization of pH indicators:

pH conditions for production: during this study, neutral and basic pH conditions were evaluated for producing pH indicators, but these led to a narrower color change window, limiting functionality and performance in indicating seafood freshness. Acidic pH conditions yielded better results; however, they posed a risk of corrosion to the coating devices. Future efforts should consider incorporating anti-corrosion coatings to mitigate this issue for commercial use.

Impact of environmental factors: anthocyanins used in pH indicators are sensitive to humidity and elevated temperatures. Water activity plays a significant role in their stability; for example, anthocyanins remain stable below a water activity of 0.3, but degradation rates increase as water activity rises due to enhanced molecular mobility [156]. Leveraging stable pigments, such as acylated anthocyanins found in black goji berries, could improve the stability of these indicators [157, 158].

3. Sourcing reliable anthocyanin dyes:

A critical challenge identified during this study was sourcing high-quality anthocyanin dyes. The concentration and quality of these dyes significantly influence the performance of colorimetric sensors. Establishing dependable suppliers for anthocyanins should be prioritized to ensure consistent functionality in future application.

4. Post-thermal treatment optimization:

Future research should explore refining post-thermal treatments, such as UV radiation or channel drying with short residence times, to prevent the degradation of anthocyanins. While UV was used in preliminary trials, drying methods using ovens provided greater consistency in results. Optimizing these treatments could improve the functionality of colorimetric sensors.

5. Safety and migration studies:

Conduct migration studies to evaluate interactions between pH indicators and food products. Ensuring there is no leaching and confirming safety for direct contact with food is essential. Guarantee that all materials used in the development of pH indicators comply with food safety regulations and standards for direct contact.

6. Collaboration and sensory analysis:

Collaborate with food scientists and technologists to better understand the interactions between pH indicators and food components, optimizing their design for practical applications and measuring process variables. Incorporate sensory analysis, texture profile analysis (TPA), and consumer testing in future studies. Correlating these results with sensor color changes, microbial activity, and chemical analyses will be vital for developing tunable and user-friendly sensors.

7. Improving laboratory lighting conditions:

Although no significant effect on color changes was observed under varying lighting conditions during this study, stable lighting environments are ideal for testing. Variability in lighting could influence participants' ability to discern color changes, which may impact the accuracy of evaluations.

8. Advanced analytical techniques

Utilize specialized columns such as CP-volatile in a GC-MS configuration to quantify low-molecular-weight chemicals, including ammonia. This approach could provide more precise measurements for monitoring freshness indicators.

* Declaration of AI and AI-assisted technologies (Quill Bot and Copilot) in the writing process.

REFERENCES

- [1] N. O. a. A. Administration. " Fisheries of the United States 2020." <https://www.fisheries.noaa.gov> (accessed.

- [2] Y. Gao, "Point-of-care colorimetric sensors for disease diagnosis and food monitoring," University of New South Wales, 2023. [Online]. Available: <http://oatd.org/oatd/record?record=oai%3Aunsw.library.unsw.edu.au%3A1959.4%2F100955&q=pH%20indicators%20for%20monitoring%20food%20spoilage>
- [3] J.-H. Cheng, D.-W. Sun, X.-A. Zeng, and D. Liu, "Recent advances in methods and techniques for freshness quality determination and evaluation of fish and fish fillets: A review," *Critical reviews in food science and nutrition*, vol. 55, no. 7, pp. 1012-1225, 2015.
- [4] J. K. Heising, M. Dekker, P. V. Bartels, and M. Van Boekel, "Monitoring the quality of perishable foods: Opportunities for intelligent packaging," *Critical reviews in food science and nutrition*, vol. 54, no. 5, pp. 645-654, 2014.
- [5] S. Jadaun, U. Sharma, R. Khapudang, and S. Siddiqui, "Biodegradable nanocellulose reinforced biocomposites for food packaging—a narrative review and future perspective," *Journal of Water and Environmental Nanotechnology*, vol. 8, no. 3, pp. 293-319, 2023.
- [6] Z. Riahi, A. Khan, G. H. Shin, J.-W. Rhim, and J. T. Kim, "Sustainable chitosan/polyvinyl alcohol composite film integrated with sulfur-modified montmorillonite for active food packaging applications," *Progress in Organic Coatings*, vol. 192, p. 108474, 2024.
- [7] J. H. Han, "Edible films and coatings: a review," *Innovations in food packaging*, pp. 213-255, 2014.
- [8] M. Ghaani, C. A. Cozzolino, G. Castelli, and S. Farris, "An overview of the intelligent packaging technologies in the food sector," *Trends in Food Science & Technology*, vol. 51, pp. 1-11, 2016.
- [9] A. Sobhan, ""Development of Bio-based Nanocomposites for Biosensor and Indicator Applications in Smart Food Packaging," PhD, Agricultural, Biosystems, & Mechanical Engineering South Dakota State University, 2021. [Online]. Available: <https://openprairie.sdstate.edu/etd/5792>
- [10] J. Kumar, K. Akhila, and K. K. Gaikwad, "Recent developments in intelligent packaging systems for food processing industry: a review," *J Food Proc Technol*, vol. 12, p. 895, 2021.
- [11] M. Xu *et al.*, "Recent advances in anthocyanin-based films and its application in sustainable intelligent food packaging: A review," *Food Control*, p. 110431, 2024.
- [12] S. S. Rosales-Murillo *et al.*, "Anthocyanin-Loaded Polymers as Promising Nature-Based, Responsive, and Bioactive Materials," *Polymers*, vol. 16, no. 1, p. 163, 2024.
- [13] D. Bhadury, H. Nadeem, M. Lin, J. M. Dyson, K. L. Tuck, and J. Tanner, "Application of on-pack pH indicators to monitor freshness of modified atmospheric packaged raw beef," *Food Quality and Safety*, vol. 8, p. fyae021, 2024.
- [14] D. Kossyvakaki, M. Contardi, A. Athanassiou, and D. Fragouli, "Colorimetric indicators based on anthocyanin polymer composites: A review," *Polymers*, vol. 14, no. 19, p. 4129, 2022.
- [15] B. A. a. Navid Etebari Alamdari a, Mediha Aksoy b, Benjamin H. Beck b, Zhihua Jiang, "A novel paper-based and pH-sensitive intelligent detector in meat and seafood packaging," *Talanta*, vol. 224, 2021, doi: [https://doi.org/10.1016/S1369-703X\(02\)00221-8](https://doi.org/10.1016/S1369-703X(02)00221-8).

- [16] Q. Xie, G. Liu, and Y. Zhang, "Edible films/coatings containing bioactive ingredients with micro/nano encapsulation: A comprehensive review of their fabrications, formulas, multifunctionality and applications in food packaging," *Critical Reviews in Food Science and Nutrition*, vol. 64, no. 16, pp. 5341-5378, 2024.
- [17] I. Azeem, B. Ashfaq, M. Sohail, and B. Yameen, "Polymer Surface Engineering in the Food Packaging Industry," in *Nanoscale Engineering of Biomaterials: Properties and Applications*: Springer, 2022, pp. 457-485.
- [18] M. Ameri, A. Ajji, and S. Kessler, "Characterization of a Food-Safe Colorimetric Indicator Based on Black Rice Anthocyanin/PET Films for Visual Analysis of Fish Spoilage," *Packaging Technology and Science*, 2024.
- [19] K. Koutsoumanis, A. Stamatiou, P. Skandamis, and G.-J. Nychas, "Development of a microbial model for the combined effect of temperature and pH on spoilage of ground meat, and validation of the model under dynamic temperature conditions," *Applied and Environmental Microbiology*, vol. 72, no. 1, pp. 124-134, 2006.
- [20] S. Mohammadalinejad, H. Almasi, and M. J. F. C. Moradi, "Immobilization of Echium amoenum anthocyanins into bacterial cellulose film: A novel colorimetric pH indicator for freshness/spoilage monitoring of shrimp," vol. 113, p. 107169, 2020.
- [21] R. Priyadarshi, P. Ezati, and J.-W. Rhim, "Recent advances in intelligent food packaging applications using natural food colorants," *ACS Food Science & Technology*, vol. 1, no. 2, pp. 124-138, 2021.
- [22] S. Kalpana, S. Priyadarshini, M. M. Leena, J. Moses, and C. Anandharamakrishnan, "Intelligent packaging: Trends and applications in food systems," *Trends in Food Science & Technology*, vol. 93, pp. 145-157, 2019.
- [23] S. Mohammadalinejad, H. Almasi, and M. Moradi, "Immobilization of Echium amoenum anthocyanins into bacterial cellulose film: A novel colorimetric pH indicator for freshness/spoilage monitoring of shrimp," *Food Control*, vol. 113, p. 107169, 2020.
- [24] J. L. Z. Zaukuu, G. Bazar, Z. Gillay, and Z. Kovacs, "Emerging trends of advanced sensor based instruments for meat, poultry and fish quality—a review," *Critical reviews in food science and nutrition*, vol. 60, no. 20, pp. 3443-3460, 2020.
- [25] S. Jafarzadeh *et al.*, "Advanced technologies in biodegradable packaging using intelligent sensing to fight food waste," *International Journal of Biological Macromolecules*, vol. 261, p. 129647, 2024/03/01/ 2024, doi: <https://doi.org/10.1016/j.ijbiomac.2024.129647>.
- [26] X. Chen, H. Lyu, J. Zhang, L. Bai, and J. Wang, "National food safety standards related to microbiological contaminants in China: Recent progress and challenges," *Foodborne Pathogens and Disease*, vol. 18, no. 8, pp. 528-537, 2021.
- [27] C. S. V. Faria, "Development of intelligent bio-based packaging to monitor fish quality during storage: Desenvolvimento de embalagens inteligentes de base biológica para monitorizar a qualidade do pescado durante o armazenamento," Universidade do Minho, 2023.
[Online]. Available: <http://oatd.org/oatd/record?record=handle%2F84663&q=pH%20indicators%20for%20fish%20freshness>

- [28] M. Cushen, J. Kerry, M. Morris, M. Cruz-Romero, and E. Cummins, "Nanotechnologies in the food industry—Recent developments, risks and regulation," *Trends in food science & technology*, vol. 24, no. 1, pp. 30-46, 2012.
- [29] G. Fuertes, I. Soto, R. Carrasco, M. Vargas, J. Sabattin, and C. Lagos, "Intelligent Packaging Systems: Sensors and Nanosensors to Monitor Food Quality and Safety," *Journal of Sensors*, vol. 2016, p. 4046061, 2016/10/20 2016, doi: 10.1155/2016/4046061.
- [30] X. Zhang, S. Lu, X. J. S. Chen, and a. B. Chemical, "A visual pH sensing film using natural dyes from *Bauhinia blakeana* Dunn," vol. 198, pp. 268-273, 2014.
- [31] J. Chen *et al.*, "Critical review and recent advances of emerging real-time and non-destructive strategies for meat spoilage monitoring," *Food Chemistry*, p. 138755, 2024.
- [32] H. Yousefi, H.-M. Su, S. M. Imani, K. Alkhaldi, C. D. M. Filipe, and T. F. Didar, "Intelligent Food Packaging: A Review of Smart Sensing Technologies for Monitoring Food Quality," *ACS Sensors*, vol. 4, no. 4, pp. 808-821, 2019/04/26 2019, doi: 10.1021/acssensors.9b00440.
- [33] E. Mohammadian, M. Alizadeh-Sani, and S. M. Jafari, "Smart monitoring of gas/temperature changes within food packaging based on natural colorants," *Comprehensive Reviews in Food Science and Food Safety*, vol. 19, no. 6, pp. 2885-2931, 2020.
- [34] M. Nami, M. Taheri, J. Siddiqui, I. A. Deen, M. Packirisamy, and M. J. Deen, "Recent Progress in Intelligent Packaging for Seafood and Meat Quality Monitoring," *Advanced Materials Technologies*, p. 2301347, 2024.
- [35] J. Zhang, S. Liu, C. Xie, C. Wang, Y. Zhong, and K. Fan, "Recent advances in pH-sensitive indicator films based on natural colorants for smart monitoring of food freshness: a review," *Critical Reviews in Food Science and Nutrition*, pp. 1-20, 2023.
- [36] H. M. C. Azeredo and D. S. Correa, "Smart choices: Mechanisms of intelligent food packaging," *Current Research in Food Science*, vol. 4, pp. 932-936, 2021/01/01/ 2021, doi: <https://doi.org/10.1016/j.crfs.2021.11.016>.
- [37] C. Rodrigues, V. G. L. Souza, I. Coelho, and A. L. Fernando, "Bio-Based Sensors for Smart Food Packaging-Current Applications and Future Trends," (in eng), *Sensors (Basel)*, vol. 21, no. 6, Mar 18 2021, doi: 10.3390/s21062148.
- [38] B. Liu, P. A. Gurr, and G. G. Qiao, "Irreversible Spoilage Sensors for Protein-Based Food," *ACS Sensors*, vol. 5, no. 9, pp. 2903-2908, 2020/09/25 2020, doi: 10.1021/acssensors.0c01211.
- [39] Y. Ma *et al.*, "Properties and applications of intelligent packaging indicators for food spoilage," *Membranes*, vol. 12, no. 5, p. 477, 2022.
- [40] M. Vanderroost, P. Ragaert, F. Devlieghere, and B. De Meulenaer, "Intelligent food packaging: The next generation," *Trends in food science & technology*, vol. 39, no. 1, pp. 47-62, 2014.
- [41] X. Luo, A. Zaitoon, and L. T. Lim, "A review on colorimetric indicators for monitoring product freshness in intelligent food packaging: Indicator dyes, preparation methods, and

- applications," *Comprehensive Reviews in Food Science and Food Safety*, vol. 21, no. 3, pp. 2489-2519, 2022.
- [42] F. Mazur, Z. Han, A. D. Tjandra, and R. Chandrawati, "Digitalization of Colorimetric Sensor Technologies for Food Safety," *Advanced Materials*, p. 2404274, 2024.
 - [43] Q. Chen, H. Li, Q. Ouyang, and J. Zhao, "Identification of spoilage bacteria using a simple colorimetric sensor array," *Sensors & Actuators: B. Chemical*, vol. 205, no. Complete, pp. 1-8, 2014, doi: 10.1016/j.snb.2014.08.025.
 - [44] N. Emanuel and H. K. Sandhu, "Food packaging development: Recent perspective," *J. Thin Film. Coat. Sci. Technol. Appl*, vol. 6, pp. 13-29, 2019.
 - [45] H. E. Tahir *et al.*, "Smart films fabricated from natural pigments for measurement of total volatile basic nitrogen (TVB-N) content of meat for freshness evaluation: A systematic review," *Food Chemistry*, vol. 396, p. 133674, 2022.
 - [46] D. Y. Kim, S. W. Park, and H. S. Shin, "Fish Freshness Indicator for Sensing Fish Quality during Storage," (in eng), *Foods*, vol. 12, no. 9, Apr 26 2023, doi: 10.3390/foods12091801.
 - [47] B. Jinadasa, "Determination of quality of marine fishes based on total volatile base nitrogen test (TVB-N)," *Nature and Science*, vol. 5, no. 12, pp. 106-111, 2014.
 - [48] X. Liu *et al.*, "An on-package colorimetric sensing label based on a sol-gel matrix for fish freshness monitoring," *Food Chemistry*, vol. 307, p. 125580, 2020/03/01/ 2020, doi: <https://doi.org/10.1016/j.foodchem.2019.125580>.
 - [49] M.-R. Chia, I. Ahmad, and S.-W. Phang, "Starch/polyaniline biopolymer film as potential intelligent food packaging with colourimetric ammonia sensor," *Polymers*, vol. 14, no. 6, p. 1122, 2022.
 - [50] M. Alizadeh-Sani, E. Mohammadian, J.-W. Rhim, and S. M. Jafari, "pH-sensitive (halochromic) smart packaging films based on natural food colorants for the monitoring of food quality and safety," *Trends in Food Science & Technology*, vol. 105, pp. 93-144, 2020/11/01/ 2020, doi: <https://doi.org/10.1016/j.tifs.2020.08.014>.
 - [51] S. T. Chan, M. W. Yao, Y. Wong, T. Wong, C. Mok, and D. W. Sin, "Evaluation of chemical indicators for monitoring freshness of food and determination of volatile amines in fish by headspace solid-phase microextraction and gas chromatography-mass spectrometry," *European Food Research and Technology*, vol. 224, pp. 67-74, 2006.
 - [52] L. Gram and H. H. Huss, "Microbiological spoilage of fish and fish products," *International journal of food microbiology*, vol. 33, no. 1, pp. 121-137, 1996.
 - [53] H.-N. Chun, B. Kim, H.-S. J. F. s. Shin, and biotechnology, "Evaluation of a freshness indicator for quality of fish products during storage," vol. 23, no. 5, pp. 1719-1725, 2014.
 - [54] I. Siró, "Active and intelligent packaging of food," *Progress in food preservation*, pp. 23-48, 2012.
 - [55] Q. Luo *et al.*, "Recent advances in the fabrication of pH-sensitive indicators films and their application for food quality evaluation," *Critical Reviews in Food Science and Nutrition*, pp. 1-17, 2021, doi: 10.1080/10408398.2021.1959296.

- [56] X. Zhang, S. Lu, and X. Chen, "A visual pH sensing film using natural dyes from *Bauhinia blakeana* Dunn," *Sensors and actuators B: Chemical*, vol. 198, pp. 268-273, 2014.
- [57] F. E. Tirtashi, M. Moradi, H. Tajik, M. Forough, P. Ezati, and B. J. I. J. o. B. M. Kuswandi, "Cellulose/chitosan pH-responsive indicator incorporated with carrot anthocyanins for intelligent food packaging," vol. 136, pp. 920-926, 2019.
- [58] M. Moradi, H. Tajik, H. Almasi, M. Forough, and P. J. C. P. Ezati, "A novel pH-sensing indicator based on bacterial cellulose nanofibers and black carrot anthocyanins for monitoring fish freshness," vol. 222, p. 115030, 2019.
- [59] S. B. Swami, S. N. Ghgare, S. S. Swami, K. J. Shinde, S. B. Kalse, and I. L. Pardeshi, "Natural pigments from plant sources: A review," *The Pharma Innovation Journal*, vol. 9, no. 10, p. 56, 2020.
- [60] J. Fang, "Classification of fruits based on anthocyanin types and relevance to their health effects," *Nutrition*, vol. 31, no. 11-12, pp. 1301-1306, 2015.
- [61] B. Yousuf, K. Gul, A. A. Wani, and P. Singh, "Health benefits of anthocyanins and their encapsulation for potential use in food systems: a review," *Critical reviews in food science and nutrition*, vol. 56, no. 13, pp. 2223-2230, 2016.
- [62] I. S. Ribeiro *et al.*, "Sustainable innovations in edible films and coatings: An overview," *Trends in Food Science & Technology*, p. 104272, 2023.
- [63] M. E. Abd El-Hack *et al.*, "Antimicrobial and antioxidant properties of chitosan and its derivatives and their applications: A review," *International Journal of Biological Macromolecules*, vol. 164, pp. 2726-2744, 2020.
- [64] S. Pourjavaher, H. Almasi, S. Meshkini, S. Pirsai, and E. J. C. p. Parandi, "Development of a colorimetric pH indicator based on bacterial cellulose nanofibers and red cabbage (*Brassica oleraceae*) extract," vol. 156, pp. 193-201, 2017.
- [65] M. Kurek, I. E. Garofulić, M. T. Bakić, M. Šćetar, V. D. Uzelac, and K. J. F. H. Galić, "Development and evaluation of a novel antioxidant and pH indicator film based on chitosan and food waste sources of antioxidants," vol. 84, pp. 238-246, 2018.
- [66] Y. Li, K. Wu, B. Wang, and X. J. I. J. o. B. M. Li, "Colorimetric indicator based on purple tomato anthocyanins and chitosan for application in intelligent packaging," vol. 174, pp. 370-376, 2021.
- [67] Z. Aghaei, B. Emadzadeh, B. Ghorani, R. J. F. Kadkhodaei, and b. technology, "Cellulose acetate nanofibres containing alizarin as a halochromic sensor for the qualitative assessment of rainbow trout fish spoilage," vol. 11, no. 5, pp. 1087-1095, 2018.
- [68] C. L. Luchese, N. Sperotto, J. C. Spada, and I. C. J. I. j. o. b. m. Tessaro, "Effect of blueberry agro-industrial waste addition to corn starch-based films for the production of a pH-indicator film," vol. 104, pp. 11-18, 2017.
- [69] F. J. Francis and P. C. Markakis, "Food colorants: Anthocyanins," *Critical Reviews in Food Science and Nutrition*, vol. 28, no. 4, pp. 273-314, 1989/01/01 1989, doi: 10.1080/10408398909527503.
- [70] H. Grisebach, *Biosynthesis of anthocyanins*. Academic Press, New York, 1982.

- [71] S. Singh, K. K. Gaikwad, Y. S. J. K. J. o. P. S. Lee, and Technology, "Anthocyanin-A natural dye for smart food packaging systems," vol. 24, no. 3, pp. 167-180, 2018.
- [72] M. Alizadeh-Sani *et al.*, "pH-responsive color indicator films based on methylcellulose/chitosan nanofiber and barberry anthocyanins for real-time monitoring of meat freshness," *International Journal of Biological Macromolecules*, vol. 166, pp. 741-750, 2021. [Online]. Available: <https://www.sciencedirect.com/science/article/pii/S0141813020348716?via%3Dihub>.
- [73] Y. Li, K. Wu, B. Wang, and X. Li, "Colorimetric indicator based on purple tomato anthocyanins and chitosan for application in intelligent packaging," (in eng), *International journal of biological macromolecules*, vol. 174, pp. 370-376, Mar 31 2021, doi: 10.1016/j.ijbiomac.2021.01.182.
- [74] T. Liang, G. Sun, L. Cao, J. Li, and L. Wang, "A pH and NH₃ sensing intelligent film based on *Artemisia sphaerocephala* Krasch. gum and red cabbage anthocyanins anchored by carboxymethyl cellulose sodium added as a host complex," *Food hydrocolloids*, vol. 87, pp. 858-868, 2019.
- [75] G. Olafsdottir, H. L. Lauzon, E. Martinsdottir, and K. Kristbergsson, "Influence of storage temperature on microbial spoilage characteristics of haddock fillets (*Melanogrammus aeglefinus*) evaluated by multivariate quality prediction," *International Journal of Food Microbiology*, vol. 111, no. 2, pp. 112-125, 2006/09/01/ 2006, doi: <https://doi.org/10.1016/j.ijfoodmicro.2006.04.045>.
- [76] S. Khan, J. K. Monteiro, A. Prasad, C. D. Filipe, Y. Li, and T. F. Didar, "Material Breakthroughs in Smart Food Monitoring: Intelligent Packaging and On-Site Testing Technologies for Spoilage and Contamination Detection," *Advanced Materials*, vol. 36, no. 1, p. 2300875, 2024.
- [77] H. Almasi, S. Forghani, and M. Moradi, "Recent advances on intelligent food freshness indicators; an update on natural colorants and methods of preparation," *Food Packaging and Shelf Life*, vol. 32, p. 100839, 2022/06/01/ 2022, doi: <https://doi.org/10.1016/j.fpsl.2022.100839>.
- [78] A. Gordon, "Introduction: effective implementation of food safety and quality systems: prerequisites and other considerations," in *Food Safety and Quality Systems in Developing Countries*: Elsevier, 2017, pp. 1-19.
- [79] S. Karanth, S. Feng, D. Patra, and A. K. Pradhan, "Linking microbial contamination to food spoilage and food waste: The role of smart packaging, spoilage risk assessments, and date labeling," *Frontiers in Microbiology*, vol. 14, p. 1198124, 2023.
- [80] S. V. G. Kumari, K. Pakshirajan, and G. Pugazhenth, "Freshness Indicator in Intelligent Food Packaging System," *Smart Food Packaging Systems: Innovations and Technology Applications*, pp. 361-386, 2024.
- [81] M. Sohail, D.-W. Sun, and Z. Zhu, "Recent developments in intelligent packaging for enhancing food quality and safety," *Critical reviews in food science and nutrition*, vol. 58, no. 15, pp. 2650-2662, 2018.

- [82] N. D. Boscher *et al.*, "Optical sensing responses of CrIII/Cl (TPP)(H₂O)-based coatings obtained by an atmospheric pressure plasma method—Application to the detection of volatile amines," *Sensors and Actuators B: Chemical*, vol. 191, pp. 553-560, 2014.
- [83] A. Pacquit *et al.*, "Development of a smart packaging for the monitoring of fish spoilage," *Food chemistry*, vol. 102, no. 2, pp. 466-470, 2007.
- [84] A. Pacquit, K. T. Lau, H. McLaughlin, J. Frisby, B. Quilty, and D. Diamond, "Development of a volatile amine sensor for the monitoring of fish spoilage," *Talanta*, vol. 69, no. 2, pp. 515-520, 2006.
- [85] B. Kuswandi, A. Restyana, A. Abdullah, L. Y. Heng, and M. Ahmad, "A novel colorimetric food package label for fish spoilage based on polyaniline film," *Food control*, vol. 25, no. 1, pp. 184-189, 2012.
- [86] B. Kuswandi, Jayus, R. Oktaviana, A. Abdullah, and L. Y. Heng, "A novel on-package sticker sensor based on methyl red for real-time monitoring of broiler chicken cut freshness," *Packaging technology and science*, vol. 27, no. 1, pp. 69-81, 2014.
- [87] B. Kuswandi, Jayus, T. S. Larasati, A. Abdullah, and L. Y. Heng, "Real-time monitoring of shrimp spoilage using on-package sticker sensor based on natural dye of curcumin," *Food Analytical Methods*, vol. 5, pp. 881-889, 2012.
- [88] M. C. Silva-Pereira, J. A. Teixeira, V. A. Pereira-Júnior, and R. Stefani, "Chitosan/corn starch blend films with extract from Brassica oleraceae (red cabbage) as a visual indicator of fish deterioration," *LWT-Food Science and Technology*, vol. 61, no. 1, pp. 258-262, 2015.
- [89] N. Wells, D. Yusufu, and A. Mills, "Colourimetric plastic film indicator for the detection of the volatile basic nitrogen compounds associated with fish spoilage," *Talanta*, vol. 194, pp. 830-836, 2019.
- [90] Y. Li, K. Wu, B. Wang, and X. Li, "Colorimetric indicator based on purple tomato anthocyanins and chitosan for application in intelligent packaging," *International Journal of Biological Macromolecules*, vol. 174, pp. 370-376, 2021.
- [91] I. Uysal Unalan, D. Boyacı, M. Ghaani, S. Trabattoni, and S. Farris, "Graphene oxide bionanocomposite coatings with high oxygen barrier properties," *Nanomaterials*, vol. 6, no. 12, p. 244, 2016.
- [92] N. Dole, K. Ahmadi, D. Solanki, V. Swaminathan, V. Keswani, and M. Keswani, "Corona Treatment of Polymer Surfaces to Enhance Adhesion," *Polymer Surface Modification to Enhance Adhesion: Techniques and Applications*, pp. 45-76, 2024.
- [93] M. Lindner, N. Rodler, M. Jesdinszki, M. Schmid, and S. J. J. o. a. p. s. Sänglerlaub, "Surface energy of corona treated PP, PE and PET films, its alteration as function of storage time and the effect of various corona dosages on their bond strength after lamination," vol. 135, no. 11, p. 45842, 2018.
- [94] C. Sun, D. Zhang, and L. C. J. A. i. P. T. J. o. t. P. P. I. Wadsworth, "Corona treatment of polyolefin films—a review," vol. 18, no. 2, pp. 171-180, 1999.
- [95] P. Fabbri and M. Messori, "Surface modification of polymers: chemical, physical, and biological routes," in *Modification of polymer properties*: Elsevier, 2017, pp. 109-130.

- [96] C. Sun, D. Zhang, and L. C. Wadsworth, "Corona treatment of polyolefin films—A review," *Advances in Polymer Technology: Journal of the Polymer Processing Institute*, vol. 18, no. 2, pp. 171-180, 1999.
- [97] M. Joshi and B. Butola, "Application technologies for coating, lamination and finishing of technical textiles," in *Advances in the dyeing and finishing of technical textiles*: Elsevier, 2013, pp. 355-411.
- [98] N. Burany, L. Huber, and P. Pejovic, "Corona discharge surface treater without high voltage transformer," *IEEE Transactions on Power Electronics*, vol. 23, no. 2, pp. 993-1002, 2008.
- [99] B. Sharma *et al.*, "Effect of cellulose nanocrystal incorporated acrylic copolymer resin on printing properties of waterborne inks," *Progress in Organic Coatings*, vol. 167, p. 106842, 2022.
- [100] C. Aydemir, B. N. Altay, and M. Akyol, "Surface analysis of polymer films for wettability and ink adhesion," *Color Research & Application*, vol. 46, no. 2, pp. 489-499, 2021.
- [101] R. Kol *et al.*, "Recent advances in pre-treatment of plastic packaging waste," *Waste Material Recycling in the Circular Economy-Challenges and Developments*, 2021.
- [102] R. Khandal, D. Khandal, G. Suri, and G. Seshadri, "Role of Surfactants in Paints, Inks, and Polishes," 2008, pp. 419-454.
- [103] R. Sharma, "Surfactants: basics and versatility in food industries," *PharmaTutor*, vol. 2, no. 3, pp. 17-29, 2014.
- [104] S. A. Stone, P. Gosavi, T. J. Athauda, and R. R. Ozer, "In situ citric acid crosslinking of alginate/polyvinyl alcohol electrospun nanofibers," *Materials Letters*, vol. 112, pp. 32-35, 2013.
- [105] L. Gautam, S. G. Warkar, S. I. Ahmad, R. Kant, and M. Jain, "A review on carboxylic acid cross-linked polyvinyl alcohol: Properties and applications," *Polymer engineering & science*, vol. 62, no. 2, pp. 225-246, 2022.
- [106] F. C. do Nascimento *et al.*, "Formulation and characterization of crosslinked polyvinyl alcohol (PVA) membranes: effects of the crosslinking agents," *Polymer Bulletin*, vol. 78, no. 2, pp. 917-929, 2021.
- [107] M. Heydari, A. Moheb, M. Ghiaci, and M. Masoomi, "Effect of cross-linking time on the thermal and mechanical properties and pervaporation performance of poly (vinyl alcohol) membrane cross-linked with fumaric acid used for dehydration of isopropanol," *Journal of applied polymer science*, vol. 128, no. 3, pp. 1640-1651, 2013.
- [108] S. Oancea, "A Review of the Current Knowledge of Thermal Stability of Anthocyanins and Approaches to Their Stabilization to Heat," *Antioxidants*, vol. 10, no. 9, p. 1337, 2021. [Online]. Available: <https://www.mdpi.com/2076-3921/10/9/1337>.
- [109] P. Loypimai, A. Moongngarm, and P. Chottanom, "Thermal and pH degradation kinetics of anthocyanins in natural food colorant prepared from black rice bran," *Journal of food science and technology*, vol. 53, pp. 461-470, 2016.
- [110] E. Commission, "Regulation (EU) No 1169/2011 on the provision of food information to consumers," 2011.

- [111] E. Commission, "Commission Regulation (EC) No 1935/2004 of 27 October 2004 on materials and articles intended to come into contact with food and repealing Directives 80/590/EEC and 89/109/EEC," 2004.
- [112] E. P. o. F. A. a. N. S. a. t. F. (ANS), "Scientific opinion on the re-evaluation of anthocyanins (E 163) as a food additive," European Food Safety Authority (EFSA), 23 May 2013 2013.
- [113] I. Konczak and W. Zhang, "Anthocyanins-More Than Nature's Colours," (in eng), *J Biomed Biotechnol*, vol. 2004, no. 5, pp. 239-240, 2004, doi: 10.1155/s1110724304407013.
- [114] E. Commission, "Regulation (EC) No.1333/2008 on food additives," 2008. [Online]. Available: <https://eur-lex.europa.eu/legal-content/EN/TXT/?uri=CELEX%3A32008R1333>
- [115] J. F. W. E. C. o. F. A. (JECFA), "Evaluation of certain food additives," 2016.
- [116] E. F. S. A. (EFSA), "Scientific Opinion on the safety of anthocyanins for use in food," 2013, vol. 11 issue 5.
- [117] E. Shim, "Coating and laminating processes and techniques for textiles," in *Smart textile coatings and laminates*: Elsevier, 2019, pp. 11-45.
- [118] H. Kipphan, *Handbook of print media: technologies and production methods*. Springer Science & Business Media, 2001.
- [119] M. Thirupathi Vasuki, V. Kadirvel, and G. Pejavara Narayana, "Smart packaging—An overview of concepts and applications in various food industries," *Food Bioengineering*, vol. 2, no. 1, pp. 25-41, 2023.
- [120] Y. Yuan and T. R. Lee, "Contact angle and wetting properties," in *Surface science techniques*: Springer, 2013, pp. 3-34.
- [121] C. Aydemir, B. N. Altay, M. J. C. R. Akyol, and Application, "Surface analysis of polymer films for wettability and ink adhesion," vol. 46, no. 2, pp. 489-499, 2021.
- [122] J. Vial, A. J. I. j. o. a. Carre, and adhesives, "Calculation of Hamaker constant and surface energy of polymers by a simple group contribution method," vol. 11, no. 3, pp. 140-143, 1991.
- [123] G. Olafsdottir *et al.*, "Methods to evaluate fish freshness in research and industry," *Trends in food science & technology*, vol. 8, no. 8, pp. 258-265, 1997.
- [124] L. Gram, L. Ravn, M. Rasch, J. B. Bruhn, A. B. Christensen, and M. Givskov, "Food spoilage—interactions between food spoilage bacteria," *International Journal of Food Microbiology*, vol. 78, no. 1, pp. 79-97, 2002/09/15/ 2002, doi: [https://doi.org/10.1016/S0168-1605\(02\)00233-7](https://doi.org/10.1016/S0168-1605(02)00233-7).
- [125] O. I. Ogidi, E. E. Charles, C. C. Okore, B. Wilfred, L. M. Oguoma, and H. E. Carbom, "Mathematical modelling of the growth of specific spoilage microorganisms in tilapia (*Oreochromis niloticus*) fish," *ASIO J Microbiol Food Sci Biotechnol Innov*, vol. 6, no. 1, pp. 09-15, 2021.
- [126] A. E.-D. A. Bekhit, B. W. Holman, S. G. Giteru, and D. L. Hopkins, "Total volatile basic nitrogen (TVB-N) and its role in meat spoilage: A review," *Trends in Food Science & Technology*, vol. 109, pp. 280-302, 2021.

- [127] S. Mohammadalinejad, I.-J. Jensen, M. Kurek, and J. Lerfall, "Novel colorimetric indicators based on alginate hydrogel beads containing anthocyanin for visual freshness monitoring of shrimp and minced chicken," *LWT*, vol. 199, p. 116127, 2024/05/01/ 2024, doi: <https://doi.org/10.1016/j.lwt.2024.116127>.
- [128] Z. Aghaei, B. Emadzadeh, B. Ghorani, and R. Kadkhodaei, "Cellulose acetate nanofibres containing alizarin as a halochromic sensor for the qualitative assessment of rainbow trout fish spoilage," *Food and bioprocess technology*, vol. 11, no. 5, pp. 1087-1095, 2018.
- [129] X. Zhai *et al.*, "Novel colorimetric films based on starch/polyvinyl alcohol incorporated with roselle anthocyanins for fish freshness monitoring," *Food Hydrocolloids*, vol. 69, pp. 308-317, 2017.
- [130] V. A. Pereira Jr, I. N. Q. de Arruda, and R. Stefani, "Active chitosan/PVA films with anthocyanins from Brassica oleraceae (Red Cabbage) as Time–Temperature Indicators for application in intelligent food packaging," *Food Hydrocolloids*, vol. 43, pp. 180-188, 2015.
- [131] M. Moradi, H. Tajik, H. Almasi, M. Forough, and P. Ezati, "A novel pH-sensing indicator based on bacterial cellulose nanofibers and black carrot anthocyanins for monitoring fish freshness," *Carbohydrate Polymers*, vol. 222, p. 115030, 2019.
- [132] J. Bremner, "Determination of nitrogen in soil by the Kjeldahl method," *The Journal of Agricultural Science*, vol. 55, no. 1, pp. 11-33, 1960.
- [133] J. Bremner and D. R. Keeney, "Steam distillation methods for determination of ammonium, nitrate and nitrite," *Analytica chimica acta*, vol. 32, pp. 485-495, 1965.
- [134] E. Conway and E. O'malley, "Microdiffusion methods. Ammonia and urea using buffered absorbents (revised methods for ranges greater than 10µg. N)," *Biochemical Journal*, vol. 36, no. 7-9, p. 655, 1942.
- [135] M. Menéndez, R. Garrido-Delgado, L. Arce, and M. Valcárcel, "Direct determination of volatile analytes from solid samples by UV-ion mobility spectrometry," *Journal of Chromatography a*, vol. 1215, no. 1-2, pp. 8-14, 2008.
- [136] D. Ripepi, R. Zaffaroni, M. Kolen, J. Middelkoop, and F. M. Mulder, "Operando isotope selective ammonia quantification in nitrogen reduction studies via gas chromatography-mass spectrometry," *Sustainable Energy & Fuels*, vol. 6, no. 8, pp. 1945-1949, 2022.
- [137] M.-L. Xu, Y. Gao, X. Wang, X. X. Han, and B. Zhao, "Comprehensive Strategy for Sample Preparation for the Analysis of Food Contaminants and Residues by GC–MS/MS: A Review of Recent Research Trends," *Foods*, vol. 10, no. 10, p. 2473, 2021. [Online]. Available: <https://www.mdpi.com/2304-8158/10/10/2473>.
- [138] N. Lorenzo-Parodi, E. Leitner, and T. C. Schmidt, "Comparison of gas chromatographic techniques for the analysis of iodinated derivatives of aromatic amines," (in eng), *Anal Bioanal Chem*, vol. 415, no. 17, pp. 3313-3325, Jul 2023, doi: 10.1007/s00216-023-04713-8.
- [139] R. Lv, X. Huang, J. H. Aheto, L. Mu, and X. Tian, "Analysis of fish spoilage by gas chromatography–mass spectrometry and electronic olfaction bionic system," *Journal of Food Safety*, vol. 38, no. 6, p. e12557, 2018.

- [140] E. J. Conway, "Microdiffusion analysis and volumetric error," *Microdiffusion analysis and volumetric error.*, 1947.
- [141] D.-Y. Kim, S.-W. Park, and H.-S. Shin, "Fish Freshness Indicator for Sensing Fish Quality during Storage," *Foods*, vol. 12, no. 9, p. 1801, 2023. [Online]. Available: <https://www.mdpi.com/2304-8158/12/9/1801>.
- [142] R. Li, L. Cai, T. Gao, C. Li, G. Zhou, and K. Ye, "Comparing the quality characteristics and bacterial communities in meatballs with or without blown pack spoilage," *LWT*, vol. 130, p. 109529, 2020/08/01/ 2020, doi: <https://doi.org/10.1016/j.lwt.2020.109529>.
- [143] E. Reynisson *et al.*, "Effects of different cooling techniques on bacterial succession and other spoilage indicators during storage of whole, gutted haddock (*Melanogrammus aeglefinus*)," *European Food Research and Technology*, vol. 231, no. 2, pp. 237-246, 2010, doi: 10.1007/s00217-010-1273-z.
- [144] M. Jouki, F. T. Yazdi, S. A. Mortazavi, A. Koocheki, and N. Khazaei, "Effect of quince seed mucilage edible films incorporated with oregano or thyme essential oil on shelf life extension of refrigerated rainbow trout fillets," *International journal of food microbiology*, vol. 174, pp. 88-97, 2014.
- [145] C. Rukchon, A. Nopwinyuwong, S. Trevanich, T. Jinkarn, and P. Suppakul, "Development of a food spoilage indicator for monitoring freshness of skinless chicken breast," *Talanta*, vol. 130, pp. 547-554, 2014.
- [146] L. Kuuliala *et al.*, "Microbiological, chemical and sensory spoilage analysis of raw Atlantic cod (*Gadus morhua*) stored under modified atmospheres," *Food Microbiology*, vol. 70, pp. 232-244, 2018/04/01/ 2018, doi: <https://doi.org/10.1016/j.fm.2017.10.011>.
- [147] L. N. Tam *et al.*, "Effects of bioactive substances to prolong the shelf-life and inhibit the formation of black spots in black tiger shrimp (*Penaeus monodon*) preserved at 0 degree C," *Vietnam Journal of Chemistry*, vol. 60, no. 2, pp. 133-139, 2022.
- [148] M. W. Apriliyanti, A. Wahyono, M. Fatoni, B. Poerwanto, and W. Suryaningsih, "The Potency of betacyanins extract from a peel of dragon fruits as a source of colourimetric indicator to develop intelligent packaging for fish freshness monitoring," in *IOP conference series: Earth and environmental science*, 2018, vol. 207, no. 1: IOP Publishing, p. 012038.
- [149] R. Husain, S. Suparmo, E. Harmayani, and C. Hidayat, "Kinetic oxidation of protein and fat in snapper (*Lutjanus* sp) fillet during storage," in *AIP Conference Proceedings*, 2016, vol. 1755, no. 1: AIP Publishing.
- [150] P. K. Prabhakar, P. P. Srivastav, S. S. Pathak, and K. Das, "Mathematical modeling of total volatile basic nitrogen and microbial biomass in stored rohu (*Labeo rohita*) fish," *Frontiers in Sustainable Food Systems*, vol. 5, p. 669473, 2021.
- [151] P. Howgate, "A critical review of total volatile bases and trimethylamine as indices of freshness of fish. Part 2. Formation of the bases, and application in quality assurance," *Electronic Journal of Environmental, Agricultural & Food Chemistry*, vol. 9, no. 1, 2010.
- [152] M. Peleg and M. G. Corradini, "Microbial Growth Curves: What the Models Tell Us and What They Cannot," *Critical Reviews in Food Science and Nutrition*, vol. 51, no. 10, pp. 917-945, 2011/12/01 2011, doi: 10.1080/10408398.2011.570463.

- [153] L. Giannuzzi, A. Pinotti, and N. Zaritzky, "Mathematical modelling of microbial growth in packaged refrigerated beef stored at different temperatures," *International Journal of Food Microbiology*, vol. 39, no. 1-2, pp. 101-110, 1998.
- [154] G. C. Vidana Gamage, J. K. Goh, and W. S. Choo, "Application of anthocyanins from black goji berry in fermented dairy model food systems: An alternate natural purple color," *LWT*, vol. 198, p. 115975, 2024/04/15/ 2024, doi: <https://doi.org/10.1016/j.lwt.2024.115975>.
- [155] D. Walkowiak-Tomczak and J. Czapski, "Colour changes of a preparation from red cabbage during storage in a model system," *Food Chemistry*, vol. 104, no. 2, pp. 709-714, 2007.
- [156] V. Lavelli, P. S. S. Harsha, M. Laureati, and E. Pagliarini, "Degradation kinetics of encapsulated grape skin phenolics and micronized grape skins in various water activity environments and criteria to develop wide-ranging and tailor-made food applications," *Innovative food science & emerging technologies*, vol. 39, pp. 156-164, 2017.
- [157] Y. Guo, H. Zhang, S. Shao, S. Sun, D. Yang, and S. Lv, "Anthocyanin: a review of plant sources, extraction, stability, content determination and modifications," *International Journal of Food Science & Technology*, vol. 57, no. 12, pp. 7573-7591, 2022, doi: <https://doi.org/10.1111/ijfs.16132>.
- [158] G. C. V. Gamage, J. K. Goh, and W. S. Choo, "Application of anthocyanins from black goji berry in fermented dairy model food systems: An alternate natural purple color," *LWT*, vol. 198, p. 115975, 2024.
- [159] B. Liang, X. Li, M. Yang, Z. Zhang, and J. Ren, "Stacking ensemble learning for gas sensor-based detection of salmon freshness and shelf life," *Journal of Food Process Engineering*, vol. 47, no. 3, p. e14593, 2024.
- [160] J. Bielecka *et al.*, "Content of Toxic Elements in 12 Groups of Rice Products Available on Polish Market: Human Health Risk Assessment," *Foods*, vol. 9, no. 12, p. 1906, 2020. [Online]. Available: <https://www.mdpi.com/2304-8158/9/12/1906>.
- [161] F. Hindle *et al.*, "Monitoring of food spoilage by high resolution THz analysis," *Analyst*, vol. 143, no. 22, pp. 5536-5544, 2018.
- [162] L. Wang, J. Heising, V. Fogliano, and M. Dekker, "Fat content and storage conditions are key factors on the partitioning and activity of carvacrol in antimicrobial packaging," *Food Packaging and Shelf Life*, vol. 24, p. 100500, 2020/06/01/ 2020, doi: <https://doi.org/10.1016/j.fpsl.2020.100500>.
- [163] Z. Yi and J. Xie, "Prediction in the dynamics and spoilage of *Shewanella putrefaciens* in Bigeye Tuna (*Thunnus obesus*) by gas sensors stored at different refrigeration temperatures," *Foods*, vol. 10, no. 9, p. 2132, 2021.
- [164] P. Ezati, J.-W. Rhim, M. Moradi, H. Tajik, and R. Molaei, "CMC and CNF-based alizarin incorporated reversible pH-responsive color indicator films," *Carbohydrate Polymers*, vol. 246, p. 116614, 2020/10/15/ 2020, doi: <https://doi.org/10.1016/j.carbpol.2020.116614>.
- [165] W. Hu, S. Chen, J. Yang, Z. Li, and H. Wang, "Functionalized bacterial cellulose derivatives and nanocomposites," *Carbohydrate Polymers*, vol. 101, pp. 1043-1060, 2014/01/30/ 2014, doi: <https://doi.org/10.1016/j.carbpol.2013.09.102>.

APPENDICES

APPENDIX A ARTICLE 1: CHARACTERIZATION OF A FOOD-SAFE COLORIMETRIC INDICATOR BASED ON BLACK RICE ANTHOCYANIN/PET FILMS FOR VISUAL ANALYSIS OF FISH SPOILAGE

A.1 Tape test

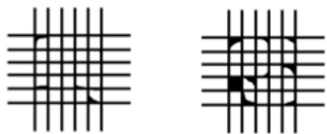

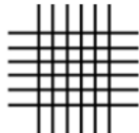

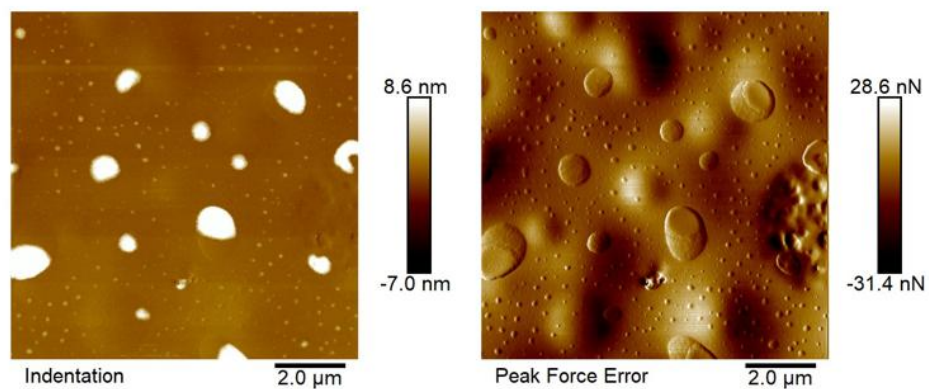
Type of samples	Classification	Percent area removed	Surface of cross-cut area from which flaking has occurred for six parallel cuts and adhesion range by percent	Picture
Coated film without Thermal treatment	3B	5-15%		
Coated film with Thermal treatment (165-5)	5B	0% Non		

Figure A.1 Final samples with proper thermal treatment (165 °C for 5 min) passed the tape test.

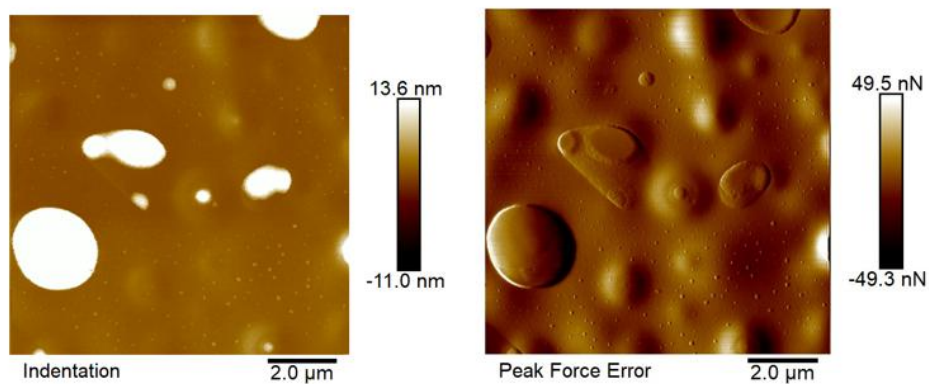
A.2 Atomic force microscope (AFM)

AFM images of the coated PET films-treated and untreated controls. Thermal treatment of coatings increases maximum roughness, while enhancing surface adhesion bonding can lead to a rise in the Root Mean Square (RMS) value measured by AFM. Improved adhesion bonding between the coating and the surface contributes to a smoother, more uniform coating, thereby resulting in higher RMS values.

(A)



(B)



(C)

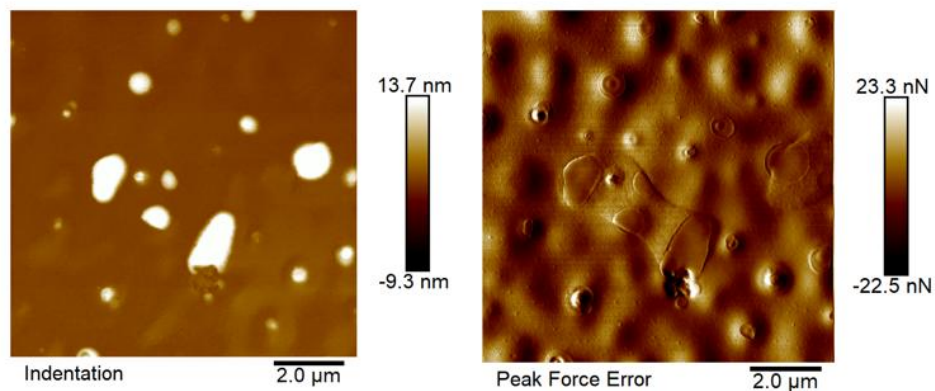


Figure A.2 The left side shows the topographic image and the right side the error-signal image of the same spot. (A) Untreated control; (B) 90 °C for 60 min treatment time; (C) 165 °C for 5 min treatment time.

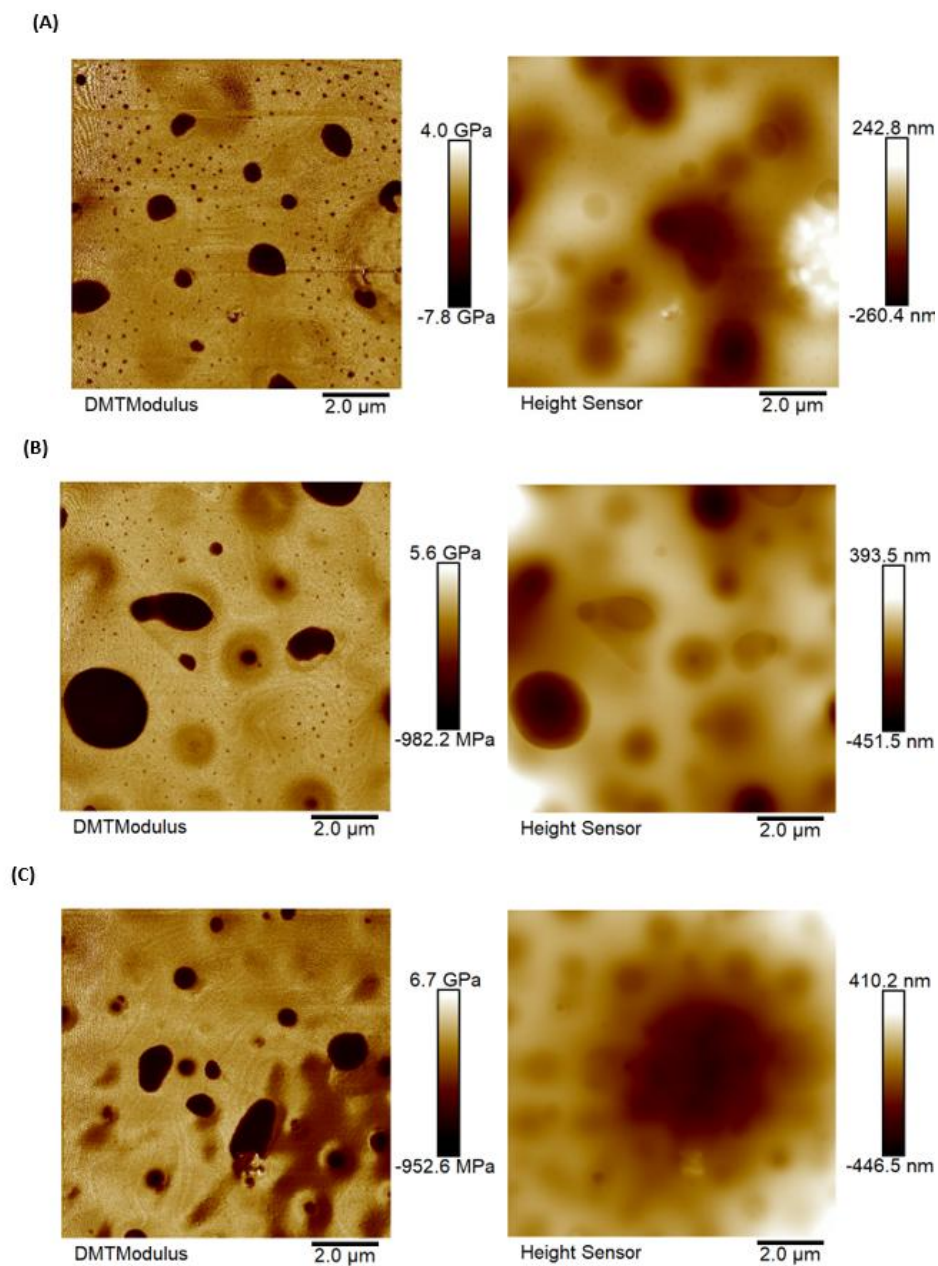


Figure A.3 The left side root-mean-square (RMS) roughness values and right side DMT modulus. (A) Untreated control; (B) 90 °C for 60 min treatment time; (C) 165 °C for 5 min treatment time.

A.3 Design of experiment for ink formulation (DOE)

The results indicated that a higher concentration of BC and CA (10–15%) can lead to a heterogeneous ink formulation, negatively impacting the uniformity and stability of the ink. Conversely, concentrations below 5% of these components may result in insufficient crosslinking, which compromises the ink's structural integrity. As a result, the pH indicator becomes prone to washing out and exhibits poor performance when exposed to high-humidity environments. Optimizing the concentration of these components is critical to achieving a balanced formulation that ensures both stability and functionality under varying environmental conditions.

Table A.1 Summary of the ink components and their corresponding design experiments. The selected range highlights the concentrations that were further investigated throughout this research study.

Design				
Run	BC	PVOH	CA	pH
1	0.05	0.15	0.132	2.25
2	0.15	0.2	0.15	1.5
3	0.15	0.1	0.05	3
4	0.05	0.1	0.05	1.5
5	0.15	0.15	0.1	2.25
6	0.15	0.1	0.1	1.5
7	0.05	0.2	0.1	1.5
8	0.15	0.2	0.05	1.5
9	0.05	0.1	0.15	1.5
10	0.05	0.15	0.05	2.25
11	0.05	0.1	0.1	3
12	0.1	0.15	0.1	3
13	0.1	0.2	0.1	2.25
14	0.1	0.15	0.05	2.25
15	0.1	0.15	0.1	1.5
16	0.1	0.1	0.1	2.25
17	0.05	0.2	0.15	3
18	0.15	0.2	0.1	3
19	0.1	0.15	0.15	2.25
20	0.15	0.1	0.15	3
21	0.05	0.2	0.05	3

APPENDIX B ARTICLE 2: ENHANCING SEAFOOD FRESHNESS MONITORING: INTEGRATION COLOR CHANGE OF A FOOD-SAFE ON-PACKAGE COLORIMETRIC SENSOR WITH MATHEMATICAL MODELS, MICROBIOLOGICAL, AND CHEMICAL ANALYSES

B.1 Mathematical model for shelf-life predication based on the experimental data

At the last step, the mathematical models were employed to experimental data to predicate the fish spoilage. The modified logistic and Howgate models provide superior performance in predicting TVB-N gas, while the modified Arrhenius models demonstrate greater performance in predicting bacterial population. The mean value of six experimental data points for TVB-N levels provides some insights but does not capture the system's full variability and complexity. With an inadequate number of samples, error estimation (RMSE and AIC) may be unreliable, and the model may overfit or underfit. Model validation requires enough data points, but splitting a limited dataset for validation is a challenge.

B.2 Mathematical model for TVB-N and Interpretation of Metrics

The simulation models were fitted using the experimental TVB-N values (mean) of Pangasius fish during storage to predict their release. According to the literature, an experimental model is suggested for storage temperatures ranging from 5 to 4 °C [150]. However, the exponential model showed the least satisfactory results, due to high RMSE and AIC compared to other models (Modified logistic and Exponential polynomial). The observed low fitting exponential model in the stored samples may be attributed to several factors, including changes in the composition of microbial activity over time, chemical interactions between TVB-N gases and other compounds in the headspace of fish samples, and the volatilization and adsorption of TVB-N gases on the surface of the fish containers during storage. The exponential model has less explanatory power. Improved model performance was achieved by a quadratic term (Bt^2) in the exponential model, significantly improving its performance by lowering the RMSE and AIC metrics, highlighting the need for incorporating additional terms to better capture the underlying processes [161]. Since, the observed

data points had an S shape curve similar to the exponential growth function, the modified logistic function is also explored as a potential model for formation of TVB-N gases during fish spoilage at 4 °C. To employ the Howgate model, we needed to parametrize Y_{\max} , Y_{\min} , K , and t_d . However, the fitting algorithm did not converge due to the limited number of observational and experimental data points. Therefore, we assumed, entered Y_{\min} as the initial value, and then proceeded to parametrize the remaining parameters. The study found that the Howgate, modified logistic, and exponential polynomials had lower RMSEs of 2.28, 2.29, and 2.88 than all the other models that were fitted to the experimental data. A lower RMSE indicates better predictive accuracy. We also obtained lower AIC values, which can suggest better model parsimony: 34.95 for both the Howgate and modified logistic models, and 37.74 for the exponential polynomial model. **Table B.1** summarizes the model parameters along with goodness of fit metrics. Therefore, the Modified logistic model and Howgate showed the best fitting performance with lowest AIC and RMSE among the models. In comparison, the modified logistic model has a reduced number of parameters and requires fewer assumptions to develop predictions. Noticeably, the A , K parameters of the Modified logistic model and Y_{\max} , t_d and K are statistically significant with p-values below 0.01 and 0.05 respectively.

B.3 Mathematical model for TVC, pseudomonas spp and Interpretation of Metrics

Food safety and quality can also be assessed using predictive microbiology instead of traditional methods. As storage conditions can alter spoiling microorganisms, we used TVC data points for fitting with available kinetic models. Initially, the logistic and modified logistic as three-parameter models were applied to the microbiological experimental data of the present study. Subsequently, the modified Gompertz model (four-parameter) were fitted [150]. In modified Gompertz model, μ_{\max} has estimated ($0.6649 \pm 0.14 \text{ day}^{-1}$) and statistically significant at p-value < 0.01 [125, 162, 163]. A "lag time" is the amount of time it takes to achieve a 50% or 100% increase. We used an arbitrary criterion to consider this parameter which is approximately 2 for Modified Gompertz equation. The "lag time" can be determined graphically as the intersection of the tangents to the growth curve at the "lag" and "exponential" phases [152]. The Logistic, modified logistic and modified Gompertz showed similar performance. Therefore, the Modified Arrhenius (I) showed the best fitting performance with lowest AIC and RMSE among the models. Noticeably, the Y_0 , K

parameters of the Modified Arrhenius (I) are statistically significant with p-values below 0.05. Hence the Modified Arrhenius (I) model appears to be the best fit model for TVC predication of current study. Comparable to the results of the TVC prediction, the best fit for the *Pseudomonas* spp population found is Modified Arrhenius (II). While both Modified Arrhenius models have similar RMSE values, Modified Arrhenius II has a significantly lower AIC than Modified Arrhenius I. Furthermore, the RMSE values for Modified Arrhenius (II), logistic, and modified logistic models are all 0.18; however, Modified Arrhenius (II) has a lower AIC value than the other models. As a result, the Modified Arrhenius (II) model appears to be the best fit model for predicting *Pseudomonas* spp population in this study.

Table B.1 Displays the parameter values derived from models based on TVB-N data obtained from the present study.

Parameters	Exponential	Modified Arrhenius (I)	Modified Arrhenius (II)	Exponential polynomial	Modified logistic	Howgate
Y_0	$11.9064 \pm 3.42^{**}$	5.2182 ± 5.49	3.28142 ± 4.31	-	-	-
A	-	-	-	$5.6052 \pm 2.35^*$	35.3510 ± 2.89 ***	-
K	$0.1343 \pm 0.04^{**}$	$3.3437 \pm 0.97^{**}$	6.70694 ± 2.69	$0.4912 \pm 0.15^{**}$	0.8666 ± 0.27 **	$0.8665 \pm 0.27^{**}$
B	-	-	-	$-0.0317 \pm 0.01^*$	11.0001 ± 7.86	-
D	-	1.2406 ± 2.45	-0.06392 ± 0.04	-	-	-

Table B.2 Displays the parameter values derived from models based on TVC data obtained from the present study.

Parameters	Modified Arrhenius (I)	Modified Arrhenius (II)	logistic	Modified logistic	Modified Gompertz
A	-	-	18.0461±29.29	18.0459±29.29	53.6758±9.43
K	0.43 ± 0.07 ***	0.30 ± 0.10**	0.1008 ± 0.07	0.1008 ± 0.07	-
B	-		13.4270 ± 29.21	3.8725 ± 7.74	-
D	-1.70 ± 1.89	0.02 ± 0.03			
μ _{Max}			-	-	0.6649 ± 0.14***
Y ₀	3.80 ± 0.22 ***	3.71 ± 0.20***	-	-	0.7894 ± 6.19

Parameters	Modified Arrhenius (I)	Modified Arrhenius (II)	logistic	Modified logistic	Modified Gompertz (Continued)
AIC	4.45	5.30	5.23	5.23	5.25
AICc	17.78	18.63	18.56	18.56	18.58
BIC	4.77	5.61	5.54	5.54	5.56
RMSE	0.19	0.20	0.20	0.20	0.20
Level of significance codes: P-value<0.01 ***, P-value<0.05 **, P-value <0.1 *					

Table B.3 Displays the parameter values derived from models based on pseudomonas spp data obtained from the present study.

Parameters	Modified Arrhenius (I)	Modified Arrhenius (II)	logistic	Modified logistic	Modified Gompertz
A	-	-	$5.5070 \pm 0.27^{***}$	$5.5071 \pm 0.27^{***}$	$2.3549 \pm 0.5180^{**}$

Parameters	Modified Arrhenius (I)	Modified Arrhenius (II)	logistic	Modified logistic	Modified Gompertz (Continued)
K	0.28090 \pm 0.04***	0.73090 \pm 0.16***	0.4385 \pm 0.10**	0.4385 \pm 0.10**	-
B	2.19637 \pm 1.02	-0.08645 \pm 0.02**	0.5567 \pm 0.31	1.2765 \pm 0.19***	-
μ_{Max}	-	-	-	-	0.7835 \pm 0.37
Y_0	2.44132 \pm 0.32***	2.38712 \pm 0.21***	-	-	3.0284 \pm 0.3151***
AIC	7.99	3.91	4.47	4.47	15.52
AICc	27.90	23.91	24.47	24.47	35.53
BIC	7.77	3.70	4.26	4.26	15.31
RMSE	0.24	0.18	0.18	0.18	0.55
Level of significance codes: P-value<0.01 ***, P-value<0.05 **, P-value <0.1 *					

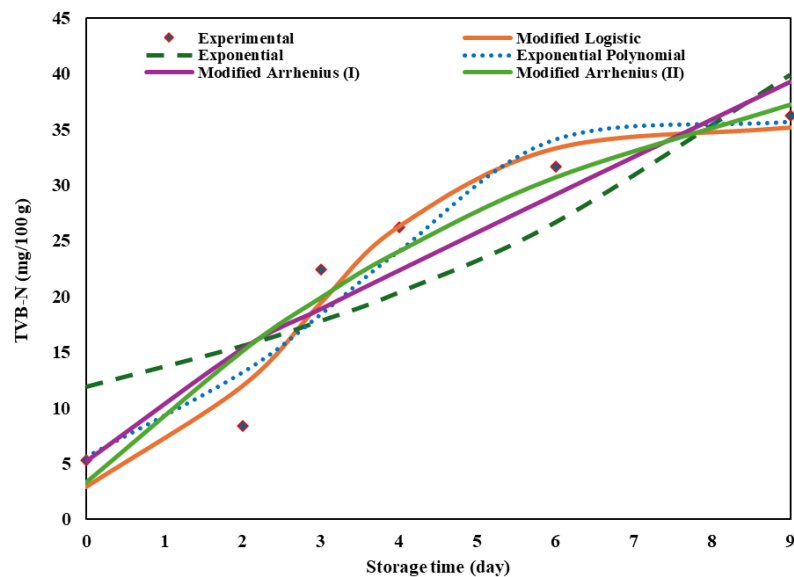


Figure B.1 Different models curve for TVB-N of Pangasius fillets during 4 °C storage for 9 days.

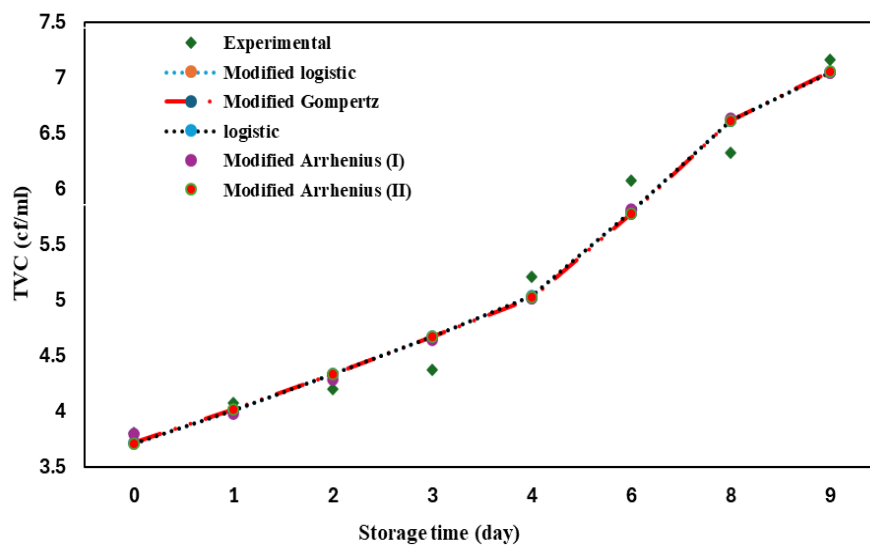


Figure B.2 Different models curve for TVC of Pangasius fillets during 4 °C storage for 9 days.

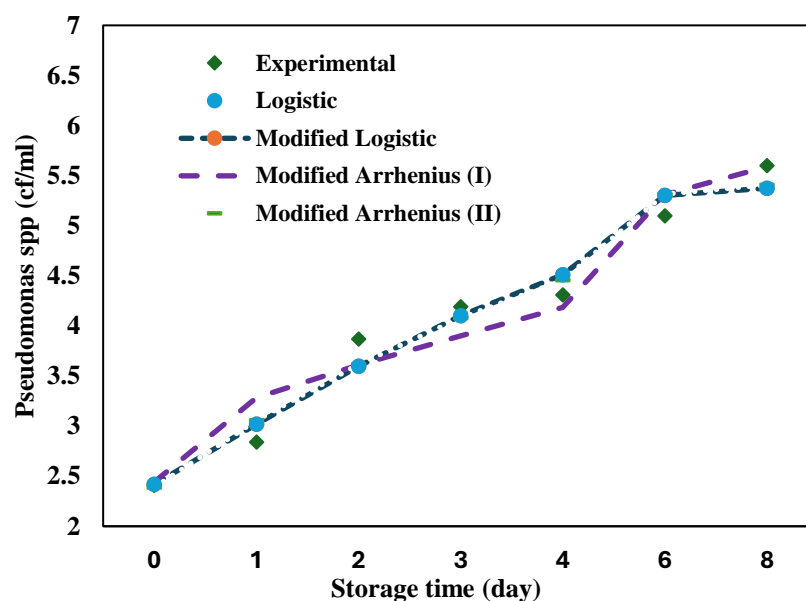


Figure B.3 Different models curve for *Pseudomonas* spp of *Pangasius* fillets during 4 °C storage for 9 days.

B.4 Sensor response to different fish weights

Figure B.4 illustrated the Δ RGB (color change) response of the pH sensor to various weights of fish samples (30, 50 and 100 g) stored over nine days in packages with different pH indicators (NTT and 165-5). According to the observations, the different weights and conditions of the fish samples impacting sensor response exhibit varying levels of sensitivity, as indicated by the range of Δ RGB values.

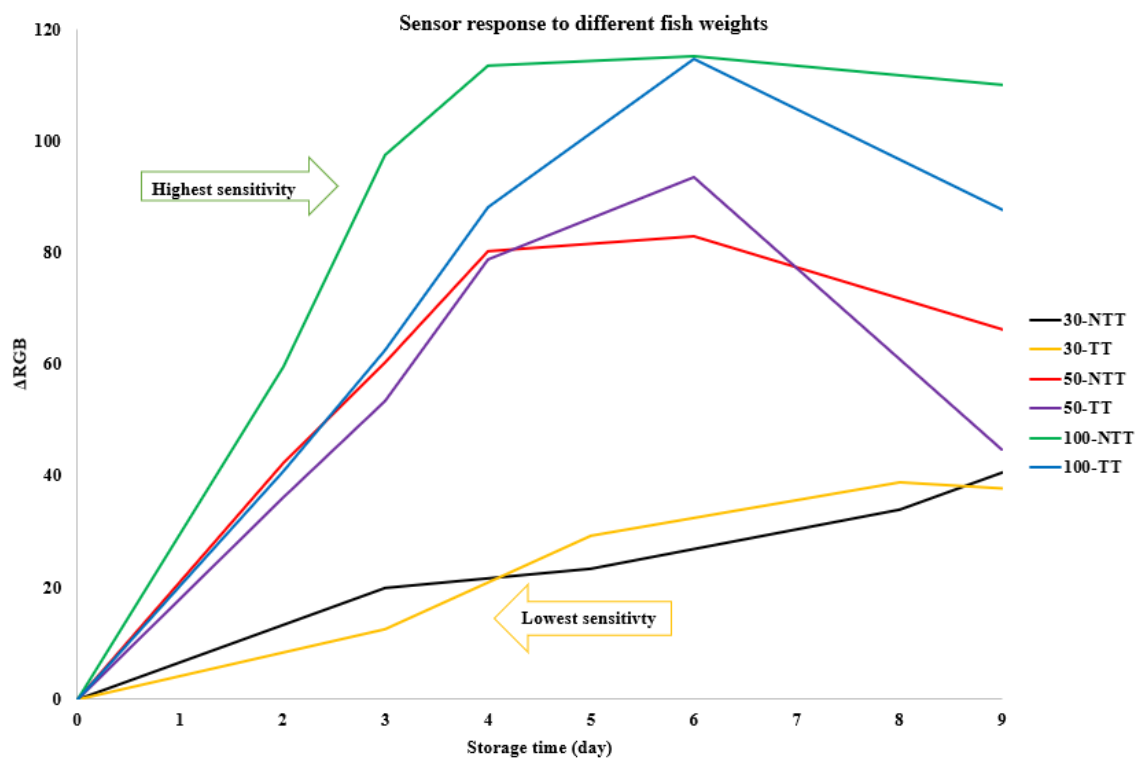


Figure B.4 Sensor response to different fish weights over storage time.

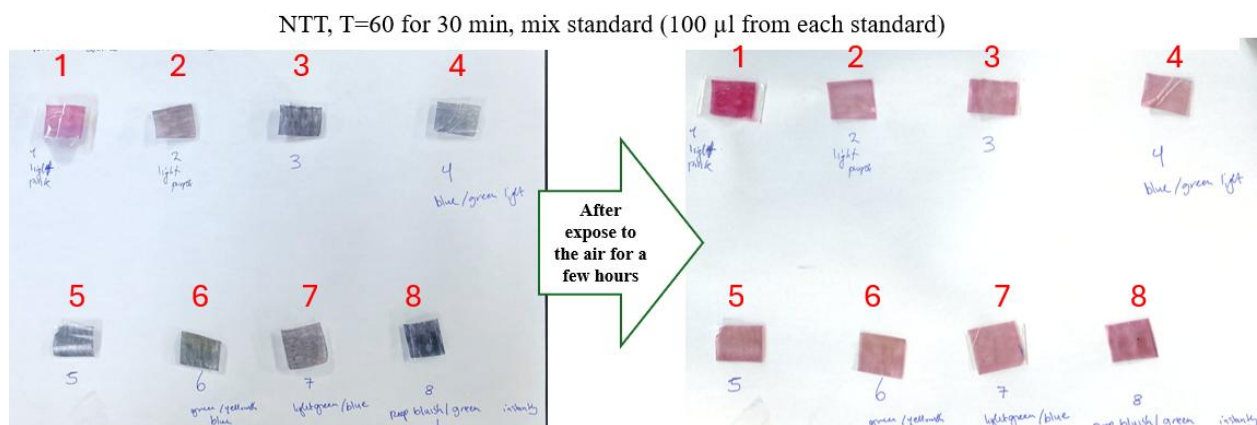


Figure B.5 Sensitivity trials for NTT pH indicators at T=60° C for 30 minutes.

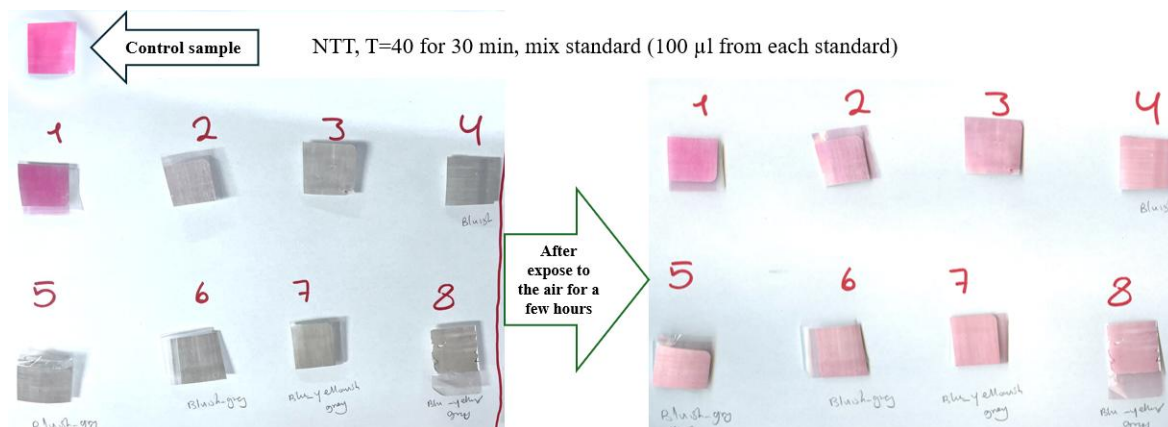


Figure B.6 Sensitivity trials for NTT pH indicators at T=40° C for 30 minutes.

B.5 Reversibility Test

Important attributes of intelligent gas sensors include high sensitivity and immediate reaction to gas vapors, to exhibit a distinct color change, as well as the ability of indicator films to be reversed [164, 165]. The reversibility of the indicator films was tested by exposing the films repeatedly to a defined volume of ammonia and Hydrochloric acid vapors for 3 min each as described [164] with some modification.

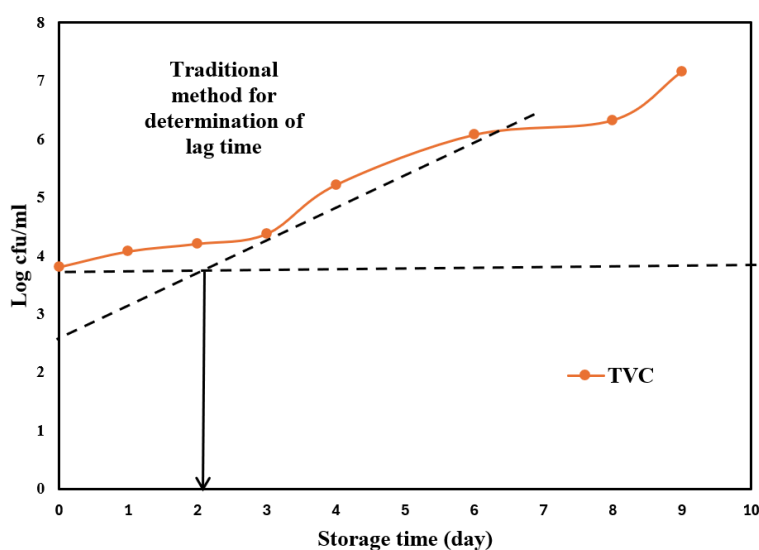


Figure B.7 Traditional method for lag time assumption: $t_0 \sim 2$ day.



Figure B.8 Colour stability of pH indicators after one month; however, the pH indicator with thermal treatment (165–5) stayed intact and its colour did not wipe out (right side).

APPENDIX C ARTICLE 3: INTELLIGENT PACKAGING SOLUTIONS FOR FISH AND MEAT PRODUCTS: VOLATILE GAS DETECTION VIA GC-MS, MICROBIAL ANALYSIS AND COLORIMETRIC MONITORING

Table C.1 Limit of detection with (TVB-N gases) at accelerated storage condition.

Type of standard	Concentration	Mean R	Mean G	Mean B	Std R	Std G	Std B	ΔRGB
NH ₃	0	204.66	41	96	4.49	16.26	8.6	0
	0.001	190.66	109.66	133.33	5.24	1.24	2.62	78.15193**
	0.01	179	137	146	6.37	6.48	5.71	108.8667***
	0.1	206.66	146.66	145.66	11.95	8.49	8.49	117.8395***
	1	174	111	102.33	4.08	2.16	4.18	72.23313**
TMA	0	204.66	41	96	4.49	16.26	8.6	0
	0.001	180	120	132.33	3.55	6.16	5.43	90.38243**
	0.01	212.33	179.66	182	3.09	2.86	2.94	163.3445***
	0.1	137.66	85.66	90.33	7.31	7.31	6.84	80.71967
	1	161	126.66	104.66	0	3.29	1.24	96.53407
DMA	0	204.66	41	96	4.49	16.26	8.6	0
	0.001	123	18.66	40.66	2.82	7.84	7.84	101.1432***
	0.01	106	7.66	68.33	8.48	4.71	4.92	107.7543***

Type of standard	Concentration	Mean R	Mean G	Mean B	Std R	Std G	Std B	Δ RGB (Continued)
	0.1	88.66	80.33	68.33	6.01	6.54	4.92	125.5726***
	1	80	64.66	33	9.41	8.57	9.27	141.6648***
<p>All values were expressed as mean \pm standard deviation (n = 3).</p> <p>Level of significance codes: P-value<0.01 ***, P-value<0.05 **, P-value <0.1 *</p>								

C.2 Freshness control in room temperature with gas tube detector

At refrigerated temperatures (0 till 4 ° C), fish typically remain fresh for several days, and ammonia production is minimal. According to several measurement, no color change was observed in gas detector tubes regarding presence of ammonia for 8 hours. Suggesting that the fish is fresh. At room temperature, spoilage occurs much more rapidly. Ammonia levels can easily increase within a few hours, depending on the initial freshness of the fish and microbial load. With increasing weights from 50 g to 200 g, the data illustrates a clear trend: larger sample sizes lead to higher ammonia concentrations over time. This can be attributed to a larger amount of organic material being decomposed, resulting in more generated ammonia. As temperatures increase and sample weights increase, spoilage accelerates, leading to faster ammonia production. The room temperature condition exacerbates this issue, making it unsuitable for preserving fish freshness. The measurements indicate that regular monitoring of ammonia levels could serve as an effective method for assessing fish freshness and ensuring product safety.

For the 50 g sample, ammonia levels increased gradually over time. The concentration reached its highest point (310 ppm) at the 8-hour mark, indicating ongoing spoilage. The concentrations fluctuate slightly, suggesting a relatively stable gradual increase. For the 100 g sample, the ammonia levels start higher and exhibit a more consistent increase, suggesting a greater rate of decomposition due to potentially higher microbes while the initial readings in the first hour were low (0 ppm for 50 g and 15 ppm for 100 g), which is typical as spoilage has not yet initiated within that timeframe. By the end of 8 hours, both samples were within ppm values that could indicate

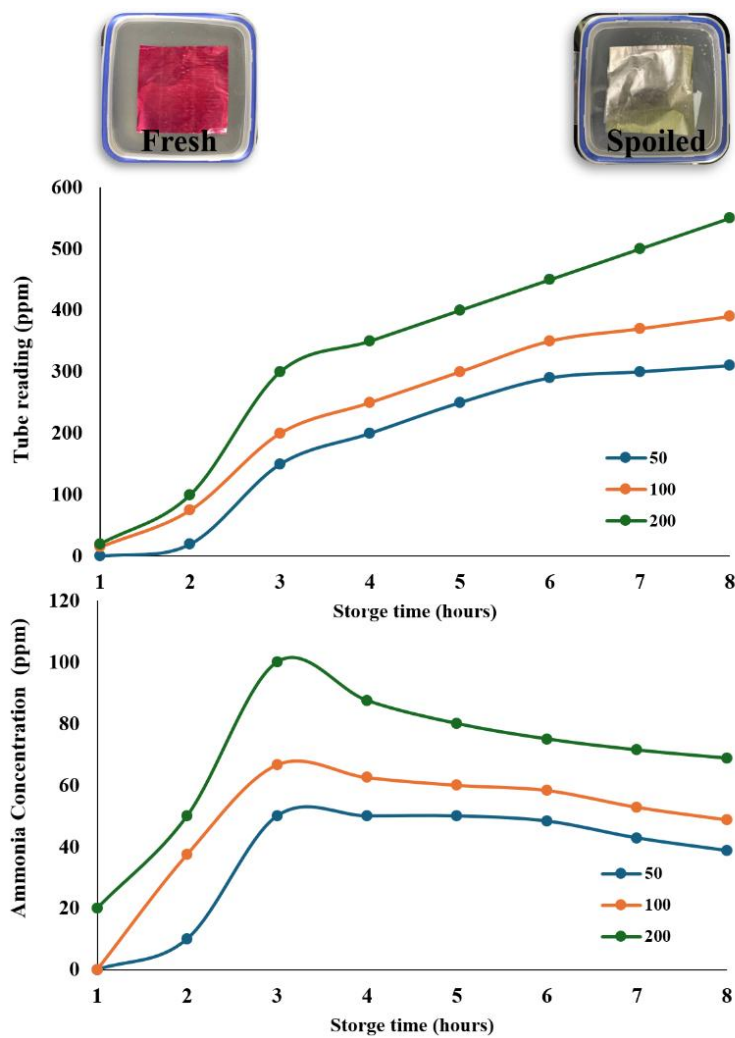


Figure C.1 The trend shows an increase in ammonia and then decrease it during 8 hours of fish storage at room temperature.

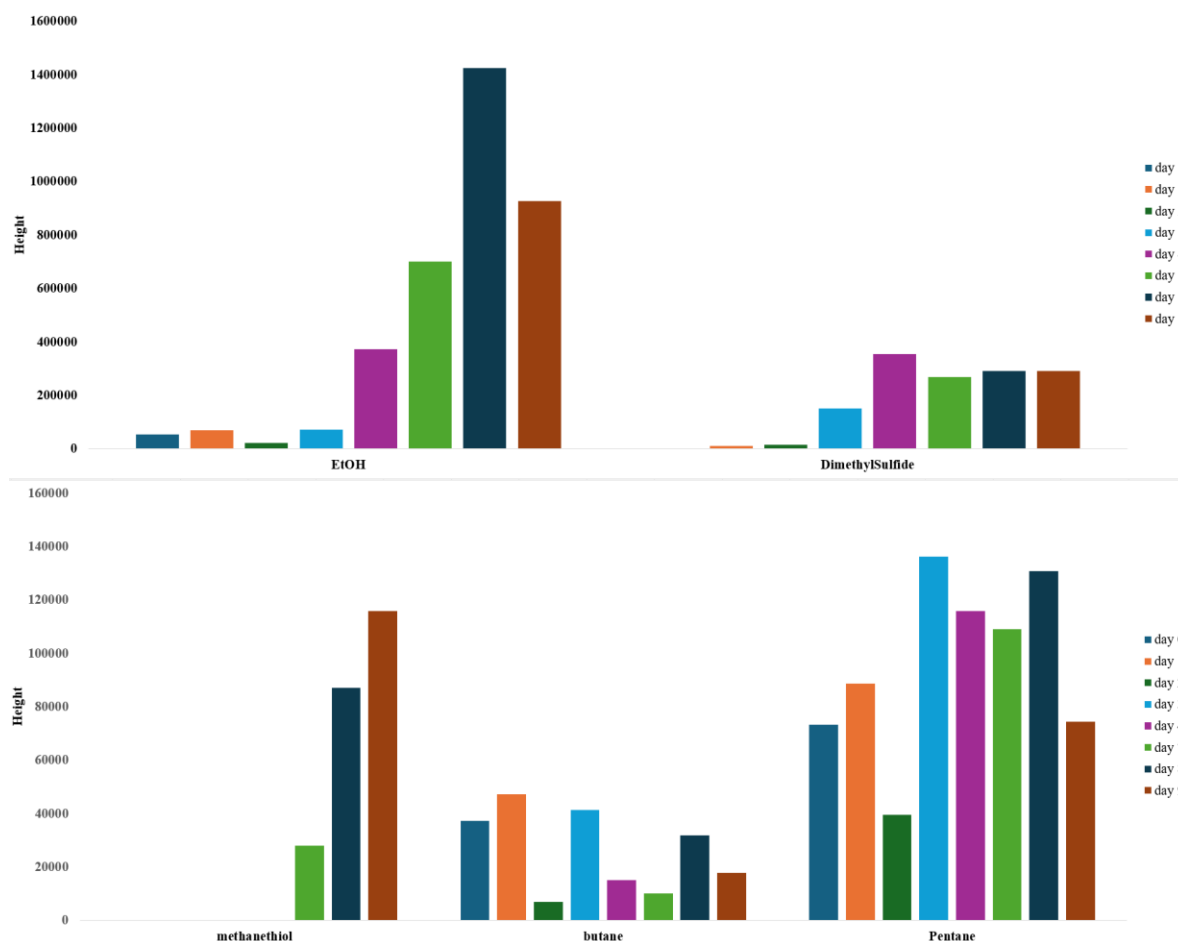


Figure C.2 Trends in the signal intensities of untargeted analytes over 9-day storage in the fridge (scan mode acquisition).

C.3 Species-Specific Analysis

The method performance for headspace GC-MS analysis was evaluated using several quality control criteria, focusing on the relative abundance of ammonia and trimethylamine in various fish samples. The issue of varying signals depending on the type of fish used was found; different fish types yielded different detectable compounds. The second experiment which performed, simultaneously with TVC and monitoring color change of sensor, with spiked fish resulted in better detection than the first, but issues with the experimental setup might continue affecting results. A comparative analysis was conducted on two fish types, pangasius and haddock. In pangasius fillets, the concentration of ammonia was found to be significantly higher compared to haddock. Conversely, haddock samples exhibited sharper and more distinct peaks for TMA, making it easier

to quantify. Notably, pangasius fillets typically contain lower levels of TMAO compared to haddock, with the marine species generally exhibiting higher concentrations of TMAO. These findings highlight the differing spoilage characteristics between freshwater (pangasius) and marine (haddock) fish, further informing quality assessment and shelf-life determination. Therefore, fluctuations in fish quality based on seasons might influence experimental outcomes.

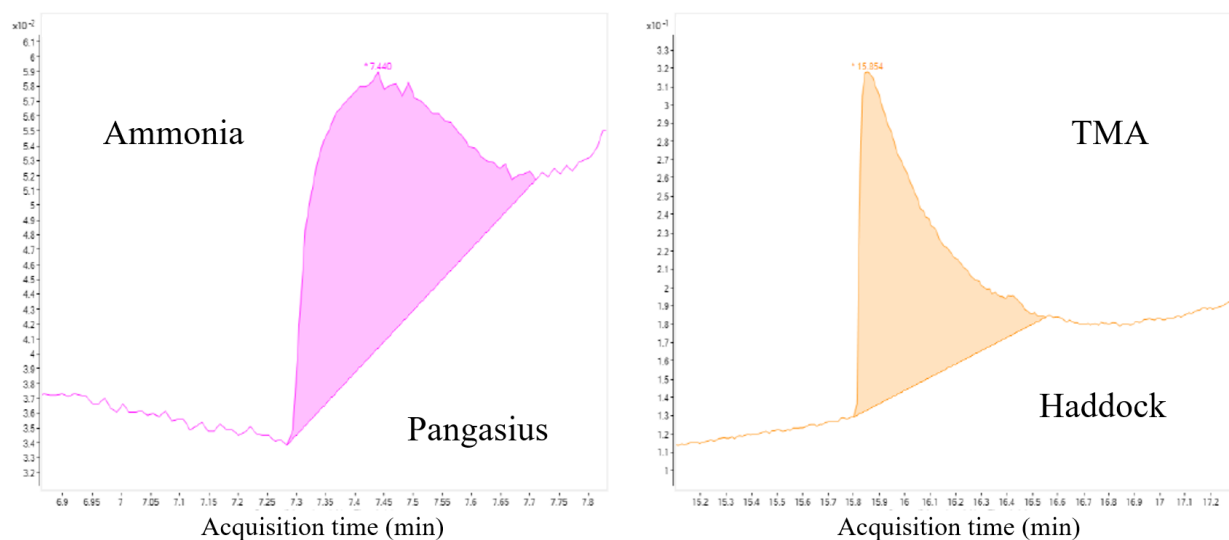


Figure C.3 Zoomed SIM chromatograms of spoiled fish samples allowing for detection of ammonia and TMA.

Some species appear to be released to the headspace after several storage days at both temperatures and could be detected by Scan mode injections. **Figure C.4** shows that ethanol and butane were identified by database search after 7 days. They could potentially be quantified by injecting their corresponding standards.

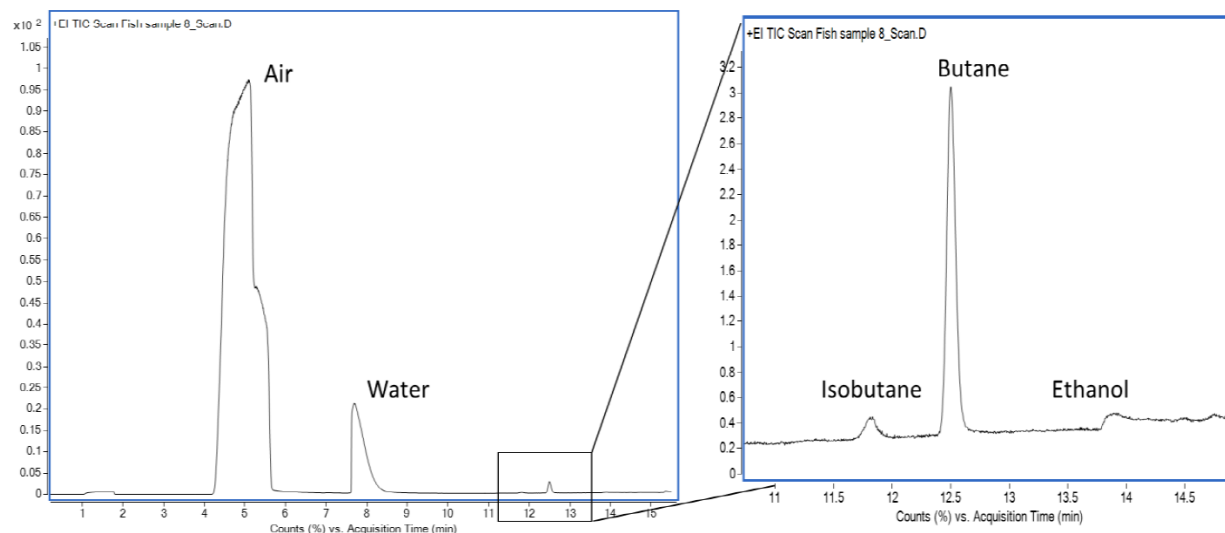


Figure C.4 Zoomed Scan chromatograms of untargeted species identified using NIST database comparison.

C.4 Performance Assessment of Colorimetric Sensing for TMA: Correlation with GC-MS Results

In this study, we compared the performance of our colorimetric sensor for detecting TMA with the established method of GC-MS. 4 samples were exposed to 100 μL TMA with different dilutions (0.001, 0.01, 0.1 and 1 M) at 25 $^{\circ}\text{C}$ for 30 min. The colorimetric sensor demonstrated a LOD of 0.01 M for 100 μL of TMA, while GC-MS achieved a lower instrumental LOD of 0.001 M for the same amount of TMA. The samples exposed to concentrations higher than 0.001 M exhibited ΔE higher than 30.

Although the GC-MS method exhibits higher sensitivity, developed colorimetric sensor's performance is significant when considering practical applications in seafood freshness monitoring. The correlation analysis between the two methods revealed a strong relationship, indicating that the colorimetric sensor can reliably detect TMA concentrations in a manner consistent with GC-MS results. To validate the effectiveness of the colorimetric sensor, we conducted repeatability and reproducibility tests, which showed consistent results across multiple trials.

The sensor's RGB values were recorded before exposure to TMA and after each subsequent acid treatment for recovery. The initial RGB values were (132, 8, 52), which changed to (176, 132, 142) after the first TMA exposure. Following the first acid treatment, the values returned to (135, 7, 47), indicating a significant change in colorimetric response. Subsequent cycles of TMA exposure and acid recovery yielded RGB values of (179, 138, 148) and (149, 34, 65), respectively, demonstrating the sensor's responsiveness to TMA concentrations. The analysis of delta RGB values revealed substantial changes, with recovery percentages indicating a high degree of sensitivity, particularly in the G channel, which showed a recovery rate of 1650%. These findings suggest that the colorimetric sensor is highly effective in detecting TMA levels, with the ability to return to baseline values after acid treatment and can offer advantages such as cost-effectiveness and ease of use. In scenarios where rapid monitoring is essential, the colorimetric sensor provides a practical alternative to GC-MS, making it a valuable tool for assessing seafood freshness.